Methods
in food science and technology.
Part 1

Monograph edited by Maria Walczycka · Urszula Błaszczyk

WYDAWNICTWO UNIWERSYTETU ROLNICZEGO W KRAKOWIE
Kraków 2022

Methods
in food science and technology.
Part 1

Monograph edited by Maria Walczycka · Urszula Błaszczyk

Publishing House of the University of Agriculture in Krakow
Krakow 2022

Reviewers

Prof. dr hab. Stanisław Mleko (Uniwersytet Przyrodniczy w Lublinie); Prof. dr hab. Iwona Wybrańska (Uniwersytet Jagielloński); Dr hab. inż. Małgorzata Karwowska, prof. UP (Uniwersytet Przyrodniczy w Lublinie); Dr hab. inż. Dariusz Stasiak, prof. UP (Uniwersytet Przyrodniczy w Lublinie); Dr hab. inż. Hanna Śmigielska, prof. UEP (Uniwersytet Ekonomiczny w Poznaniu); Dr hab. Ireneusz Kapusta, prof. UR (Uniwersytet Rzeszowski); Dr hab. Monika Sujka, prof. UP (Uniwersytet Przyrodniczy w Lublinie); Dr hab. Marta Tomczyńska-Mleko, prof. UP (Uniwersytet Przyrodniczy w Lublinie); Dr inż. Joanna Kaszuba (Uniwersytet Rzeszowski); Dr inż. Karolina Pycia (Uniwersytet Rzeszowski); Dr Agata Pawłowska (Uniwersytet Rzeszowski)

Editor in Chief
Dr hab. inż. Andrzej Wałęga, prof. URK

Scientific Editor
Prof. dr hab. inż. Krzysztof Surówka

Cover design
Anna Podczaszy

Picture on the cover
Yaroslav Pavlov, dreamstime.com

Layout
Regina Wojtyłko

Published with approval from the Rector of the University of Agriculture in Krakow

ISBN 978-83-66602-61-8

http://dx.doi.org/10.15576/978-83-66602-61-8

Publishing House of the University of Agriculture in Krakow
31-425 Kraków, al. 29 Listopada 46
Phone (+48) 12 662 51 51 or 12 662 51 57
e-mail: wydawnictwo@urk.edu.pl
www.wydawnictwo.urk.edu.pl

Editor sheets 18

CONTENT

Dear Readers,

We would like to present to you a monograph entitled "Methods in food science and technology – part 1", which we hope will be warmly accepted and continued. Our intention was to gather in one place descriptions of modern methods used in science related to food and human nutrition. Although the monograph is written in English, it has been prepared in such a way that it can be used in the didactic process by teachers and their students and doctoral students. Each chapter is a separate whole, i.e. it is devoted to a different method or group of methods or techniques for food analysis, both in terms of its chemical composition, physical properties, sensory qualities, as well as its quality, stability and safety. The aim of the monograph is to present terminology and specialist vocabulary in an accessible way for a reader who is not a specialist in a given discipline. Importantly, individual chapters have been reviewed by at least two experts.
We wish you pleasant reading and fruitful use of the monograph.

Dean of Faculty of Food Technology,
Authors and Editors of the monograph
University of Agriculture in Krakow

ION CHROMATOGRAPHY TECHNIQUES IN THE ANALYSIS OF FOOD SAMPLES WITH A FOCUS ON THE BIOFERMENTATION MONITORING

Robert DULIŃSKI

Department of Biotechnology and General Technology of Food,
Faculty of Food Technology, University of Agriculture in Krakow,
Aleja Mickiewicza 21, 31-120 Krakow, Poland

robert.dulinski@urk.edu.pl
ORCID: https://orcid.org/0000-0002-0370-2556

Abstract. Ion chromatography, an HPLC technique originally developed for the determination of inorganic cations and anions, in recent years has found application in food analysis and brewing industry. The separation mechanism based on the interaction of ionic substances with counterions bound on the column allows to broaden the spectrum of analyzed substances with biologically active compounds such as carbohydrates, amino acids, proteins and organic acids. The paper presents selected aspects of the application of this method with particular emphasis on fermentation samples related to instrument requirements, column selection, detection system and comparison of advantages and limitations of ion chromatography. From the brewing technology point of view, the possibility of simultaneous analysis of amino acids and fermentable sugars, or the profile of oligosaccharides with the number of subunits up to DP30, is an important argument for the choice of this technique. The sensitive pulsed amperometric and conductivity-suppressed conductometric detection systems described in this paper are an alternative to classical UV/Vis systems and refractometric index measurements for the determination of amino acids, saccharides and sugar alcohols.

Keywords: ion chromatography, electrochemical detector, suppressed conductivity

1. Introduction

In the last decade, significant progress has been made in the control of bioprocesses carried out in the food industry. In addition to gas chromatography, high-performance liquid chromatography, enzymatic methods and classical techniques of instrumental chemical analysis, a relatively new variant of HPLC – ion chromatography (High Performance Ion Chromatography) has developed dynamically [Lucy and Wahab 2013; Michalski 2016].

The separation principle in ion chromatography, which in the initial stage of development was dedicated to the separation of inorganic cations and anions, is similar to the mechanism used in ion exchange chromatography (IEC) [Cummins et al. 2017]. However, through the use of modified polystyrene and polyvinylbenzene latex matrices with varying bed diameters controlled by the degree of crosslinking, better results can be achieved while reducing the ionic strength of buffer [Michalski 2016]. Depending on the substances load to be analyzed, a column with bound counterions that selectively interact with the analyte molecules is selected. The strength of this interaction depends on the load value of ions flowing through the column, which leads to selective inhibition and longer residence time of substances on the column, which are eventually eluted from the bed through the solution with increased ionic strength. An additional argument to increase selectivity is the skillful profiling of an often three-component gradient elution program. The relatively high ionic strength of eluents in some applications has been reduced to solutions of 10–50 mM by using sensitive detection systems.

2. Apparatus

Theoretically, a classical HPLC apparatus with a gradient pump, degasser and an appropriately selected ion exchange column with an operating pressure of 1500––4000 psi is sufficient to perform chromatographic separation. However, in practice, the use of conventional stainless steel tubing connecting the various components of the system during gradient execution with a strong acid or alkali leads to progressive corrosion of these components and, as a consequence, to a decrease in sensitivity or even destruction of the sensitive detection systems. Thus, companies specializing in the manufacture of ion chromatography apparatus use so-called biocompatible materials, i.e. PEEK (polydieter ketone), for all components in contact with the mobile phase [Huang et al. 2021]. Additional elements are also

conductivity supressors that allow the exchange of cations and anions flowing out of the column into OH^- and H^+ respectively, which reduces the signal-to-noise ratio for conductometric detection to a minimum, thus increasing the sensitivity of system from mg/mL to μg/mL [Haddad et al. 2003; Pohl 2021]. It is also important to ensure that the eluents are of sufficient purity and even the so-called HPLC-pure water (conductivity approx. 18 milliOhm-cm) used for RP-HPLC can be contaminated with cations and anions to such an extent that the baseline noise is significantly increased (Fig. 1).

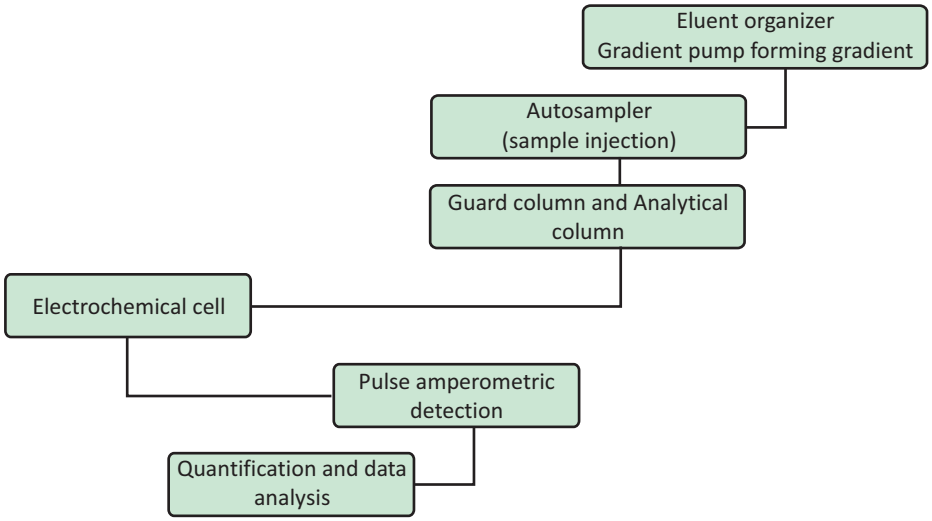

Fig. 1. System diagram for ion chromatography with electrochemical detection (source: own elaboration)

3. Columns

Column with ion-exchange matrix is a key component of the overall chromatographic system and in contrast to classical RP-HPLC columns made of stainless steel, here the bed is packed in a housing of biocompatible PEEK material. The dimensions of columns used for the analysis of carbohydrates and polyols range from 5 × 250 mm to 350 mm (Aminex HPX-87, CarboPack MA, PA 1-200) and are slightly larger than in the case of reversed-phase HPLC columns filled with octadecylsilane C-18. However, this does not result in a significant increase in analysis time, which in 80% of applications is in the range of 15–30 minutes. The

stationary phase consists of cation exchangers, able to exchange cations in solution, or anion exchangers allowing separation of negatively charged substances. The active centers of anion exchangers are quaternary ammonium groups ($-NR_3^+$) and tertiary protonated amines ($-NR_2H^+$) or sulfonium groups ($-SR_2^+$) (Fig. 2). In case of cationite beds, the functional groups are of acidic nature (e.g. carboxylic COOH, sulfonic SO_3H), undergoing dissociation with release of H^+ atom, they are able to exchange a particular ion for other cations. The structure of column core, the number and type of functional groups and the degree of crosslinking determine the properties of column filling.

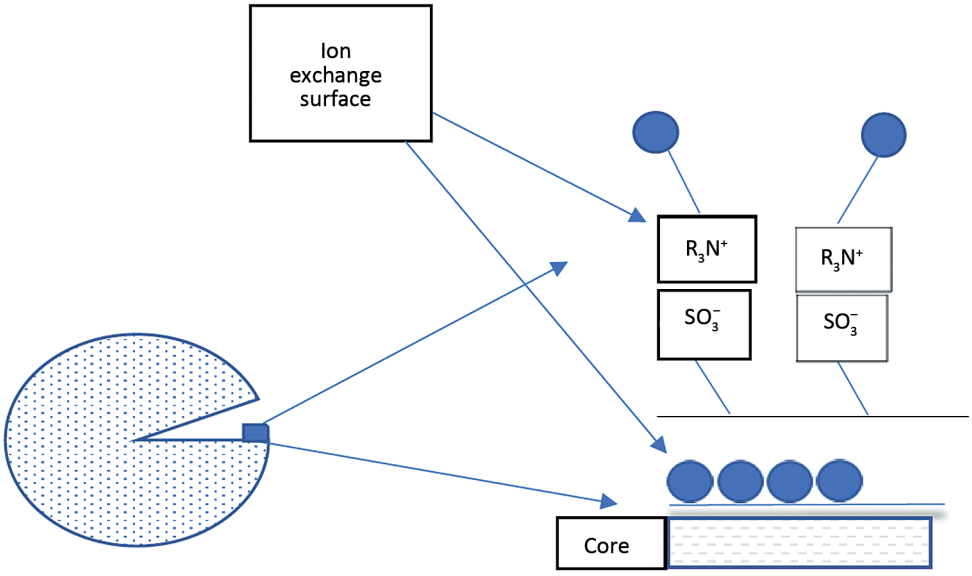

Fig. 2. Schematic cross-section of a bed used in high-performance anion exchange chromatography (source: own elaboration)

A great advantage of HPLC is the fact that the sample introduced to the column is not subjected to rigorous preliminary purification procedures as is often the case in other types of chromatography. Manufacturers' application notes mainly recommend filtering the sample through syringe strainers with a pore diameter of 0.2–0.44 μm and a nylon filter layer, although it is not recommended to introduce highly saline samples (concentrations below 50 mM) onto the column.

4. Analysis in electrochemical detection mode

Detection system of the ion chromatograph can theoretically use known from classical HPLC the universal UV/Vis detectors, more advanced with photodiode array (PDA) [Logan 1994], or refractometric [Swartz 2010]. However, the often minimal changes in the profiles of saccharides or sugar alcohols at the mashing or saccharification stage, which are so important from the fermentation process point of view, can be traced using sensitive detectors such as conductometric detection (CD) or pulse amperometric detector (PAD), without giving up the possibility of gradient elution and the necessity of thermostating the system as in the case of RI detector [Zdaniewicz et al. 2021; Maio et al. 2022]. Their principle of operation is based on potential changes in the electrochemical cell realized by oxidation-reduction processes of analyte molecules e.g. monosaccharide flowing out of the column [Cataldi et al. 2000] preceded in the case of CD measurement by a process of conductivity suppression of the interfering eluent component [Haddad et al. 2003].

The primary problem of electrochemical detectors used in HPIC was the successive wear of working electrode that was used in the electrochemical reaction. This has been solved by introducing a sequential process of electrode excitation and subsequent regeneration, all taking place over milliseconds. In addition, repeatability and reproducibility can be increased by using disposable electrodes calculated for 7 working days of continuous operation [Hanko et al. 2004]. The design of electrochemical cell minimizes signal drift by using very thin tubing lines (0.2 mm).

The use of ion chromatography coupled to pulsed amperometric detection eliminated the problems associated with contamination of the electrode surface with products of the sugar oxidation reaction. The process is based on a three-step change in the potential applied to the gold electrode:

(E1) oxidation of OH groups of carbohydrates (potential about 200 mV);

(E2) surface of the Au electrode is oxidized to remove the reaction products (800 mV);

(E3) electrode is reduced to its initial state by applying a third potential (–800 mV).

Sugars due to pKa values between 12–14 must be separated as anions in a high pressure anion-exchange chromatography with pulse amperometric detection (HPAEC-PAD) system in which the required electrochemical reaction conditions are correlated with an alkaline mobile phase (> 12 pH) [Corradini et al. 2012; Rohrer et al. 2013]. These parameters allow the determination of saccharides with a detection limit of 10–12 nanomoles, a result several orders of magnitude better than the classical RI detection system for sugars [Chávez-Servín et al. 2004].

5. Selected applications in food

This chapter focuses mainly on applications in the fermentation industry, because this is where ion chromatography offers significant advantages in terms of increased sensitivity and broadening the spectrum of molecules analyzed. For example, in the beer or wine industry, where the final product may contain up to 1000 different substances, the most important compounds are organic acids, inorganic ions, which determine the taste and aroma of beverage, as well as proteins, carbohydrates and alcohols, the analysis of which allows the monitoring of fermentation process progress. An additional element is the determination of preservatives and colorants. Most of these compounds are of ionic nature, which includes them in the area of HPIC interest.

The first stage of brewing process involves soaking barley grains, sometimes other cereal grains, in warm water, enzymes of the grain, mainly amylases and proteinases degrade the starch present through oligosaccharides to fermentable sugars: glucose, maltose and maltotriose. Beginning at this stage, through malting, mashing, and finally to the final product, compounds with a very wide range of molecular weights are generated. Ion chromatography, through the use of modified polymer column beds, allows for the analysis of most of these substances and the monitoring of individual stages of the technological process in the brewery.

5.1. Fermentable sugars, oligo- and polysaccharides

For the analysis of sugars fermentable to DP3, the most important from the brewing industry point of view as they are converted to alcohol, anion exchangers from Carbo-Pack MA and PA-1 series (Dionex) and Aminex HPX-87C cation exchange columns are used [Castellari et al. 2001; Corradini et al. 2012; Langenaeken et al. 2020] were analysed at 28 key points in the process. The barley starch content decreased during malting from 75.0% to 69.7%. During mashing, malt starch was converted to fermentable sugars (75.3%]. In the latter case, isocratic separation with deionized water as eluent can be coupled to both RI (Fig. 3) and PAD detection, but in this situation post-column derivatization with 1 M NaOH is required.

In general, sugars larger than DP3 are unfermentable, but can potentially contribute to altering the caloric value of beer and its aroma quality. In this case, columns with a slightly lower degree of crosslinking e.g. Aminex 42A, Carbo-Pack PA-10 to 100 (55%, 8.5 μm internal diameter) are recommended, although the

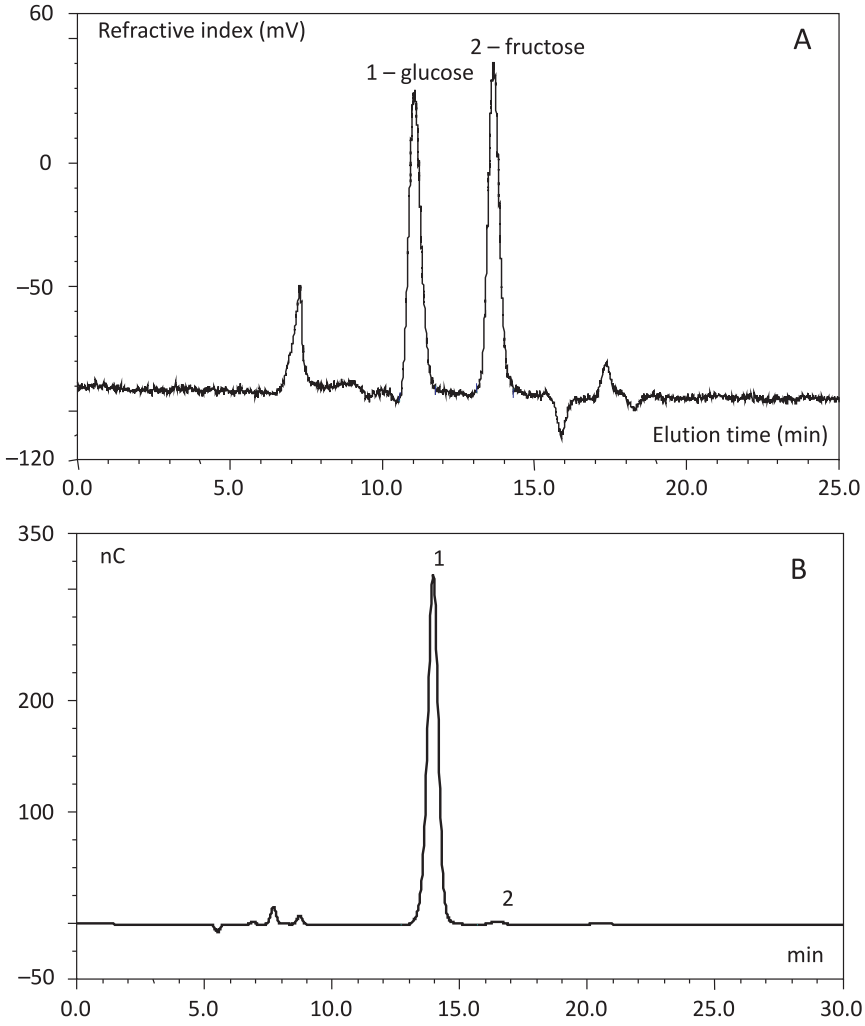

Fig. 3. Separation of mono- and disaccharides by ion chromatography in a wine sample (Swenson Red) on an Aminex HPX-87C cation exchange column, eluent: deionized water, UV detection 210nm/RI, temp. 85°C (A); in a glucose syrup sample on a CarboPack MA-1 anion exchange column, eluent 1M NaOH, PAD detection, 1-glucose, 2-maltose (B) (source: own research)

basic separation mechanism and detection system (PAD) remain the same as for mono and disaccharides [Mechelke et al. 2017].

The wide range of polymer columns used in HPIC allows the separation of maltooligosacchrides with subunit numbers from DP3 to DP10 on a Carbo--Pack PA-100 column. However, programming a ternary gradient involving

DI water, 500mM sodium acetate (increases ionic strength, reducing retention time), and 1 M NaOH allow clear separation of maltose oligomers up to DP15 (Dionex, AN 67), and there are also papers documenting the separation of sugars with a polymerization degree of 60 (Tab. 1) [Vinogradov and Bock 1998; Cataldi et al. 2000].

Table 1. Official methods for the analysis of sugars in food with a dedicated technique of ion chromatography coupled to electrochemical detection (source: own elaboration)

Analysis	Technique	Official method
Sugars in molasses	HPAE-PAD	AOAC 996.06 ICUMSA (1994)
Carbohydrates in instant coffee	HPAE-PAD	AOAC 995.13 ISO 11292
Fructans in food	HPAE-PAD	AOAC 997.08
Polydextrose	HPAE-PAD	AOAC 2000.11

Figure 4 shows the separation of carbohydrates at different stages of the brewery process: glucose syrup, wort, and beer, which allows effective monitoring of potential undesirable changes in the saccharide profile. Such possibilities are offered, among others, by Carbo-Pack PA-100 and Aminex Bio--Fermentation Analysis columns [Hanko et al. 2004], the competition here are size exclusion chromatography (SEC) columns based on a different retention mechanism.

5.2. Sugar alcohols

Among the sugar alcohols that play an important role in brewing are ethanol and glycerol [Zhao et al. 2015]. Both alcohols are subject to separation on both monosaccharide columns (Carbo-Pack MA-1, Aminex HPX-87H) (Fig. 5) and a variant of HPIC called ion exclusion chromatography (column: IonPac ICE-AS6) [Dionex AN 122, 2004], however the separation of ethanol and glycerol in beer is possible on the last column involving a pulsed amperometric detection system using a platinum working electrode [Wu et al. 2009].

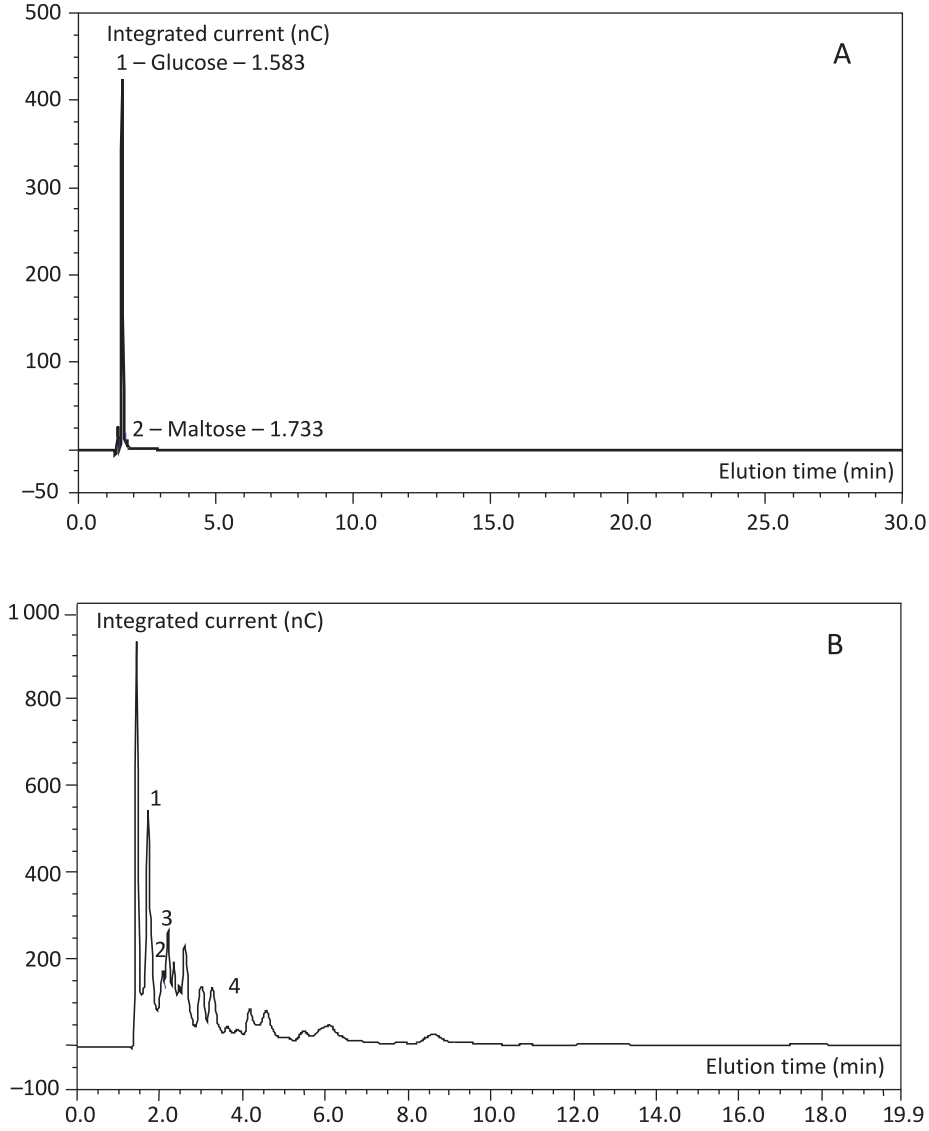

Fig. 4. Oligosaccharide profile of glucose syrup sample (A) (1 : 100 dilution) and light beer sample (B) (1 : 10 dilution) on CarboPack PA-100 anion exchange column, PAD detection, 0.175 mM NaOH/0.150 mM sodium acetate isocratic separation. 1 – glucose, 2 – maltose, 3 – matotriose, 4 – maltopentaose, unidentified peaks represent maltooligosaccharides DP 4–20 (source: own research)

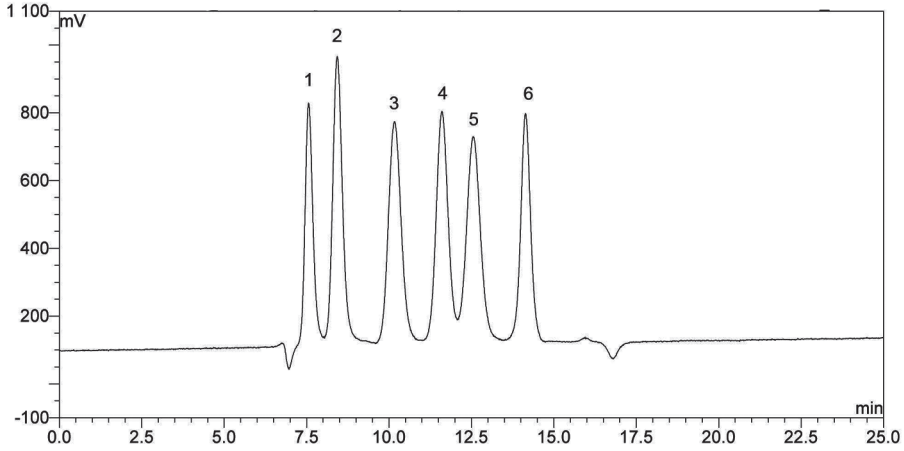

Fig. 5. Separation of sugar alcohols and saccharides on Aminex HPX-87C column, RI/UV detection. 1 – melcytose, 2 – maltose, 3 – glucose, 4 – mannose, 5 – fructose, 6 – ribitol (source: own research)

5.3. Bioactive inositols

The bioactive and functional properties of beer intended for a special group of consumers (gluten-free beer) can be improved by using unconventional ingredients in the malting process such as buckwheat, an additional aspect arises here from the high content of bioactive inositols: D-*chiro*- and *myo*-inositol. These are substances with potential positive effects on glycemic index, immunomodulatory, signaling, and cell growth-stimulating properties [Al-Suod et al. 2016; Rendle et al. 2016; Duliński et al. 2020]. P-type phosphoglycans containing D-*chiro*-inositol and galactosamine may function as secondary transmitters to mimic the effects of insulin or to enhance the signal generated by this blood sugar regulator [Bevilacqua and Bizzarri 2018]. The relatively high level of anti-nutritive phytates in buckwheat and buckwheat malt and low activity of endogenous enzymes, limiting the effective use of substrates for fermentation and yeast metabolism (starch, proteins, minerals), also justify the use of phosphatases in beer production technology [Duliński et al. 2017]. Monitoring of changes in the content of these polyols is possible precisely thanks to unique solutions offered by HPAEC-PAD chromatography (Fig. 6) [Duliński et al. 2019; Zdaniewicz et al. 2020].

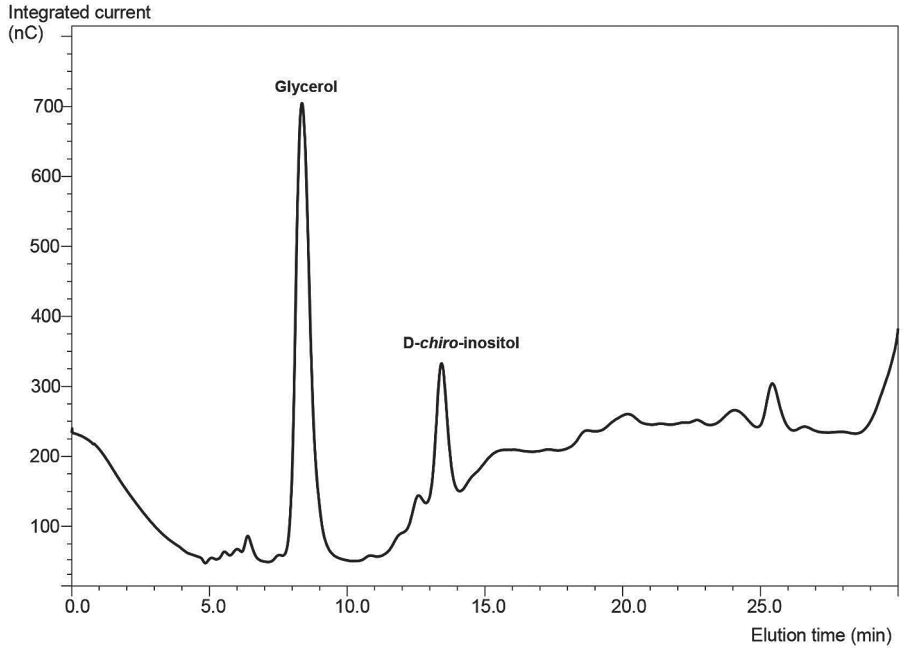

Fig. 6. Sample chromatogram from the analysis of D-*chiro*-inositol in buckwheat beer by HPAEC–PAD chromatography on CarboPack MA1 column (source: own research)

5.4. Amino acids and peptides

Proteins can originate both from the primary raw material for mashing and from intermediate fermentation biocatalysts, yeast cells and components of their cell wall. The thousands of proteins present in beer from the brewing point of view are most conveniently ranked by molecular weight. Large protein complexes can be separated on IEC or RP-HPLC columns and in this case ion chromatography is an overly refined technique. However, smaller protein polymers with a molecular weight of 30 kDa or less can be separated on a ProteinPac column with AAA-Direct detection system (Dionex, TN 50). Amino acids and peptides are important components in the final stages of fermentation, indicative of the metabolic activity of yeast cells and proteolytic enzymes of the grain [Ferreira and Guido 2018; Koller and Perkins 2022]. Amino acids are usually weak chromophores and monitoring fermentation samples containing as in brewing cellular components leads to interference and generates high noise in conventional UV detection mode at 220 nm (peptide bond absorption band) or 280 nm (aromatic amino acids). Am-

inoPac PA-10 columns allow simultaneous separation in such complex matrices of amino acids and oligosaccharides (Fig. 7) [Hanko et al. 2004; Jandik et al. 2004; Cuomo et al. 2022]. In order to eliminate one of components from the chromatogram, it is possible to purify the sample using AminoTrap Cartridge columns [Thiele et al. 2002; Cheng and Kaplan 2003; Jandik et al. 2003].

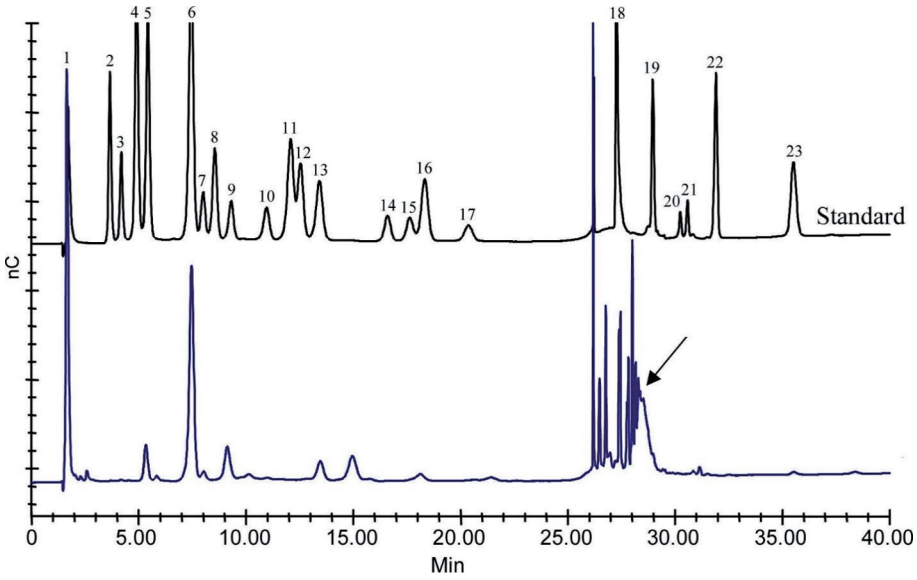

Fig. 7. Simultaneous separation of amino acids and maltooligosaccharides on AminoPac PA-10 ion exchange column, PAD detection, Eluent 1: deionized water; E2: 250 mM NaOH; E3: 1 M sodium acetate Standards of the amino acids (black line) 1. Arginine; 2. Hydroxylysine; 3. Lysine; 4. Galactosamine; 5. Glucosamine; 6. Glucose; 7. Alanine; 8. Threonine; 9. Glycine; 10. Valine; 11. Hydroxyproline; 12. Serine; 13. Proline; 14. Isoleucine; 15. Leucine; 16. Methionine; 17. Norleucine; 18. Histidine; 19. Phenylalanine; 20. Glutamate; 21. Aspartame; 22. Cysteine; 23. Tyrosine; Beer sample (blue line): maltoligosaccharides – indicated by the arrow (source: based on AminoPac AAA Direct Manual, thanks to Thermo-Dionex Corp. courtesy)

5.5. Organic acids

The qualitative and quantitative analysis of organic acids, at all stages of beer production, allows to identify metabolic products associated with yeast fermentation and correlate them with the direction of changes in the aroma of beverage. The previously mentioned IonPac ICE-AS6 column provides an efficient separation of low molecular weight aliphatic organic acids including hydroxy-substituted

acids [Fischer et al. 1999]. The mechanism is based on weak ionization of compounds eluted from the column according to differences in their pKa constant with monoprotonic acids. The signal of analytes is measured in conductivity-suppressed conductometric detection mode (AMMS™-ICE). Determinations include maleic, citric, formic, pyruvic, lactic, and succinic acids. The presence of acetate may indicate the degree of oxidation; pyruvate is an intermediate product of ethanol fermentation. A high level of lactate is an unfavorable factor, it may prove a high metabolic activity of acetic bacteria, lowering the glucose pool for primary fermentation of *Saccharomyces* cells. This process is eligible in sour beer production process [Dysvik et al. 2020].

5.6. Inorganic ions

Inorganic anions are separated by HPAEC on an IonPac AS11 column coupled to conductometric detection [Park et al. 2017]. Due to potential ion contamination of the eluent and baseline drift, an Anion Trap Column (ATC) system should be installed between the gradient pump and the injection valve. In addition, the use of NaOH as eluent is recommended to eliminate high background conductivity. The reproducibility of this method is 0.5% for retention times and 2% for peak areas with good linearity of the calibration curve (r2 = 0.999) (Dionex, AN 67).

Inorganic cations Na, K, Mg, Ca may be involved in regulating the pH of mash or affecting the beverage aroma [Zeng et al. 2006]. Magnesium ions are an important cofactor for yeast enzymes (10–20 mg/L), but at concentrations higher than 5 mg they contribute to the bitter taste of beer. Calcium ions play a similar role, although their contribution to the taste and aroma of product is marginal. It is also worth monitoring the levels of heavy metals such as Hg, Pb, Zn, as most of them are toxic at the lowest detection level of ppm.

6. Conclusion

Ion chromatography coupled with amperometric detection modes offers a precise tool for analyzing the profile of key components and changes occurring in fermentation products. It covers all stages of the fermentation process: from the stage of substrates (syrup), through intermediate products (wort) to the final product (beer). They also are not so time-consuming because of a simple extraction procedures, in most cases reduced to dilution and filtration of the

samples, so from the perspective of challenging monitoring of the bioprocesses it is an important advantage. The pulsed amperometric and conductivity-suppressed electrochemical detection systems will be better tools to detection of full array of saccharides and ion compounds considering: sensitivity, resolution, mobile phase modifications, need of thermostatisation and the general robustness of the method in relation to methods coupled with Refractive index or UV-Vis detection.

References

Al-Suod H., Ligor M., Rațiu I.A., Rafińska K., Górecki R., Buszewski B. 2016. A window on cyclitols: Characterization and analytics of inositols. Phytochemistry Letters, 20. https://doi.org/10.1016/j.phytol.2016.12.009

Bevilacqua A., Bizzarri M. 2018. Inositols in insulin signaling and glucose metabolism. International Journal of Endocrinology, 2018, 1968450. https://doi.org/10.1155/2018/1968450

Castellari M., Sartini E., Spinabelli U., Riponi C., Galass S. 2001. Determination of carboxylic acids, carbohydrates, glycerol, ethanol, and 5-HMF in beer by high-performance liquid chromatography and UV-refractive index double detection. Journal of Chromatographic Science, 39, 235–238. https://doi.org/10.1093/chromsci/39.6.235

Cataldi T.R.I., Campa C., De Benedetto G.E. 2000. Carbohydrate analysis by high-performance anion-exchange chromatography with pulsed amperometric detection: The potential is still growing. Fresenius. Journal of Analytical Chemistry, 368, 739–758. https://doi.org/10.1007/s002160000588

Chávez-Servín J.L., Castellote A.I., López-Sabater M.C. 2004. Analysis of mono- and disaccharides in milk-based formulae by high-performance liquid chromatography with refractive index detection. Journal of Chromatography A, 1043, 211–215. https://doi.org/10.1016/j.chroma.2004.06.002

Cheng X., Kaplan L.A. 2003. Simultaneous analyses of neutral carbohydrates and amino sugars in freshwaters with HPLC-PAD. Journal of Chromatographic Science, 41, 434–438. https://doi.org/10.1093/chromsci/41.8.434

Corradini C., Cavazza A., Bignardi C. 2012. High-Performance anion-exchange chromatography coupled with pulsed electrochemical detection as a powerful tool to evaluate carbohydrates of food interest: Principles and applications. International Journal of Carbohydrate Chemistry, 2012, 487564. https://doi.org/10.1155/2012/487564

Cummins P.M., Rochfort K.D., O'Connor B.F. 2017. Ion-exchange chromatography: Basic principles and application. Methods in Molecular Biology, 1485, 209–223. https://doi.org/10.1007/978-1-4939-6412-3_11

Cuomo F., Trivisonno M.C., Iacovino S., Messia M.C., Marconi E. 2022. Sustainable re-use of brewers spent grain for the production of high protein and fibre pasta. Foods, 11, 642. https://doi.org/10.3390/foods11050642

Duliński R., Starzyńska-Janiszewska A., Byczyński Ł., Błaszczyk U. 2017. Myo-inositol phosphates profile of buckwheat and quinoa seeds: Effects of hydrothermal processing and solid-state fermentation with Rhizopus oligosporus. International Journal of Food Properties, 20, 2088–2095. https://doi.org/10.1080/10942912.2016.1230871

Duliński R., Zdaniewicz M., Pater A., Poniewska D., Żyła K. 2020. The impact of phytases on the release of bioactive inositols, the profile of inositol phosphates, and the release of selected minerals in the technology of buckwheat beer production. Biomolecules, 10(2). https://doi.org/10.3390/biom10020166

Duliński R., Zdaniewicz M., Pater A., Żyła K. 2019. Impact of two commercial enzymes on the release of inositols, fermentable sugars, and peptides in the technology of buckwheat beer. Journal of the American Society of Brewing Chemists, 77(2), 119–125. https://doi.org/10.1080/03610470.2019.1589910

Dysvik A., La Rosa S.L., Liland K.H., Myhrer K.S., Østlie H.M., De Rouck G., Rukke E.O., Westereng B., Wicklund T. 2020. Co-fermentation involving Saccharomyces cerevisiae and Lactobacillus species tolerant to brewing-related stress factors for controlled and rapid production of sour beer. Frontiers in Microbiology, 11, 279. https://doi.org/10.3389/fmicb.2020.00279

Ferreira I.M., Guido L.F. 2018. Impact of wort amino acids on beer flavour: A review. Fermentation 4. https://doi.org/10.3390/fermentation4020023

Fischer K., Kotalik J., Kettrup A. 1999. Chromatographic properties of the ion-exclusion column lonPac ICE-AS6 and application in environmental Analysis Part I: Chromatographic Properties. Journal of Chromatographic Science, 37, 477–485. https://doi.org/10.1093/chromsci/37.12.477

Haddad P.R., Jackson P.E., Shaw M.J. 2003. Developments in suppressor technology for inorganic ion analysis by ion chromatography using conductivity detection. Journal of Chromatography A, 1000, 725–742. https://doi.org/https://doi.org/10.1016/S0021-9673(02)01999-4

Hanko V.P., Heckenberg A., Rohrer J.S. 2004. Determination of amino acids in cell culture and fermentation broth media using anion-exchange chromatography with integrated pulsed amperometric detection. Journal of Biomolecular Techniques, 15(4), 317–324.

Huang W., Plistil A., Stearns S.D., Dasgupta P.K. 2021. Gradient nanopump based suppressed ion chromatography using PEEK open tubular columns. Talanta Open, 3, 100029. https://doi.org/10.1016/j.talo.2020.100029

Jandik P., Cheng J., Avdalovic N. 2003. Amino acid analysis in protein hydrolysates using anion exchange chromatography and IPAD detection BT. [In:] Protein Sequencing Protocols. Ed. B.J. Smith. Humana Press, Totowa, NJ, 155–167.

Jandik P., Cheng J., Avdalovic N. 2004. Analysis of amino acid-carbohydrate mixtures by anion exchange chromatography and integrated pulsed amperometric detection. Journal

of Biochemical and Biophysical Methods, 60(3), 191–203. https://doi.org/10.1016/j.jbbm.2004.01.003

Koller H., Perkins L.B. 2022. Brewing and the chemical composition of amine-containing compounds in beer: A review. Foods (Basel, Switzerland), 11, 257. https://doi.org/10.3390/foods11030257

Langenaeken N.A., De Schepper C.F., De Schutter D.P., Courtin C.M. 2020. Carbohydrate content and structure during malting and brewing: A mass balance study. Journal of the Institute of Brewing, 126, 253–262. https://doi.org/https://doi.org/10.1002/jib.619

Logan B.K. 1994. Liquid chromatography with photodiode array spectrophotometric detection in the forensic sciences. Analytica Chimica Acta, 288(1–2), 111–122. https://doi.org/10.1016/0003-2670(94)85120-4

Lucy C.A., Wahab M.F. 2013. Advances in high-speed and high-resolution ion chromatography. LCGC Supplements, 38–42.

Maio M., Di Fiore C., Iannone A., Carriera F., Notardonato I., Avino P. 2022. Review of the analytical methods based on HPLC-electrochemical detection coupling for the evaluation of organic compounds of nutritional and environmental interest. Analytica. https://doi.org/10.3390/analytica3010005

Mechelke M., Herlet J., Benz J.P., Schwarz W.H., Zverlov V.V., Liebl W., Kornberger P. 2017. HPAEC-PAD for oligosaccharide analysis – novel insights into analyte sensitivity and response stability. Analytical and Bioanalytical Chemistry, 409, 7169–7181. https://doi.org/10.1007/s00216-017-0678-y

Michalski R. 2016. Principles and applications of ion chromatography. [In:] Application of IC-MS and IC-ICP-MS in Environmental Research. Ed. R. Michalski. John Wiley & Sons, Ltd, New Jersey, United States, 1–46.

Park J.M., Shin J.A., Lee J.H., Lee K.T. 2017. Development of a quantitative method for organic acid in wine and beer using high performance liquid chromatography. Food Science and Biotechnology 26, 349–355. https://doi.org/10.1007/s10068-017-0047-9

Pohl C. 2021. Stationary phases and suppressors in ion chromatography, 1975–2000. [In:] Ion Chromatography. Eds. C. Pohl, N. Avdalovic, K. Srinivasan. Academic Press, Cambridge, United States, 15–42. https://doi.org/10.1016/B978-0-12-813075-9.00005-4

Rendle P.M., Kassibawi F., Johnston K.A., Hart J.B., Cameron S.A., Falshaw A., Painter G.F., Loomes K.M. 2016. Synthesis and biological activities of d-chiro-inositol analogues with insulin-like actions. European Journal of Medicinal Chemistry, 122, 442–451. https://doi.org/10.1016/j.ejmech.2016.06.047

Rohrer J.S., Basumallick L., Hurum D. 2013. High-performance anion-exchange chromatography with pulsed amperometric detection for carbohydrate analysis of glycoproteins. Biochemistry (Moscow), 78(7), 697–709. https://doi.org/ 10.1134/S000629791307002X

Swartz M. 2010. HPLC detectors: A brief review. Journal of Liquid Chromatography & Related Technologies, 33(9–12), 1130–1150. https://doi.org/10.1080/10826076.2010.484356

Thiele C., Gänzle M.G., Vogel R.F. 2002. Sample preparation for amino acid determination by integrated pulsed amperometric detection in foods. Analytical Biochemistry, 310, 171––178. https://doi.org/10.1016/s0003-2697(02)00283-x

Vinogradov E., Bock K. 1998. Structural determination of some new oligosaccharides and analysis of the branching pattern of isomaltooligosaccharides from beer. Carbohydrate Research, 309, 57–64. https://doi.org/https://doi.org/10.1016/S0008-6215(98)00119-0

Wu P., Tian J.C., Walker C.E., Wang F.C. 2009. Determination of phytic acid in cereals – A brief review. International Journal of Food Science & Technology, 44, 1671–1676. https://doi.org/10.1111/j.1365-2621.2009.01991.x

Zdaniewicz M., Pater A., Hrabia O., Duliński R., Cioch-Skoneczny M., 2020. Tritordeum malt: An innovative raw material for beer production. Journal of Cereal Science, 96. https://doi.org/10.1016/j.jcs.2020.103095

Zdaniewicz M., Pater A., Knapik A., Duliński R., 2021. The effect of different oat (Avena sativa L) malt contents in a top-fermented beer recipe on the brewing process performance and product quality. Journal of Cereal Science, 101, 1–8. https://doi.org/10.1016/j.jcs.2021.103301

Zeng W., Chen Y., Cui H., Wu F., Zhu Y., Fritz J.S. 2006. Single-column method of ion chromatography for the determination of common cations and some transition metals. Journal of Chromatography A, 1118(1), 68–72. https://doi.org/10.1016/j.chroma.2006.01.065

Zhao X., Procopio S., Becker T. 2015. Flavor impacts of glycerol in the processing of yeast fermented beverages: A review. Journal of Food Science and Technology, 52 (12), 7588––7598. https://doi.org/10.1007/s13197-015-1977-y

II DETERMINATION OF MOLECULAR WEIGHT OF BIOPOLYMERS USING HPSEC-MALLS-RI METHOD

Ewelina NOWAK, Anna WISŁA-ŚWIDER

Department of Chemistry,
Faculty of Food Technology, University of Agriculture in Krakow,
Aleja Mickiewicza 21, 31-120 Krakow, Poland

ewelina.nowak@urk.edu.pl
ORCID: https://orcid.org/0000-0001-6186-023X

anna.wisla-swider@urk.edu.pl
ORCID: https://orcid.org/0000-0001-8889-2960

Abstract. The chapter presents a brief overview of the methods for determining the average molecular weight of biopolymers used in food technology. These analyzes are most often based on size exclusion chromatography (SEC). Mass detection and scattering intensity can be determined with different detectors: LALLS, MALLS, UV, DRI and others. An exemplary chromatogram obtained during the separation of starch polysaccharide chains by the HPSEC-MALLS--RI method has been presented. The work also presents the plots of differential weight fraction for native and modified starches with their interpretation. Selected results of molecular weights of polysaccharide chains described in the literature are discussed.

Keywords: HPSEC-MALLS-RI, molecular weight, polysaccharide chains, size exclusion chromatography, starch

1. Introduction

Biopolymers are the main components occurring in living organisms and the whole environment and they are the basis of the food technology. The most popular biopolymers are: polysaccharides (e.g. starch, cellulose, chitosan, alginic acid, pectins), oligosaccharides, proteins and enzymes.

The molar mass distributions and molecular structure significantly influences their digestibility, viscosity [Bello-Perez et al. 2019], solubility, hydration rate and extent [Nishinari and Fang 2020] and another functional properties. For example, determining the molar mass of hydrocolloids is important in controlling the viscosity of fluid foods. A small addition of high molar mass polysaccharides may increase the viscosity of the fluid (assuming the polysaccharide is not completely random coil). However, many factors have an influence on viscosity of liquid foods on viscosity: molar mass, structural characteristics, conformation, molecular shape and molecule stiffness [Nishinari and Fang 2020].

Degree of polysaccharides branching also play a key role for viscosity of liquids. It is thus very essential for application properties to understand the architecture of especially highly branched polymers.

According to the literature, there are several methods to determine the molecular weight and radii of gyration e.g. high-performance anion-exchange chromatography (HPAEC) [Bertoft 2007; Bertoft et al. 2010; Zhao et al. 2021], with pulsed amperometric detection (PAD) [Bello-Perez et al. 1996; Hanashiro et al. 1996; Blennow et al. 2000; Sanderson et al. 2006; Villas-Boas et al. 2019; Ye et al. 2021].

Flow field-flow fractionation (FIFFF) is another important technique for analysis of ultra-large biopolimer molecules like starch (amylopectin). The method is used in molecular analysis of water-soluble polymers, colloids, liposomes, DNAs and another natural organic matters [Lee et al. 2003]. The asymmetrical-flow field-flow fractionated system (AF4) with MALLS-DRI detectors is also a type of method to assess molecular weight and radii of gyration [Hoyos-Leyva et al. 2017; Bello-Pérez et al. 2018]. This methods has been used for analysis of colloidal particles, polysaccharides, celluloses, κ-carragenian, xanthan, cationic potato amylopectin and dextran [Lee et al. 2003], red wine macromolecules [Pascotto et al. 2020] and glycogen [Rolland-Sabate et al. 2007]. Nevertheless, the size-exclusion chromatography (SEC) is a very important method to characterize the molecular weights distribution of polymers [Bertolini et al. 2001; Gaborieau and Castignolles 2011], average molecular weight and degree of polymerization or separate the polymer mixture into various components.

2. High performance size exclusion chromatography methods

Natural biopolymers are investigated using SEC method which is the most widely accepted one, for the measurement of molecular weight (M_w) distribution and molecular weight averages of macromolecules [Kostanski et al. 2004]. Futhermore, this system is suitable for separation of small molecules.

Multiple-detection SEC allows molecular weights to be denoted with two different types of detection: viscometry and light scattering method. The M_w sensitive detectors being commonly used are: low-angle laser light scattering (LALLS), multiangle laser light scattering (MALLS) and two types of viscosity (VISC) detectors (differential viscometers and single or dual capillary viscometers) [Kostanski et al. 2004]. Viscometry needs a universal calibration curve to determine true molecular weights. Light-scattering detectors enable the determination of absolute molecular weights through low-angle laser light scattering, multi-angle laser light scattering, or triple detection [Gaborieau and Castignolles 2011].

Multi-angle light scattering coupled with size-exclusion chromatography (SEC-MALS) is very useful method for the determination of polymer molecular weights, their averages, their distributions. SEC-MALS provides a useful tool for determination of accurate monomer and fragment of the absolute molecular weight, oligomeric state and hydrodynamic radius. SEC-MALS can be used to characterize the molecular weight and types of aggregates present in protein products, to confirm the molecular weight of the biopolymers. We can apply multi-angle light scattering coupled to size-exclusion chromatography (SEC--MALS) or field flow fractionation (FFF-MALS) in the characterization of protein conformational and colloidal stability and the characterization of both specific and non-specific protein-protein interaction [Sahin and Roberts 2012]. The general characteristics of detectors used in the size-exclusion chromatography are collected in Table 1.

Size-exclusion chromatography coupled with a multi-angle laser light scattering detector is one of the widely-used techniques for the characterization of macromolecules and particles in solution in chemical, biological, biopharmaceutical sciences and food science [Wyatt 1993; Nettleship et al. 2008; Minton 2016].

The weight-average molecular weight and hydrodynamic radius, of some proteins was determined by high performance size exclusion chromatography coupled with on-line multi-angle laser light scattering and refractive index detectors (HPSEC-MALLS-RI) [Zhou et al. 2006]. The molecular structure of polysaccharide could be analyzed using HPSEC-MALLS-RI [Zhang et al. 2021], especially

native [Fiedorowicz et al. 2001; Xia et al. 2017], retrogradated [Villas-Boas et al. 2020], acetylated, oxidized and hydrolyzed starch samples and their nanocomposites [Khachatryan et al. 2015; Khachatryan et al. 2016a], amylopectins [Bello-Perez et al. 1998; Zhao et al. 2021]. Literature data shows that this method is suitable for molecular analysis of κ-carragenian derivatives [Júnior et al. 2021], arabinoglucans [Ye et al. 2021], hyaluronan, hyaluronan-lecithin composites [Khachatryan et al. 2016b] and DNAs [Porsch et al. 2009; Nowak et al. 2019]. Hyaluronan's molar analysis [Harmon et al. 2012] and cationic cellulose derivatives [Liu et al. 2006] were also carried out with triple detection (SEC-TD) (dual-angle light scattering detector along with a differential refractometer and viscometer). Dervilly et al. [2000] studied macromolecular characteristics of arabinoxylans using HPSEC methods combined with four detectors, MALLS-RI-VISC and UV detector.

Table 1. Characteristics of detectors (source: based on Kilz and Pasch [2000]; Kostanski et al. [2004])

Detector	Sensitivity to	Calibration	SEC method application	MMD	R_g distribution	Chain conformation
RI	concentration	+	absolute M_w	requires *dn*/*dc* values	+	–
UV	concentration	+	requires chromophores, used for copolymers and sample contaminations	signal – not proportional to M_w	–	–
MALLS	molar mass	-	*MMD*, R_g distribution	requires precise *n* and *dn*/*dc* values	+	R_g vs *M* plot
LALLS	molar mass	-	MMD	requires precise n and *dn*/*dc* values	–	–
VISC	molar mass	+	[η] distribution, *MMD*, R_g distribution, Copolymer *Mn*	requires universal calibration and *K*, *a*-parameters	calculable from [η]*M*	[η] vs *M* plot, R_g vs *M* plot

M_w – molecular weight
MMD – molar mass distribution

It has been reported that high-performance size-exclusion chromatography (HPSEC-MALLS-RI) is used to measure the weight-average molecular weight of pectin samples [Li et al. 2019; Reichembach and de Oliveira Petkowicz 2020]. The HPSEC method with different detector; MALLS coupled with a viscometer (VIS) [Ma et al. 2008; Chen et al. 2009] and RID–MALSD [Chen et al. 2013] were using to determine β-D-glucans isolated from a common edible mushrooms.

SEC method can be used to monitoring the progress of enzymatic hydrolysis of biopolymers, especially polysaccharides or proteins. One example might be hydrolysis of cellulose and lignocellulose. Is commonly observed that hydrolysis usually causes the changes in molecular weight (M_w) distribution toward lower M_w range. Hence, changes in M_w directly affect the DP (*degree of polymerization*) values. Cateto et al. [2011] and Du et al. [2013] carried out enzymatic hydrolysis of lignocellulose. The researches have determined e.g the molecular weight distribution, molecular size distribution and DP. They observed similar phenomenon: during enzymatic hydrolysis M_w of both cellulose and hemicellulose fraction remarkably shift towards lower values. As reported by Ottøy et al. [1996] the M_w of cellulose derivatives might be overestimated if only the SEC method is used (in view of M_w calibration with M_w of standards). The application of SEC-MALLS--RI is consider as an absolute approach without calibration to measure M_w, R_g, *DP* and polydispersity of biopolymers [Du et al 2013]. Nevertheless, complicated enzymatic processes dependent on many factors (for instance various cellulosic substrates, digestion time, enzymes used, enzymes complexes) could induce the increase in M_w and DP at later stage of hydrolysis. Similar observations were presented in Zhang et al. [2011] studies. The authors analysed M_w, *DP*, R_g using SEC-MALLS-RI method after enzymatic hydrolysis of celulose filter paper and microcrystalline celulose.

The molecular weight and size distribution of arabinogalactan (AG) and arabinogalactan-protein (AGP) fractions have been investigated by Renard et al. [2014]. The reseacher were analysed AGP and AG parts (hydrolysed using proteases) in order to determine the conformation and structure of the Acacia senegal gum. The research were performed by HPSEC method coupled with 3 detectors (MALLS-RI-VISC). The use of triple detection allowed to go deeper insight into the structure of these two main fractions and examine molecular associations of structural units, covalent linkages and/or hydrophobic associations, formation of the AGP macromolecular assemblies (using hydrogen bondings) [Renard et al 2014].

Nevertheless, to fully understand the mechanism of enzymatic hydrolysis the researchers have to used another methods (e.g. XRD, HPLC, CD,SANS) besides SEC-MALS analysis.

2.1. Principle of the SEC method

Size exclusion chromatography is a type of high performance liquid chromatography (HPLC). This method separates molecules based on their size using columns packed with small, round, porous particles e.g. spherical silicas, cross-linked polymers or rigid inorganic packing particles [Kostanski et al. 2004]. The most important conditions in SEC analysis are: sample dissolution (the use of polar organic solvents with lithium salts is suitable for starch and cellulose dissolution), absence of chains interaction with the stationary phase (no adsorption, interaction could provide a complex and specious separation) and degradation (polymers with ultrahigh molecular weight could be degradated by shearing during separation process). However, optimal injection concentration is necessary [Gaborieau and Castignolles 2011]. The separating mechanism of different sizes molecules is shown in Figure 1.

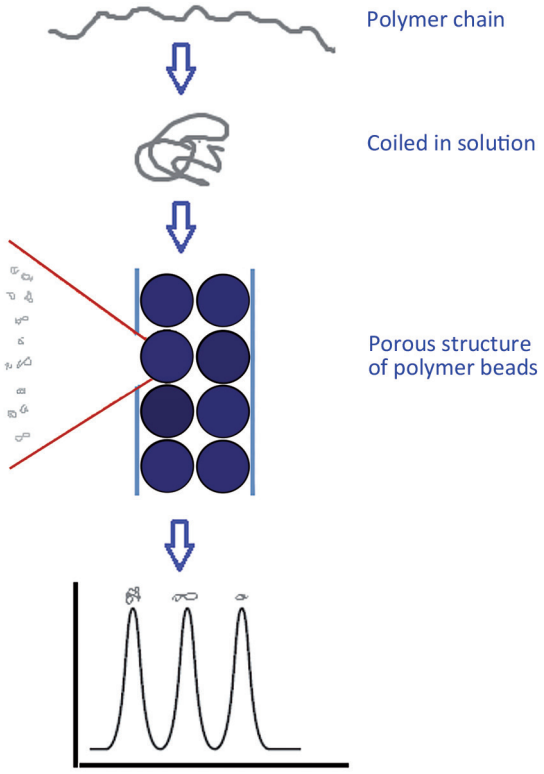

Fig. 1. Principle of the SEC method (source: based on: An Introduction to Gel Permeation Chromatography and Size Exclusion Chromatography, Agilent Technologies, Inc.)

Dissolved polymer molecules (coils) are carried in a column through the mobile phase. The size of the pores in the beads is important to pass sample through the column. Small polymer coils could enter many pores in the beads and it takes them a long time to leave the column. Larger polymer coils cannot enter the pores and consequently are carried by the mobile phase without entering the pores. Therefore, large coils have shorter retention time in the pores than smaller ones and they are eluted from the column faster [Kostanski et al. 2004]. Nevertheless, intermediate polymer molecules eluate from the column between small and big coils. SEC results give information regarding the size of polymer molecules in solution. Obtained data are converted into molecular weights through the calibration.

2.2. Detector calibration

The calibration constant for the refractive index detector (RI) was determined by injecting five known concentrations of aqueous sodium chloride solution (0.05–0.50 mg/mL) into the detector. The Rical 2 software (Wyatt Technology, Santa Barbara CA, USA) collected the output voltage from the detector and the calibration constant was calculated from the slope of the graph of $\Delta n = c\ dn/dc\ vs$ voltages. Calculation of M_w and R_g of pullulan, dextran and starch were used the *dn/dc* values of 0.148, 0.142 and 0.146, respectively.

Laser light scattering detector (LS) calibration constant for the diode at 90° was determined with the LS intensity of toluene. BSA (*bovine serum albumin)* was used to normalization of the responses of photodiodes arranged around the scattering cell to the diode at 90°.

Recovery of injected standards was over 95% and the determined M_w values were 9.9×10^5 for pullulan P-100, 6.2×10^5 for dextran D-580 and 2.0×10^6 for dextran D-2000. Obtained M_w values for standards were in line to those given by the manufacturer [Fiedorowicz et al. 1999; Fiedorowicz et al. 2001; Fiedorowicz and Chaczatrian 2004].

2.3. Determination of molecular weight (M_w) and radii of gyration (R_g) with HPSEC-MALLS-RI methods

The method of determining molecular weight using HPSEC – MALLS – RI has been successfully used in recent years to calculate the molecular weights of polymers. Aberle et al. [1994] described the theory and principle of MALLS analysis. In this method, the eluate flowing from the gel column containing polymer parti-

cles is introduced into a laser light scattering detector. The laser light is scattered on the polymer molecules present in the solution. The detector used in the present study (DAWN DSP-F) provides up to 18 laser light scattering chromatograms, each taken at a different angle to the incident beam. An additional chromatogram is provided by the RI detector. The software used (Astra 4.73.04) divides the area under the chromatogram line into small sections. Each section corresponds to a small volume of eluate leaving the column (750 μL). If the light intensity scattered by the polymer at a given angle Θ is known, as well as its concentration in a given volume, the mean radii of gyration and the average molecular weight of the polymer can be calculated from following Eq. 1:

$$(R_\Theta/K^*c)_i = M_i - 16\,\Pi^2/3\,\lambda^2\,R_{gi}^2\,M_i\sin^2(\Theta/2) \tag{1}$$

where:

R_Θ – the excess Rayleigh ratio of the solute under angle Θ;
K^* – instrumental optical constant;
λ – the wavelength of the incident laser beam.

R_Θ was defined by Eq. 2:

$$R_\Theta = f(I_s/I_0) \tag{2}$$

where:

f – geometrical constant;
I_s – intensity of scattered light.
I_0 – intensity of incident light.

Instrumental constant K^* could be calculated from the following Eq. 3:

$$K^* = 4\Pi^2\,n_0^2(dn/dc)^2/\lambda^4\,N_A \tag{3}$$

where:

n_0 – the index of refraction of the solvent,
N_A – Avogadro's number,
dn/dc – the differencial refractive index increment of the polymer.

According to Eq. 1, by plotting the dependence ($R\Theta$ / $K\,c$) and on $\sin^2(\Theta/2)$ on the basis of the slope of the line and its point of intersection with the Y axis, the values of R_g and M_w for the polymer molecules eluted in a given small volume of eluate will be obtained. Such a plot is called a Debey plot. R_g and M_w values can also be obtained from the Zimm ($K^*\,c\,/\,R_\Theta$ vs $\sin^2(\Theta/2)$) and Berry (vs $\sin^2(\Theta/2)$) plots. The average values of M_w and R_g for the entire chromatogram are

obtained by summing up the values obtained for the selected small volumes. Literature data shows that for polymers with very high molecular weights the most accurate results for both R_g and M_w are obtained using the Berry plot [Aberle et al. 1994; Hanselmann et al. 1995]. In our studies the Debye plot for eluted polysaccharides was expressed by the Berry metod using a 3rd order polynomial fit to take care of a curvature at the low angles [Aberle et al. 1994; Bello-Perez et al. 1996].

2.4. Differential weight fraction

Differential weight fraction is defined as a mass share of the sample containing molecules of M_w constituting given fraction in relation to the total mass of the sample. [Fiedorowicz et al. 2001; Fiedorowicz and Chaczatrian 2004; Khachatryan et al. 2014].

It is available from the Schrott Eq. (4) [Schrott 1993]:

$$x(M) = \frac{dW(M)}{d(\log M)} = \frac{-h(V)}{f(V)} \tag{4}$$

where:
$h(V)$ is a normalized polymer concentration in a given volume V, and $f(V) = \mathrm{d}(\log M)/dV$ is available from the slope of the calibration curve for the LS detector, $h(V)$ is estimated from Eq. (5):

$$(V) = c_i / \Sigma c_i \, \Delta V \tag{5}$$

where:
c_i denotes concentration in a ΔV volume of the eluate.

2.5. HPSEC-MALLS-RI apparatus

The chromatograph consisted of a pump (Ultimate 3000, Dionex, Palo Alto, California, USA), an injection valve (model 7021, Rheodyne, Palo Alto, California, USA), a precolumn (TSK PWH, Tosoh, Tokyo, Japan), two columns (TSKgel GMPWXL (300 × 7.8 mm, Tosoh) and a TSKgel 2500 PWXL (300 × 7.8 mm, Tosoh). Dawn-DSP-F (Wyatt, Santa Barbara CA, USA) and refractometric (model SE71, Shodex, Tokyo, Japan) multi-angle laser light scattering (MALLS) detec-

tors were connected to the columns [Fiedorowicz et al. 2001]. The columns were kept at 40°C and the RI detector at 35°C. A 0.15 M $NaNO_3$ solution and a 0.02% NaN_3 solution constituted the mobile phase. The HPSEC-MALLS-RI system is presented in Figure 2.

For the calculations of M_w and R_g it was assumed that *dn/dc* (refractive index change depending on the concentration change) = 0.146. The flow rate of the mobile phase and the injection volume of the sample were 0.4 cm^3 min^{-1} and

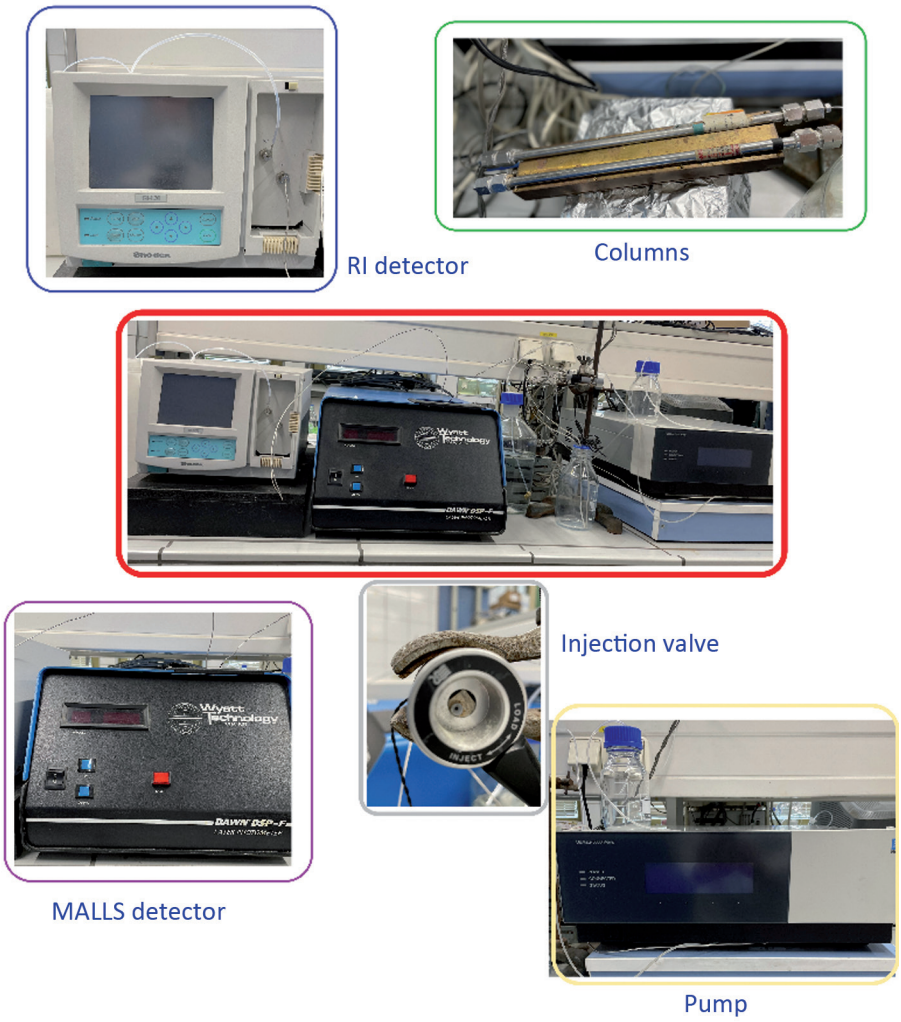

Fig. 2. HPSEC-MALLS-RI apparatus (source: own photo)

500 µl, respectively. The data obtained from the RI and MALLS detectors were used to calculate the mean molecular weight (M_w) and gyration radii (R_g) using the Astra 4.73.04 program (Wyatt Technology, Santa Barbara CA, USA). A Berry plot with a third order polynomial fit was used to calculate the M_w and R_g values [Bello-Pérez et al. 1996].

2.5.1. Sample preparation for HPSEC – starch polysaccharide molecules

Dissolution and SEC analysis in DMSO have been widely used for more than 25 years. Researchers have observed that DMSO with 5–10% H_2O (wet DMSO) was making the starch granules swell faster than dry DMSO [Gaborieau and Castignolles 2011].

The solutions to be measured were obtained by adding the appropriate starch to a volumetric flask containing water. The contents were gently mixed with a magnetic stirrer to moisten and disperse the starch granules. With continued stirring, dimethyl sulfoxide (DMSO) was added and the temperature was gradually increased to 80°C while continually stirring until clear solutions were obtained. After the solution had cooled to 25°C, the flask was filled with DMSO to a final volume. Prior to HPSEC injection, the solution was filtered through a 0.8 µm filter (Whatman, England).

2.5.2. Sample chromatogram – starch

Molecular structure of branched polymers, like starch, are characterized by distribution of molecular weight of the polymer chains and branches, topology and degree of branching. In this study, the HPSEC-MALLS-RI technique was used to determine the molecular weights and radii of gyration of polymer chains. This method allowed us to determine the molecular weights of the polysaccharides included in the amylopectin fraction. The chromatogram for starch taken with both, the LS detector diode at a 90° angle and RI detector, are presented in Figure 3.

Based on the shape, the chromatograms were divided arbitrarily into two regions corresponding to the amylopectin (I) and amylose (II) fractions, respectively. Analysis, with the Astra software, of the superimposed chromatograms allowed for molar mass distribution for the whole complex peak of the eluate and for each of its regions.

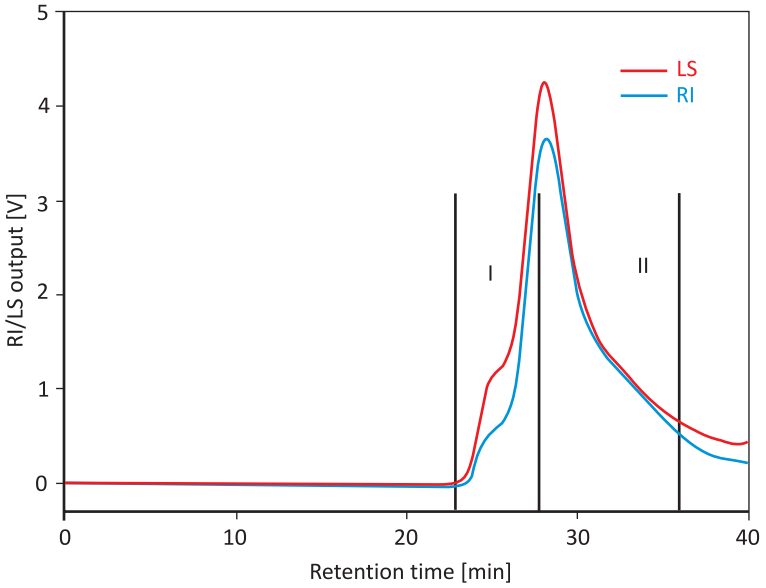

Fig. 3. Superimposed chromatograms of RI and LS detector outputs for native spelt starch eluted from SEC columns (source: Nowak – unpublished data)

2.5.3. Differential weight fraction – sample

HPSEC is used to determine the molecular weight distributions of polymers. Based on the data provided by the LS and RI detectors, the Astra software provided the calculation of the differential molecular weight distributions for the polymer molecules eluted from the column.

We presented a differential weight fraction of spelt starches, native and modified physically (illuminated). Diagrams of differential weight fraction vs. M_w for the examined samples are given in Figure 4.

Native starch polysaccharides exhibited much broader molecular weight distribution than polysaccharide chains originating from modified samples. From the chromatogram presented above it can be concluded that the modification for 15 hours leads to the formation of chains starch polysaccharides with the lowest polydispersity (highest homogeneity). Physical modification (illumination) of spelt starch results in a lower polydispersion of molecular weight values compared to native starch. Illumination for 5 hours led to a slight decrease in the M_w of molecules. Further modification (15 hours) exhibited a narrow M_w distribution and a considerable increase in molecular weight of eluted polysaccharide chains. At the same time, a significant decrease in the dispersity of the eluted molecules

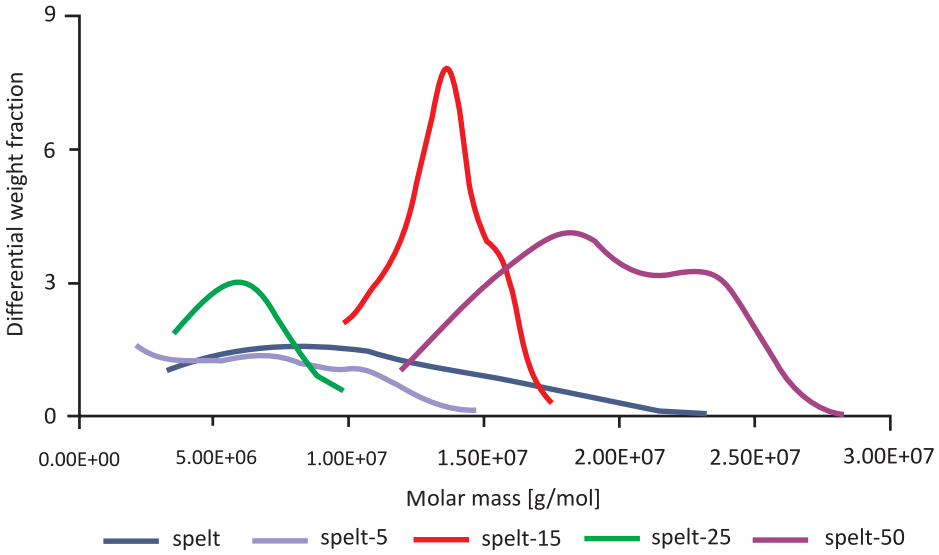

Fig. 4. Plots of differential weight fraction vs molar mass for native and illuminated for 5 h, 15 h, 25 h and 50 h spelt starches (source: Nowak – unpublished data)

was observed. Further illumination up to 25 h and 50 h provided subsequent changes in molecular weights and polydispersity of molecules eluted from the starch samples. It is worthy to note that the 25-hour illumination changed significantly the values of the average molecular weights. However, the polysaccharide chains eluted from a 50-hour illuminated sample presented a much wider range of M_w distribution compared to the molecules eluted from starch illuminated for 25 hours. Nevertheless, prolonged modification provided widely increased M_w parameters as well as the dispersity of the sample.

3. Advantages of using HPSEC methods for different starches

The main application of HPSEC methods is the determination of polymers molecular weight (M_w). In this work we have presented the results of use multiple-detection SEC (MALLS-RI) to determine the average molecular mass of polysaccharide chains of starches of various origins. Starch is one the most abundant and complex branched polymer to characterize. Amylose and amylopectin are different in terms of the branch content. Amylopectin is highly branched (con-

tains many clusters of short chains) while amylose has only a few branches [Gaborieau and Castignolles 2011]. This technique is also widely used for determination of amylopectin chains length distribution. Molecular structure (e.g. M_w) affects functional properties of starch and hence determine its applications. Food industries utilize starch as gelling agents, thickeners, emulsifiers and encapsulating agents.

Selected molecular weights and radius of gyration of different starches obtained with HPSEC-MALLS-RI method are summarized in Table 2.

Using HPSEC-MALLS-RI system and other methods described above, it is possible to measure average molar mass and radius of gyration of solubilized polymers. The solubilisation of starch is necessary and depends on the method and solvent used in procedure [Bello-Perez et al. 2019].

Literature reports on molecular weight distributions (M_w) for starches of various botanical origin indicate that the starch solubilisation method and the method for determining average molecular weights have a large influence on these values. A study by Fishman et al. [1996] on native and waxy maize starch solubilised by heating in a microwave indicated values of 15×10^6 and 26×10^6 g/mol, respectively. Depending on the determination method used, the molecular weight measurement for waxy maize starch as tested by Klavons et al. [1997] was 412×10^6 and 224×10^6 g/mol. Using the HPSEC-MALLS-RI method, Fiedorowicz et al. [1999] determined the molecular weight values of native and irradiated aerobic and anaerobic corn starch (30% w/w) solubilised in a base solution. The values of molecular weights and radii of gyration were respectively 41.1×10^6 g/mol and 185.5 nm for native corn starch. Bello-Perez et al. [2019] studies showed that HPSEC-MALLS-RI and AF4 techniques are accurate to characterization of different maize starch structure. Their concluded that estimated results (M_w, R_g, apparent particle density) obtained with SEC method were in line with the literature data. Different values were observed for AF4 system. Authors confirmed that the HPSEC-MALLS-RI is the right strategy for the accurate characterization of starch structure.

According to the literature data [Zhu 2017], the molecular mass of amaranth (amylopectin fraction) varies from $1 - 70 \times 10^7$ [g/mol]. Author proposes that M_w depends on the dissolving conditions and instrumentation used. Research carried out by Nowak et al. [2021] showed that average M_w of amaranth polysaccharide chains is 4.51×10^7 g/mol. Similar value was provided by Zhu [2017].

Nevertheless, Bello-Perez et al. [2018] studies suggests that the molecular structure of amaranth amylopectin vary based on its diverse botanical origin. They concluded that amylopectin from translucent and opaque perisperm had a different molecular weight (6.2×10^7 g/mol and 7.0×10^7 g/mol, respectively).

Table 2. The M_w (g/mol) and R_g values of different starches (source: own elaboration)

Sample	M_w x 10^7 [g/mol] Whole peak	R_g [nm] Whole peak	References
Hylon V	0.646	69.7	Khachatryan et al. [2014]
	5.4	152.0	Bello-Perez et al. [2019]
Hylon VII	0.125	31.8	Khachatryan et al. [2014]
Cassava	42.00	NR	Bertolini et al. [2001]
	13.00	186.0	Tetchi et al. [2007]
	2.19	NR	Xia et al. [2017]
Waxy corn	9.43	NR	Fiedorowicz et al. [2004]
	25.0	232.0	Bello-Perez et al. [2019]
Spelt	0.820	66.8	Nowak et al. [2014]
Normal maize	18.0	209.0	Tetchi et al. [2007]
	14.0	203.0	Bello-Perez et al. [2019]
Wheat	2.31	77.4	Nowak et al. [2014]
	16.8	NR	Guo et al. [2020]
	16.39	242.9	Yang et al. [2020]
	17.80	205.0	Tetchi et al. [2007]
Potato	12.30	NR	Fiedorowicz [2004]
	18.7	NR	Guo et al. [2020]
	9.40	178.0	Tetchi et al. [2007]
Corn	4.11	185.5	Fiedorowicz et al. [1999]
	14.2	NR	Guo et al. [2020]
	13.40	NR	Fiedorowicz et al. [2001]
Amaranth	4.51	146.7	Nowak et al. [2021]

NR – not reported

The HPSEC-MALLS-RI method is successfully applied to analyze the structure of modified starch polysaccharide chains. Some of the authors [Fiedorowicz et al. 2001; Fiedorowicz and Chaczatrian 2004; Khachatryan et al. 2014; Nowak et al. 2021] did a research on modified starch with electromagnetic radiation. The authors measured the M_w of the starch fractions both, native and illuminated. This method allows the determination of changes in the molecu-

lar structure of amylose and amylopectin fractions. For instance, Khachatryan et al. [2014] studied the effect of illumination with linearly polarised visible light on high-amylose starches (Hylon V and Hylon VII). Fiedorowicz et al. [1999] conducted a research based on UV-illumination of corn starches. The authors found a higher M_w values for the corn starch amylopectin fraction after increasing time of exposure. On the other hand, the studies of Bertolini et al. [2001] shows that the molecular weight values of corn amylopectin decrease with increasing UV exposure time. The authors also investigated the effect of UV light on the molecular structure of starch using the size exclusion chromatography method with dual detection (SEC-MALLS-RI).

According to the literature HPSEC-MALLS-RI system could be used to determine the molecular weight and radii of gyration of nanocomposites [Khachatryan et al. 2015; Khachatryan et al. 2016a]. The reasearchers generated quantum dots (QDs), core shell nanocrystals or nanoparticles (nanosilver and nanogold) in different starch matrix. Measurement of M_w and R_g of the polysaccharide chains from the nanocomposites samples showed that the generation of QDs within the amylopectin starch fraction was favored [Khachatryan et al. 2015]. The estimation of average molecular weights of composites with nanometals using the SEC method led to interesting conclusions. The authors proposed that formation of nanosilver in tapioca starch matrix led to partial degradation of amylose molecules. The resulting short amylose chains were attached to the amylopectin fraction. This was reflected in an increase in the molecular weight of the amylopectin macromolecules. However, synthesis of gold nanoparticles induced depolymerisation of polysaccharide chains from amylose and amylopectin fractions [Khachatryan et al. 2016a].

4. Conclusion

Determination of molecular structure of biopolymers chains (M_w, R_g) is one of the most important factors in food industry. This structure influences functional properties of foods. Despite of the availability of various methods, size-exclusion chromatography (SEC) coupled with molar-mass-sensitive detector and concentration sensitive detector is generally used to define these parameters. One of the main features of HPSEC-MALLS-RI is the possibility to measure high-molar masses fractions. Differential weight fraction of biopolymers and their composites influence functional parameters such as intrinsic viscosity or susceptibility for hydrolysis by α-amylase.

Generally, literature data indicates that SEC technique is the most frequently used method for polysaccharides molecular structure determination. This method could be used in the future for determination of the molecular structure parameters of new composites and nanocomposites used in special-purpose products.

References

Aberle T., Burchard W., Vorwerg W., Radosta S. 1994. Conformational contributions of amylose and amylopectin to the structural properties of starches from various sources. Starch/Stärke, 46, 329–335. https://doi.org/10.1002/star.19940460903

An Introduction to Gel Permeation Chromatography and Size Exclusion Chromatography 2015. Agilent Technologies, Inc., Printed in US, 5990-6969EN.

Bello-Perez L.A., Paredes-Lopez O., Roger P., Colonna P. 1996. Amylopectin – properties and fine structure. Food Chemistry, 56, 171–176. https://doi.org/10.1016/0308-8146(95)00152-2

Bello-Perez L.A., Roger P., Baud B., Colonna P. 1998. Macromolecular features of starches determined by aqueous high-performance size exclusion chromatography. Journal of Cereal Science, 27, 267–278. https://doi.org/10.1006/jcrs.1998.0186

Bello-Perez L.A., Rodriguez-Ambriz S.L., Hoyos-Leyva J.D., Agama-Acevedo E., Pacheco--Vargas G., Alvarez-Ramirez J. 2018. Characteristics of starch from opaque and translucent perisperm of amaranth (A. hypochondriacus) grains. Starch/Starke, 70(11), 1700260. https://doi.org/10.1002/star.201700260

Bello-Perez L.A., Agama-Acevedo E., Lopez-Silva M., Alvarez-Ramirez J. 2019. Molecular characterization of corn starches by HPSEC-MALS-RI: A comparison with AF4 MALS-RI system. Food Hydrocolloids, 96, 373–376. https://doi.org/10.1016/j.foodhyd.2019.04.067

Bertoft E. 2007. Composition of clusters and their arrangement in potato amylopectin. Carbohydrate Polymers, 68, 3, 433–446. https://doi.org/10.1016/j.carbpol.2006.11.012

Bertoft E., Laohaphatanalert K., Piyachomkwan K., Sriroth K. 2010. The fine structure of cassava starch amylopectin. Part 2: Building block structure of clusters. International Journal of Biological Macromolecules, 47, 325–335. https://doi.org/10.1016/j.ijbiomac.2010.05.018

Bertolini A.C., Mestres C., Raffi J., Buleon A., Lerner D., Colonna P. 2001. Photodegradation of cassava and corn starches. Journal of Agricultural and Food Chemistry, 49, 675–682. https://doi.org/10.1021/jf0010174

Blennow A., Engelsen S.B., Munck L., Møller B.L. 2000. Starch molecular structure and phosphorylation investigated by a combined chromatographic and chemometric approach. Carbohydrate Polymers, 41, 163–174. https://doi.org/10.1016/S0144-8617(99)00082-X

Cateto C., Hu G., Ragauskas A. 2011. Enzymatic hydrolysis of Organosolv Kanlow switchgrass and its impact on cellulose crystallinity and degree of polymerization. Energy & Environmental Science, 4, 4, 1516–1521.

Chen X.Y., Xu X.J., Zhang L., Kennedy J.F. 2009. Flexible chain conformation of (1,3)-beta--D-glucan from Poria cocos sclerotium in NaOH/urea aqueous solution. Carbohydrate Polymers, 75, 586–591. https://doi.org/10.1016/j.carbpol.2008.08.027

Chen Y.W., Hu D.J., Cheong K.L., Li J., Xie J., Zhao J., Li S.P. 2013. Quality evaluation of lentinan injection produced in China. Journal of Pharmaceutical and Biomedical Analysis, 78–79, 176–182. https://doi.org/10.1016/j.jpba.2013.02.012

Dervilly G., Saulnier L., Roger P., Thibault J.F. 2000. Isolation of homogeneous fractions from wheat water-soluble arabinoxylans. Influence of the structure on their macromolecular characteristics. Journal of Agricultural and Food Chemistry, 48, 270–278. https://doi.org/10.1021/jf990222k

Du R., Huang R., Su R., Zhang M., Wang M., Yang J., Qi W., He Z. 2013. Enzymatic hydrolysis of lignocellulose: SEC-MALLS analysis and reaction mechanism. RSC Advances, 3, 1871–1877. https://doi.org/10.1039/C2RA21781C

Fiedorowicz M., Tomasik P., You S., Lim S.T. 1999. Molecular distribution and pasting properties of UV-irradiated corn starches. Starch/Starke, 51, 126–131. https://doi.org/10.1002/(SICI)1521-379X(199904)51:4<126::AID-STAR126>3.0.CO;2-N

Fiedorowicz M., Tomasik P., Lii C.Y. 2001. Degradation of starch by polarized light. Carbohydrate Polymers, 45, 79–87. https://doi.org/10.1016/S0144-8617(00)00238-1

Fiedorowicz M., Chaczatrian G. 2004. Selected functional properties of waxy corn and potato starches after illumination with linearly polarized visible light. Journal of the Science of Food Agriculture, 84, 1, 36–42. https://doi.org/10.1002/jsfa.1601

Fishman M.L., Rodriguez L., Chau K.H. 1996. Molar masses and sizes of starches by high performance size exclusion chromatography with on-line multi angle laser light scattering detection. Journal of Agricultural and Food Chemistry, 44, 3182. https://doi.org/10.1021/jf9600162

Gaborieau M., Castignolles P. 2011. Size-exclusion chromatography (SEC) of branched polymers and polysaccharides. Analytical & Bioanalytical Chemistry, 399, 1413–1423. https://doi.org/10.1007/s00216-010-4221-7

Guo L., Li J., Gui Y., Zhua Y., Yua B., Tana C., Fanga Y., Cui B. 2020. Porous starches modified with double enzymes: Structure and adsorption properties. International Journal of Biological Macromolecules, 164, 1758–1765. https://doi.org/10.1016/j.ijbiomac.2020.07.323

Hanashiro I., Abe J.I., Hizukuri S. 1996. A periodic distribution of the chain length of amylopectin as revealed by high-performance anion-exchange chromatography. Carbohydrate Research, 283, 151–159. https://doi.org/10.1016/0008-6215(95)00408-4

Hanselmann R., Ehrat M., Widmer H.M. 1995. Sedimentation field flow fractionation combined with multi angle laser light scattering applied for characterization of starch polymers. Starch/Stärke, 46, 345–349. https://doi.org/10.1002/star.19950470905

Harmon P.S., Maziar E.P., Liu X.M. 2012. Detailed characterization of hyaluronan using aqueous size exclusion chromatography with triple detection and multiangle light scattering detection. Journal of Biomedical Materials Research B: Applied Biomaterials, 100B, 7, 1955–1960. https://doi.org/10.1002/jbm.b.32762

Hoyos-Leyva J.D., Bello-Pérez L.A., Alvarez-Ramirez J., Agama-Acevedo E. 2017. Structural characterization of aroid starches by means of chromatographic techniques. Food Hydrocolloids, 69, 97–102. https://doi.org/10.1016/j.foodhyd.2017.01.034

Júnior E.H., Gonçalves A.G., Noseda M.D., Duarte M.E.R., Murakami F.S., Ducatti D.R.B. 2021. Semi-synthesis of N-alkyl-kappa-carrageenan derivatives and evaluation of their antibacterial activity. Carbohydrate Research, 499, 108234. https://doi.org/10.1016/j.carres.2021.108234

Khachatryan G., Krzeminska-Fiedorowicz L., Nowak E., Fiedorowicz M. 2014. Molecular structure and physicochemical properties of Hylon V and Hylon VII starches illuminated with linearly polarised visible light. LWT – Food Science and Technology, 58, 256–262. https://doi.org/10.1016/j.lwt.2014.02.020

Khachatryan K., Khachatryan G., Fiedorowicz M. 2016a. Silver and gold nanoparticles embedded in potato starch gel films. Journal of Materials Science and Chemical Engineering, 4, 22–31. https://doi.org/10.4236/msce.2016.42003

Khachatryan K., Khachatryan G., Fiedorowicz M. 2015. Synthesis of ZnS, CdS and core-shell mixed CdS/ZnS, ZnS/CdS nanocrystals in tapioca starch matrix. Journal of Materials Science and Chemical Engineering, 3, 30–38. https://doi.org/10.4236/msce.2015.311005

Khachatryan K., Khachatryan G., Grzyb J., Fiedorowicz M. 2016b. Formation and properties of hyaluronan/nano Ag and hyaluronan-lecithin/nano Ag films. Carbohydrate Polymers, 151, 452–457. https://doi.org/10.1016/j.carbpol.2016.05.104

Kilz P., Pasch H. 2000. Coupled liquid chromatographic techniques in molecular characterization. [In:] Encyclopedia of Analytical Chemistry. Ed. R.A. Meyers. John Wiley & Sons, Ltd, Chichester, 7495–7543.

Klavons J.A., Dintzis F.R., Millard M.M. 1997. Hydrodynamic chromatography of waxy maize starch. Cereal Chemistry, 74, 832. https://doi.org/10.1094/CCHEM.1997.74.6.832

Kostanski J.K., Keller D., Hamielec A.E. 2004. Size-exclusion chromatography – A review of calibration methodologies. Journal of Biochemical and Biophysical Methods, 58(2), 159–186. https://doi.org/10.1016/j.jbbm.2003.10.001

Lee S., Nilsson P.O., Nilsson G.S., Wahlund K.G. 2003. Development of asymmetrical flow field-flow fractionation–multi angle laser light scattering analysis for molecular mass characterization of cationic potato amylopectin. Journal of Chromatography A, 1011, 111–123. https://doi.org/10.1016/s0021-9673(03)01144-0

Li W.J., Fan Z.G., Wu Y.Y, Jianga Z.G., Shia R.Ch. 2019. Eco-friendly extraction and physicochemical properties of pectin from jackfruit peel waste with subcritical water. Journal of the Science of Food and Agriculture, 99, 5283–5292. https://doi.org/10.1002/jsfa.9729

Liu X.M., Gao W., Maziarz E.P., Salamone J.C., Duex J., Xia E. 2006. Detailed characterization of cationic hydroxyethylcellulose derivatives using aqueous size-exclusion chromatography with on-line triple detection. Journal of Chromatography A, 1104, 1–2, 145–153. https://doi.org/10.1016/j.chroma.2005.11.094

Ma Z.C., Wang J.G., Zhang L.N. 2008. Structure and chain conformation of ss-glucan isolated from Auricularia auricula-judae. Biopolymers, 89, 614–622. https://doi.org/10.1002/bip.20971

Minton A.P. 2016. Recent applications of light scattering measurement in the biological and biopharmaceutical sciences. Analytical Biochemistry, 501, 4–22. https://doi.org/10.1016/j.ab.2016.02.007

Nettleship J.E., Brown J., Groves M.R., Geerlof A. 2008. Methods for protein characterization by mass spectrometry, thermal shift (ThermoFluor) assay, and multiangle or static light scattering. Methods in Molecular Biology, 426, 299–318. https://doi.org/10.1007/978-1-60327-058-8_19

Nishinari K., Fang Y. 2020. Molar mass effect in food and health. Food Hydrocolloids, 122, 106110. https://doi.org/10.1016/j.foodhyd.2020.106110

Nowak E., Krzeminska-Fiedorowicz L., Khachatryan G., Fiedorowicz M. 2014. Comparison of molecular structure and selected Physicochemical properties of spelt wheat and common wheat starches. Journal of Food And Nutrition Research, 53(1), 31–38.

Nowak E., Wisła-Świder A., Khachatryan G., Fiedorowicz M., Danel K. 2019. Possible sensor applications of selected DNA-surfactant complexes. European Biophysics Journal, 48, 371–381. https://doi.org/10.1007/s00249-019-01367-2

Nowak E., Khachatryan G., Wisła-Świder A. 2021. Structural changes of different starches illuminated with linearly polarised visible light. Food Chemistry, 344, 128693. https://doi.org/10.1016/j.foodchem.2020.128693

Ottøy M.H., Vårum K.M., Christensen B.E., Anthonsen M.W., Smidsrød O. 1996. Preparative and analytical size-exclusion chromatography of chitosans. Carbohydrate Polymers, 31, 253–261. https://doi.org/10.1016/S0144-8617(96)00096-3

Pascotto K., Cheynier V., Williams P., Geffroy O., Violleau F. 2020. Fractionation and characterization of polyphenolic compounds and macromolecules in red wine by asymmetrical flow field-flow fractionation. Journal of Chromatography A, 1629, 461464. https://doi.org/10.1016/j.chroma.2020.461464

Porsch B., Laga R., Horský J., Koňák Č., Ulbrich K. 2009. Molecular weight and polydispersity of calf-thymus DNA: Static light-scattering and size-exclusion chromatography with dual detection. Biomacromolecules, 10(11), 3148–3150. https://doi.org/10.1021/bm900768j

Reichembach L.H., de Oliveira Petkowicz C.L. 2020. Extraction and characterization of a pectin from coffee (Coffea arabica L.) pulp with gelling properties. Carbohydrate Polymers, 245, 116473. https://doi.org/10.1016/j.carbpol.2020.116473

Renard D., Lavenant-Gourgon L., Lapp A., Nigen M., Sanchez Ch. 2014. Enzymatic hydrolysis studies of arabinogalactan-protein structure from Acacia gum: the self-similarity

hypothesis of assembly from a common building block. Carbohydrate Polymers, 112, 648–661. https://doi.org/10.1016/j.carbpol.2014.06.041

Rolland-Sabate A., Colonna P., Mendez-Montealvo M.G., Planchot V. 2007. Branching features of amylopectins and glycogen determined by asymmetrical flow field flow fractionation coupled with multiangle laser light scattering. Biomacromolecules, 8, 2520–2532. https://doi.org/10.1021/bm070024z

Sahin E., Roberts C.J. 2012. Size-exclusion chromatography with multi-angle light scattering for elucidating protein aggregation mechanisms. [In:] Therapeutic Proteins. Methods in Molecular Biology (Methods and Protocols). Eds. V. Voynov, J. Caravella. Humana Press, Totowa, NJ, 403–423. https://doi.org/10.1007/978-1-61779-921-1_25

Sanderson J.S, Daniels R.D., Donald A.M., Blennow A., Søren B., Engelsen S.B. 2006. Exploratory SAXS and HPAEC-PAD studies of starches from diverse plant genotypes. Carbohydrate Polymers, 64, 433–443. https://doi.org/10.1016/j.carbpol.2005.12.026

Schrott D.W. 1993. Differential molecular weight distributions in high performance size exclusion chromatography. Journal of Liquid Chromatography, 16, 3371–3391. https://doi.org/10.1080/10826079308019695

Tetchi F.A., Rolland-Sabate A., N'Guessan Amani G., Colonna P. 2007. Molecular and physicochemical characterisation of starches from yam, cocoyam, cassava, sweet potato and ginger produced in the Ivory Coast. Journal of the Science of Food and Agriculture, 87, 1906–1916. https://doi.org/10.1002/jsfa.2928

Villas-Boas F., Yamauti Y., Moretti M.M.S., Franco C.M.L. 2019. Influence of molecular structure on the susceptibility of starch to α-amylase. Carbohydrate Research, 479, 23–30. https://doi.org/10.1016/j.carres.2019.05.001

Villas-Boas F., Facchinatto W.M., Colnago L.A., Volanti D.P., Landi Franco C.M. 2020. Effect of amylolysis on the formation, the molecular, crystalline and thermal characteristics and the digestibility of retrograded starches. International Journal of Biological Macromolecules, 163, 1333–1343. https://doi.org/10.1016/j.ijbiomac.2020.07.181

Wyatt P.J. 1993. Light scattering and the absolute characterization of macromolecules. Analytica Chimica Acta, 272, 1–40. https://doi.org/10.1016/0003-2670(93)80373-S

Xia H., Li B.Z., Gao Q. 2017. Effect of molecular weight of starch on the properties of cassava starch microspheres prepared in aqueous two-phase system. Carbohydrate Polymers, 177, 334–340. https://doi.org/10.1016/j.carbpol.2017.08.074

Yang Y., Li T., Li Y., Qiana H., Qia X., Zhanga H., Wang L. 2020. Understanding the molecular weight distribution, in vitro digestibility and rheological properties of the deep-fried wheat starch. Food Chemistry, 331, 127315. https://doi.org/10.1016/j.foodchem.2020.127315

Ye J., Hua X,. Lyu X., Zhao W., Zhang W., Yang R. 2021. Structure and chain conformation characterization of arabinoglucan from by-product of peanut oil processing. Carbohydrate Polymers, 255, 117327. https://doi.org/10.1016/j.carbpol.2020.117327

Zhang M., Su R., Qi W., Du R., He Z. 2011. Enzymatic hydrolysis of cellulose with different crystallinities studied by means of SEC-MALLS. Chinese Journal of Chemical Engineering, 19, 5, 773–778.

Zhang H., Li C., Lai P.F.H, Chen J., Xie F., Xia Y., Ai L. 2021. Fractionation, chemical characterization and immunostimulatory activity of β-glucan and galactoglucan from Russula vinosa Lindblad. Carbohydrate Polymers, 256, 117559. https://doi.org/10.1016/j.carbpol.2020.117559

Zhao X., Andersson M., Andersson R. 2021. A simplified method of determining the internal structure of amylopectin from barley starch without amylopectin isolation. Carbohydrate Polymers, 255, 117503. https://doi.org/10.1016/j.carbpol.2020.117503

Zhou W.B., Bi J.X., Janson J.C., Li Y., Huang Y.D., Zhang Y., Su Z.G. 2006. Molecular characterization of recombinant Hepatitis B surface antigen from Chinese hamster ovary and Hansenula polymorpha cells by high-performance size exclusion chromatography and multi-angle laser light scattering. Journal of Chromatography B, 838, 71–77. https://doi.org/10.1016/j.jchromb.2006.03.064

Zhu F. 2017. Structures, physicochemical properties, and applications of amaranth starch. Critical Reviews in Food Science and Nutrition, 57(2), 313–325. https://doi.org/10.1080/10408398.2013.862784

III APPLICATION OF SIZE EXCLUSION CHROMATOGRAPHY (SEC) IN THE ANALYSIS OF POLYSACCHARIDES

Krzysztof BUKSA

Department of Carbohydrate Technology and Cereal Processing,
Faculty of Food Technology, University of Agriculture in Krakow,
Aleja Mickiewicza 21, 31-120 Krakow, Poland

krzysztof.buksa@urk.edu.pl
ORCID: https://orcid.org/0000-0002-2509-5881

Abstract. An overview of the application of size exclusion chromatography (SEC) in the analysis of polysaccharides in foods is presented. The most important issues regarding sample preparation and possibilities of application of post-column derivatization for detection of polysaccharides in complex samples are demonstrated. SEC is an important separation technique used to separate molecules such as polysaccharides based on size and shape (hydrodynamic radius), however, sample preparation is crucial to obtain robust and useful data. In the case of complex samples containing more than one kind of polysaccharide, what usually takes place in polysaccharides obtained from plant material, application of even the state-of-the-art detection systems is of limited use. In such a case, a solution could be the application of post-column derivatization and selective detection of derivatized polysaccharides. The techniques highlighted in this work are still developing and could be a very useful tool for the investigation of transformations and interactions of polysaccharides in food products during processing.

Keywords: size exclusion chromatography, gel filtration chromatography, polysaccharide

1. Introduction

Size exclusion chromatography (SEC) is a technique that separates molecules based on their size by filtration through a gel and is used for the determination of the molecular mass of different molecules. The concept of size-based separations by chromatography was first speculated in 1950 by Synge and Tiselius based on the observation that molecules could be separated as a function of their molecular size using zeolites [Hong et al. 2012]. For over last 5 years we observe a continuous interest in this technique (www.trends.google.com). Nowadays, the highest interest in SEC is observed in China, but also in other countries such as the USA, Canada, Australia, or in Western Europe. From the countries of Eastern Europe, this technique is distinctly popular among researchers in Poland (www.trends.google.com).

Size exclusion chromatography has been known under several other names such as exclusion chromatography, steric-exclusion chromatography, restricted-diffusion chromatography, liquid-exclusion chromatography, gel-filtration chromatography, and gel-permeation chromatography [Hong et al. 2012]. The separation in these techniques is based on size exclusion, which is why IUPAC (International Union of Pure and Applied Chemistry) recommends using the term SEC instead of GPC [Gaborieau and Castignolles 2011]. Often the difference between the two terms GPC and SEC is that SEC is for aqueous applications and at room temperatures while GPC is with organic solvents and can be performed at high temperatures necessary to dissolve high molecular weight polymers. In general, the term GPC is used for those analyzing plastics or synthetic polymers using either organic or aqueous-containing eluents. By comparison, SEC is more commonly used to describe size-based separations of biological compounds such as polysaccharides and proteins [Held 2018].

The performance, quality, and safety of polysaccharide-based products depend on their molar mass, molecular weight distribution, and structure. If the molar mass of the polysaccharide is too high, then the final product may be too brittle and/or firm, while a low molar mass may result in a far more weakly structured product and a deterioration other technological properties. Furthermore, at low molar mass, polysaccharides tend to be linear, but as molar mass increases, so does the likelihood that the molecule will branch. Branching also directly influences the quality of a finished product, so controlling both properties is crucial to ensure a safe, high-quality product that behaves as required [Ball 2016].

SEC with multiple detection was proven for effective polysaccharide characterization. However all detection systems have some limitations [Striegel 2016;

Williams 2018], especially when polysaccharides of the object are not sufficiently purified or other polysaccharides are present in the samples, which is especially challenging in samples derived from biological (plant) material. In such a case post-column derivatization and detection of derivatized polysaccharides in samples containing other polysaccharides seems to be a promising and innovative solution, however, information concerning this kind of SEC is scarce. This work aimed to present an overview of the application of SEC in the analysis of polysaccharides in foods with a special emphasis on the sample preparation and possibilities of application of post-column derivatization for detection of polysaccharides in complex samples.

2. Size exclusion chromatography (SEC)

Size exclusion chromatography (SEC) system separates polysaccharides by their hydrodynamic radius, a property determined both by the size and shape of the molecule. The principle of SEC separation is shown in Figure 1. Large molecules cannot enter pores in the gel, their way through the column is shorter and are eluted sooner, whereas small molecules can enter gel pores their way through the column is more complicated, longer and are eluted later.

Unlike other chromatographic methods, saccharides do not bind to a stationary phase during SEC. In contrast, saccharides are separated by the rate at which they navigate through an inert stationary phase called size-exclusion resin [Hong et al. 2012].

The gel consists of spherical beads containing pores of specific size distribution. Separation occurs when molecules of different sizes are included or excluded from the pores within the matrix. Small molecules diffuse into the pores and their flow through the column is retarded according to their size, while large molecules do not enter the pores and are eluted in the column's void volume. Consequently, molecules separate based on their size as they pass through the column and are eluted in order of decreasing molecular weight (M_w). Operating conditions and gel selection depend on the application and the desired resolution [Hong et al. 2012].

The basic components of a typical SEC system (Fig. 2) are the pump, injection system, SEC column, detection system, and specific SEC software.

Pumps used in SEC must have low pulsations and high accuracy of flow. A change of the flow rate of only 0,1% can cause an error in molar mass of up to 10%. The injection system should provide an introduction of the sample without

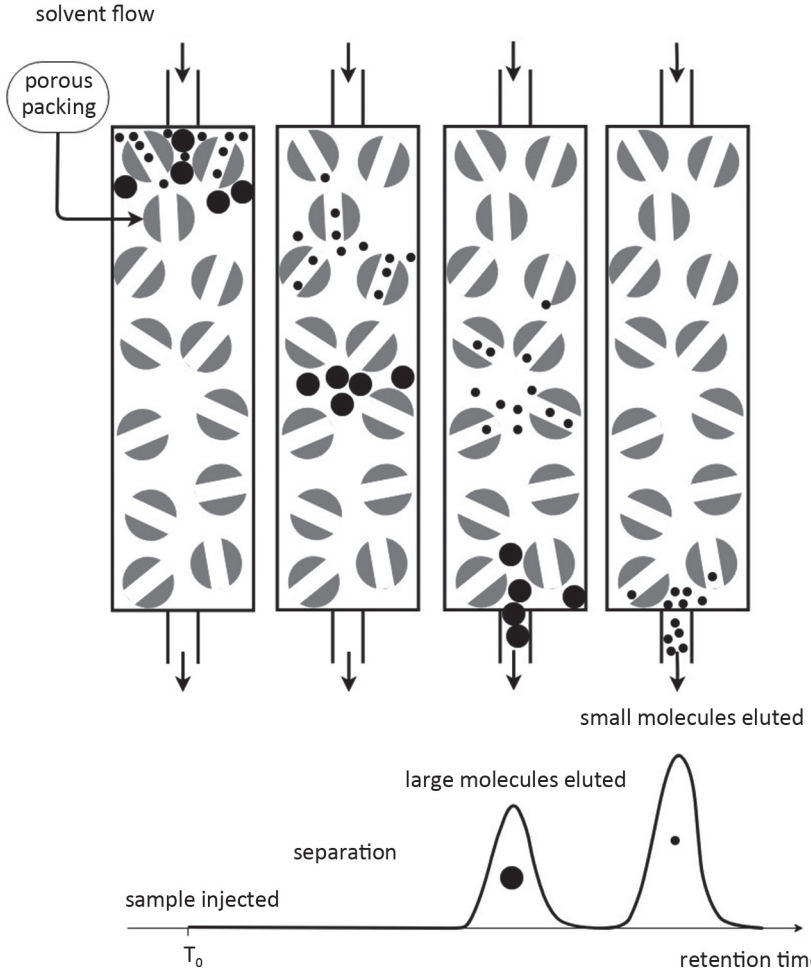

Fig. 1. Schematic representation of the separation mechanism of molecules based on size (and shape) on the SEC column (source: own elaboration)

jump of pressure. SEC columns should be maintained at a constant temperature during the whole analysis. Temperature control of the detector is also desirable. More extended SEC systems used for the analysis of carbohydrates have often series of columns connected in line, multidetection system, post-column derivatization system, and equipment providing the possibility of collection fractions. Application of SEC columns of different target molecular weight range connected inline provide the possibility of separation molecules in a wide range of their size. Multidetection system provides possibility of detection of various

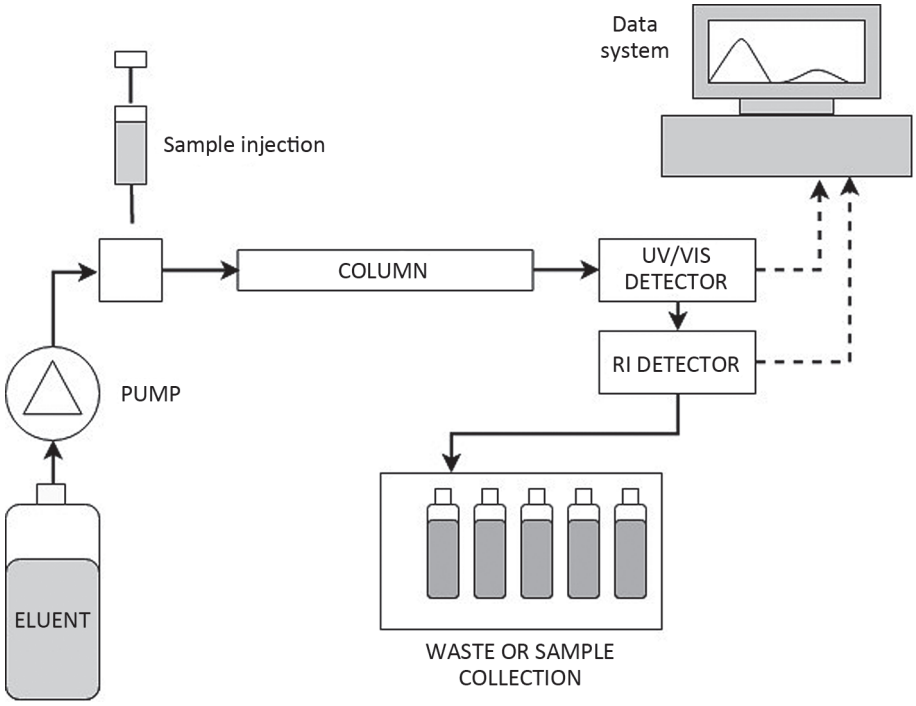

Fig. 2. Schematic representation of the SEC system (source: own elaboration)

substituents of polysaccharide chain, as well as contaminants in the sample. In the analysis of molecular weight distribution of polysaccharides isolated from plant material refractometric detector (for sugars detection) completed by UV detection (for detection of proteinaceous material) is especially useful. Polysaccharides obtained from biological sources are usually a mixture of different ones. For example, purified starch contains significant amounts of non-starch polysaccharides. Both molecular weight distribution profile, as well as molar mass, may be strongly affected by these contaminants because detectors used for sugar detection cannot distinguish between different kinds of polysaccharides. Post-column derivatization allows distinguishing one kind of polysaccharide from another after their separation on the SEC column at the detection stage. The SEC system equipped with post-column derivatization system (Fig. 3) at the output of SEC columns has a mixer and reaction coil where separated polysaccharides are mixed with derivatization reagent provided by the second pump at a constant rate, and derivatized polysaccharides are further detected by UV or fluorescence detectors [Shewry and Ward 2009]. The SEC system equipped

with fraction collector enables the possibility of further examination of obtained fractions as well as production of higher amounts of selected fractions more efficiently in combination with preparative SEC columns. If results of SEC analysis are to be compared or are to be followed, specific SEC software is needed to generate the results [Held 2018].

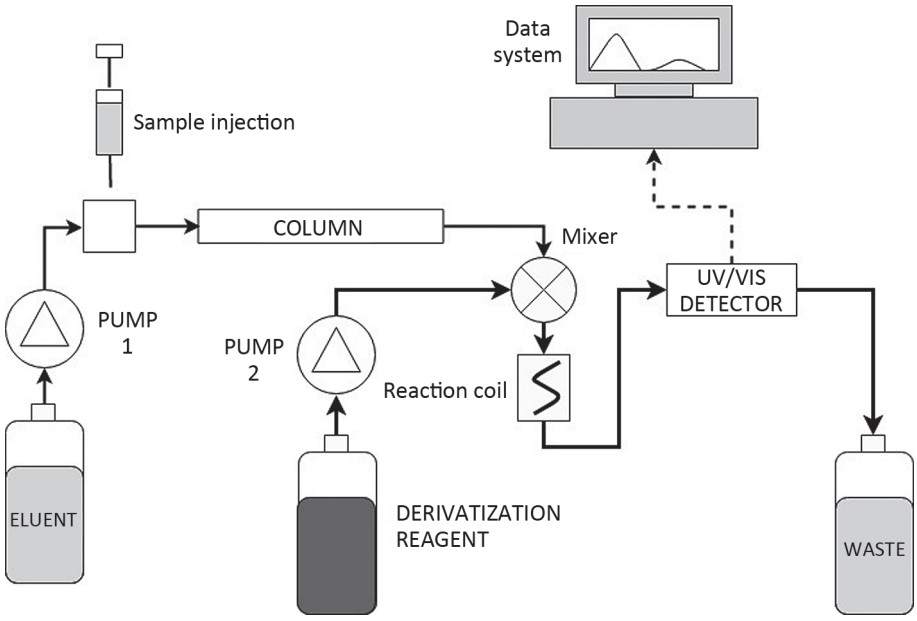

Fig. 3. Schematic representation of the SEC with post-column derivatization system (source: own elaboration)

3. Sample preparation for SEC analysis

Sample preparation is the most important stage in the analysis of the molar mass of different biopolymers, including polysaccharides by SEC [Gaborieau and Castignolles 2010; Hong et al. 2012; Buksa et al. 2018]. Conditions applied during sample preparation must ensure a complete dissolving of biopolymer in the solvent used. If dissolution will be incomplete there will be a question of what part was not dissolved and if the dissolved fraction is representative to the whole sample. After dissolving centrifugation and/or filtration is applied and in most cases after these steps material that was not completely dissolved is excluded from further analysis. If these steps will not be applied the undissolved mate-

rial could be retained in the guard column or at the top of the main column and finally also be excluded from the analysis, or strongly modified by high shearing forces (this often could be observed as a pressure jump immediately after injection), and apart of the high risk of column blockage this approach leads to distorted results of SEC analysis. What is more, the undissolved fraction has not an average but rather a high molar mass, and exclusion of this fraction causes significant underestimation of the average molar mass determined. The second problem associated with not properly dissolved polymers is that the molecules may be in a form of complexes, aggregates and deliver an overestimated results [Gaborieau and Castignolles 2011; Hong et al. 2012]. This is especially dangerous when MALS (multi angle light scattering) detection is applied which is very sensitive to aggregates.

The issue which must be considered in the case of sample preparation is a selection of a suitable solvent. Also, the conditions such as temperature, pH, time, the intensity of dissolving, etc. must be selected carefully as one or all may affect the natural structure of polysaccharides and their substituents, changing their molecular properties. As an example using alkali solvents is not acceptable for the investigation of esterified molecules as it causes de-esterification.

To summarize the above-mentioned issues the examined polysaccharide should be properly dissolved and every time the recovery after centrifugation/filtration should be measured and clearly presented. In some cases, such as research concerning cross-linking, further analysis of undissolved material with other techniques is justified [Buksa et al. 2018; Buksa and Krystyjan 2019].

In the molecular mass analysis of starch and modified starches, the problem of incomplete dissolving still remains, and there is no universal method of complete starch dissolving without controversies about interference with its natural molecular structure [Gilbert et al 2010].

4. Standards used in SEC analysis of polysaccharides

The SEC system calibrated with proper standards of known molar mass allows the measurement of the molecular masses of unknown molecules. The standards should be as similar to the molecules of interest (polysaccharides) as possible. Any difference in the structure, branching, degree of substitution with different molecules or groups, etc. will generate differences which finally cause under- or overestimation of the true molar mass of examined polysaccharides. In such a case, the not absolute molar mass is determined but related to standards,

apparent molar mass. However, this apparent molar mass should be close to an absolute molar mass as far as possible, because when abstract values are reported for biopolymers of rather widely reported molar mass (for example starches), for which molar mass is also determined by other techniques, this causes controversy and confusion [Gilbert et al. 2010; Ball 2016; Williams 2018].

The SEC standards may have narrow or broad distribution. Broad distribution standards may help in the situation when narrow standards are not available. For the determination of the molar mass of glucans, dextran or pullulans are commonly used [Ball 2016]. For molar mass analysis of protein, different proteins of known molar mass are used. For analysis of pentose-based polysaccharides, xylans of known molar mass should be used, but these are poorly available. For other biopolymers, available standards could be used, but the reported molecular parameters must be clearly explained as apparent in relation to kind of standards.

The inclusion of a light scattering detector in a SEC system eliminates the need to run a series of standards to generate a calibration curve, as the sample's molecular weight is measured directly by the light scattering detector. This ability, in addition to the measurement of a sample's absolute molecular weight, is one of the main advantages of using a system with a light scattering detector. However, while a long-lasting process to generate a calibration curve is not needed when using a light scattering detector, a quick calibration step involving the analysis of a single, narrow standard is still required. The two reasons for this are to determine the detector response factors and to calculate detector offsets and corresponding band broadening corrections [Gaborieau and Castignolles 2011; Ball 2016; Williams 2018].

5. Characterization of SEC columns

In SEC analysis the type of resin used and the length of the column play a critical role. The choice of the resin depends on the molar mass of the polysaccharides which are intended to be separated and the conditions under which the separation will be performed. For the complex mixture of polysaccharides not one column but series of columns, of different exclusion ranges, connected in line is often applied. Comprised exclusion ranges of columns in series provide more good separation conditions in a broad range of molar mass.

The most popular columns in SEC are Shodex SB-800 Series, Tosoh Bioscience TSKgel PW & PWxl, Agilent PL aquagel-OH, Waters Ultrahydrogel Phe-

nomenex PolySep, and PSS SUPREMA. Recently so-called mixed-bed HPSEC columns are available. These columns have particles with different pore size ranges and are designed to extend the linear range. Such columns are recommended to use for dietary fiber polysaccharides since they significantly simplify the calibration of the SEC system [Shewry and Ward 2009].

The main parameters of SEC columns are particle and pore size and column dimensions. In general the smaller the particle size, the higher the resolution. Pore size controls the exclusion limit and the fractionation range of the media. Resolution increases with the column length, and as the column diameter increases, the capacity of the column increases due to the larger column or bed volume. Column packing is critical to resolution. As a result of pressure jumps (for example at the sample injections) bed in the column may be destroyed. Dead volume at the top of the column can significantly reduce resolution as the sample is allowed to diffuse prior to entering the column bed, resulting in "band broadening" or wider peaks. Dead volume at the top of the column is possibly the most critical consideration because the loss in resolution is then multiplied as the molecules travel through the column [Hong et al. 2012].

The elution volume decreases nearly linear with the log of the molecular hydrodynamic volume. The elution volume between V_0 and V_t can be expressed as a function of molecular size and represents the working range where the column is capable of size separation (Fig. 4). It is possible to calibrate the column for molecular size determination within this range if standards with well-defined molecular sizes are available. However, the parameter of interest is often the molar mass rather than the molecular size. Therefore, the relationship between molecular size and molar mass becomes important. Within a type of polysaccharide, this relationship is linear if the fine structure and conformation are constant. This means that elution volume only can be translated into molar mass if standard samples of the correct structure were used for calibration. A calibration performed under good conditions should show a nearly straight line when log molar mass is plotted against elution volume. However, if the SEC system consists of more than one column this relationship could be more complicated. V_0 and V_t should always be determined in order to avoid extrapolations outside of the working range [Shewry and Ward 2009; Hong et al. 2012; Held 2018].

SEC separations are generally performed using materials composed of dextrose, agarose, polyacrylamide, or silica which have different physical characteristics. Polymer combinations are also used. Ideally, the materials will have no interaction with the examined biopolymers [Hong et al. 2012].

For a successful SEC separation, the selection of both column packing as well as solvent system is required. The mobile phase should consist of a very

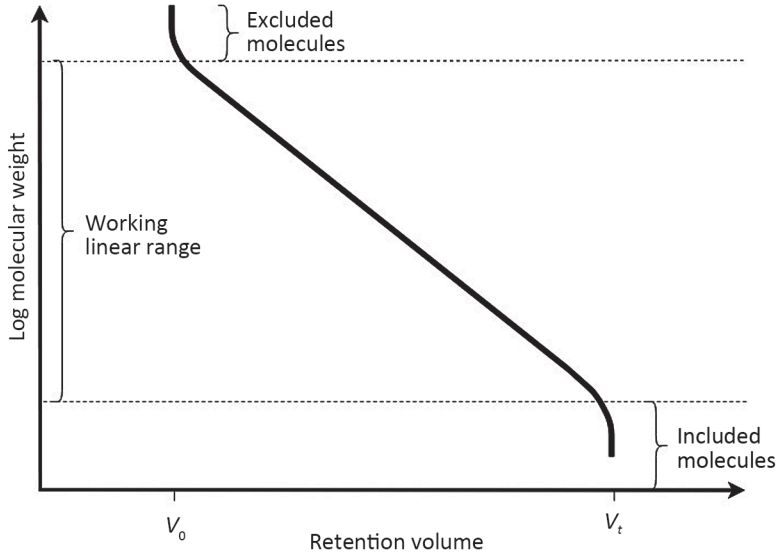

Fig. 4. Schematic representation of the relationship between molecular weight and retention volume in size exclusion chromatography (source: own elaboration)

high purity solvent that should not react with sample or column packing and there should not be any interference with the detector. A common approach to reduce electrostatic interactions in SEC involves increasing the ionic strength or salt concentration of the mobile phase. This can reduce secondary interactions and improve peak symmetry, retention time, and quantitation. Mobile phases used for SEC of polysaccharides are alkali or $NaNO_3$ (salts) solutions [Shewry and Ward 2009; Hong et al. 2012]. Considering flow rates used in SEC – the moderate flow rates offer the highest resolution. Moderate flow rates allow the molecules to fully access the surface area of the stationary phase permitting the smaller molar mass species the time to enter the pores, resulting in improved partitioning of the different molar mass species. Flow rates that are too slow will reduce resolution since the peaks or bands will diffuse too much as they travel through the column. In SEC where elution could be carried out by using physiological buffers, the speed of SEC can result in the quantitative purification of enzymes with full activity. For labile enzymes, SEC can be performed in the cold and at the highest possible flow rate. For those biopolymers which show aggregation, detergents, generally 0.1% SDS (sodium dodecyl sulfate), can be included in the mobile phase [Tayyab et al. 1991].

6. Characterization of most common detection systems in SEC

Several types of detectors are used in SEC systems. Two main groups are concentration-sensitive detectors and molar mass-sensitive detectors. Among concentration-sensitive detectors, bulk property detectors with the most common in sugar analysis Refractive Index (RI) Detector should be mentioned. Other concentration-sensitive detectors are the Ultraviolet UV Absorption Detector which is a solute property detector and Evaporative Light Scattering Detector (ELSD) belonging to evaporative detectors. Among molar mass sensitive detectors, the Light Scattering Detectors including Low Angle Light Scattering (LALS) and Multiangle Light Scattering (MALS) detectors should be mentioned. To the group of molar mass sensitive detectors also Viscosity detectors (Differential Viscometers, VISC) are classified [Striegel 2016]. There are also other detectors used in SEC systems such as Flame Ionization Detector (FID), a Mass Spectrometer, or a Fourier Transform Infrared (FTIR) Spectrometer. For multidetection SEC systems, the offset and band broadening calculations are necessary to align and coordinate the responses of multiple detectors positioned in series [Williams 2018].

It must be noted that for measurements with advanced detectors complete dissolving and exact purification of the sample polysaccharide from co-eluting contaminants is crucial to generate useful data [Shewry and Ward 2009; Hong et al. 2012; Williams 2018].

7. Molecular parameters determined by SEC

There are many parameters influencing calculated molar mass, so in order to ensure comparable conditions of calculations for estimation of molecular parameters, a special software should be applied [Shewry and Ward 2009; Held 2018]. The most common parameters are: number average molar mass, mass (weight) average molar mass and dispersity.

The number average molecular mass (M_n) is the ordinary arithmetic mean or the average of the molecular masses of the individual macromolecules. It is determined by measuring the molecular mass of n polymer molecules, summing the masses, and dividing by n.

$$\bar{M}_n = \frac{\Sigma_i N_i M_i}{\Sigma_i N_i}$$

The mass average molar mass (M_w) is another way of describing the molar mass of a polymer. Some properties are dependent on molecular size, so a larger molecules will have a larger contribution than a smaller molecules.

$$\bar{M}_w = \frac{\Sigma_i N_i M_i^2}{\Sigma_i N_i M_i}$$

Where N_i is the number of molecules of molar mass M_i.
The ratio of the mass average to the number average is called the dispersity *Đ*.

$$Đ = \frac{\bar{M}_w}{\bar{M}_n}$$

To avoid misinterpretation the calculated parameters should be compared with the same parameters determined by other techniques. Surprisingly, only very few SEC characterizations have been validated by determining the molecular weight with at least two different methods [Shewry and Ward 2009; Gaborieau and Castignolles 2011].

8. Examples of application of SEC in analysis of polysaccharides

SEC is not a high-resolution technique. Although SEC does not discern similar molar mass species particularly well, it is very good at separating molecules that may not be fully resolved by other methods. The resolution of separation depends on particle size, pore size, flow rate, column length and diameter, and sample volume. Generally, the highest possible resolution is the ability to measure a twofold difference in molar mass. This is obtained with moderate flow rates, long, narrow columns, small particle size gels, small sample volumes, and a sample viscosity that is the same as the eluent.

8.1. Molecular mass determination

SEC enables measurement of the average molecular weights and molecular-weight distributions of polymers. Because these characteristics may be correlated with important properties of hydrocolloids such as water absorption, SEC is an essential analytical technique for characterization of macromolecules.

8.2. Proteins and polysaccharide fractionation

Polysaccharides are obtained from natural sources using various isolation and purification techniques. For example, non-starch polysaccharides are obtained from cereal grain by water extraction [Shewry and Ward 2009]. Hyaluronic acid is obtained from rooster combs by extraction with sodium acetate and precipitation with an ethanol solution. Dextran is now synthesized by lactic acid bacteria, such as *Leuconostoc mesenteroides* using sucrose [Krawczyk et al. 2018]. During preliminary purification, polysaccharides can be precipitated from their aqueous solution with organic solvents, such as acetone, acetonitrile, or ethanol, sometimes with the aid of salts. The disadvantage of this method is the possibility of co-precipitation of impurities. For technological, biochemical, and medicine-related applications it is also important to separate a particular fraction of a polysaccharide with a suitable molar mass. For example, 200 000–2 000 000 g/mol fractions of inulin, β-glucan, levan, and hyaluronic acid are usually used for pharmaceutical-related purposes [Krawczyk et al. 2018]. One of the reasons is molar mass dependent properties of polysaccharides. Therefore, methods of purification from natural sources and separation of polysaccharides into fractions of a particular molar mass suitable for analytical and preparative purposes are necessary. The most commonly used methods are: capillary electrophoresis (CE), a combination of CE and HPLC, nanofiltration, and SEC [Hong et al. 2012; Krawczyk et al. 2018].

8.3. Purification

SEC is generally used near the end of the purification process for a polysaccharide of interest. SEC can also be used extensively to guide the development of the purification process for biopharmaceuticals [Hong et al. 2012]. Often, size exclusion chromatography is used as a faster and more reliable buffer exchange method than dialysis because it is compatible with several solvents and requires less buffer. A single solvent is used throughout the procedure, and the available resins are compatible with the most commonly used buffers. SEC enables the separation of not only sugars but also protein, peptides, nucleic acids, and others on the basis of their size. Various species of RNA and viruses have been purified using SEC. This technique is used in biopharmaceutical areas, including the purification of viruses such as coronaviruses including SARS-CoV-2 [Loa et al 2002; Esposito et al. 2020], adenovirus, lentivirus, influenza virus, antibody fragment vaccine against HIV1, plasmid, or viral clearance [Stein et al. 2016].

8.4. Desalting

A common use of SEC is for desalting especially of a protein or nucleic acid samples. The molecule of interest is eluted in the void volume, while smaller molecules are retained in the gel pores. To obtain the desired separation, the gel should have an exclusion limit significantly smaller than the molecule of interest.

8.5. Aggregation studies

SEC is also a great tool commonly applied for the investigation of protein-polysaccharide interactions, complex formation, and complexes in food matrixes [Tao and Zhang 2008; Liu et al. 2017; Buksa et al. 2018; Buksa and Krystyjan 2019; Cao and Mezzenga 2020]. SEC is also commonly used for studying modifications of biopolymers which strongly affect their molar mass. SEC could be very useful to determine the advancement of hydrolysis and cross-linking, where decrease or increase of molar mass can be monitored respectively [Boeriu 2008; Rasmussen and Meyer 2010; Buksa et al. 2016b; Akhtar and Ding 2017; Raak et al. 2018].

8.6. Studies of molar mass of polysaccharides in complex samples

Preparation of extracts prior to molecular weight determinations is a crucial step, because there is a compromise between using mild conditions that preserve molecular weight and on the other hand, obtaining a high yield of the polysaccharide. One way to eliminate the need for purification of extracts is to use selective detection. If only the molecules of interest are detected, co-eluting molecules do not interfere with the determination of the molecular weight distribution. Such selective detection is possible by applying techniques of post-column derivatization followed by detection of selectively derivatized molecules. For food samples of post-column derivatization techniques are available for the detection of ß-glucans, pentose-based polysaccharides (arabinoxylans), and starch fractions (Table 1). Application of post-column derivatization and multidetection allow determining molecular mass distribution profiles of polysaccharides such as starch, ß-glucan, arabinoxylan in the samples where other polysaccharides are present.

Table 1. Examples of SEC with post-column derivatization applications in the analysis of polysaccharides (source: own elaboration)

Kind of polysaccharide	SEC column system	Mobile phase used	Post-column derivatization	Detection	Reference
Amylose in starch	SB-G and OHpak SB-806 and SB-804	0.1M $NaNO_3$ at 0.6 mL/min	10% I_2-DMSO solution (90% DMSO, 10% water, 0.006M I2), 10% 6M urea and 80% water solution at a flow rate of 0.4 mL/min	UV/VIS detector at 640 nm	Buksa [2018]
Arabinoxylan	Fractogel HW40 and Superose6 and 2 × Fractogel HW40	50mM NaCl at 0.6 mL/min	Determination of hexose-based polysaccharides: To 0.5 mL of each fraction 1 mL of anthrone reagent (0.2 g of anthrone per 100 mL of H_2SO_4); Determination of pentose-based polysaccharides (arabinoxylan): To 0.3 mL of each fraction 0.7 mL of H_2O, 50 µL of ferric ammonium citrate solution (10 mg ferric ammonium citrate per 1 mL H_2O) and 1 mL of orcinol reagent (0.2 g orcinol in 100 mL of H_2SO_4)	Spectrofotometric detection – absorbance of each fraction after derivatizations was measured at: 620 nm for hexose -based polysaccharides; 660 nm for pentose-based polysaccharides. The absorbance of fractions without derivatization at 280 nm was used for detetection of protein	Buksa et al. [2016a]
β-glucan	µHydrogel 250 and 2000	50mM NaOH at 0.5 mL/min	Calcofluor solution (30 mg/L in 50mM NaOH) at 0.6 mL/min	Fluorescent detector 415 nm (λ_{ex}), 445 nm (λ_{em})	Suortti [1993]
β-glucan	OHpak SB806HQ and SB-804HQ	0.1M $NaNO_3$ at 0.5 mL/min	Calcofluor solution (25 mg/L in 0.1M Tris) at 0.5 mL/min	Fluorescent detector 415 nm (λ_{ex}), 445 nm (λ_{em})	Shewry and Ward [2009]

ß-glucan forms complex with the dye Calcofluor that can be selectively measured with a fluorescence detector. Calcofluor in post-column derivatization SEC system (Fig. 3) is delivered post-column to the eluting sample and the complex is formed in a mixer and reaction coil prior to the detector. Different wavelengths for the detection of the complex have been reported in the literature. Wood et al. [1991] used 360 nm excitation and 425 nm emission while Suortti [1993] used 415 and 445 nm respectively. The emitted light measured is proportional to the mass of ß-glucan in the detector thus providing a signal showing a weight distribution of molecular weight. It must be underlined that there is a need for calibration standards with known molar mass for calibration of SEC system, and no such commercial standards are available for ß-glucan, but it is possible to calibrate a Calcofluor post derivatization SEC system by combining light scattering and micro fractionation [Shewry and Ward 2009].

Similarly, as it was described for ß-glucan post-column derivatization system may be used for the determination of molar mass and molecular mass distribution of arabinoxylans extracted from cereal grain. In extracts containing other polysaccharides such as starch or ß-glucan, pentoses may be selectively measured by means of specific staining reaction in the collected fractions with orcinol-based spectrometric method [Buksa et al. 2016a].

Recently, the post-column derivatization SEC system was applied for examination of molecular properties of starch fractions and resistant starch. The linear regions in starch molecules form complexes with iodine and such complexes could be examined by means of colorimetric measurements. This is a great opportunity to apply the SEC with post-column derivatization using iodine solution in order to investigate the molecular structure of starch fractions and resistant starch in the samples [Buksa 2018]. An exemplary elution profile of starch, amylose, and amylopectin is shown in Figure 5.

8.7. Analysis of molar mass of starches

SEC is commonly used for the determination of molecular parameters of starches. However, the analysis of the molar mass of starch still is a challenge. Despite 10 years, the problems of molar mass analysis of starch highlighted in 2010 [Gilbert et al. 2010] are still unresolved. Critical steps in the analysis of molecular properties of starch that generate the highest mistakes are especially: extraction and purification, dissolving and solvent selection, and availability of appropriate standards.

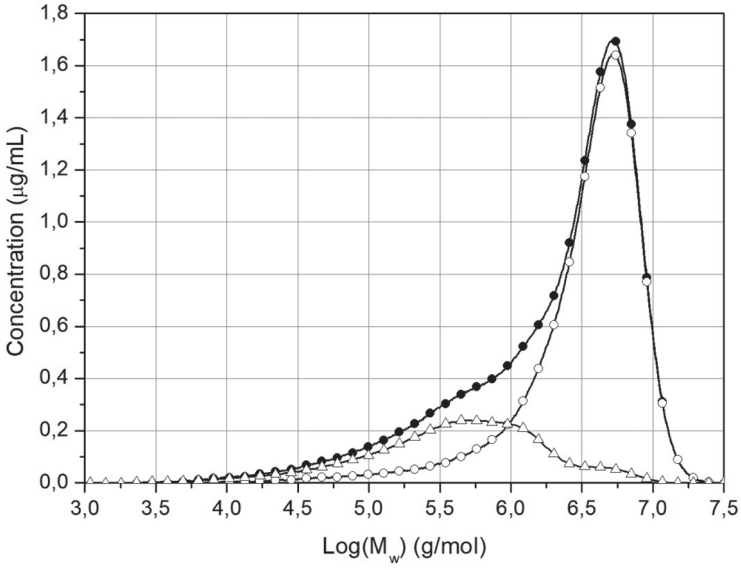

Fig. 5. Molecular mass distribution profiles of whole starch (-●-), amylose (-Δ-), amylopectin (-○-) (source: own elaboration)

9. Conclusion

Size exclusion chromatography (SEC) is a separation technique used to separate molecules on the basis of size and shape (hydrodynamic radius). This is a great tool for the analysis of biopolymers such as polysaccharides. However, sample preparation is crucial to obtain robust and useful data. For investigation of polysaccharides isolated from various raw food resources (especially plant material) using the state-of-the-art detection systems extremely thorough purification is required which affects all determined molecular parameters. In the case of such complex samples, a solution could be the application of post-column derivatization and selective detection of derivatized polysaccharides but, the advantages of SEC with post-column derivatization seems to be underappreciated in the current studies. The technique highlighted in this work in all its modifications is still being developed and could be a very useful tool for the investigation of transformations and interactions of polysaccharides in food products during processing.

References

Akhtar M., Ding R. 2017. Covalently cross-linked proteins & polysaccharides: Formation, characterisation and potential applications. Current Opinion in Colloid & Interface Science, 28, 31–36. https://doi.org/10.1016/j.cocis.2017.01.002

Ball S. 2016. Exploring the value of GPC/SEC in polysaccharide characterization. https://www.americanlaboratory.com/914-Application-Notes/191847-Exploring-the-Value-of-GPC--SEC-in-Polysaccharide-Characterization/ [accessed: March 27, 2021].

Boeriu C.G. 2008. Peroxidases in food industry: Crosslinking of proteins and polysaccharides to impart novel functional properties. Roumanian Biotechnological Letters, 13(5), Suppl., 81–86.

Buksa K. 2018. Extraction and characterization of rye grain starch and its susceptibility to resistant starch formation. Carbohydrate Polymers, 194, 184–192. https://doi.org/10.1016/j.carbpol.2018.04.024

Buksa K., Krystyjan M. 2019. Arabinoxylan-starch-protein interactions in specially modified rye dough during a simulated baking process. Food Chemistry, 287, 176–185. https://doi.org/doi.org/10.1016/j.foodchem.2019.02.077

Buksa K., Łakomy A., Nowotna A., Krystyjan M. 2018. Arabinoxylan-starch-protein interactions in specially modified rye dough during a simulated fermentation process. Food Chemistry, 253, 156–163. https://doi.org/10.1016/j.foodchem.2018.01.153.

Buksa K., Praznik W., Loeppert R., Nowotna A. 2016a. Characterization of water and alkali extractable arabinoxylan from wheat and rye under standardized conditions. Journal of Food Science and Technology, 53(3), 1389–1398. https://doi.org/10.1007/s13197-015-2135-2

Buksa K., Nowotna A., Ziobro R. 2016b. Application of cross-linked and hydrolyzed arabinoxylans in baking of model rye bread. Food Chemistry, 192, 991–996. https://doi.org/10.1016/j.foodchem.2015.07.104

Cao Y., Mezzenga R. 2020. Design principles of food gels. Nature Food, 1, 106–118. https://doi.org/doi.org/10.1038/s43016-019-0009-x

Esposito D., Mehalko J., Drew M., Snead K., Wall V., Taylor T., Frank P., Denson J.P., Hong M., Gulten G., Sadtler K., Messing S., Gillette W. 2020. Optimizing high-yield production of SARS-CoV-2 soluble spike trimers for serology assays. Protein Expression and Purification, 174, 105686. https://doi.org/10.1016/j.pep.2020.105686

Gaborieau M., Castignolles P. 2011. Size-exclusion chromatography (SEC) of branched polymers and polysaccharides. Analitical and Bioanalitical Chemistry, 399, 1413–1423. https://doi.org/10.1007/s00216-010-4221-7

Gilbert R.G., Gidley M.J., Hill S., Kilz P., Rolland-Sabate A., Stevenson D.G., Cave R.A. 2010. Characterizing the size and molecular weight distribution of starch: Why it is important and why it is hard. Cereal Foods World, 55(3), 139–143. https://doi.org/doi.org/10.1094/CFW-55-3-0139

Held D. 2018. Tips & Tricks GPC/SEC: What are the differences between GPC, SEC, and GFC, and how do you get started with the technique? The Column, 14(10), 2–8.

Hong P., Koza S., Bouvier E.S.P. 2012. A review. Size-exclusion chromatography for the analysis of protein biotherapeutics and their aggregates. Journal of Liquid Chromatography & Related Technologies, 35, 2923–2950. https://doi.org/10.1080/10826076.2012.743724

Krawczyk T., Zalewski M., Janeta A., Hodurek P. 2018. SEC Separation of polysaccharides using macroporous spherical silica gel as a stationary phase. Chromatographia, 81, 1365––1372. https://doi.org/10.1007/s10337-018-3582-5

Liu F., Ma C., Gao Y., McClements D.J. 2017. Food-grade covalent complexes and their application as nutraceutical delivery systems: A review. Comprehensive Reviews in Food Science and Food Safety, 16, 76–95. https://doi.org/10.1111/1541-4337.12229

Loa C.C., Lin T.L., Wu C.C., Bryan T.A., Thacker H.L., Hooper T., Schrader D. 2002. Purification of turkey coronavirus by Sephacryl size-exclusion chromatography. Journal of Virological Methods, 104(2), 187–194. https://doi.org/10.1016/S0166-0934(02)00069-1

Raak N., Abbate R.A., Lederer A., Rohm H., Jaros D. 2018. Size separation techniques for the characterisation of cross-linked casein: A review of methods and their applications. Separations, 5(1), 14. https://doi.org/10.3390/separations5010014

Rasmussen L.E., Meyer A.S. 2010. Size exclusion chromatography for the quantitative profiling of the enzyme-catalyzed hydrolysis of xylo-oligosaccharides. Journal of Agricultural and Food Chemistry, 58(2), 762–769. https://doi.org/10.1021/jf903200h

Shewry P.R., Ward J.L. 2009. Analysis of bioactive components in small grain cereals. AACC International Inc., St. Paul, Minnesota.

Stein A., Heinen-Kreuzig A., Kiesewetter A., Schwarm S. 2016. Size-exclusion chromatography for preparative purification of biomolecules. BioPharm International, 29(4), 30–37.

Striegel A.M. 2016. Viscometric detection in size-exclusion chromatography: Principles and select applications. Chromatographia, 79, 945–960. https://doi.org/10.1007/s10337-016-3078-0

Suortti T. 1993. Size-exclusion chromatographic determination of β-glucan with postcolumn reaction detection. Journal of Chromatography A, 632(1–2), 105–110. https://doi.org/doi.org/10.1016/0021-9673(93)80032-4

Tao Y., Zhang L. 2008. Characterization of polysaccharide-protein complexes by size-exclusion chromatography combined with three detectors. Carbohydrate Research, 343(13), 2251–2257. https://doi.org/10.1016/j.carres.2008.04.030

Tayyab S., Qamar S., Islam M. 1991. Size exclusion chromatography and size exclusion HPLC of proteins. Biochemical Education, 19(3), 149–152. https://doi.org/10.1016/0307-4412(91)90060-L

Williams K. 2018. Why do I need a standard if I have a GPC/SEC system with a light scattering detector? https://www.materials-talks.com/blog/2018/07/12/why-do-i-need-a-standard-if-i-have-a-gpcsec-system-with-a-light-scattering-detector/ [accessed: March 27, 2021]

Wood P.J., Weisz J., Mahn. W. 1991. Molecular characterization of cereal beta-glucans. II. Size-exclusion chromatography for comparison of molecular weight. Cereal Chemistry, 68, 530–536.

IV APPLICATION OF ELECTRONIC NOSE AND GAS CHROMATOGRAPHY WITH OLFACTOMETRIC DETECTOR FOR THE ANALYSIS OF ALCOHOLIC BEVERAGES

Magdalena JANUSZEK

Department of Fermentation Technology and Microbiology,
Faculty of Food Technology, University of Agriculture in Krakow,
Aleja Mickiewicza 21, 31-120 Krakow, Poland

magdalena.januszek@urk.edu.pl
ORCID: https://orcid.org/0000-0003-4128-3636

Abstract. Most volatile fraction components of alcoholic beverages can be quantified and qualitatively determined by chromatographic techniques. Olfactometry is a method that allows the simultaneous separation and identification of volatile compounds. At the same time it aids the perception of the given compound's smell by the human nose. Non-chromatographic methods used to determine the flavour profile of alcoholic beverages include i.a. electronic nose. The purpose of this work is to present and compare the principles of these two methods. In order to facilitate an understanding of the principles the schemes are presented. For both methods advantages and limitations are presented. There are various possibilities of electronic nose and gas chromatography with olfactometric detector application. The methods may be used for the analysis of alcoholic beverages, as well as the most common esters and terpenes in alcoholic beverages, taking into consideration the characteristic aromas and detection threshold.

Keywords: volatile compounds, gas chromatography, olfactometric detector, electronic nose, alcoholic beverages

1. Introduction

Volatile compounds in alcoholic beverages are responsible for their taste and aroma. The word "volatile" is used to describe the compounds not undergoing any chemical procesess, detectable in room temperature in low concentrations. Most often the concentration of these compounds in alcoholic beverages is within a range of ppm, ppb or sometimes ppt. Each of these substances has own sensory threshold value. Those values are well known in the case of aqueus solutions, however, there is little or no data regarding wines. Aroma compounds can be divided into three groups depending on their source. There are primary aromas coming from grapes and secondary aromas produced by yeasts during fermentation process. There are also compounds known as tertiary aromas, formed during the storage period in the wooden barrels or glass bottles. The most important volatiles in alcoholic beverages are higher alcohols, esters, volatile acids, carbonyl compounds and lesser-known terpenoids. However, esters and terpenoids contribute to sweet, floral and fruity aroma of alcoholic beverages, even if they occur at a low concentration [Clarke and Bakker 2004; Kostrz and Satora 2018]. Therefore in current chapter these compounds are focused on (Table 1 and Table 2).

Esters are compounds derived from organic or inorganic acids in which at least one hydroxyl group is replaced by alkoxy group [IUPAC, 1997]. These compounds could also be synthesised by yeast during fermentation as a result of reaction between alcohols and acetyl-CoA (catalyzed by acetyltransferase), which caused higher concentration of these compounds in alcoholic beverages [Sparkman et al. 2011; Januszek et al. 2020].

Terpenoids are present in low concentrations in alcoholic beverages, which significantly affect their flavour. Bacteria, fungi and several invertebrates are responsible for terpenoids biosynthesis. However, these compounds are also known to be secondary metabolites derived from plants. About 60,000 terpenoid structures have been identified from natural materials so far and since terpenes are built up from isoprene, they are also called isoprenoids. That compounds may be divided on the basis of their C-skeleton, e.g. 10 carbons (monoterpenes), 15 carbons (sesquiterpenes), 20 carbons (diterpenes), 30 carbons (triterpenes) [Arrhenius et al. 1996; Grassmann 2005; Brattoli et al. 2014; Kostrz and Satora 2018].

Table 1. Selected terpenoids in alcoholic beverages (source: own modification based on Burdock [2006])

Terpenoids	Aroma threshold detection at:	Characteristic aroma	Type of alcoholic beverages
b-caryophyllene	64 to 90 ppb	woody, spicy, dry, clove-like aroma	beer
m-cresol	n/a	aroma characteristics at 1.0%: phenolic, spicy eugenol-like, medicinal, smoky powdery with a leather like note	beer, rum, sherry, whiskey
o-cresol	n/a	musty, medicinal, sweet spicy, phenolic aftertaste	rum, sherry, whiskey
cycloionone	n/a	woody, cedar wood, raspberry, orris root	cognac
a-damascenone	*d*-form,100 ppb *l*-form, 1.5 ppb	sweet, fruity, woody with a green seedy background	wine
b-damascenone	0.0007 to 0.009 ppb	sweet, brown woody, tobacco, davana-like, fruity, with a spicy balsamic undernote	hop oil rum, white wine, red wine, beer, cognac, rum, whiskies, scotch, cider, grape wines
farnesol	1 ppm	floral, rose, sweet, fruity, green lavender and haylike nuances	beer, whiskey
limonene	4 to 229 ppb	*d-, l-* or *dl*-limonene has a pleasant, lemon-like odor free from camphoraceous and turpentine-like notes	apple brandies
linalol	4 to 10 ppb	pleasant floral aroma, free from camphoraceous and terpenic notes	grape wines, rum, cider
linalol oxide	320 ppb	sweet, woody, penetrating aroma with floral, woody-earthy undertones	grape wines, apple brandies
citral	n/s; Dection at 1.0%:	strong, lemon-like odor characterizing lemon-like, distilled lime peel, intense aldehydic citrus like	beer, wine, apple brandies

Table 1. cont.

Terpenoids	Aroma threshold detection at:	Characteristic aroma	Type of alcoholic beverages
citronellol	11 ppb to 2.2 ppm	characteristic rose-like odor *l*-Citronellol - sweet, peach -like flavor *d*-citronellol – bitter taste	beer, rum and apple distillates
geraniol	4 to 75 ppb	rose-like aroma	whiskey, apple distillates
eugenol	6 to 100 ppb	strong aromatic odor of clove and a spicy pungent taste	whiskey, grape wines, apple distillates
a-ionol	n/a	woody, ionone-like with a woody, floral powdery note	raspberry brandy
b-ionone	0.6 to 10 ppb	violet-like aroma, woody, floral, berry, fruity.with powdery nuances	cognac, rum, whisky, white wine, raspberry, apple, brandy

Table 2. Selected esters in alcoholic beverages (source: own modification based on Burdock [2006])

Esters	Aroma or taste treshold	Characteristic aroma	Type of alcoholic beverages
amyl hexanoate	n/a	characteristic fruit-like (banana, pineapple) aroma Taste characteristics at 20 ppm: green, waxy, sweet and fruity with cognac-like notes	beer, rum, cider, white wine
amyl octanoate	n/a	fruity and earthy aroma	malt whiskey, cider, white wine, sparkling wine
butyl laurate	n/a	characteristic fruity, peanut -like aroma Taste characteristic at 100 ppm: harsh and sulfuraceous with fruit notes	cognac, cider and white wine, whiskey

Esters	Aroma or taste treshold	Characteristic aroma	Type of alcoholic beverages
decyl butyrate	detection: 225 to 1000 ppb	floral, orange-rose aroma	cognac
diethyl malate	n/a	fruity aroma with a pleasant herbaceous undertone	cognac, malt whiskey, cider, sherry,white, red, port, sparkling, rose, strawberry and bilberry wines
diethyl succinate	n/a	aroma characteristics at 1.0%: fruity, waxy, floral and slightly musty	cognac, rum, whiskey, cider, sherry, plum brandy, apple brandy, grape brandy, cherry brandy, cocoa, arrack and red, white, port, strawberry and sparkling wines
diethyl sulfide	n/a	garlic/ethereal aroma	beer, grape, brandy (cognac, armagnac, weinbrand)
ethyl acetate	5 ppb to 5 ppm	pleasant ethereal fruity, brandy-like odor, reminiscent of pineapple, somewhat nauseating in high concentration	cognac, beer, whiskies, cider, sherry, grape wines, rum
ethyl benzoate	100 ppb to 150 ppb	fruity aroma similar to ylang-ylang	white wine, red wine, cider, whiskies, apple brandy, cherry brandy, Bourbon vanilla
ethyl butyrate	0.1 to 18 ppb	fruity, sweet, tutti-frutti, apple, fresh and lifting, ethereal	beer, cognac, rum, whiskies, cider, sherry, grape wines
ethyl cinnamate	17 to 40 ppb	sweet balsamic honey-note aroma	apple brandy, quince, prickly pear, strawberry wine, Bourbon vanilla, clove brandy, rum, sherry, grape wines

Table 2. cont.

Esters	Aroma or taste treshold	Characteristic aroma	Type of alcoholic beverages
ethyl decanoate	8 to 12 ppb	waxy, fruity, sweet apple	cognac and apple brandy
hexyl acetate	2 to 480 ppb	fruity, green, fresh, sweet, banana peel, apple and pear	beer, rum, cognac, whiskies, cider, sherry, grape wines, pear and apple brandy, Bourbon vanilla
isoamyl acetate	2 to 43 ppb	sweet fruity, banana-like with a green ripe nuance	beer, cognac, grape wines, rum, whiskies, cider, sherry
2-methylbutyl acetate	5 to 11 ppb	fruity, sweet, banana, juicy fruit and tutti-frutti note	Scotch whiskey, white wine, Bantu beer, beer, cider
methyl cyclohexane-carboxylate	n/a	cooling, sweet, fruity and floral	Bourbon vanilla

2. Electronic nose

Electronic nose (e-nose) is one of the non-chromatographic methods of food analyses. Electronic nose mimic the human smell and the sense's communication with the brain (Fig. 1). The human olfactory ability is more complex and contains thousands of receptors that bind aroma molecules and enable the detection of some volatile compounds at the concentration reaching ppt. The human brain detects these signals and recognizes the substance consumed. On the other hand, electronic noses are the systems built from appropriately selected electronic sensors (transducers), that interact with aroma molecules showing different chemical affinity [Mielle 1996; Plutowska 2008; Payel et al. 2018]. Generally, the principle of e-nose operation can be divided into three parts. The first one is a simple delivery system, which is able to release volatiles from the sample headspace after its injection into the detection system. The second mentioned detection system has got a sensor which plays the role of the transducer and a converter. When volatiles get adsorbed on the sensor surface, they tend to change physical and elec-

trical properties of the sensor. The last part is a computing system, functioning of which is based on a statistical model [Wilkes et al. 2000; Turek and Chmielewski 2006; Payel et al. 2018].

Electronic noses, similarly to human noses are more able to distinguish specific aromas than characteristic compounds, however, e-noses detects the smell more effectively. Moreover, e-noses also detects hazardous subtances (e.g. poisonous gas), which are undetectable by human nose. Even though, sensors are very sensitive, they are only able to detect volatiles in the range of ppm with very few decimal places [Mielle and Marquis 1999; Wilkes et al. 2000; Turek and Chmielewski 2006; Payel et al. 2018].

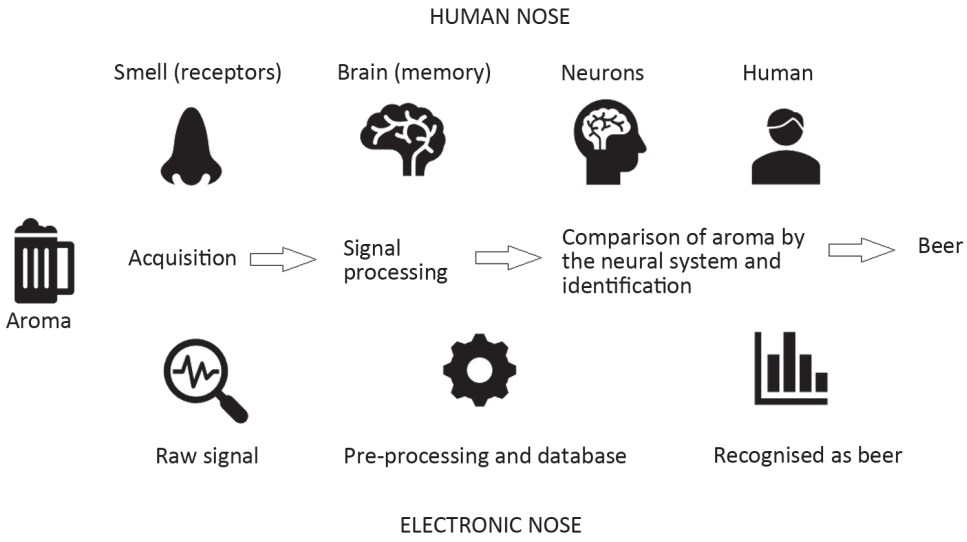

Fig. 1. Interpretation of data – e-nose vs human nose (source: own modification based on Payel et al. [2018] and Santos et al. [2017])

3. Gas chromatography with olfactometric detector

Application of gas chromatography method with olfactometric detector uses the skills of trained users to organoleptically distinguish the eluate from a chromatographic column in order to recognise aroma volatiles. This method allows to determine whether the given aroma compounds is present in a concentration enabling its human sensory detection, what is the aroma's type and the duration of its sensory activity. Determination of volatiles is possible due to the application of special

equipment, which is the olfactometric connector pipe. It is usually connected parallelly to standard detectors, e.g. flame detector and mass specttrometer, as well as the ionizing detector. Provided that the quantity of the compound is sufficiently large, several users are able to concurrently detect it in several ports (Fig. 2) [Ferreira et al. 2001; Ferreira 2002; Triqui and Bouchriti 2003; Ferrari et al. 2004; Plutowska 2008].

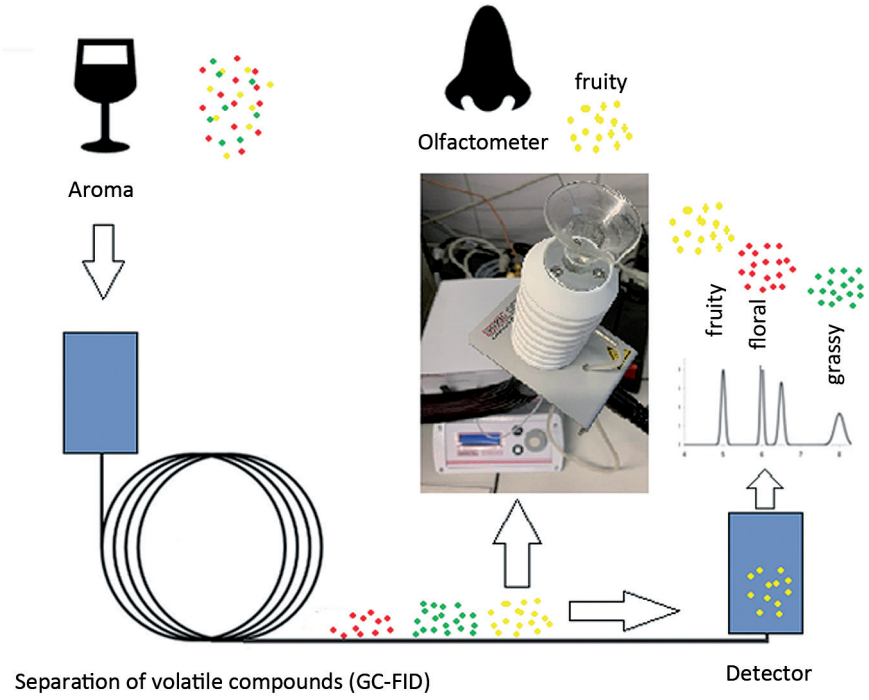

Fig. 2. Scheme of GC-O (source: own modification based on Internet source 1 [2018])

Separation method as well as equipment set up may influence the quality of obtained results. Subsequently, that may cause differences in the response of the human detector [Delahunty et al. 2006]. It is very important to choose properly extraction technique of volatile compounds, and to eliminate of distraction stimuli during the evaluation of sensory assessment, e.g. foreign odors and distracting sounds. Another limiting factor is too many samples for identification, at a short time, causing sensory fatigue. Sensory panel should, within tens of minutes, identify many specific aroma which are felt at irregular intervals just for few seconds. It is advisable to exchange panelists who recognise the aroma every few minutes [Bernet et al. 2002; Delahunty et al. 2006; Plutowska 2008].

Usually, the application of gas chromatography olfactometry method is typical for the comparison of the organoleptic properties of beer, wine, cognac, whisky, and other alcoholic beverages. For comparison, classical sensory analysis, e.g. (duo-trio method, taste profixing method) is very often used at the same time. The majority of these descriptive methods principle is described as suitable sensory attributes which are selected and rated in intensity [Meilgaard et al. 1983; Escudero et al. 2004; De Souza 2006; Plutowska 2008]. The characterising descriptors of aroma samples are ascribed to each scent. Chromatography with an olfactometric detector use determines the compounds, corresponding to given descriptors. The application of chemometric methods (the smallest partial square method, procrust analysis) [Fur et al. 2003; Lee and Noble 2003; Campo et al. 2005; Plutowska 2008] justifies each time that the descriptors and analytes are more comprehensively correlated.

One of the major obstacles, of volatile compounds analysis by GC-O, is related to the differences in the sensory sensibility thresholds. Sometimes the comparison of the results obtained during the GC-O analysis with traditional methods e.g. using flame ionization detector or mass spectrometry detector is impossible due to sensibility tresholds. High signals obtained by conventional detectors may be poorly perceptible in the column eluate or not detectable at all. Moreover, the pics that show up on the olfactogram will not always appear also on the chromatogram. In the above-mentioned situation, the preliminary olfactometric analysis allows to determine the analyte's retention time [Callemien 2006; Plutowska 2008].

4. Advantages and disadvantages of using electronic nose and GC-O methods

The most important advantages of using electronic nose method certainly are: short time of analysis and short recovery time. In addition, this method is relatively inexpensive. Other advantage is the fact, that there is a portable version of e-nose avaliable on the market. Analysed samples of alcoholic beverages do not require special preparation and analysed mixtures do not have to be separated. Sampling headspace technique could be chosen based on the type of sample and the specific requirements of the method. SHS (static headspace) is the most simple method to use. It requires optimisation of some parameters, e.g. quantity and temperature of analysed samples, equilibration of time and vial size. Due to the fact that volatiles are not preconcentrated, in some cases static headspace

has a low sensitivity. To improve the sensitivity, the DHS (dynamic headspace) technique is used. However, this method has got some disadvantages – the time of the analysis is increased because a supplementarny stage is introduce and it requires special equipment. Other type of the extraction of volatiles is SPME (solid-phase microextraction) which has a considerable concentration capacity. Relatively new method is SBSE (stir bar sorptive extraction) which is promising technique that provides very high sensitivity [Martí 2005]. The application of e-noses in analysis of alcoholic beverages comes from their high sensitivity, repeatability and reproducibility, which is higher than using GC-O. The ability to obtain the same chromatograms over a short intervals of time using the same equipment is called repeatability. The definition of reproducibility is the same, however, it aplies when using different instrument. It is possible to assess both of those parameters for e-nose when we calculate corelation coefficient between two measurments of the same sample [Mamat et al. 2011; Wardnecki et al. 2013].

The most important disadvantages of using e-nose are due to the presence of sensors, which are moisture-sensitive and suffer from ageing. Moreover, depending on the type of sensor used, it is possible to 'poison' sensors, e.g. conducting polymer sensors showed resistance to sensor poisoning, while, metal oxides semi-conducting (MOS) is prone to sulfur and weak acid poisoning. An electronic nose uses non- or partially-specific sensors distinguishing between different aroma, however, with lower sensitivity than human olfactory system [Wilson and Baietto 2009; Wardnecki et al. 2013].

The major advantage of the GC-O method is simultaneous quantitative and qualitative evaluation of the aroma with simultaneous assessment of the importance of individual components for the assessed flavour. This method allows the selection of active volatiles from complex mixtures specifying the sensory detection threshold and determining time of sensory activity and the intensity of aroma compounds [Wardnecki et al. 2013].

GC-O has significantly more disadvantages than the electronic nose. The first one is the fact, that this method is time-consuming and requires user experience and training. Even though, the operators are thoroughly trained, there is a risk of errors and difficulties with the detection of some volatiles at the end of aroma region. Moreover, we must bear in mind that human responses of flavour is always subjective. It is necessery that before main analysis the analytes have to be isolated, enriched and separated. Moreover, it is relatively expensive method, and to obtain qualitative and quantitative results it is required to connect with other detectors, e.g. GC-O-MS or GC-O-FID. It should be mentioned that the information regarding behaviour of compounds in the mixture is very scarce.

Additionally, the behaviour of compounds varies from one piece of equipment to another. Finally, the time of human responses differs among individuals [Wardnecki et al. 2013].

5. Electronic nose and gas chromatography with olfactometric detector in the analysis of alcoholic beverages

Before the analysis of alcoholic beverages using e-nose, it is usually required to remove ethanol from the sample [Mielle 1996; Turek and Chmielewski 2006]. It is another disadvantage of this method. For this reason, it is really crucial to provide proper conditions of the detection, e.g. the temperature should be controlled with a high accuracy (+/– 0.1°C) as its fluctuations affect changes practically in all types of sensors, moisture changes should not be grater than +/– 0.1%, reference gases should be applied to provide stable baseline signal and reduce interferences of undesired aromas, gas flow should be monitored and should not exceed 1% of the fixed value [Gardner 2002; Turek and Chmielewski 2006]. Different possibilities of using e-nose and GC-O methods in the analysis of alcoholic beverages are summarised in the Table 3.

6. Conclusion

The application of electronic nose and gas chromatography with olfactometric detector are suitable methods for the analysis of aromatically active volatile compounds of alcoholic beverages. There are many advantages and disadvantages in using both methods, however, e-nose is cheaper and much less demanding. On the other hand, olfactometry method determines the meaning of individual compounds for the assessed aroma of alcoholic beverages.

Acknowledgments

Findings reported in the current paper were reported in the research grant 2020/04/X/NZ9/01357 funded by National Science Centre, Poland.

Table 3. Different possibilities of using e-nose and GC-O methods in the analysis of alcoholic beverages (source: own elaboration)

Type of alcoholic beverages	Methods	The diferent possibilities of using e-nose and GC-O	References
Beer	E-nose	Detection of aroma compounds showing defects, which in higher concentration decreasing quality of beer, e.g., dimethyl sulfide, 1-hexanol, ethyl acetate, oct-1-en-3-ol and diacetyl.	Santos et al. [2017]
Beer	E-nose prototype	Determination of ethanol concentration in a wide spectrum of beers using a prototype of an electronic nose.	Voss et al. [2019]
Beer	Optical e-nose	Optical e-nose usage, in order to investigate alcohol decay in breath after drinking beer.	Santos et al. [2017]
Wine	E-nose	Determination of aroma compounds in wine focused on spoilage thresholds.	Rodriguez Gamboa et al. [2019]
Wine	E-nose	Identification of acetic acid in wine.	Lozano et al. [2011]
Chinese Liquors	E-nose	Classification of Chinese Liquors quality combining discriminant principal component analysis.	Wu et al. [2019]
Chinese Rice Wine	E-nose	Classification of Chinese rice wine as based on the (wine) age.	Yu et al. [2014]
Cherry Liqueurs	E-nose	Determination of Polish homemade liqueurs called Nalewka authenticity.	Śliwińska et al. [2016]

Type of alcoholic beverages	Methods	The diferent possibilities of using e-nose and GC-O	References
Beer	GC-O	Specification of the increasing aldehydes concentration resulting from the compliant with the Strecker's amino acids degradation reaction. That might take place during the maturation of beer, which may be an ageing and its organoleptic properties deterioration indicator.	Soares da Costa et al. [2004]; Plutowska and Wardnecki [2012]
Beer	GC-O	The aroma compounds concentration which can play an indicator role in controlling and optimising pH during malting and brewing determination.	Gijs et al. [2002]; Plutowska and Wardnecki [2012]
Beer	GC-O	Determination of aroma profile during Lambic beer ageing (increased quantities of aroma compounds with ageing time).	Witrick et al. [2020]
Wine	GC-O	Changes determination in the profile of aroma compounds which are related to the young, white wines oxidation process (e.g. presence of paper, boiled or rotten food odor).	Escudero et al. [2004]; Plutowska and Wardnecki [2012]
Wine	GC-O	The impact of vine managment (e.g. spacing between vine rows, fastening shoots upwards, load on buds and irrigation) on aroma profile and sensory assessment of wines determination.	Nicolli et al. [2018]
Cognac spirits	GC-O	Contribution of volatile terpenoid compounds in Cognac spirits ageing (e.g. concentration of geraniol, α-terpinene, α-terpineol and 1.8-cineole increased during ageing, wherease content of nerol decreased). The perceptual synergic effect was also observed between β-damascenone and lactone whisky.	Thibaud et al. [2020]
Chinese "Yanghe Daqu" liquors	GC-O	Aroma profiles of young and aged liquors comparison.	Fan and Qian [2005]

References

Arrhenius S.P., McCloskey L.P., Sylvan M. 1996. Chemical markers for aroma of Victis vinifera var. Chardonnay region wines. Journal of Agricultural and Food Chemistry, 44, 1085–1090. https://doi.org/10.1021/jf9505943

Bernet C., Dirninger N., Claudel P., Etievant P., Schaeffer A. 2002. Application of finger span cross modality matching method (FSCM) by naive assessors for olfactometric discrimination of Gewurztraminer wines. Lebensmittel-Wissenschaft und Technologie, 35, 244–253.

Brattoli M., Cisternino E., Gennaro G., Giungato P., Mazzone A., Palmisani J., Tutino M. 2014. Gas chromatography analysis with olfactometric detection (GC-O): An innovative approach for chemical characterization of odor active volatile organic compounds (VOCs) emitted from a consumer product. The Italian Association of Chemical Engineering, 40, 121–126.

Burdock G.A. 2006. Fenaroli's Handbook of Flavor Ingredients. CRC Press, New York, NY, USA.

Callemien D., Dasnoy S., Collin S. 2006. Identification of a stale-beer-like odorant in extracts of naturally ages beer. Journal of Agricultural and Food Chemistry, 54, 1409–1413. https://doi.org/10.1021/jf051772n

Campo E., Ferreira V., Escudero A., Cacho J. 2005. Prediction of the wine sensory properties related to grape variety from dynamic-headspace gas chromatography-olfactometry data. Journal of Agricultural and Food Chemistry, 53, 5682–5690. https://doi.org/doi.org/10.1021/jf047870a

Clarke R.J., Bakker J. 2004. Wine Flavour Chemistry. Blackwell Publishing, Oxford, UK.

Delahunty C.M., Eyres G., Dufour J.P. 2006. Gas chromatography-olfactometry. Journal of Separation Science, 29, 2107–2125.

De Souza M.D.C.A., Vasquez P., Mastro N.L., Acree T.E., Lavin E.H. 2006. Characterization of cachaca and rum aroma. Journal of Agricultural and Food Chemistry, 54, 485–488.

Escudero A., Gogorza B., Melus M.A., Ortin N., Cacho J., Ferreira V. 2004. Characterization of the aroma of a wine from from Maccabeo. Key role played by compound with low odor activity values. Journal of Agricultural and Food Chemistry, 52, 3516–3524.

Fan W., Qian M. 2005. Headspace solid phase microextraction and gas chromatography-olfactometry dilution analysis of young and aged Chinese "Yanghe Daqu" liquors. Journal of Agricultural and Food Chemistry, 53(20), 7931–7938. https://doi.org/10.1021/jf051011k

Ferrari G., Lablanquie O., Cantagrel R., Ledauphin J., Payot T., Fournier N., Guichard E. 2004. Determination of key odorant compoundsin freshly distilled cognac using GC-O, GC-MS, and sensory evaluation. Journal of Agricultural and Food Chemistry, 52, 5670––5676.

Ferreira V., Aznar M., López R., Cacho J. 2001. Quantitative gas chromatography-olfactometry carried out at different dilutions of an extract. Key differences in the odor profiles of four high-quality Spanish aged red wines. Journal of Agricultural and Food Chemistry, 49, 4818–4824.

Ferreira V., Ortin N., Escudero A., Lopez R., Cacho J. 2002. Chemical characterization of the aroma of Grenache Rose wines: Aroma extract dilution analysis, quantitative determination, and sensory reconstitution studies. Journal of Agricultural and Food Chemistry, 50, 4048–4054.

Fur Y., Mercurio V., Moio L., Blanquet J., Meunier J.M. 2003. A new approach to examine the relationship between sensory and gas chromatography – olfactometry data using generalized Procrustes analysis applied to six French Chardonnay wines. Journal of Agricultural Food Chemistry, 51, 443–452. https://doi.org/10.1021/jf0205458

Gardner J.W. 2002. Applications of Electronic Noses. Proceeidngs of 1st NOSE Short Course, National Institute of Matter Physics & University of Brescia, Chemistry and Physiscs Department, Italy.

Gijs L., Chevance F., Jerkovic V., Collin S. 2002. How low pH can intensify b-damascenone and dimethyl trisulfide production through beer aging. Journal of Agricultural and Food Chemistry, 50, 5612–5616.

Grassmann J. 2005. Terpenoids as plant antioxidants in vitamins and hormones. Plant Hormones, 72, 505–535.

Internet source 1. 2018. www/https//odourobservatory.org/measuring-odour/gas-chromatography-olfactometry/ [accessed: November 10, 2021].

IUPAC. 1997. Esters [In:] Compendium of Chemical Terminology. Second Edition. Online corrected version (2006). https://goldbook.iupac.org/ [accessed: October 7, 2022]. https://doi.org/10.1351/goldbook.E02219

Januszek M., Satora P., Tarko T. 2020. Oenological characteristics of fermented apple musts and volatile profile of brandies obtained from different apple cultivars. Biomolecules, 10, 853. https://doi.org/10.3390/biom10060853

Kostrz M., Satora P. 2018. Formation of terpenes in grapes and wines. Folia Pomeranae Universitatis Technologiae Stetinensis, seria Agricultura, Alimentaria, Piscaria et Zootechnica, 340(45), 1, 31–38.

Lee S.J., Noble A.C. 2003. Characterization of odor-active compounds in Californian Chardonnay wines using GC-olfactometry and GC-mass spectrometry. Journal of Agricultural and Food Chemistry, 51, 8036–8044.

Lozano J., Álvareza F., Santos J.P., Horrillo C. 2011. Detection of acetic acid in wine by means of an electronic nose. AIP Conference Proceedings, 1362, 176. https://doi.org/10.1063/1.3627188

Mamat M., Samad S.A., Hannan M.A. 2011. An electronic nose for reliable measurement and correct classification of beverages. Sensors (Basel), 11, 6, 6435–6453.

Martí M.P., Busto O., Guasch J., Boqué R. 2005. Electronic noses in the quality control of alcoholic beverages. Trends in Analitical Chemistry, 24, 57–66. https://doi.org/doi.org/10.1016/j.trac.2004.09.006

Meilgaard M.C., Agis A., de Banchs N.M., Babcook D.R., Berndt R., Blaschke E.F., Boersma J., Buckee G., Canales A., Chen E., Clarke B.J., Dravnieks A., Garza Cantu R., Harper R., Hawley J.S., Hoff J.T., Hysert D.W., Konis T.J., Larmond E., Larson J.W., Lepage M., Lewis M.J., Likens S., McGill L., Markl K.S., Moll M., Rolfe Morrison G., Muller J.E., Noble A.C., O'Brien T.J., Palamand R.S., Pangborn R.M., Pastrana F., Powers J.J., Prell P.A., Schmitt D.J., Schwiesow M., Seigel J., Vargas G., Williams R.S., Word K., Cutaia A.J. 1983. Sensory analysis. Journal of the American Society of Brewing Chemists. The Science of Beer. Sensory Analysis. Journal of the American Society of Brewing Chemists, 41(3), 95–98. https://doi.org/10.1094/ASBCJ-41-0095

Mielle P. 1996. Electronic noses: Towards the objective instrumental characterization of food aroma. Trends in Food Science and Technology, 7, 432–438.

Mielle P., Marquis F. 1999. Gas sensor arrays (electronic noses): A study about the speed/accuracy ratio. Proceedings of Eurosensors, 68, 9–16. https://doi.org 10.1016/S0925-4005(00)00509-8

Nicolli K.P., Biasoto A.C.T., Souza-Silva E.A., Guerra C.C., dos Santos H.P., Welke J.E., Zini C.A. 2018. Sensory, olfactometry and comprehensive two-dimensional gas chromatography analyses as appropriate tools to characterize the effects of vine management on wine aroma. Food Chemistry, 15(243), 103–117. https://doi.org. 10.1016/j.foodchem.2017.09.078

Payel D., Piyush K., Navdeep J., Ruchi R. 2018. Role of Electronic Nose Technology in Food Industry. Conference: Emerging Sustainable Technolgies in Food Processing (ESTFP-2018).

Plutowska B. 2008. Wykorzystanie technik instrumentalnych do oceny jakości organoleptycznej i rozróżniania destylatów rolniczych i miodów. Rozprawa doktorska, Katedra Chemii Analitycznej, Wydział Chemii, Politechnika Gdańska.

Plutowska B., Wardnecki W. 2012. Gas chromatography-olfactometry of alcoholic beverages. [In:] Alcoholic Beverages. Sensory Evaluation and Consumer Research. Ed. J. Piggott. Woodhead Publishing Limited, 101–130. https://doi.org/10.1533/9780857095176.1.101

Rodriguez Gamboa J.C., Albarracin E.S., da Silva A.J., Ferreira T.A.E. 2019. Electronic nose dataset for detection of wine spoilage thresholds. Data in Brief, 25, 104202. https://doi.org/doi.org/10.1016/j.dib.2019.104202

Santos J.P., Lozano J., Aleixandre M. 2017. Electronic noses applications in beer technology. [In:] Brewing Technology. Intech Open. 177–200. https://doi.org/10.5772/intechopen.68822

Soares da Costa M., Goncalves C., Ferreira A., Ibsen C., Guedes dePincho P., Silva Ferreira A.C. 2004. Further insights into the role of methional and phenylacetaldehyde in lager beer flavor stability. Journal of Agricultural and Food Chemistry, 52, 7911–7917.

Sparkman O.D., Penton Z.E., Fulton G.K. 2011. Esters. [In:] Gas Chromatography and Mass Spectometry. A Practical Guide. Second Edition. Eds. O.D. Sparkman, Z.E. Penton, G.K. Fulton. Elsevier, Netherlands.

Śliwińska M., Wiśniewska P., Dymerski T., Wardencki W., Namieśnik J. 2016. Application of electronic nose based on fast GC for authenticity assessment of Polish homemade liqueurs called nalewka. Food Analytical Methods, 9, 2670–2681.

Thibaud F., Courregelongue M., Darriet P. 2020. Contribution of volatile odorous terpenoid compounds to aged cognac spirits aroma in a context of multicomponent odor mixtures. Journal of Agricultural and Food Chemistry, 68(47), 13310–13318. https://doi.org/10.1021/acs.jafc.9b06656

Triqui H., Bouchriti N. 2003. Freshness assessments of Moroccan sardine (Sardina pilchardus): comparison of overall sensory changes to instrumentally determined volatiles. Journal of Agricultural and Food Chemistry, 51, 7540–7546.

Turek P., Chmielewski J. 2006. Nos elektroniczny jako nowoczesne narzędzie w ocenie jakości wyrobów. Zeszyty Naukowe Akademii Ekonomicznej w Krakowie, 718, 147–160.

Wardnecki W., Chmiel T., Dymerski T. 2013. Gas chromatography-olfactometry (GC-O), electronic noses (e-noses) and electronic tongues (e-tongues) for in vivo food flavour measurement. [In:] Instrumental Assessment of Food Sensory Quality. Ed. D. Kilcast. Woodhead Publishing Limited, Cambridge (UK), Philadelphia (USA), 195–229. https://doi.org/10.1533/9780857098856.2.195

Wilkes J.G., Conte E.D., Kim Y., Holcomb M., Sutherland J.B., Miller D.W. 2000. Sample preparation for the analysis of flavors and off-flavors in foods. Journal of Chromatography A, 880, 3–33.

Wilson A.D., Baietto M. 2009. Applications and advances in electronic-nose technologies. Sensors (Basel), 9(7), 5099–5148. https://doi.org/10.3390/s90705099

Witrick K., Pitts E.R., O'Keefe S.F. 2020. Analysis of lambic beer volatiles during aging using gas chromatography-mass spectrometry (GCMS) and gas chromatography-olfactometry (GCO). Beverages, 6(2), 31. https://doi.org/10.3390/beverages6020031

Wu X., Zhu J., Wu B., Zhao C., Sun J., Dail C. 2019. Discrimination of Chinese liquors based on electronic nose and fuzzy discriminant principal component analysis. Foods, 8(1), 38. https://doi.org/10.3390/foods8010038

Voss H.G.J., Júnior J.J.A.M., Farinelli M.E., Stevan S.L. 2019. A prototype to detect the alcohol content of beers based on an electronic nose. Sensors (Basel), 19(11), 2646. https://doi.org/10.3390/s1911264

Yu H., Dai X., Yao G., Xiao Z. 2014. Application of gas chromatography-based electronic nose for classification of chinese rice wine by wine age. Food Analytical Methods, 7(7), 1489–1497. https://doi.org/10.1007/s12161-013-9778-2

V IMAGE ANALYSIS AS A USEFUL TOOL IN MEASURING PHYSICAL PROPERTIES OF OBJECTS

Wiktor BERSKI

Department of Carbohydrates Technology and Cereal Processing,
Faculty of Food Technology, University of Agriculture in Krakow,
Aleja Mickiewicza 21, 31-120 Krakow, Poland

wiktor.berski@urk.edu.pl
ORCID: https://orcid.org/0000-0002-0183-933X

Abstract. Image analysis (IA) is a powerful tool allowing to extract numerical information from acquired images, like for example physical dimensions, color or shape. This method can be applied both for scientific purposes or industrial processing and quality control.

This manuscript briefly discusses about methods applied for physical dimensions measurement by tests based on different principles. Therefore, a concept of equivalent sphere is introduced. Also the importance of particle size distribution (PSD) is analyzed, and method to transform numeric based distribution into volume one is described. Moreover, some IA open source software utilization in measurement of physical dimensions is discussed.

Keywords: image analysis, physical property, quality control

1. Introduction

Usually, when we think about image analysis (IA), we mean sophisticated devices (digital IA), but we forget that our minds also have equally complicated operations related to the perception, recognition and analysis of the perceived objects, which in turn translates into the actions we take. Image analysis (IA) is a powerful tool providing information about size, shape, color or other feature that can be drawn from a picture of object(s) by means of digital image processing techniques. Artificial IA can be as simple as reading bar coded tags or as sophisticated as identifying a person from their face or potato chips color during online inspection. It is a common practice for manufacturers of image acquisition devices to provide dedicated image processing software, but usually these programs are not very complex and do not allow more complex image manipulations. But there are plenty of public domain (its source code is openly available and its use is license free) image processing programs already available. Among them, ImageJ[1] holds a unique position because it runs on any operating system, is easy to use, and can perform a full set of imaging manipulations and it has already a huge and knowledgeable user community [Abramoff et al. 2004; Solomon and Breckon 2011].

2. Measurement of physical dimensions

Physical dimensions can be measured by different means, and scaled ruler can be the simplest example. The classically used methods for a measurement of physical dimensions of various material are summarized below and in Table 1 [Fayed and Otten 1997; Jillavenkatesa et al. 2001; Allen 2003; Masuda et al. 2006]:

- Sieving is material separation based on size or some other physical characteristic, and it is among the most often used and least expensive techniques for PS and PSD determination over a broad size range, from over 100 mm to about 20 μm. A sieve is a measuring device designed to retain particles larger than a designated size, while allowing smaller particles to pass through openings. PSD is reported as the mass of the material

[1] ImageJ can be easily downloaded from https://imagej.nih.gov/ij/index.html
Manual for ImageJ https://imagej.nih.gov/ij/docs/guide/user-guide.pdf
Similar program can be obtained from this site in different language version http://www.pl.euhou.net/

retained on a mesh of given size. An example of such analysis is grain selectiveness and uniformity (homogeneity) (Celność i wyrównanie ziarna) [Jillavenkatesa et al. 2001].

- Sedimentation-based methods rely on the measurement of the velocity with which particles in a fluid settle due to the gravitational forces acting on the particle, against the buoyancy of the fluid and other drag forces acting against the settling of particles. This relationship is expressed by Stokes' law, which is valid only for particles settling under conditions of terminal velocity and non-turbulent. This principle was adopted in development of different sedimentation scales, and also in pipette method [Jillavenkatesa et al. 2001].
- Microscopy-based techniques for PS measurement involve direct observation of particles and the consequent determination of size based on a defined measure of diameter. Typically, the calculated sizes are expressed as the equivalent diameter (diameter of a sphere that has the same projected area as the projected image of the particle). When compared to other techniques of particle size analysis, a significant advantage of microscopy-based techniques lies in the ability to determine the particle shape, in addition to making a direct measurement of size. Unfortunately this method is time consuming and tedious. Introduction of VEM (Video Enhanced Microscopy) and application of IA software allowed to decrease amount of time needed to perform analysis and increased an accuracy and replication of measurements. Different types of instruments can be applied, from optical microscopes scanning electron microscopes (SEM) transmission electron microscopes (TEM) and atomic force microscopy (AFM). The type of the applied instrument is governed by the size range of the materials being studied, magnification, and resolution that is desired [Jillavenkatesa et al. 2001; Sikora et al. 2015, 2017; Krystyjan et al. 2016; Dobosz et al. 2019].
- Laser instruments for PS and PSD determination are based upon the same general principles of laser beam diffraction, but the application of different components, configurations, and algorithms gives rise to a broad selection of instruments with analysis capabilities covering a broad range of sizes. The interaction of a particle and light incident upon it gives rise to four different but inherently related scattering phenomena, namely, diffraction, refraction, reflection and absorption. The basic principle laser diffraction measurements is that the scattered light pattern formed at the detector is a summation of the scattering pattern produced by each particle that is being sampled. Deconvolution of the resultant pattern can

generate information about the scattering pattern produced by each particle and, upon inversion, information about the size of that particle. Some problems can occur as a consequence of light multiple scattering, i.e. the phenomenon where light scattered from one particle interacts with another particle and gets scattered again. So such situations has to be eliminated by the sample concentration limit [Jillavenkatesa et al. 2001; Ptaszek and Ptaszek 2006; Sikora et al. 2015].

- Image analysis can be applied to measure, as previously mentioned, a objects dimensions extracted from microscopic images, but also from image acquired by other means like desktop scanner or digital camera [Shouche et al. 2001; Wiwart et al. 2006, 2012; Kumari and Rana 2015; Laucka et al. 2020]

Image analysis (IA) allows to perform measuring procedure on previously stored images acquired by different means like video/digital camera, mobile phone camera or camera attached to the microscope (VEM). But it should be taken into consideration, that in order to know exact dimension extracted from a digital image, a scaling procedure has to be implemented[2], because digital images, even taken by the same equipment, can be collected at different conditions (different resolution of images, or the same camera can be applied to take the image of bread loaf, or attached to microscope can take digital images of yeast cell for instance). Measured dimension will depend on the shape of the object, and on the principle of the applied method. In some instances there is no a good mean to characterize an investigated object dimension. For spherical objects the most obvious choice it will be diameter (denoted as D or d), and for elongated or irregular shape objects the longest distances among two points on object (also called as Feret) will be more appropriate. We should keep in mind, that various measurement methods provide different information about tested material. For example, laser light scattering (laser diffraction) is reporting in terms of Equivalent Spherical Diameter (or Volume Weighted Equivalent Spherical Diameter), and data obtained from microscopy analyze can be given as Feret or as an equivalent diameter calculated from the object surface area. Equivalent spherical diameter is defined by ISO 9276-1 [1998] as the diameter of a sphere having the same physical properties as the particle under examination. Because there is no ideal way to describe the size of actual object, therefore a concept of equivalent diameter was introduced (Figs. 1–2).

[2] An example of such procedure is described below https://imagej.nih.gov/ij/docs/pdfs/examples.pdf [accessed: February 17, 2021].

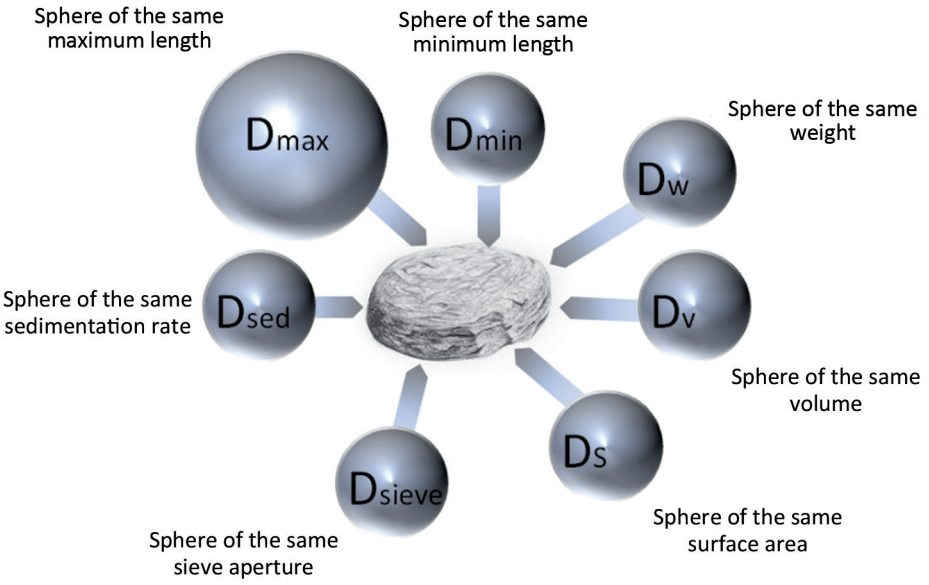

Fig. 1. Concept of equivalent spheres (source: based on Malvern [2015])

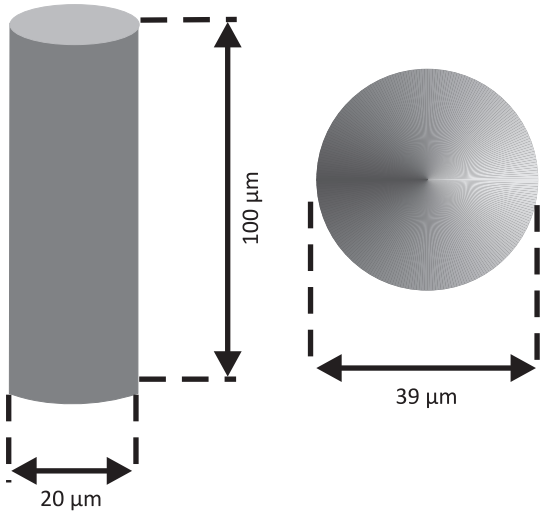

Fig. 2. Volume equivalent rod and sphere (source: based on Rawle [2003])

But it should be kept in mind, that various measurement methods provide different information about tested material. For example, laser light scattering (laser diffraction) is reporting in terms of Equivalent Spherical Diameter (or Volume Weighted Equivalent Spherical Diameter).

In order to characterize the sample by the specific values: the mean (average value), median and mode can be used. Mean is the average size of a population, median: size where 50% of the population is below/above this value and mode is the size with highest frequency (highest occurrence). In other word mode value represents a peak value.

There are various means, that can be defined depending upon how the distribution data are collected and analysed[3]. The most common in use are number length mean, surface area mean and volume moment mean. Number length mean (D[1,0] or Xnl) is just the arithmetic mean. It is most valid where the number of particles is of interest. It can be calculated only if the total number of particles in the sample is known. Surface area mean (D[3, 2] or Xsv) is also known as Sauter Mean Diameter. It is applicable, where specific surface area is important (bioavailability, reactivity, solubility). It is very sensitive to the presence of fine particulates in the size distribution. Finally, the volume moment mean (D[4, 3] or Xvm), or De Brouckere Mean Diameter is relevant for many samples as it reflects the size of those particles which constitute the bulk of the sample volume. It is very sensitive to the presence of large particles.

ImageJ procedure of analysis

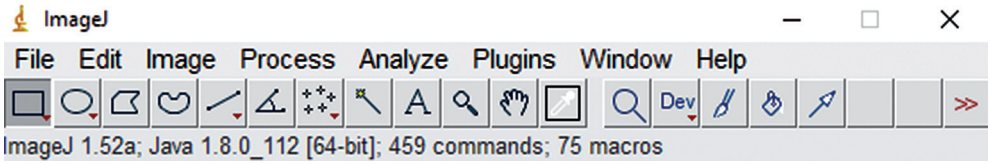

Fig. 3. ImageJ panel (source: based on Ferreira and Rasband [2012])

In order to perform a measurement procedure using ImageJ the following steps has have to be performed. After launching a ImageJ (Fig. 3) scaling procedure has to be performed. A picture containing scale or object of known dimensions has to be open. It is important, that all pictures used in this procedure have

[3] Description of some different means, used to describe different material was presented as appendix.

to be in the same resolution, because initial measurement is performed in pixels, and later on pixels are converted to the right unit [Solomon and Breckon 2011; Ferreira and Rasband 2012].

Then select straight (as indicated by the arrow) and draw a line over a scale. Next use Analyse → Set Scale. In Set Scale window enter appropriate value into the "Known Distance" box and change the "Unit of Measurement" box to appropriate value, check "Global". Next draw a new line and confirm that the measurement scale is correct Analyze → Measure or Ctrl+M). Now measurement procedure in manual mode can be done by simply drawing a line over object of interest.

In order to perform analysis in automatic mode the picture has to be converted to grayscale (Image → Type → 8-bi). Then threshold the image using the automated routine (Process → Binary →Make Binary). In order to measure/analyse objects it has to be decided what values will be chosen (Analyze → Set Measurements), and the direct measurement will be performed (Analyze → Analyze Particles). In a new window an appropriate particle size should be entered in order to eliminate too small objects or "noise". Other factor allowing to eliminate undesirable object is circularity (Circ), which is defined as $Circ = 4\pi \cdot \frac{Area}{Perimeter^2}$ (it takes values among 0 (increasingly elongated shape) and 1 (perfect circle); values may not be valid for very small particles) [Ferreira and Rasband 2012]. Then toggle "Show Outlines", check "Display Results", "Summarize" and "Record Stats" and click "OK".

3. Particle size distribution (PSD)

In industrial processing, including food industry, some raw bulky materials, and products are in the form of powder or fine/coarse particles (flours, groats, sugar, salt etc.). Knowledge of particle sizes (PS) and the particles size distribution (PSD) is required for most production and processing operations. PS and PSD influences many properties of particulate materials and provides a valuable information about their quality and performance. It applies for powders, suspensions, emulsions, and aerosols. Both the size and shape of powders influences their flow and compaction properties. Larger, more spherical particles will typically flow more easily than smaller. Smaller particles dissolve more quickly and lead to higher suspension viscosities than larger ones. Smaller droplet sizes and higher surface charge (zeta potential) will typically improve suspension and emulsion stability.

Powder or droplets in the range of 2–5 μm aerosolize better and will penetrate into lungs deeper than larger sizes. For these and many other reasons it is important to measure and control the particle size distribution (PSD) of many products. Substantial production losses can be incurred due to high rejection rates if size and size distribution of material applied in a process are not adequately controlled [Jillavenkatesa et al. 2001; Horiba 2013; Kumari and Rana 2015; Malvern 2015; Laucka et al. 2020]

Material size and size distribution can be determined using numerous techniques and instruments, depending on the material size and nature (Tab. 1) [Jillavenkatesa et al. 2001].

Table 1. Particle size analysis instruments (source: based on Jillavenkatesa et al. [2001])

Instrumental Technique	Physical Principle	Size Range (μm)
Acoustic Attenuation Spectroscopy (N) [Ulltrasonic Attenuation Spectroscopy]	ultrasonics	0.05 to 10
Centrifugal Sedimentation-Optical (E)	sedimentation	0.01 to 30
Centrifugal Sedimentation-X-Ray (E)	sedimentation	0.01 to 100
Electrical Resistance Zone Sensing (E) [Particle Counting, Coulter Counter]	particle counting	0.4 to 1200
Electroacoustic Spectroscopy (N) [Electrokinetic Sonic Amplitude]	ultrasonics	0.1 to 10
Gas Absorption Surface Area Analysis (E) [BET Absorption]	surface area analysis	NA
Laser Light Diffraction (E) [Static Light Scattering, Mie Scattering, Elastic Light Scattering]	electromagnetic wave interaction and scattering	0.04 to 1000
Light Microscopy (E)	particle counting	> 1.0
Quasi-Elastic Light Scattering (E) [Dynamic Light Scattering, Photon Correlation Spectroscopy, Optical Beating Spectroscopy]		< 0.005

Instrumental Technique	Physical Principle	Size Range (μm)
Scanning Electron Microscopy (E)	particle counting	> 0.1
X-Ray Gravitational Sedimentation (E)	sedimentation	0.5 to 100
Colloid Vibration Current (N) [Single Frequency]	ultrasonics	< 10
Electrokinetic Sonic Amplitude (N) [single frequency]	ultrasonics	< 10
Microelectrophoresis (E) [Laser Light Scattering, Quasi-Elastic Light Scattering]	electromagnetic wave interaction and scattering	0.1 to 1
Sieving (E)	sieving	5 to 100,000

E – Established Technique; N – Emerging Technique; ID – Instrument Dependent

It is important to understand that different instruments are operating on different physical principles, so some discrepancies in the results obtained from these instruments can be encountered. Furthermore, even when applying equipment based on the same physical principle, the algorithms or components applied by the manufacturer, and variations in adaptations of the same basic physical principle, and even a sample treatment can influence the result [Fayed and Otten 1997; Jillavenkatesa et al. 2001; Allen 2003; Masuda et al. 2006; Kumari and Rana 2015; Laucka et al. 2020].

In order to characterize a population of particles an average (mean) is not a sufficient tool, as well as median or mode. More appropriate way to describe a population is to create PSD. According to Vigneau et al. [2000] the minimal number of objects necessary to prepare it is 500.

Using classical microscopic method it would be really time consuming, boring and hard work to measure this 500 objects manually. Fortunately with the application of VEM and IA such task can be performed much easier and faster. Obtained data can be presented as histogram or cumulative curve (Figs. 4–5). Both ways of presentation can provide an important information.

In order to prepare histogram collected data should be divided into classes (bins), that can be equal in size or not. The number of classes depends on data application. A good practice is to establish the total number of classes (n), and class span (s) could be calculated:

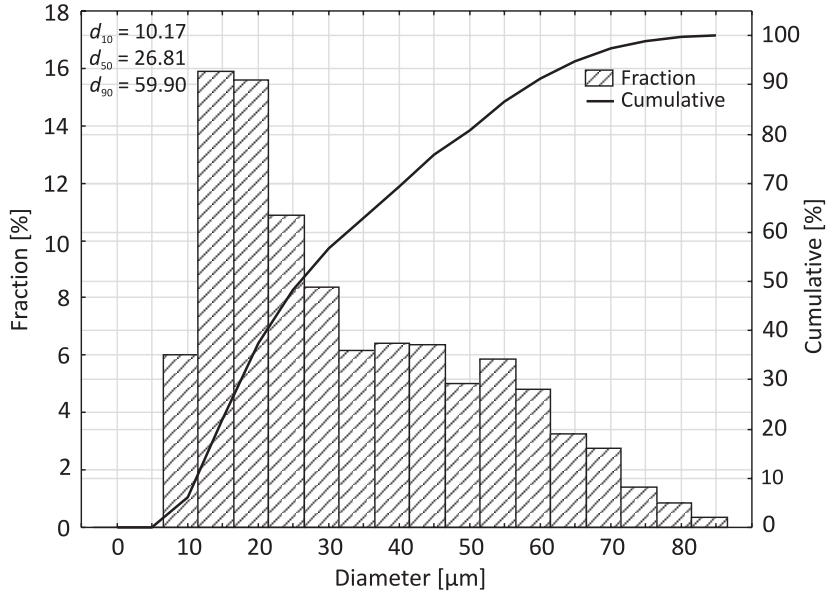

Fig. 4. Particle size distribution (PSD) of potato starch (source: own research)

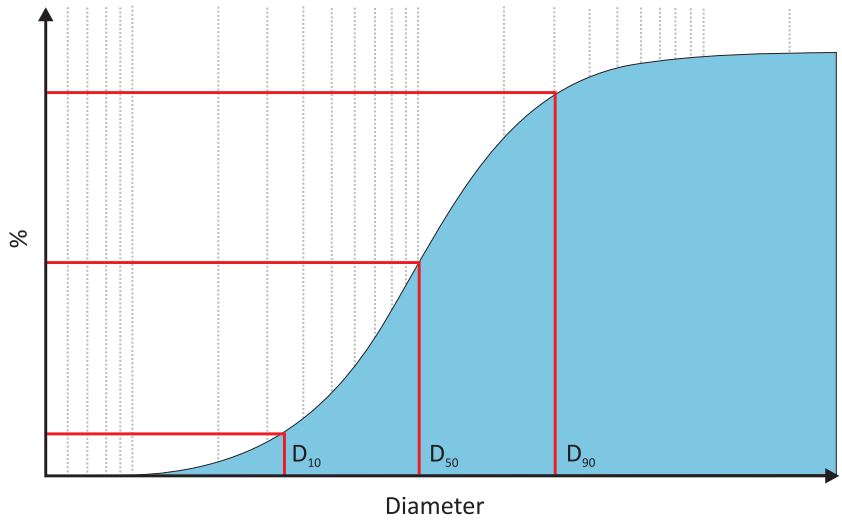

Fig. 5. Illustration of the most common percentiles reported (Dv10, Dv50 and Dv90), as illustrated in the frequency and cumulative plots (source: based on Malvern [2015])

$$S = \frac{d_{\max} - d_{\min}}{n},$$

where $d_{\max}$ and $d_{\min}$ are maximum and minimum diameter, respectively (numerator value is called a range). Histogram can be easily converted into cumulative curve, just as sum of consecutive value of classes (graphically depicted as histogram columns).

Besides graphical representation of PSD data are also percentiles denoted as d_{10}, d_{50} or d_{90} (D_{10}, D_{50} and D_{90}) (Fig. 5). For example, d_{50}^4 refers to the 50th percentile, meaning the diameter of a particle at which 50% of the particles in the sample are smaller. Other terminology for the same value is D(v, 0.5), and "v" represents a volume weighted basis. Similarly, d_{10} is the 10th percentile = the diameter of a sphere at which 10% of the particles in the sample are smaller (D(v, 0.1) on a volume basis), and so on. The percentiles values can be extracted from cumulative curve.

ImageJ software allows to create a histogram of already measured sample. It is not possible to choose the span (or resolution/width) of the class, but only the number of classes can be selected.

4. Transformation of numeric based distribution into volume based

Interpretation of PS measurement results requires an understanding of which principle/technique was applied and the basis of the calculations. Each technique provides a different result since each measures different physical properties of the sample. The resulting PSD can be calculated based on several models: most often as a number or volume/mass distribution [Jillavenkatesa et al. 2001; Horiba 2013; Malvern 2015]. So it is really hard to compare data obtained by different techniques. Data extracted from microscopic images by means of IA procedure can be expressed as Feret or equivalent diameter, but they are number length based, and created PSD will be number based. On other hand data from laser scattering will be volume based, and those obtained by sieving or sedimentation method will be mass based.

But taking into considerations some assumptions it will be possible to make comparison. It will be explained on the following example. During IA of microscopic pictures a size of each particle is measured, and numeric value is assigned. It will allow to build a number based distribution – each particle has the same

weighting once the final distribution is calculated. Investigated particle population (Fig. 6) consists of ten elements in four diameter classes: three particles are 1μm, three are 2 μm, three are 3 μm and one is 5 μm. Building a number based PSD for this population will give result shown in Figure 6, where three first particle classes (1, 2 and 3 μm) account for 90% of the total (3 · 30%), and remaining class (single 5 μm diameter particle) for remaining 10%. In order to transform this number based into volume base distribution it has to be assumed that each particle is a perfect sphere, so it volume (v) is $v = \frac{4}{3} \cdot \pi \cdot r^3$, where r is radius ($r = d/2$). The volume of each particle is calculated, then the sum of volume for each class, and finally the total volume for all particles. Then the share of each class is calculated and volume based PSD is finally created. The smallest granules class (1 μm) now accounts for only 1.29%, 2 μm class for 10.30%, 3 μm class for 34.76%. And finally, the last class – single 5 μm particle accounts for more than 50%, 53.65% to be specific.

Pabst et al. [2006] proposed a more elaborated method of construction of volume-weighted PSD from image analysis data. The size distributions ob-

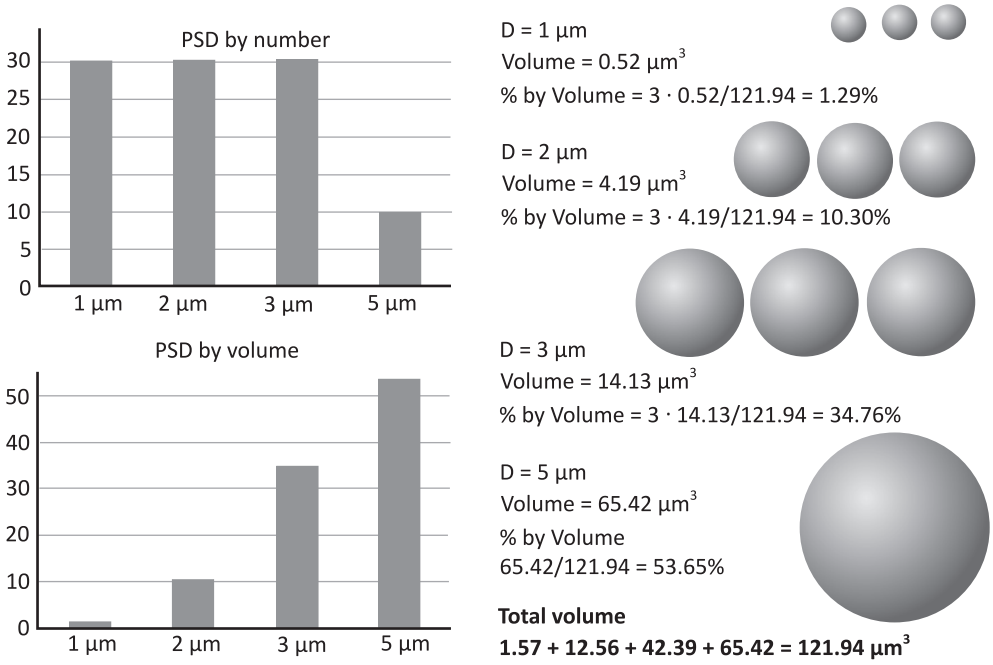

Fig. 6. Transformation of number based PSD into volume based one (source: based on Horiba [2013])

tained by image analysis (primary data in the form of number-weighted frequency histograms, denoted as $\boldsymbol{q_0}$) will required a transformation in order to obtain volume-weighted histogram denoted $\boldsymbol{Q_3}$). Such transformation can be termed $\boldsymbol{q_0} \rightarrow \boldsymbol{Q_3}$. This proposal PSD is based on projected area diameter ($\boldsymbol{D_p}$), $D_p = 2\sqrt{\frac{A}{\pi}}$, where A is the area of particle. The resolution/width of this PSD is 3.0 and total count of particles is 1308 (Tab. 2). First column contains Projected area diameter ($\boldsymbol{D_p}$), third absolute frequency (before first re-ordering) i.e. number of objects in each class $\boldsymbol{q_0}$ (Fig. 7A). There are few singular objects counted in the large-size region >85.5 m are solely due to statistical scatter ("noise"). Due to their large size (D_p) these few objects will have an extremely large volume ($\boldsymbol{D_p^3}$, data in second column) and therefore, can have a great impact on the volume weighted size distribution. This scatter is a consequence of the finite (i.e. relatively small) number of objects counted. A detailed inspection shows that similar conclusions hold for all values in the region > 58.5. Of course, the exact value of this **"cut-off size"** ($\boldsymbol{D_c}$) has to be individually fixed by inspection of each data set. The selection of D_c is a subjective decision, and cannot be done automatically. When D_c is defined, the absolute frequencies in the size range > D_C are re-ordered ("first re-ordering" – fourth column) and are shifted in decreasing order. The new, re-ordered frequency histogram as a whole ends at smaller sizes than the original one ("artificial damping") (Fig. 7B). In order to transform the re-ordered q_0 frequency histogram (number-weighted) into a volume-weighted q_3 histogram (relative partial volumes of the respective size classes, with the volume of the whole system normalized to unity). In order to perform it, just multiply values of $\boldsymbol{D_p^3}$ (second column) by corresponding q_0 values (third column). The resulting values (fifth column) must be added up, and then share for each class calculated (sixth column). Obtained data allowed to create a new volume based histogram (Fig. 7C).

It can be observed (Fig. 7C) peaks (so-called "modes") in the q_3 histogram (here at 64.5, 79.5 and 97.5) which are a consequence of the finite data set (too small number of objects counted). So as previously, a "second reordering" has to be performed for all relative partial volumes in the size range > *Dc* (here >58.5), and resulting data are stored in seventh column, allowing to create final histogram (Fig. 7D).

The proposed $q_0 \rightarrow q_3$ transformation can be summarized [Pabst et al. 2006]:

- choosing a "cut-off size" D_c,
- first re-ordering", corresponding to artificial damping (q_0 histogram),
- calculation of relative volumes ($q_0 \rightarrow q_3$),
- second re-ordering" (q_3 histogram)

Table 2. Size distribution in terms of projected area diameters D_p (source: based on Pabst et al. [2006])

D_p	D_p^3	Absolute frequency (before first re-ordering)	Absolute frequency (after first re-ordering) q_o	$D_p^3 \cdot q_0$	Relative volume (%) (before second re-ordering) q_3	Relative volume (%) (after second re-ordering) q_3
10.5	1157.6	15	15	17364.4	0.04	0.04
13.5	2460.4	112	112	275562.0	0.63	0.63
16.5	4492.1	197	197	884948.6	2.02	2.02
19.5	7414.9	197	197	1460730.4	3.33	3.33
22.5	11390.6	189	189	2152828.1	4.91	4.91
25.5	16581.4	151	151	2503787.6	5.71	5.71
28.5	23149.1	108	108	2500105.5	5.71	5.71
31.5	31255.9	76	76	2375446.5	5.42	5.42
34.5	41063.6	48	48	1971054.0	4.5	4.5
37.5	52734.4	42	42	2214843.8	5.06	5.06
40.5	66430.1	41	41	2723635.1	6.22	6.22
43.5	82312.9	26	26	2140134.8	4.88	4.88
46.5	100544.6	21	21	2111437.1	4.82	4.82
49.5	121287.4	22	22	2668322.3	6.09	6.09
52.5	144703.1	14	14	2025843.8	4.62	4.62
55.5	170953.9	11	11	1880492.6	4.29	4.29
58.5	200201.6	6	6	1201209.8	2.74	3.67
61.5	232608.4	5	6	1395650.3	3.19	3.51
64.5	268336.1	6	6	1610016.8	3.67	3.19
67.5	307546.9	3	5	1537734.4	3.51	2.74
70.5	350402.6	2	3	1051207.9	2.4	2.4

D_p	D_p^3	Absolute frequency (before first re-ordering)	Absolute frequency (after first re-ordering) q_o	$D_p^3 \cdot q_0$	Relative volume (%) (before second re-ordering) q_3	Relative volume (%) (after second re-ordering) q_3
73.5	397065.4	2	2	794130.8	1.81	2.29
76.5	447697.1	6	2	895394.3	2.04	2.12
79.5	502459.9	2	2	1004919.8	2.29	2.04
82.5	561515.6	0	1	561515.6	1.28	1.93
85.5	625026.4	0	1	625026.4	1.43	1.81
88.5	693154.1	1	1	693154.1	1.58	1.75
91.5	766060.9	1	1	766060.9	1.75	1.58
94.5	843908.6	1	1	843908.6	1.93	1.43
97.5	926859.4	0	1	926859.4	2.12	1.28
100.5	1015075.1	1	0	0.0	0.00	0
103.5	1108717.9	0	0	0.0	0.00	0
106.5	1207949.6	1	0	0.0	0.00	0
109.5	1312932.4	0	0	0.0	0.00	0
112.5	1423828.1	1	0	0.0	0.00	0
	Σ	1308	1308	43813325,3	100	

Shaded cell contain data subjected to first and second re-ordering

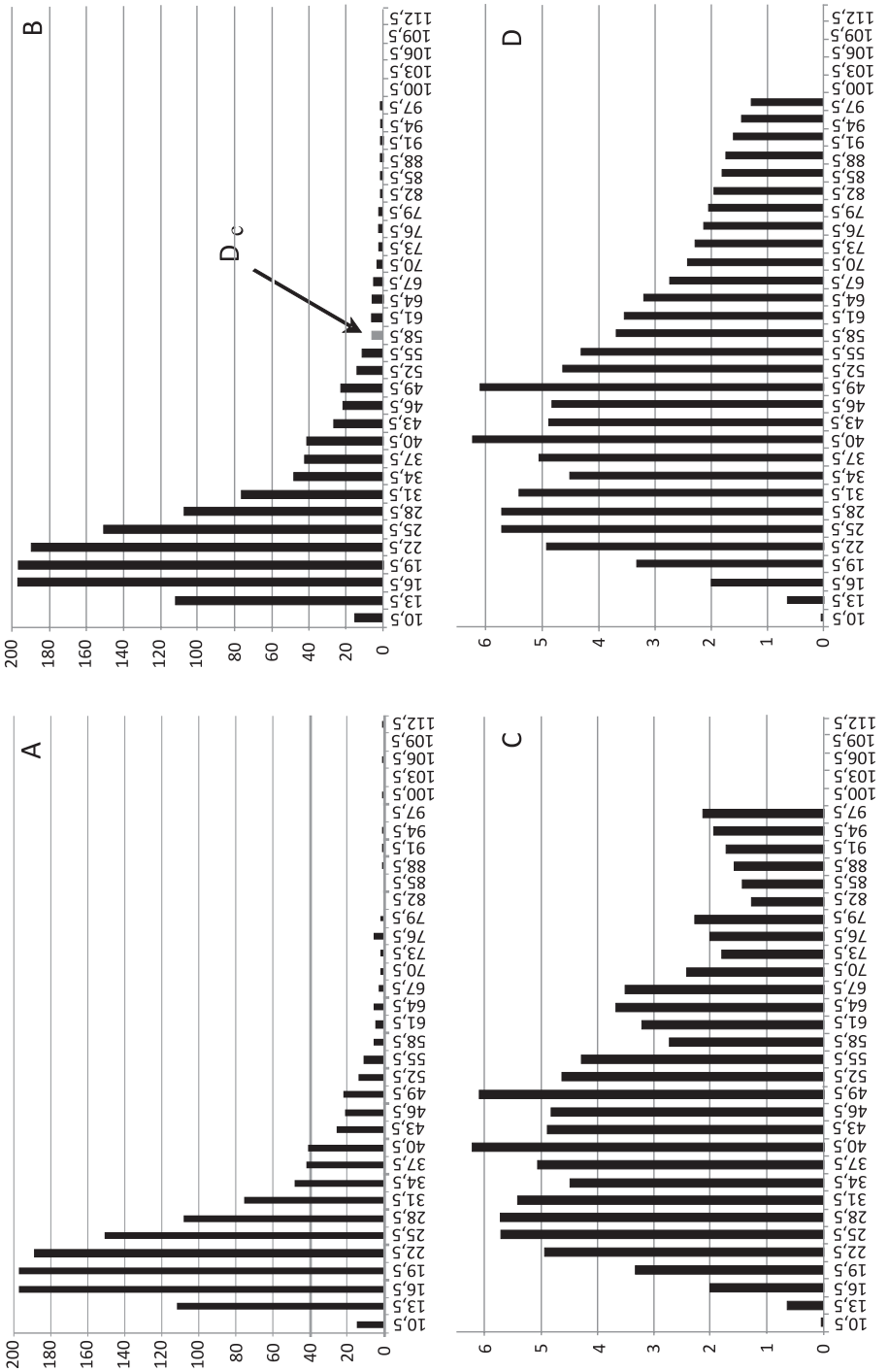

Fig. 7. Size distribution in terms of projected area diameters: number-weighted frequency (q_0) histogram before first re-ordering (A), number-weighted frequency (q_0) histogram after first re-ordering (B), volume-weighted frequency (q_3) histogram before second reordering (C), volume-weighted frequency (q_3) histogram after second reordering (D) (source: based on Pabst et al. [2006])

5. Aeration measurements

The field, which seems to be perfectly suited for the application of IA is an investigation of aeration (expansion) of food products, among others. It will include measurements of bread crumb pores size (porosity) [Gonzales-Barron and Butler 2006; Wang et al. 2013; Ziobro et al. 2013; Gumul et al. 2015; Korus et al. 2015; Rathnayake et al. 2018] and also foam gas bubbles diameters [Ptaszek et al. 2014; Żmudziński et al. 2014].

In classical approach bread porosity was measured by crumb sample pressing, which physical dimensions were previously measured, in order to remove pores. Crumb deprived of pores was formed into balls, which were submerged in a graduated cylinder with known volume of oil. Knowing the initial volume of crumb (with pores) and crumb deprived of pores it was possible to calculate porosity [Korus et al. 2012]. Unfortunately this method gave no idea about pores size distribution, but only general idea about porosity.

For bubble size measurement a different method can be applied [Pugh 2016] also optical fibre probe analysis, X-ray tomographic imaging, nuclear magnetic resonance imaging and terahertz spectroscopy, ultrasonic imaging and multiple light scattering and back-scattering can be employed. All these methods will require a rather complicated (and costly) equipment, so IA seems to the best cost-effect option.

6. Conclusion

Year by year, image analysis finds new and new applications in many areas of life, including obtaining data for the purposes of scientific research. Its development is largely influenced by the availability of free software, such as the discussed above ImageJ. The above-mentioned possibilities for obtaining information with image analysis are only a small part of the wide spectrum of possibilities offered by this method. In addition to direct measurement of the size of objects, it is possible to further analyse the obtained data using shape descriptors, or to determine the porosity of bread, the size of foam gas bubbles forming foam, or to determine the color.

References

Abramoff M.D., Magalhães P.J., Ram S.J. 2004. Image processing with ImageJ. Biophotonics International, 11(7), 36–42.

Allen T. 2003. Powder SAMPLING and Particle Size Determination (1st ed.). Elsevier Science. https://www.elsevier.com/books/powder-sampling-and-particle-size-determination/allen/978-0-444-51564-3 [accessed: February 17, 2021].

Anonymous. 2013. MaS control ANALYSETTE 22. Software Manual version 1.035. Fritsch GmbH. Milling and Sizing.

Dobosz A., Sikora M., Krystyjan M., Tomasik P., Lach R., Borczak B., Berski W., Lukasiewicz M. 2019. Short- and long-term retrogradation of potato starches with varying amylose content. Journal of the Science of Food and Agriculture, 99(5), 2393––2403. https://doi.org/10.1002/jsfa.9446

Fayed M., Otten L. 1997. Handbook of Powder Science & Technology (2nd ed.). Springer US. https://doi.org/10.1007/978-1-4615-6373-0

Ferreira T., Rasband W. 2012. ImageJ User GuideIJ 1.46r. http://imagej.nih.gov/ij/docs/guide [accessed: October 3, 2022].

Gonzales-Barron U., Butler F. 2006. A comparison of seven thresholding techniques with the k-means clustering algorithm for measurement of bread-crumb features by digital image analysis. Journal of Food Engineering, 74(2), 268–278. https://doi.org/10.1016/j.jfoodeng.2005.03.007

Gumul D., Ziobro R., Korus J., Krystyjan M., Witczak T., Zięba T., Gambuś H. 2015. Effect of potato starch extrudates on the physical properties and staling of wheat bread. Starch – Stärke, 67(5–6), 540–548. https://doi.org/10.1002/star.201400229

Horiba. 2013. A Guidebook to Particle Size Analysis. Horiba Instruments, Inc. https://www.horiba.com/en_en/en-en/products/by-segment/scientific/particle-characterization/particle-guidebook/ [accessed: February 17, 2021].

ISO. 1998. ISO 9276-1 Representation of Results of Particle Size Analysis – Part 1: Graphical Representation. https://www.iso.org/cms/render/live/en/sites/isoorg/contents/data/standard/02/58/25860.html [accessed: February 17, 2021].

Jillavenkatesa A., Lum L.S.H., Dapkunas S. 2001. NIST Recommended Practice Guide: Particle Size Characterization. https://www.nist.gov/publications/nist-recommended-practice-guide-particle-size-characterization [accessed: February 17, 2021].

Korus J., Juszczak L., Ziobro R., Witczak M., Grzelak K., Sójka M. 2012. Defatted strawberry and blackcurrant seeds as functional ingredients of gluten-free bread. Journal of Texture Studies, 43(1), 29–39. https://doi.org/10.1111/j.1745-4603.2011.00314.x

Korus J., Witczak M., Ziobro R., Juszczak L. 2015. The influence of acorn flour on rheological properties of gluten-free dough and physical characteristics of the bread. European Food Research and Technology, 240(6), 1135–1143. https://doi.org/10.1007/s00217-015-2417-y

Krystyjan M., Sikora M., Adamczyk G., Dobosz A., Tomasik P., Berski W., Łukasiewicz M., Izak P. 2016. Thixotropic properties of waxy potato starch depending on the degree of the granules pasting. Carbohydrate Polymers, 141, 126–134. https://doi.org/10.1016/j.carbpol.2015.12.063

Kumari R., Rana N. 2015. Particle size and shape analysis using imageJ with customized tools for segmentation of particles. International Journal of Engineering Research & Technology, 4(11). https://www.ijert.org/research/particle-size-and-shape-analysis-using-imagej-with-customized-tools-for-segmentation-of-particles-IJERTV4IS110211.pdf, https://www.ijert.org/particle-size-and-shape-analysis-using-imagej-with-customized-tools-for-segmentation-of-particles [accessed: February 17, 2021].

Laucka A., Andriukaitis D., Valinevicius A., Navikas D., Zilys M., Markevicius V., Klimenta D., Sotner R., Jerabek J. 2020. Method for volume of irregular shape pellets estimation using 2D imaging measurement. Applied Sciences, 10(8), 2650. https://doi.org/10.3390/app10082650

Malvern. 2015. A Basic Guide to Particle Characterization. Malvern Instruments Limited. www.malvern.com [accessed: February 17, 2021].

Masuda H., Higashitani K., Yoshida H. 2006. Powder Technology Handbook. CRC Press, Boca Raton. https://doi.org/10.1201/9781439831885

Pabst W., Berthold C., Gregorová E. 2006. Size and shape characterization of polydisperse short-fiber systems. Journal of the European Ceramic Society, 26(7), 1121–1130. https://doi.org/10.1016/j.jeurceramsoc.2005.01.053

Ptaszek P., Ptaszek A. 2006. Zastosowanie metod rozpraszania światła w analizie żywności. Laboratorium, 3, 47–50.

Ptaszek P., Żmudziński D., Kruk J., Kaczmarczyk K., Rożnowski W., Berski W. 2014. The physical and linear viscoelastic properties of fresh wet foams based on egg white proteins and selected hydrocolloids. Food Biophysics, 9(1), 76–87. https://doi.org/10.1007/s11483-013-9320-5

Pugh R.. 2016. Bubble Size Measurements and Foam Test Methods. [In:] Bubble and Foam Chemistry. Ed. R. Pugh (pp. 372–404). Cambridge University Press, Cambridge. https://doi.org/10.1017/CBO9781316106938.012

Rathnayake H.A., Navaratne S.B., Navaratne C.M. 2018. Porous crumb structure of leavened baked products. International Journal of Food Science, 2018, e8187318. https://doi.org/10.1155/2018/8187318

Rawle A. 2003. The basic principles of particle size analysis. Surface Coatings International Part A. Coatings Journal, 86(2), 58–65.

Shouche S.P., Rastogi R., Bhagwat S.G., Sainis J.K. 2001. Shape analysis of grains of Indian wheat varieties. Computers and Electronics in Agriculture, 33(1), 55–76. https://doi.org/10.1016/S0168-1699(01)00174-0

Sikora M., Adamczyk G., Krystyjan M., Dobosz A., Tomasik P., Berski W., Lukasiewicz M., Izak P. 2015. Thixotropic properties of normal potato starch depending on the degree of the granules pasting. Carbohydrate Polymers, 121, 254–264. https://doi.org/10.1016/j.carbpol.2014.12.059

Sikora M., Dobosz A., Krystyjan M., Adamczyk G., Tomasik P., Berski W., Kutyła-Kupidura E.M. 2017. Thixotropic properties of the normal potato starch – Locust bean gum blends. Lebensmittel-Wissenschaft & Technologie, 75, 590–598. https://doi.org/10.1016/j.lwt.2016.10.011

Solomon C.J., Breckon T.P. 2011. Fundamentals of Digital Image Processing: A Practical Approach with Examples in Matlab. John Wiley & Sons, Ltd. https://doi.org/10.1002/9780470689776

Vigneau E., Loisel C., Devaux M.F., Cantoni P. 2000. Number of particles for the determination of size distribution from microscopic images. Powder Technology, 107(3), 243–250. https://doi.org/10.1016/S0032-5910(99)00192-8

Wang J., Xie A., Zhang C. 2013. Feature of air classification product in wheat milling: Physicochemical, rheological properties of filter flour. Journal of Cereal Science, 57(3), 537–542. https://doi.org/10.1016/j.jcs.2013.03.001

Wiwart M., Moś M., Wójtowicz T. 2006. Studies on the imbibition of triticale kernels with a different degree of sprouting, using digital shape analysis. Plant, Soil and Environment, 52(7), 328–334.

Wiwart M., Suchowilska E., Lajszner W., Graban Ł. 2012. Identification of hybrids of spelt and wheat and their parental forms using shape and color descriptors. Computers and Electronics in Agriculture, 83, 68–76. https://doi.org/10.1016/j.compag.2012.01.015

Ziobro R., Korus J., Juszczak L., Witczak T. 2013. Influence of inulin on physical characteristics and staling rate of gluten-free bread. Journal of Food Engineering, 116(1), 21–27. https://doi.org/10.1016/j.jfoodeng.2012.10.049

Żmudziński D., Ptaszek P., Kruk J., Kaczmarczyk K., Rożnowski W., Berski W., Ptaszek A., Grzesik M. 2014. The role of hydrocolloids in mechanical properties of fresh foams based on egg white proteins. Journal of Food Engineering, 121, 128–134. https://doi.org/10.1016/j.jfoodeng.2013.08.020

Appendix

This section is intended to describe the meaning of different notations used in description of different diameter values, that can be encountered when working with laser size meters. This description is based on Fritsch manual (Anonymous, 2013).

1. Length-related average value of the number distribution

How to express an average diameter of three balls with diameters 1, 2 and 3 units. The most natural answer is 2, because all the diameters were added together ($\Sigma d = 1 + 2 + 3$) and divided this by the number of particles ($n = 3$).

This is a numerical mean (more specifically, the length-related mean of the number distribution) (Anonymous, 2013), because the number of particles appears in the equation:

$$D\left[1,0\right] = \frac{1+2+3}{3} = \frac{\sum d^1}{\sum d^0} = 2.00$$

Mathematically, itis described as $D[1,0]$ because the diameters (d^1) appear in the top of the equation and no diameters (d^0) appear in the bottom of the equation, but rather the number of particles. The first index is the exponent of the grain size d; the second index is the quantity type of the measured distribution.

In some areas (i.e. catalysis), the aforementioned balls should be compared on the basis of their surface area, because the efficiency of a catalyst increases when its surface area increases (Anonymous, 2013). The surface area of a ball is $4 \cdot \pi \cdot r^2$. In order to make the comparisons based on this factor (surface area), it is necessary to calculate the square of the diameters, divided by the number of particles, and then take the square root in order to get back to a mean diameter:

$$D\left[2,0\right] = \sqrt[2]{\frac{\left(1^2+2^2+3^2\right)}{3}} = \sqrt[2]{\frac{\left(1+4+9\right)}{3}\frac{\sum d^2}{\sum d^0}} = 2.16$$

This is the area-related mean value (numerical mean) of the number distribution. Denominator of the equation contains the number of particles. It was calculated the total of the square roots of the diameter, which is referred to math-

ematically as the $D[2,0]$ diameter. Squares of the diameters in the numerator (d^2), whereas the number (d^0) in the denominator of the equation.

For other applications (i.e. chemistry), balls are compared on the basis of their weight. The weight of a ball is $\frac{4}{3} \cdot \pi \cdot r^3 \cdot \rho$, which means that the volume of the diameters has to be calculated and divided the total number of particles and the cube root has to be taken in order to get back to a mean diameter (Anonymous, 2013).

$$D\left[3,0\right] = \sqrt[3]{\frac{(1^3 + 2^3 + 3^3)}{3}} = \sqrt[3]{\frac{(1+8+27)}{3}} = \frac{\sum d^3}{\sum d^0} = 2.29$$

This is the volume (or mass) related mean value of the number distribution, because the number of particles appears in the denominator of the equation. The $D[3,0]$ value is normally described as the volume mean diameter (VMD).

2. Area-related average value of the length distribution

Average values for the length distribution relate to the length, which means the length is the unit used in denominator (Anonymous, 2013). Average values are the mean x^2 of the length distribution D[2,1]:

$$D\left[2,1\right] = \frac{1^2 + 2^2 + 3^2}{1+2+3} = \frac{1+4+9}{6} \frac{\sum d^2}{\sum d^1} = 2.33$$

and the mean x^3 of the length distribution $D[3,1]$:

$$D\left[3,1\right] = \sqrt[2]{\frac{\left(1^3 + 2^3 + 3^3\right)}{\left(1+2+3\right)}} = \sqrt[2]{\frac{\left(1+8+27\right)}{6}} = \sqrt[2]{\frac{\sum d^2}{\sum d^1}} = 2.45$$

3. Volume-related average value of the area distribution

An average value of the area distribution is the mean x3 of the area distribution $D[3,2]$, also referred to as the Sauter mean diameter (SMD) or equivalent surface area (Anonymous, 2013):

$$D\left[3,2\right]=\frac{1^3+2^3+3^3}{1^2+2^2+3^2}=\frac{1+8+27}{1+4+9}=\frac{\sum d^3}{\sum d^2}=2.57$$

4. Volume-related mean value of the volume distribution

The volume-related mean value of the volume distribution (volume weighted mean diameter) can be calculated by the following equation:

$$D\left[4,3\right]=\frac{1^4+2^4+3^4}{1^3+2^3+3^3}=\frac{1+16+81}{1+8+27}=\frac{\sum d^4}{\sum d^3}=2.72$$

i.e. when calculating the average, each particle is assigned its relative volume as weight.

With regard to the last three average values, it should be noted that the number of particles does not appear in the denominator of the equation. Techniques such as laser diffraction that measure a distribution proportional to d^3 do not require the number of particles in order to obtain the average result [Anonymous, 2013].

VI INSTRUMENTAL COLOUR ANALYSIS AS AN INDICATOR OF THE QUALITY OF RAW MATERIALS AND FOOD PRODUCTS

Marta LISZKA-SKOCZYLAS

Department of Engineering and Machinery for Food Industry,
Faculty of Food Technology, University of Agriculture in Krakow,
Aleja Mickiewicza 21, 31-120 Krakow, Poland

marta.liszka-skoczylas@urk.edu.pl
ORCID: https://orcid.org/0000-0001-7281-3711

Abstract. The chapter describes the colour as one of the main attributes of food quality, that has strong influence on the consumers' choice. It determines their expectations as to the taste and smell of food. Color may also be related to the perceived energy value of food and the nutritional value. For the consumer, it can be a guide when choosing food in terms of safety and attractiveness assessment. It is also a sensory stimulus for accepting or rejecting a specific product. Color is also one of the most frequently measured quality features of products in post-harvest proceedings and in food processing research and industry because it reflects the influence of many factors both on the raw material and on the finished product, e.g. temperature, humidity and biochemical changes during maturation, growth, post-harvest activities and processing.

The first part of chapter concerns the main color characteristics such as hue, saturation and brightness. Due to the fact that these features cannot be systematized on a plane and are presented spatially, the color systems, most often used in the food industry, have also been characterized (CIE XYZ, CIE L*a*b*, CIE L*C*h*). Main and related parameters, describing food color in a quantitative and qualitative manner, were characterized. Chroma (C*) is used as a quantitative attribute of the object's color while the hue (or hue angle) (h*) is considered to be a quality attribute of a color. Using the CIE L*a*b* system also allows the calculation of the total (absolute) color

difference (ΔE*), which is measured as the vector modulus of the distance between the initial color values and the actual color coordinates. Derived color parameters include whiteness index (WI), Yellowness Index (YI) and Browning Index (BI).

Color measurements can be carried out by visual inspection (visual analysis) and with usage of traditional instruments (instrumental analysis): such as a colorimeter or computer vision. In the chapter the methodology of measurements, advantages and disadvantages of individual methods used for color assessment are also presented.

In the second part of the article, literature based application of color measurements in the food is described.

Keywords: color, food quality, hue, brightness, saturation, CIE LAB

1. Introduction

The sensory attractiveness of food raw materials, food products and dishes prepared on their basis is the basic criterion for the acceptance of the product selection by the consumer. The set of features that create sensory attractiveness, apart from availability and health, contribute to the generally understood quality of a food product. Each type of product has a specific set of quality characteristics. The basic characteristics are color, taste (palatability) and smell. The palatability is perceived when assessed orally as the sum of the smell, taste and feeling impressions. Color is one of a qualitative features of the external appearance of food, which is registered through visual impressions [Vivek et al. 2020].

The visual appearance of a food in terms of color has a strong influence on the consumer's opinion about its quality [Pereira et al. 2009; Nisha et al. 2011]. The color of the food surface is the first quality parameter assessed by the consumer. It determines expectations as to the taste and smell of food. Color may also be related to the perceived energy value of food and the nutritional value [Foroni et al. 2016]. For the consumer, it can be a guide when choosing food in terms of safety and attractiveness assessment [Hidaka and Shimoda 2014]. It is also a tool for accepting or rejecting a specific product [León et al. 2006].

Color can be defined as a psychophysical impression felt, through the sense of sight, under the influence of electromagnetic radiation with a wavelength of 390 to 760 nm, which is applied to the human eye's retina. Retinal cells may only be sensitive to black and white (rods) or to red, green, and blue light (cones). Retinal cells transmit a signal through the optic nerve to the brain, which in turn interprets responses in terms of what we call color [Francis 1995]. Observed object's

color can influence on our impression of surface structure, gloss and intensity of incident light. The color observed by the human eye corresponds to the quantity of radiation reflected from the illuminated object [Kazimierska 2014].

The aim of this chapter is to familiarize the reader with one of the main attributes of the quality of raw materials and food products, which is color. The first part of the chapter characterizes main (hue, saturation and brightness) and related (Chroma, total color index, Whiteness Index, Yellowness Index, Browning Index) color characteristics and color systems, most often used in the food industry. The chapter also presents the methodology of color measurements and presents the advantages and disadvantages of individual methods. In the second part of the article, based on the literature, the use of color measurements in food is described.

2. Color as an attribute of food quality

Quality is not a single, well-defined attribute, but rather a compromise between many features or properties. When making a decision about the purchase and consumption of food, the consumer uses appearance indicators to determine the freshness and flavor of products. The color of the food surface is usually considered the first, most important aspect of the appearance and has a great influence on consumers' choice, especially when it is related to other aspects of the food, such as the freshness of the products. It depends on many factors including temperature, humidity and biochemical changes during maturation, growth, post-harvest activities and processing. Consequently, color is one of the attributes of product quality, as it takes into account the above-mentioned parameters and is one of the most frequently measured quality features of products in post-harvest proceedings and in food processing research and industry [Lazaro et al. 2019].

Certain foods are closely related to certain color attributes. In the case of raw food materials such as fruit and vegetables, the color changes with the degree of maturity, but also during storage [Buvé et al. 2018]. Consumers have strictly defined expectations to the color of a given product. Research shows that consumers perceive yellow to go with 'lemon' or 'banana' and pink to go with 'grapefruit'. Inverting the colors changes their perception. Consumers have misdiagnosed the taste of yellow mandarin and orange raspberry or considered them inferior to the correct match. Inadequate color for fruit or vegetables suggests a lack of maturity. Yellowing of green vegetables due to the loss of chlorophyll, browning or tarnishing of the color of fruit and vegetables during storage suggest the loss of freshness of the product and is an unacceptable feature by consumers [Shewfelt 1984, 2002].

Color may also be associated with various taste sensations [Velasco et al. 2016] and it has been shown that it modifies taste reactions in various types of products, e.g. in fruit drinks [Garber et al. 2000], in fruit-flavored yoghurts [Calvo et al. 2001], in sugar-coated chocolates [Levitan et al. 2008] and noodles [Zhou et al. 2015] etc. Its change may affect the quality and intensity of the perceived taste and smell, their identification and the overall acceptability of the product. Some consumers are able to reject sweet bananas (yellow with brown spots), nutritious tomatoes high in b-carotene (orange), and aromatic cherries (yellow with a red blush) due to their unexpected coloration. Spence [2018] showed that the unusual color of a food product (blue potato) influences consumer perception and choice. However, it should be remembered that consumer groups may differ depending on nutritional neophobia and age [Paakki et al. 2016]. Consumers may have conflicting views on the acceptance of blue food and drink [Spence 2018]. However, recent advances in the cultivation of plants have resulted in new varieties of fruit and vegetables, the colors of the skin or flesh of which differ from the traditional ones, e.g. yellow tomatoes, strawberries, golden kiwi.

Color also affects the apparent sweetness level. Consumers perceive a drink with a strong red color and a strawberry flavor as sweeter than the version with a less intense color [Griffiths 2005]. Yellow and green are commonly associated with acidic fruit, which may lead to the assumption that unknown yellow or green foods will also be acidic. Naturally blue foods are quite rare, but blue sweets and sweetened beverages are more popular than other blue colored food. As a consequence, consumers can be expected to associate blue and sweetness together [Hidaka and Shimoda 2014].

The color of the raw material may be a source of information of the chemical composition of the product (e.g. the content of carotenoids in citrus products or in tomatoes), and thus determine its suitability for processing, storage or transport. By assessing the color of the food surface, it is possible, almost immediately, to control and diagnose visible defects or hidden deterioration of raw materials or food products [Francis 1995]. In industry, thanks to the use of online imaging systems, it is possible to monitor and control the quality of raw materials and food products. Changes in color parameters may be an indicator of other changes, for example of nutritional or textural changes, that occurred in the product during its processing [Mieszkalska and Piotrowski 2014]. For example, a change in the internal structure of extrudates is manifested by a change in the brightness of the color [Ekielski 2013]. Detecting peel defects of fruit and vegetables (e.g. their discoloration) using image analysis is a valuable tool in the quality control of food raw materials [Yu et al. 2003; Pereira et al. 2009; Cubero et al. 2011]. Color measurement is also used to optimize and select the conditions of technological pro-

cesses, e.g. drying or expansion process, which is related to the change of physical and chemical properties occurring during such a process. Such changes may be caused by pigment concentration due to changes in humidity, dye degradation, browning process or gas exchange. As a result of drying, all color parameters change, and the intensity of the changes depends on many factors, including the temperature and drying time or the type of dried material [Krokida et al. 2001]. For dried products, obtaining the most acceptable color to the consumer must comply with technological process parameters which minimize adverse reactions (e.g. non-enzymatic browning, oxidation of vitamin C) causing a change in color. Also, the standardization of the quality of powdered milk products may be based on the color measurement [Caron et al. 1997].

3. Color attributes

The concept of color has two meanings. Firstly, color is a visual impression perceived by a human (or an animal) when a mixture of electromagnetic waves in the visible range hits his eye and remains in the sphere of subjective sensations. Secondly, it is a quantity that tries to objectify and systematize the description of these impressions (a measure of the impression described above). Clear identification of the color is possible on the basis of 3 color attributes. These are: hue, saturation and brightness. These features cannot be systematized on a plane, therefore they are presented spatially. Each of the three dimensions of space is subscribed to one of these characteristics.

Hue is a color feature that depends on the type of radiation that hits the receptors in the eye and gives the impression of a specific color, e.g. red, blue or green (Fig. 1). This is a qualitative difference in color defined by the dominant wavelength. Not all colors have a shade. Those that have it are called chromatic colors.

Saturation is the feeling of a chromatic color in its mixture with achromatic (white, black, gray). It is a measure of the deviation of color from white (red, pink, white). Pastel colors, containing a lot of white, belong to unsaturated colors.

Brightness is the sensation of the intensity of the radiation that produces the impression of color (it is the quantity that changes color with the intensity of the light). The physical measure of this color characteristic is luminance. In daytime vision, the highest luminance shows yellow-green radiation at a wavelength of 555 nm, and in scotopic (night) vision, blue-green radiation at a wavelength of 510 nm [Kazimierska 2014].

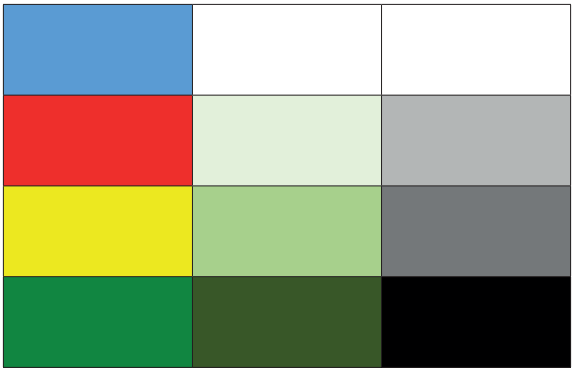

Fig. 1. Color attributes. Four different colors: blue, red, yellow, green. Four different saturations: green 0%, 20%, 60%, 100%. Four different brightness levels – pure white, 30% gray, 60% gray, black (source: own elaboration)

4. Color System (Color Spaces)

There are several color coordinate systems by which it can be described. The most popular are RGB (red, green, blue), Hunter Lab, Commission Internationale de l'Eclairage (CIE) XYZ, CIE L*a*b*, CIE L*u*v*, CIE Yxy and CIE LCH. They differ in the symmetry of the color space and the coordinate system used to determine the location of the point in space [Pathare et al. 2013; Siswantoro 2019].

At the beginning of the 20th century, attempts were made to create a color model that would be device-independent. In 1931, such a model was developed at the request of the Commission Internationale de l'Eclairage (International Commission on Illumination) and is actually valid till today. In the meantime, several newer models have been created, but all of them are based on that former one. This model was called CIE XYZ 1931. The basis for building the model was the examination of a group of about twenty people correctly distinguishing colors. These people were presented with different colors in a very narrow field of view (2°) and asked to differentiate between them. Based on the statistical analysis of the responses, a standard observer model was developed that represents the averaged human color perception capabilities (e.g. sensitivity, wavelength range, resolution, etc.). The standard observer model provided the basis for the development of the first device-independent color model [Gozdecka 2006; Pathare et al. 2013].

The basic property of this space is that it allows each perceived color to be uniquely defined by three coordinates. This space uses three primary colors *X*, *Y*, *Z*, which do not occur in nature, but are created for the needs of this space, used to describe real colors. This model uses a chromaticity diagram to denote the different colors. The *Y* component always corresponds to the brightness of the color. The application of the weighting to a reflectance curve gives the tristimulus values. Each of these values are denoted by the capital letters *X*, *Y* and *Z* and used to calculate the chromaticity coordinates, designated by lowercase letters *x* (red), *y* (green) and *z* (blue) [Pathare et al. 2013]. The *x* and *y* coordinates can be calculated as (eq. 1 and 2):

$$x = \frac{X}{X + Y + Z} \tag{1}$$

$$y = \frac{Y}{X + Y + Z} \tag{2}$$

It follows from the above expressions that the third coordinate must be $z = 1 - x - y$ [Sahin and Sumnu 2006].

The Hunter L a b color space was created in 1948 and its CIE $L^*a^*b^*$ modification was standardized in 1976 by CIE. This color space provides a more uniform color difference with respect to the human perception of differences. In this model, we use three values of L^*, a^*, b^* (LAB) in the form of axes contained in the three-dimensional color space (Fig. 2). The vertical axis of this coordinate system is expressed by the L^* parameter, which is an approximate measure of brightness. This parameter takes values from 0 – black to 100 – white. The a^* parameter roughly describes the color deviation towards red (positive values) or green (negative values). The b^* parameter, on the other hand, characterizes the color deviation towards yellow (positive values) and blue (negative values). Today, this space is widely used in the food industry [Segura et al. 2017].

The CIE L^*, a^*, b^* coordinates can be converted to cylindrical L^*, C^*, h coordinates using the appropriate equations. They define the Munsell color space variables. Similarly to the CIE LAB system, the L^* value determines the brightness, while the C^* value expresses the color saturation and grows along the radius of the circle. The h value, called the tone angle, defines the hue and is measured on a circle from the a^* axis (Fig. 2).

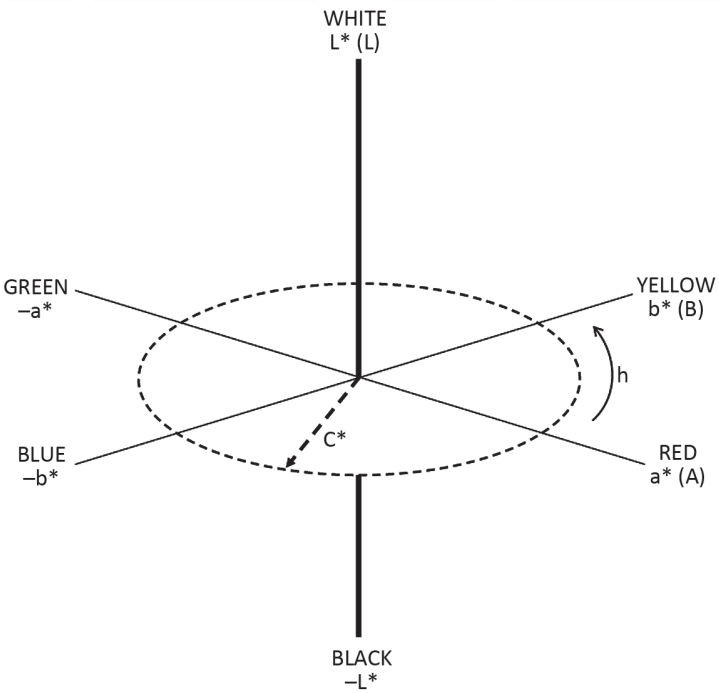

Fig. 2. Color spaces: CIE LAB (L*a*b*), L*C*h (source: Gozdecka [2006], p. 36)

5. Quantification of color

Chroma (C^*) is used as a quantitative attribute of the object's color, which is used to define the difference in hue compared to the gray color of the same lightness. The higher the values of the C^* parameter, the higher color intensity of objects perceived by humans. The saturation of C* takes values from 0 (in the center of the coordinate system) and increases as it moves away from the center. This parameter can be determined from equation (3):

$$C^* = \sqrt{a^{*2} + b^{*2}} \tag{3}$$

The hue (or hue angle) (h^*), where hue is traditionally defined as red, blue, etc., is considered to be a quality attribute of a color. This parameter indicates the difference of a specific color with respect to a gray of the same lightness. This parameter is defined by the following formula (eq. 4):

$$h^* = tan^{-1}\left(\frac{b^*}{a^*}\right) \tag{4}$$

An angle of 0° or 360° corresponds to red hue, while angles of 90°, 180° and 270° correspond to yellow, green and blue, respectively. This parameter is widely used in the assessment of the color parameters of green vegetables, fruit and meats [Pathare et al. 2013].

Using the CIE $L^*a^*b^*$ system also allows the calculation of the total (absolute) color difference (ΔE^*), which is measured as the vector modulus of the distance between the initial color values and the actual color coordinates. The total color difference indicates the size of the color difference between control and test samples (e.g. after storage or after specific agrotechnical treatments or technological processes) [Lewicki et al. 1998; Özkan et al. 2003; Patras et al. 2009; Skoczylas et al. 2020]. This parameter is calculated as the Euclidean distance between two points in the three-dimensional space determined by L^*, a^*, and b^* using the following equation (eq. 5):

$$\Delta E^* = \sqrt{\Delta a^{*2} + \Delta b^{*2} + \Delta L^{*2}} \tag{5}$$

where Da^*, Db^* and ΔL^* is the difference of these parameters between the control sample and the test sample. A perceivable color difference can be classified as very pronounced when $\Delta E^* > 3$, pronounced when $1.5 < \Delta E^* < 3$ or a slight $\Delta E^* < 1.5$ [Hutchings 2011].

The whiteness index is a parameter that mathematically combines lightness and yellow-blue into a single index. According to Rhim et al. [1999] indicates the degree of whiteness (*WI*) as calculated according to the following formula (eq. 6):

$$WI = \sqrt{\left(100 - L^{*2}\right) + a^{*2} + b^{*2}} \tag{6}$$

The Yellowness Index (*YI*) indicates the degree of yellowing of raw materials or food products. Yellowing may be the result of degradation processes that occur in the food item under the influence of light, air or other - chemical agents, it can be associated with processing operations or dirt. This indicator is calculated according to the following formula (eq. 7):

$$YI = \frac{142.86\, b^*}{L^*} \tag{7}$$

The parameter to characterize the change in color browning is the browning index (*BI*) [Quitão-Teixeira et al. 2007]. Defined as the purity of the brown color, and it is one of the most common indicators of browning sugar-containing foods. In the case of this indicator, the CIE $L^*a^*b^*$ color space is the most widely used color model due to the homogeneity of the distribution of colors in the space [Yam and Papadakis 2004]. Based on the CIE $L^*a^*b^*$ coordinates, especially the L^* value or the CIE XYZ color space, indicators of fruit browning were developed [Pristijono et al. 2006; Lu et al. 2007]. The BI parameter is calculated using the following expression [Maskan 2001; Mohapatra et al. 2010] (eq. 8–9):

$$BI = 100 \cdot \left(\frac{X - 0.31}{0.17} \right) \tag{8}$$

where

$$X = \frac{\left(a^* + 1.75\,L\right)a^*}{\left(5.645\,L + a^* - 3.012b^*\right)} \tag{9}$$

In the literature of the subject, one can find color indicators that allow for a direct relationship with the external appearance of specific raw materials and food products such as: fruit, vegetables, meat, juices, pasta, etc. [Pathare et al. 2013]. These indicators can directly determine the degree of maturity of the raw material, the stage of the technological process or the time and conditions of the food product storage. For example, sugar syrup clarity is determined using the Yellow color value = a^* / b^* [García and Calixto 2000], the brightness of mashed potatoes using the ratio White / yellow ratio = L / b [O'Leary et al. 2000] or sherry wine color intensity is determined by absorbance at 470 nm using a spectrophotometer [Palacios et al. 2002] and according to Meléndez-Martínez et al. [2011] a good indicator of the color of orange juice is the K / S index.

6. Color measurement

Color measurements can be carried out by visual inspection (visual analysis) and with usage of traditional instruments (instrumental analysis): such as a colorimeter or computer vision.

Visual assessment of the color of the food consists of observing the sample through a trained panel, using the senses (without instruments) but under strictly controlled lighting conditions together with a set of color standards for the com-

parison. As a result of visual measurement, a specific color description is obtained using strictly defined vocabulary [Meléndez-Martínez et al. 2005]. Although the human assessment of color is quite reliable, it is subjective due to the variability occurring among people (age, sex, origin, body mass index (BMI), human psychophysical state) and depending on changes in physical parameters of the environment at the time of color assessment, e.g. lighting [Francis 1995; Hoppu et al. 2018]. Besides subjectivity, human assessment of color is laborious and tedious and is not suitable for routine color scale measurements [McCaig 2002; León et al. 2006]. For this reason, the parametric interpretation of color is of particular importance in assessing the quality of food products. In instrumental measurement, color is expressed in terms of color coordinates.

In the food industry, traditional instruments such as colorimeters and spectrophotometers are the most often used to measure color [Balaban and Odabasi 2006]. Under certain lighting conditions, these instruments provide a quantitative measurement of color by simulating the way the average human eye perceives the color of an object [McCaig 2002].

Colorimeters measure the color of primary radiation sources that emit light and secondary radiation sources, i.e. those that reflect or transmit external light [Meléndez-Martínez et al. 2005; León et al. 2006]. For this reason, tristimulus values are obtained optically and not mathematically. The color parameter values obtained with the different colorimeters differ from each other because the instruments simulate the response of only a standard observer and a standard light source. Based on the structure of the human eye (the three types of cones in the retina), a trichromatic colorimeter has been constructed with three filters that work like each of the three types of cones. A trichromatic colorimeter consists of three main components: (1) a light source, (2) a combination of filters to modify the energy distribution of the incident / reflected light, and (3) a photoelectric detector that converts the reflected light into an electrical output. Measurements made on a tristimulus colorimeter are usually comparative. Therefore, it is necessary to use calibrated standards with similar colors to the measured materials in order to obtain the most accurate measurements [Pathare et al. 2013].

Spectrometers operating in an extended spectral range including the visible range (VNIR spectrometer) are widely used for measuring the color of food in the food industry and agriculture [McCaig 2002]. Spectrophotometers measure the spectral distribution of transmittance or reflectance of the sample. The obtained values of X, Y and Z depend on the light source, measurement geometry and the observer [Hutchings 2011] and are mathematically obtained according to the CIE definitions. The advantage of spectrophotometers over colorimeters is

that the relevant color information can be obtained by calculating the color value for any light source and lighting.

Although a simple color measurement of an object can be made quickly with a colorimeter and spectrophotometer, there are potential limitations to their use. In order to obtain an accurate average color, special attention should be paid to the number of readings and the sampling location. Traditional instrumental measurements can only accurately measure uniform sample surfaces which are rather small. In the event that the sample has a non-uniform color, the measurement should be repeated as long as it covers the entire surface and yet may still be unrepresentative of the sample, making global food analysis difficult. Another limitation is the size and shape of the tested sample surface. When the samples are too small - the rice grain, or the shape is not a circle – a shrimp, the measurement may not be accurate. Moreover, in order to assess the color of the food in detail, it is required to obtain the color value of each pixel on the sample surface in order to obtain a color distribution map on the surface of the tested object [León et al. 2006]. This requirement cannot be achieved with traditional color measuring instruments. This possibility is given by computer vision, which extracts information about the color from digital images. The main difference in color measurement between traditional and computer vision instruments is the amount of spatial information provided, which enables the measurement of heterogeneous shapes and colors, and a flexible choice of the range of interest. This technique allows for investigating of larger surface at one time, generating a color distribution map and ensuring permanent image recording [Balaban and Odabasi 2006; León et al. 2006]. Such a system usually consists of 5 components: a light source, a digital camera, an image storage card, computer hardware and image processing software [Quevedo et al. 2010]. The first step in computer vision is image acquisition. The digital image is recorded in such a way that light from the visible spectrum falls on a partially reflecting surface and the scattered photons are collected in the camera lens and converted into an electrical signal using a vacuum lamp or CCD (charge-coupled device) and then stored on the hard disk for further display and analyze the image. A digital monochrome image is a two-dimensional (2-D) function of the radiation intensity I in the spatial coordinates x, y (function I (x, y)). The intensity of the radiation (read as a gray level) is proportional to the energy of the radiation received by the sensor or detector over a small area around the point (x, y) [Gunasekaran 1996]. In food color assessment usage of the computer vision color space transformation is the most common pixel pre-processing method. Typically, color images are stored in the three-dimensional RGB color space. However, this space does not represent the colors naturally perceived by the human eye, and the RGB model is device

dependent and not identical to the intensities of the CIE system. To overcome this problem, RGB values are converted to other color spaces such as L*a*b* [Menesatti et al. 2012]. The exact method of converting RGB to L*a*b* is presented in the work of León et al. [2006].

Image acquisition and analysis are the two most important steps in applying this technique. The accuracy of the acquisition equipment must be high to capture the required details and enough coarse to enable fast image processing. The image analysis consists of numerous algorithms and measurement classification methods [Krutz et al. 2000]. Automatic color measurement with computer vision is fast, accurate and economical.

7. The use of color measurements in the food industry

Nowadays, the measurement of food color using instrumental methods, especially computer vision, has found wide application in the food industry as one of the key methods of quality control of raw materials and food products. Precise control and increased throughput of the production process during packaging is possible thanks to the implementation of computer vision systems on technological lines.

Based on color measurements, determination of appropriate indicators and their analysis, it is possible to optimize the conditions of a given process. Patras et al. [2011] found in their research that the most sensitive indicator for measuring the color degradation of heat-treated strawberry jam was the total color difference (ΔE^*) and the color saturation (C^*). Longer heat treatment of *Agua-mel* (Mediterranean honey-like groceries) during processing led to a significant color increase, which can be attributed to the accumulation of brown pigment [Cavaco et al. 2022]. Cazzaniga et al. [2021] found in their study that baking time reduction allowed a similar color to be obtained between snacks made with and without dehydrated cassava puree substitution. The browning index increased with the proportion of cassava in flour and cakes, but not in baked snacks. Adekunte et al. [2010] and Tiwari et al. [2008] proved that sonification in tomato and orange juice contributed to an increase in the value of the total color difference. High pressure homogenization (HPH) is a non-thermal technology that can be used as a partial or complete replacement for the thermal treatment of food liquids. According to Salehi [2020], in many cases, juices from high pressure homogenization (HPH) retain better parameters indicative of freshness, such as color, than those subjected to heat treatment. The effects of HPH on color of juice could

strongly depend on food matrices and treatments. The processing of HPH did not show a significant effect on the change of color parameters of mixed apple, carrot and peach juices, and in the case of kiwi juice their significant increase was noted. In the studies of Dede et al. [2007] it was found that the high-pressure treatment of carrot and tomato juices had less effect on the difference in color (compared to fresh juice) than conventional heat treatment. Similar conclusions were reached by Patras et al. [2009] examining strawberry and blackberry purees. Also, biofortification of carrots at the growth stage resulted in the total color difference of obtained carrot juice [Skoczylas et al. 2020].

In the work of Hsu et al. [2003] the *WI* index was used as a measure of the degree of discoloration of white products during the drying process. The white color of the surface is a feature that determines the quality of Camembert cheeses. For the samples of cheese packed in the modified atmosphere, this index remained constant, while for the control samples the *WI* values clearly decreased during the storage of the product [Rodriguez-Aguilera et al. 2011].

In the Qin et al. [2010] work the nutritional composition and physical properties of flour obtained from buckwheat and buckwheat tartars were analyzed. Tartar buckwheat flour was characterized by a lower whiteness index *WI* than common buckwheat flour. Wheat bread with the addition of buckwheat showed a lower value of the WI parameter [Lin et al. 2009].

According to Kotwaliwale et al. [2007] the *WI* parameter of mushrooms decreased while the yellowness index *YI* increased during drying. However, the values of these parameters behaved in reverse with the progress of irrigation of these fungi. Rice *YI* increased with increasing infrared radiation intensity or with increased heating [Das et al. 2004].

The color of the dried fruit changes as a result of browning, which is often caused by the Maillard reaction [Baini and Langrish 2009]. Krokida et al. [1998] in their work assessed the color development of dried apples and bananas. Based on the evaluation of the formation of browning in the dried food, an appropriate drying technique and optimal process conditions can be selected, which can improve the color quality of the product. Visually, the degree of browning of fried dishes is also considered as one of the most important parameters of their quality [Scanlon et al. 1994].

The color change during storage is the main parameter that predicts the shelf life of fruit-based products. During the storage of fruit leather (fruit bar), the decrease in the content of anthocyanins strongly correlated with the decrease in the red chromatic parameter (a^* value), which suggests that a^* values can be used as an indicator of anthocyanin degradation in this type of products [da Silva Simão et al. 2022]. The percentage of consumers rejecting the color analysis was strong-

ly correlated with the *a* * value, which can be used as an analytical indicator for estimating the durability of strawberry skin. Based on this result, the authors developed mathematical functions predicting the change in *a* * value as a function of the probability of the product being rejected by the consumer. The approach used in this study, which integrates instrumental and sensory data to assess color changes during storage and predict the shelf life of a product in the marketplace, is a useful tool for use in industry-specific quality control programs.

Lyu et al. [2022] showed that pre-treatment of carrots with ultrasound (40 Hz, 100 W, 10 min) and ascorbic acid (2%, w / v) –$CaCl_2$ (1%, w / v) solution (UAA-$CaCl_2$) significantly improves the parameters colors of freeze-dried carrots. The redness (29.66%), chroma (16.59%) of freeze-dried carrots at 120-day (25° C) was significantly higher than the control carrots.

The color of the product is one of the basic incentives for its purchase by the consumer. The red and light red color of beef is associated by consumers with fresh meat, while the brownish color is considered an indicator of its deterioration. Larrain et al. [2008]investigated the differences in the color of fresh beef using colorimeters. However, that assessment has limitations in scanning a small area. Computer vision is considered a promising method for meat color prediction [Mancini and Hunt 2005]. Using the above method, Tan [2004] assessed the color of pork as an indicator of freshness and tenderness of meat.

Consumers' choice to buy fish is the most often based on color. Gormley [1992] concluded, that consumers associate the color of fish products with the freshness, better taste and higher quality. In the fish industry, color charts such as the SalmonFan™ card are usually used for comparison. However, determining the color on this basis is subjective and time-consuming. Thanks to the camera vision method, it was possible to assign a color score to a salmon fillet according to the SalmonFan™ card [Quevedo et al. 2010].

There are studies in the literature that indicate that the color of a drink is related to the consumer's perception of taste, sweetness and other quality characteristics [Meléndez-Martínez et al. 2005; Fernández-Vázquez et al. 2011]. The color of orange drinks has been found to influence the perceived sweetness and flavor intensity of most fruit drinks by the consumer. To assess the color of the orange juice both traditional instrumental methods (colorimeter) were used [Meléndez-Martínez et al. 2005] as well as the computer vision method [Fernández-Vázquez et al. 2011].

The above-mentioned examples of the use of color measurements in the food industry are only a small part of the possibilities that both traditional instrumental methods and camera vision give us in determining the quality characteristics of raw materials and food products. The color of wine is one of the main parame-

ters determining its acceptance by the consumer [Martin et al. 2007], the color of potato chips is an important quality attribute for the potato processing industry, which is closely related to consumer perception [Pedreschi et al. 2006], the color of bananas depends on the degree of ripeness [Mendoza and Aguilera 2004]. There are many examples.

8. Conclusion

Color is one of the most important quality attributes of food influencing its perception, purchase and thus the nutritional choice of consumers. For a long time, color has been used as an indicator of product changes in the production process. Color of an object indicates maturity, freshness or doneness. Color measurement and analysis is therefore important both at the harvest stage for plant raw materials and in post-harvest, processing and marketing. It helps to optimize the quality and nutritional value of the food.

While non-destructive measurement of the external color of products is now routine practice in research and industry, predicting internal color remains both a technological and practical challenge. The variety of indicators used to describe the color of fresh and processed foods, even of the same type, makes it difficult to compare the results. There is a need for their standardization. Given the importance of color in consumer food choices and preferences, and the growing consumer demand for intrinsic quality of food products, there is a need to develop fast, non-destructive methods of measuring the color and to elaborate indicators connected to nutrition value. Recent advances in acquiring and interpreting images obtained with camera vision are very promising for that task.

References

Adekunte A.O., Tiwari B.K., Cullen P.J., Scannell A.G.M., O'Donnell C.P. 2010. Effect of sonication on colour, ascorbic acid and yeast inactivation in tomato juice. Food Chemistry, 122(3), 500–507. https://doi.org/10.1016/j.foodchem.2010.01.026

Baini R., Langrish T.A.G. 2009. Assessment of colour development in dried bananas – measurements and implications for modelling. Journal of Food Engineering, 93(2), 177–182. https://doi.org/10.1016/j.jfoodeng.2009.01.012

Balaban M.O., Odabasi A.Z. 2006. Measuring color with machine vision. Food Technology, 60(12), 32–36.

Buvé C., Kebede B.T., De Batselier C., Carillo C., Pham H, Hendrickx M., Grauwet T., van Loey A. 2018. Kinetics of colour changes in pasteurised strawberry juice during storage. Journal of Food Engineering, 216, 42–51. https://doi.org/10.1016/j.jfoodeng.2017.08.002

Calvo C., Salvador A., Fiszman S.M. 2001. Influence of colour intensity on the perception of colour and sweetness in various fruit-flavoured yoghurts. European Food Research and Technology, 213(2), 99–103. https://10.1007/s002170100359

Caron A., St-Gelais D., Pouliot Y. 1997. Coagulation of milk enriched with ultrafiltered or diafiltered microfiltered milk retentate powders. International Dairy Journal, 7(6), 445–451. https://doi.org/10.1016/S0958-6946(97)00024-1

Cavaco T., Figueira A.C., González-Domínguez R., Sayago A., Fernández-Recamales Á. 2022. Evolution of physicochemical parameters during the thermal-based production of Água-mel, a traditional Portuguese honey-related food product. Molecules, 27(1), 57. https://10.3390/molecules27010057

Cazzaniga A., Brousse M.M., Linares R.A. 2021. Variation of color with baking time in snacks made with pregelatinized cassava. Journal of Food Science, 86(9), 4100–4109. https://10.1111/1750-3841.15870

Cubero S., Aleixos N., Moltó E., Gómez-Sanchis J., Blasco J. 2011. Advances in machine vision applications for automatic inspection and quality evaluation of fruits and vegetables. Food and Bioprocess Technology, 4(4), 487–504. https://10.1007/s11947-010-0411-8

Das I., Das S.K., Bal S. 2004. Specific energy and quality aspects of infrared (IR) dried parboiled rice. Journal of Food Engineering, 62(1), 9–14. https://10.1016/S0260-8774(03)00164-X

Dede S., Alpas H., Bayındırlı A. 2007. High hydrostatic pressure treatment and storage of carrot and tomato juices: Antioxidant activity and microbial safety. Journal of the Science of Food Agriculture, 87(5), 773–782. https://doi.org/10.1002/jsfa.2758

Ekielski A. 2013. Application of Image Analysis to Evaluate Selected Parameters Describing Porous Structures at the Output of Cereal Extrudates. Wydawnictwo Wieś Jutra, Warszawa.

Fernández-Vázquez R., Stinco C.M., Meléndez-Martínez A.J., Heredia F.J., Vicario I.M. 2011. Visual and instrumental evaluation of orange juice color: A consumers preference study. Journal of Sensory Studies, 26(6), 436–444. https://doi.org/10.1111/j.1745-459X.2011.00360.x

Foroni F., Pergola G., Rumiati R.I. 2016. Food color is in the eye of the beholder: The role of human trichromatic vision in food evaluation. Scientific Reports-UK, 6(1), 37034. https://doi.org/10.1038/srep37034

Francis F.J. 1995. Quality as influenced by color. Food Quality and Preference, 6(3), 149–155. https://doi.org/10.1016/0950-3293(94)00026-R

Garber L.L., Hyatt E.M., Starr R.G. 2000. The effects of food color on perceived flavor. Journal of Marketing Theory and Practice, 8(4), 59–72.

García J.A.L., Calixto F.S. 2000. Evaluation of CIE-lab colour parameters during the clarification of a sugar syrup from Mesquite pods (Prosopis Pallida L.). International Journal of Food Science and Technology, 35(4), 385–389. https://doi.org/10.1046/j.1365-2621.2000.00394.x

Gormley T.R. 1992. A note on consumer preference of smoked salmon colour. Irish Journal of Agricultural and Food Research, 31(2), 199–202.

Gozdecka G. 2006. Zastosowanie obiektywnej metody kolorymetrycznej do oceny barwy mięsa. Postępy Techniki Przetwórstwa Spożywczego, 16(2), 35–37.

Griffiths J.C. 2005. Coloring Foods and Beverages. Food Technology 59, 38–44.

Gunasekaran S. 1996. Computer vision technology for food quality assurance. Trends in Food Science & Technology, 7(8), 245–256. https://doi.org/10.1016/0924-2244(96)10028-5

Hidaka S., Shimoda K. 2014. Investigation of the effects of color on judgments of sweetness using a taste adaptation method. Multisensory Research, 27, 189–205. https://doi.org/10.1163/22134808-00002455

Hoppu U., Puputti S., Aisala H., Laaksonen O., Sandell M. 2018. Individual differences in the perception of color solutions. Foods (Basel, Switzerland), 7(9), 154. https://doi.org/10.3390/foods7090154

Hsu C.L., Chen W., Weng Y.M., Tseng C.Y. 2003. Chemical composition, physical properties, and antioxidant activities of yam flours as affected by different drying methods. Food Chemistry, 83(1), 85–92. https://doi.org/10.1016/S0308-8146(03)00053-0

Hutchings J.B. 2011. Food colour and appearance. Springer, New York. https://doi.org/10.1007/978-1-4615-2123-5

Kazimierska M. 2014. Objective evaluation of colour of usable products. Technology and Quality of Products, 59, 44–47.

Kotwaliwale N., Bakane P., Verma A. 2007. Changes in textural and optical properties of oyster mushroom during hot air drying. Journal of Food Engineering, 78(4), 1207–1211. https://doi.org/10.1016/j.jfoodeng.2005.12.033

Krokida M.K., Tsami E., Maroulis Z.B. 1998. Kinetics on color changes during drying of some fruits and vegetables. Drying Technology, 16(3–5), 667–685. https://doi.org/10.1080/07373939808917429

Krokida M.K., Maroulis Z.B., Saravacos G.D. 2001. The effect of the method of drying on the colour of dehydrated products. International Journal of Food Science and Technology 36(1), 53–59. https://doi.org/10.1046/j.1365-2621.2001.00426.x

Krutz G.W., Gibson H.G., Cassens D.L., Min Z. 2000. Colour vision in forest and wood engineering. Landwards, 55(1), 2–9.

Larraín R.E., Schaefer D.M., Reed J.D. 2008. Use of digital images to estimate CIE color coordinates of beef. Food Research International, 41(4), 380–385. https://doi.org/10.1016/j.foodres.2008.01.002

Lazaro A., Boada M., Villarino R., Girbau D. 2019. Color measurement and analysis of fruit with a battery-less NFC sensor. Sensors 19(7), 1741. https://doi.org/10.3390/s19071741

León K., Mery D., Pedreschi F., León J. 2006. Color measurement in L*a*b* units from RGB digital images. Food Research International, 39(10), 1084–1091. https://doi.org/10.1016/j.foodres.2006.03.006

Levitan C.A., Zampini M., Li R., Spence C. 2008. Assessing the role of color cues and people's beliefs about color–flavor associations on the discrimination of the flavor of sugar-coated chocolates. Chemical Senses, 33(5), 415–423. https://doi.org/10.1093/chemse/bjn008

Lewicki P.P., Pomaranska-Lazuka W., Witrowa-Rajchert D., Nowak D. 1998. Effect of mode of drying on storage stability of colour of dried onion. Polish Journal of Food and Nutrition Science, 7/48(4), 701–706.

Lin L.Y., Liu H.M., Yu Y.W., Li S.D., Mau J.L. 2009. Quality and antioxidant property of buckwheat enhanced wheat bread. Food Chemistry, 112(4), 987–991. https://doi.org/10.1016/j.foodchem.2008.07.022

Lu S., Luo Y., Turner E., Feng H. 2007. Efficacy of sodium chlorite as an inhibitor of enzymatic browning in apple slices. Food Chemistry, 104(2), 824–829. https://doi.org/10.1016/j.foodchem.2006.12.050

Lyu Y., Bi J., Chen Q., Li X., Wu X., Gou M. 2022. Effects of ultrasound, heat, ascorbic acid and $CaCl_2$ treatments on color enhancement and flavor changes of freeze-dried carrots during the storage period. Food Chemistry, 373B(30), 131526. https://10.1016/j.foodchem.2021.131526

Mancini R.A. Hunt M.C. 2005. Current research in meat color. Meat Science, 71(1), 100–121. https://doi.org/10.1016/j.meatsci.2005.03.003

Martin M.L.G.M., Ji W., Luo R., Hutchings J., Heredia F.J. 2007. Measuring colour appearance of red wines. Food Quality and Preference, 18(6), 862–871. https://doi.org/10.1016/j.foodqual.2007.01.013

Maskan M. 2001. Kinetics of colour change of kiwifruits during hot air and microwave drying. Journal of Food Engineering, 48(2), 169–175. https://doi.org/10.1016/S0260-8774(00)00154-0

McCaig T.N. 2002. Extending the use of visible/near-infrared reflectance spectrophotometers to measure colour of food and agricultural products. Food Research International, 35(8), 731–736. https://doi.org/10.1016/S0963-9969(02)00068-6

Meléndez-Martínez A.J., Vicario I.M., Heredia F.J. 2005. Instrumental measurement of orange juice colour: A review. Journal of the Science of Food and Agriculture, 85(6), 894–901. https://doi.org/10.1002/jsfa.2115

Meléndez-Martínez A.J., Gómez-Robledo L., Melgosa M., Vicario I.M., Heredia F.J. 2011. Color of orange juices in relation to their carotenoid contents as assessed from different spectroscopic data. Journal of Food Composition and Analysis, 24(6), 837–844. https://doi.org/10.1016/j.jfca.2011.05.001

Mendoza F., Aguilera J.M. 2004. Application of image analysis for classification of ripening bananas. Journal of Food Science, 69(9), E471–E477. https://doi.org/10.1111/j.1365-2621.2004.tb09932.x

Menesatti P., Angelini C., Pallottino F., Antonucci F., Aguzzi J., Costa C. 2012. RGB color calibration for quantitative image analysis: The "3D thin-plate spline" warping approach. Sensors, 12(6), 7063–79. https://doi.org/ 10.3390/s120607063

Mieszkalska A., Piotrowski D. 2014. The use of color models to evaluate dried plants. Technological Progress in Food Processing, 2, 105–111.

Mohapatra D., Bira Z.M., Kerry J.P., Frías J.M., Rodrigues F.A. 2010. Postharvest hardness and color evolution of white button mushrooms (Agaricus bisporus). Journal of Food Science, 75(3), E146–E152. https://doi.org/10.1111/j.1750-3841.2010.01518.x

Nisha P., Singhal R.S., Pandit A.B. 2011. Kinetic modelling of colour degradation in tomato puree (Lycopersicon esculentum L.). Food and Bioprocess Technology, 4(5), 781–787. https://doi.org/10.1007/s11947-009-0300-1

O'Leary E., Gormley T., Butler F., Shilton N. 2000. The effect of freeze-chilling on the quality of ready-meal components. LWT – Food Science and Technology, 33, 217–224. https://doi.org/10.1006/fstl.2000.0645

Özkan M., Kirca A., Cemeroğlu B. 2003. Effect of moisture content on CIE color values in dried apricots. European Food Research and Technology, 216(3), 217–219. https://doi.org/10.1007/s00217-002-0627-6

Paakki M., Sandell M., Hopia A. 2016. Consumer's reactions to natural, atypically colored foods: An investigation using blue potatoes. Journal of Sensory Studies, 31(1), 78–89. https://doi.org/10.1111/joss.12193

Palacios V.M., Caro I., Pérez L. 2002. Comparative study of crossflow microfiltration with conventional filtration of sherry wines. Journal of Food Engineering, 54(2), 95–102. https://doi.org/10.1016/S0260-8774(01)00189-3

Pathare P.B., Opara U.L., Al-Said F.A.J. 2013. Colour measurement and analysis in fresh and processed foods: A Review. Food and Bioprocess Technology, 1(6), 36–60. https://doi.org/10.1007/s11947-012-0867-9

Patras A., Brunton N.P., Da Pieve S., Butler F. 2009. Impact of high pressure processing on total antioxidant activity, phenolic, ascorbic acid, anthocyanin content and colour of strawberry and blackberry purées. Innovative Food Science & Emerging Technologies, 10(3), 308–313. https://doi.org/10.1016/j.ifset.2008.12.004

Patras A., Brunton N., Brijesh Kumar T., Butler F. 2011. Stability and degradation kinetics of bioactive compounds and colour in strawberry jam during storage. Food and Bioprocess Technology, 4, 1245–1252. https://10.1007/s11947-009-0226-7

Pedreschi F., León J., Mery D., Moyano P. 2006. Development of a computer vision system to measure the color of potato chips. Food Research International, 39(10), 1092–1098. https://doi.org/10.1016/j.foodres.2006.03.009

Pereira A.C., Reis M.S., Saraiva P.M. 2009. Quality control of food products using image analysis and multivariate statistical tools. Industrial & Engineering Chemistry Research, 48(2), 988–998. https://doi.org/10.1021/ie071610b

Pristijono P., Wills R.B.H., Golding J.B. 2006. Inhibition of browning on the surface of apple slices by short term exposure to nitric oxide (NO) gas. Postharvest Biology and Technology, 42(3), 256–259. https://doi.org/10.1016/j.postharvbio.2006.07.006

Qin P., Wang Q., Shan F., Hou Z., Ren G. 2010. Nutritional composition and flavonoids content of flour from different buckwheat cultivars. International Journal of Food Science and Technology, 45, 951–958. https://doi.org/10.1111/j.1365-2621.2010.02231.x

Quevedo R.A., Aguilera J.M., Pedreschi F. 2010. Color of salmon fillets by computer vision and sensory panel. Food and Bioprocess Technology, 3(5), 637–643. https://doi.org/10.1007/s11947-008-0106-6

Quitão-Teixeira L.J., Aguiló-Aguayo I., Ramos A.M., Martín-Belloso O. 2008. Inactivation of oxidative enzymes by high-intensity pulsed electric field for retention of color in carrot juice. Food and Bioprocess Technology, 1(4), 364. https://doi.org/10.1007/s11947-007-0018-x

Rhim J.W., Wu Y., Weller C.L., Schnepf M. 1999. Physical characteristics of a composite film of soy protein isolate and propyleneglycol alginate. Journal of Food Science, 64(1), 149––152. https://doi.org/10.1111/j.1365-2621.1999.tb09880.x

Rodriguez-Aguilera R., Oliveira J.C., Montanez J.C., Mahajan P.V. 2011. Effect of modified atmosphere packaging on quality factors and shelf-life of mould surface-ripened cheese: Part II varying storage temperature. LWT – Food Science and Technology, 44(1), 337––342. https://doi.org/10.1016/j.lwt.2010.06.014

Sahin S., Sumnu S.G. 2006. Physical Properties of Foods. Springer-Verlag, New York. https://doi.org/ 10.1007/0-387-30808-3

Salehi, F. 2020. Physico-chemical and rheological properties of fruit and vegetable juices as affected by high pressure homogenization: A review. International Journal of Food Properties 23(1), 1136–1149. https://doi.org/10.1080/10942912.2020.1781167

Scanlon M.G., Roller R., Mazza G., Pritchard M.K. 1994. Computerized video image analysis to quantify color of potato chips. American Journal of Potato Research, 71(11), 717. https://doi.org/10.1007/BF02849210

Segura L.I., Salvadori V.O., Goñi S.M. 2017. Characterisation of liquid food colour from digital images. International Journal of Food Properties 20(sup1), S467–S477. https://doi.org/10.1080/10942912.2017.1299758

Shewfelt R.L. 2002. Color. [In:] Postharvest Physiology and Pathology of Vegetables, Eds. J.A. Bartz, J.K. Brecht. CRC Press, New York, 313–323.

Shewfelt R.L., Heaton E.K., Batal K.M. 1984. Nondestructive color measurement of fresh broccoli. Journal of Food Science, 49(6), 1612–1613. https://doi.org/10.1111/j.1365-2621.1984.tb12857.x

da Silva Simão R., de Moraes J.O., Lopes J.B., Frabetti A.C.C., Carciofi B.A.M., Laurindo J.B. 2022. Survival analysis to predict how color influences the shelf life of strawberry leather. Foods 11(2), 218. https://10.3390/foods11020218

Siswantoro, J. 2019. Application of color and size measurement in food products inspection. Indonesian Journal of Information Systems 1(2), 90–107. https://doi.org/10.24002/ijis.v1i2.1923

Skoczylas Ł., Tabaszewska M., Smoleń S., Słupski J., Liszka-Skoczylas M., Barański R. 2020. Carrots (Daucus carota L.) biofortified with iodine and selenium as a raw material for the production of juice with additional nutritional functions. Agronomy 10(9), 1360. https://doi.org/10.3390/agronomy10091360

Spence C. 2018. What is so unappealing about blue food and drink? International Journal of Gastronomy and Food Science, 14, 1–8. https://doi.org/10.1016/j.ijgfs.2018.08.001

Tan J. 2004. Meat quality evaluation by computer vision. Journal of Food Engineering, 61(1), 27–35. https://doi.org/10.1016/S0260-8774(03)00185-7

Tiwari B.K., Muthukumarappan K., O'Donnell C.P., Cullen P.J. 2008. Effects of sonication on the kinetics of orange juice quality parameters. Journal of Agricultural and Food Chemistry, 56(7), 2423–2428. https://doi.org/10.1021/jf073503y

Velasco C., Michel C., Youssef J., Gamez X., Cheok A., Spence C. 2016. Colour–taste correspondences: Designing food experiences to meet expectations or to surprise. International Journal of Food Design, 1, 83–102. https://doi.org/10.1386/ijfd.1.2.83_1

Vivek K., Subbarao K.V., Routray W., Kamini N.R., Dash K.K. 2020. Application of fuzzy logic in sensory evaluation of food products: A comprehensive study. Food and Bioprocess Technology, 13(1), 1–29. https://doi.org/10.1007/s11947-019-02337-4

Yam K.L., Papadakis S.E. 2004. A simple digital imaging method for measuring and analyzing color of food surfaces. Journal of Food Engineering, 61(1), 137–142. https://doi.org/10.1016/S0260-8774(03)00195-X

Yu H., MacGregor J.F., Haarsma G., Bourg W. 2003. Digital imaging for online monitoring and control of industrial snack food processes. Industrial and Engineering Chemistry Research, 42(13), 3036–3044. https://doi.org/10.1021/ie020941f

Zhou X., Wan X., Mu B., Du D., Spence C. 2015. Crossmodal associations and subjective ratings of Asian noodles and the impact of the receptacle. Food Quality and Preference, 41, 141–150. https://doi.org/10.1016/j.foodqual.2014.11.013

VII APPLICATION OF CIRCULAR DICHROISM SPECTROSCOPY IN FOOD RESEARCH

Urszula BŁASZCZYK

Department of Fermentation Technology and Microbiology,
Faculty of Food Technology, University of Agriculture in Krakow,
Aleja Mickiewicza 21, 31-120 Krakow, Poland

urszula.blaszczyk@urk.edu.pl
ORCID: https://orcid.org/0000-0003-2905-4937

Abstract. Circular dichroism spectroscopy is an excellent method for studying the secondary and tertiary structure of proteins in solution. The technique has found many applications in food research. Abundant research is focused on monitoring conformational changes in food proteins occurring during physical (e.g. high temperature, ultrasound, high pressure) or chemical (e.g. phosphorylation, Maillard reaction, acylation) processing. Even slight modifications to the conformation of proteins can significantly change their physicochemical and functional properties, thus changing their use as ingredients in the food industry. Another group of circular dichroism studies concerns the interaction of proteins with ligands and the determination of structural alterations of proteins due to ligand binding. In this work, examples of such application are given, covering the interaction of serum albumin with food dyes (quinoline yellow, allura red or curcumin) important from the point of view of toxicological studies, as well as interactions of serum albumin with tea polyphenols.

Keywords: circular dichroism, food protein, conformational change, interaction of ligand-protein

1. Introduction

Circular dichroism (CD) spectroscopy is based on a phenomenon discovered by Aimé Cotton in the 1890s. He found that optically active molecules absorb right and left circularly polarized light unequally. Thus, circular dichroism spectroscopy allows the recording of the wavelength-dependent differences in the absorption of two components of circularly polarized light by chiral molecules or symmetric molecules in asymmetric environment (Fig. 1) [Gopal et al. 2012]. Quantitatively, circular dichroism can be expressed as the difference of molar coefficients absorption of left and right circularly polarized light: $\Delta\varepsilon = \varepsilon L - \varepsilon R$, where: εL and εR are molar absorption coefficients of left- and right circularly polarized light. Because the CD spectra are differential, the measured effect can be positive or negative; and therefore, in the case of a stronger absorption of the left-handed component, the difference in the absorption coefficients is positive, and the spectrum shows a positive Cotton effect. In turn, when the difference absorption coefficient is negative, it is observed a negative Cotton effect (Fig. 1) [Matera-Witkiewicz and Janicka-Kłos 2015].

Circular dichroism (CD) spectroscopy is one of the spectroscopic techniques used to study the conformation of biomolecules in a solution and provides important information that complements the data obtained by other methods [Greenfield 2006]. Since the CD spectra reflect the overall structure of the protein, the circular dichroism technique can be used to monitor any structural alterations

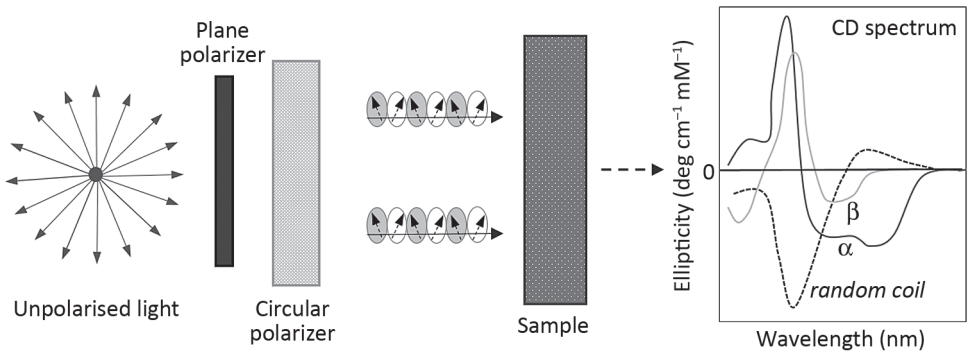

Fig. 1. A schematic diagram of CD technique. The plane polarized light passes through the modulator; circular dichroism occurs when the absorption of left- and right-handed circularly polarized components by optically active sample is not equal. The shape and magnitude of CD spectra in far-UV for different types of protein secondary structure are characteristic (source: own modification based on Ranjbar and Gill [2009])

that might result from changes in environmental conditions, such as temperature, pH, ionic strength, etc. CD spectroscopy is also used to study the influence of targeted mutations on the structure and stability of proteins. Moreover, the technique allows to monitor the unfolding of a polypeptide chain as a function of temperature or chemical denaturants, and is also applicable to the determination of conformational changes due to macromolecule-ligand and macromolecule-macromolecule interactions [Martin and Schilstra 2008; Birnbaum 2018]. The CD spectroscopy is an excellent method for studying the secondary and tertiary structure of proteins. The measurements of CD spectra in the far-UV range (160–240 nm) are particularly useful because singlet electron transitions resulting from the backbone peptide bond occur at 190 and 220 nm. The spectra of CD proteins in the far-UV region allow for observing the differences between the random coil and ordered structures such as α-helix or β-sheet, and estimating the content of individual secondary structures [Rogers et al. 2019]. The CD spectrum of disordered peptides or proteins has a single negative band near 195 nm, while α-helical structures typically have two negative bands at 208 and 222 nm along with one positive band at 192 nm [Greenfield 2006; Gopal et al. 2012]. For antiparallel β-pleated sheet structures, a negative band at 218 nm and a positive band at 195 nm are usually observed [Greenfield 2006]. The use of reference databases, consisting of spectra of proteins with known structures, allows for the decomposition of the CD spectrum of an unknown protein and provides information on the secondary structure of the analyzed protein [Choi and Ma 2007]. In contrast to far-UV, CD spectra in the near-UV region (250–320 nm) can provide useful information related to the presence of aromatic chromophores in a protein, such as the amino acid residues Phe, Tyr, and Trp (phenylalanine, tyrosine and tryptophan), in an asymmetric environment. The shape and magnitude of the CD spectrum in the near-UV depend on not only the particular aromatic amino acids, but their mobility as well as the nature of their environment (hydrogen bonds, polar groups) and their spatial distribution in the protein [Zhuo et al. 2013]. This information is used to evaluate the tertiary and sometimes quaternary structure of proteins during processing. The increase in band size and intensity demonstrates structural changes that are associated with loss of native structure and increasing aromatic amino acid residue interactions during processing [He et al. 2014; Wang et al. 2017].

2. Relationship between conformation and functional properties of food proteins

The rapid characterization of proteins is crucial not only in the field of proteomics, but also in food science. Functional properties of food proteins are closely related to their chemical structure, which can be changed by different external factors such as temperature, pH and ionic strength of the environment [Wang et al. 2017]. The amino acid sequence of a protein determines its spatial structure [Berg et al. 2018]. Some observations indicate that the native structure of proteins found in a living cell might be also dependent on interactions with other proteins or nucleic acids. Proteins fold into the structures with the lowest energy. According to Anfinsen's [1973] hypothesis, the amino acid sequence of a protein unequivocally determines its structure. This rule is certainly true for small globular proteins. Anfinsen found that the native structure usually corresponds to the minimum free energy of the system in which the protein is located [Anfinsen 1973].

The secondary structure of proteins defines the way the polypeptide chain is arranged in certain regular spatial structures, such as the α-helix, β-sheet, β-turn or hairpin, etc. The tertiary structure is the arrangement of the entire polypeptide chain along with all secondary structures in space. The tertiary organization of proteins is stabilized by disulfide bridges, hydrogen bonds, and hydrophobic, ionic and van der Waals interactions between the side groups of amino acids. For most known proteins, the correct spatial structure is necessary for their physiological role. It is believed that serious diseases such as Alzheimer's and Creutzfeldt-Jakob's diseases are a consequence of incorrect folding of proteins. When the polypeptide chain takes a different conformation from the proper structure, it usually leads to the formation of a protein with different properties, which in some cases can be toxic to the body (prion proteins may be an example) [Berg et al. 2018].

The chemical nature of the amino acid side chain groups determines the hydrophobicity and shape of proteins. In general, proteins tend to become globular when they contain a large number of hydrophobic residues, while an elongated rodlike shape appears when polypeptide chain contains many hydrophilic amino acid residues that are distributed uniformly in its sequence. Mostly when the protein takes the native structure, the hydrophobic segments are buried in the core. The hydrophobicity and hydrophilicity of the surface of proteins significantly affect their solubility, and thus such functional properties as foaming, emulsifying, thickening and gelling [Hettiarachchy et al. 2012]. The pH of the environment

has a significant influence on the solubility of proteins in aqueous solutions. At the isoelectric point, proteins are characterized by the lowest solubility and viscosity, and the hydrophobic interactions reach the maximum. At a pH above or below the isoelectric point, electrostatic repulsion and hydration tend to promote protein dissolution. Under such conditions, some functional properties can be improved. It might be related to protein unfolding and activation of buried sulfhydryl groups. Other environmental factors such as ionic strength as well as temperature-induced protein denaturation might also influence the solubility of the protein [Wang et al. 2017].

Various physical, chemical or enzymatic modifications are used to change the conformation and functionality of food proteins. The functional properties of denatured food proteins differ from those in their native state. For example, the process of denaturing proteins may reveal more amino acid residues and thus facilitate their proteolysis and improve protein digestibility [Perreault et al. 2017]. Exposure of hydrophobic regions can lower solubility and influence the surface activity of proteins [Shen and Tang 2012; Wang et al. 2017]. Moreover, a change in the conformation of protein toxins may inhibit their activity. In addition to modifications, the functional properties of food proteins also depend on the state of the protein: wet or dry, liquid or frozen, globular or fibrous protein etc. [Kuan et al. 2013; Wang et al. 2017]. In summary, the modification of the functionality of food proteins is accompanied by conformational changes that affect the quality of the final product. Studies towards a thorough understanding of the relationship between structure and function of the protein are essential for the proper and effective use of this protein in the food industry.

3. Application of the circular dichroism method in food research

3.1. Influence of physical and chemical modifications on the conformation of food proteins

Even slight changes of the conformation of proteins occurring during physical and/or chemical modifications can significantly influence their physicochemical and functional properties, thus changing their use as ingredients in the food industry. In Table 1 are presented examples of the application of circular dichroism spectroscopy in the study of structural alterations of food proteins as a result of physical and chemical treatments.

Studies by Farrell et al. [2001] were devoted to the analysis of the secondary structure of bovine β-casein. This fraction in milk accounts for approximately 36% of casein proteins. The CD spectra indicated a structural similarity between β-casein and proteins known to contain a characteristic structural motif found in polyproline II, called polyproline helix. During heating, some changes in the content of secondary structures in β-casein was observed, which suggests the unfolding of these local structures. The only significant change was the increase in polyproline helix content. The analysis of the CD spectra suggests that the structure of the β-casein monomer becomes more compact with increase of temperature [Farrell et al. 2001].

Circular dichroism spectroscopy has been also used in studies of the influence of environmental conditions and heat treatment on the conformation of the globulin derived from buckwheat (*Fagopyrum esculentum* Moench) [Choi and Ma 2007]. The buckwheat globulin is a storage protein composed of six non-identical monomers that interact non-covalently with each other. The CD analysis of secondary structures showed that in the buckwheat globulin, the content α-helix is 15.0%, the β-sheet 25.8%; in addition 28.9% of the common buckwheat globulin is the β-turn, while 30.3% is a random coil. A decrease in pH to a value in the range of 3–5 led to a disturbance of the native protein structure, indicating unfolding and denaturation. Heating at 100°C resulted in lower content of the α-helix, the appearance of the anti-parallel β-sheet, and an increase in the content of a random coil, suggesting protein denaturation and aggregation [Choi and Ma 2007]. It has also been shown that both non-covalent and covalent interactions play an important role in stabilizing the conformation of the buckwheat globulin.

Whey protein is a mixture of globular proteins found in whey, which is a by-product of cheese production. This group of proteins includes β-lactoglobulin, α-lactalbumin, bovine albumin, casein glicoomacropeptide, immunoglobulins and lactoferrin. Whey proteins and their products are widely used in the food industry due to their high nutritional value and functional properties (solubility, emulsification, gelling, antioxidant activity). As a source of bioactive peptides, they have a favorable physiological effect on the human body [Miwa et al. 2013]. In study conducted by Birnbaum [2018], CD spectroscopy was used to analyze of 10 whey protein products. Taking into account the variety of processing, storage and transport conditions for whey products, it was analyzed whether these differences could be reflected in the structure of whey proteins. The obtained CD spectra showed many differences in the secondary and tertiary structure of whey proteins in the analyzed products. These alterations were due to thermal denaturation caused by different whey protein processing techniques (e.g. spray drying) as well as storage or transport conditions depending on the manufacturer. It was

Table 1. Application of CD spectroscopy to study conformational changes in food proteins as a result of various processing methods (source: own modification based on Wang et al. [2017])

Protein	Processing method	References
Bovine haemoglobin	Heat	Bhomi et al. [2016]
Egg ovotransferrin	Heat	Tong et al. [2012]
Whey protein isolate	Heat	Zhang and Zhong [2012]; Tomczyńska-Mleko et al. [2014]
Bovine β-lactoglobulin	Heat	Manderson et al. [1999]
Beer protein Z	Mashing, boiling	Han et al. [2015]
Rapeseed protein isolate	High pressure, heat	He et al. [2014]
Myofibrillar protein	High pressure	Qiu et al. [2014]
Soybean protein isolate	High hydrostatic pressure	Li et al. [2012]
Skeletal muscle myoglobin	High pressure carbon dioxide	Yan et al. [2016]
Bovine β-lactoglobulin	High pressure microfluidization	Zhong et al. [2012]
α-lactalbumin and β-lactoglobulin	High intensity ultrasound	Chandrapala et al. [2012]
Soybean β-conglycinin and glycinin	High intensity ultrasound	Hu et al. [2015]
Soybean glycinin	High intensity ultrasound	Zhou et al. [2016]
Black bean protein isolates	Ultrasound	Jiang et al. [2014]
Soybean protein isolate	Ultrasound	Hu et al. [2013]
β-conglycinin	Ultrasound and Maillard reaction	Zhang et al. [2014]
Peanut protein isolate	Maillard reaction	Liu et al. [2012]
Soybean protein isolate	Maillard reaction	Zhuo et al. [2013]
Whey protein isolate	Maillard reaction	Wang et al. [2013]
Soybean protein	Glycosylation, enzymatic cross-linking	Song and Zhao [2014]
Whey protein isolate	Enzymatic deamidation	Miwa et al. [2013]

noted that the CD technique can be a good tool to evaluate the impact of food processing and handling proteins in dry powder form [Birnbaum 2018].

The aim of the research undertaken by Tong et al. [2012] was to determine changes in the structure and potential allergenicity of ovotransferrin (OVT) caused by heat. Using the CD technique, reversible changes in the protein structure were observed at 55–60°C, while at temperature in range of 70–80°C, the structural alterations were irreversible. The results of the analysis of potential OVT allergenicity correlated well with the observed structural changes. The increase in antigenicity and potential allergenicity of ovotransferrin heated at a relatively low temperature (55–60°C) was probably caused by structure unfolding. As a result of this process, hydrophobic groups and intermolecular disulfide bonds as well as more antigenic epitopes hidden inside the native molecule might be exposed to the surface of the protein molecule. On the other hand, the decrease in antigenicity and potential allergenicity of the OVT protein observed during heating at higher temperatures (70–80°C) may be caused by the cleavage and rearrangement of disulfide bonds. It seems that in some cases controlled heat treatment of an allergic product can be a good way to reduce its allergenicity and adverse effect on the human body [Tong et al. 2012].

Ultrasound application is another way to modify food properties [Ozuna et al. 2015]. Several studies have investigated the effect of sonication on the secondary structure of proteins using the circular dichroism method. The obtained results are inconsistent. In an experiment performed by Frydenberg et al. [2016], the influence of high intensity ultrasound (HIU) on the thermal behavior, structure and nature of intra- and intermolecular bonds during protein heat gelation in whey protein isolates was investigated. Ultrasound (24 kHz, 300 W/cm^2, 2078 J/ml) significantly reduced the denaturation enthalpy, but the far-UV CD spectra remained unchanged, indicating that there were no differences in protein secondary structure. The lack of influence on the secondary structure can be attributed to the experimental system. CD measurements were taken 24 h after ultrasound, which could have influenced the results. It is possible that proteins had been partially unfolded during the ultrasound application, but this was a reversible process, therefore no changes in the secondary structure were detected after 24 h.

Another protein which structure has been analyzed using CD spectroscopy is soy protein. This protein consists of 4 major water-extractable fractions (named 2S, 7S, 11S and 15S) which are classified according to their sedimentation rates. Soy protein is widely used in food products due to its high nutritional value as well as good functional properties (e.g. emulsifying, gelling) [Zhou et al. 2016]. When applying high intensity ultrasound (HIU) to a soy protein isolate,

an increase in surface hydrophobicity, emulsifying activity, emulsion stability and protein solubility was observed, as well as change in rheological properties [Hu et al. 2013]. The use of HIU with lower power (20 kHz, 200 W) on the soy protein isolate resulted in a reduction in the α-helix and random coil content and an increase in the β-sheet structure. On the other hand, during processing with higher power (20 kHz, 600 W), the increase in the α-helix and disordered coil and the decrease in the β-sheet were observed [Hu et al. 2013]. In other studies by Chandrapala et al. [2011] it was also reported that the use of HIU led to an increase in the content of α-helix, while a decrease in the β-turn and β-sheet in the β-lactoglobulin protein. Chandrapala et al. [2012] also analyzed structural and functional changes of pure and mixtures of β-lactoglobulin (β-LG) and α-lactoglobulin (α-LA) after sonication at 20 kHz, 31 W, up to 60 min. During sonication, the content of reactive thiols and the hydrophobicity of the surface of the analyzed proteins had been increasing continuously, which indicated the unfolding of proteins. The CD spectra confirmed some secondary and tertiary structural changes. The results suggest that sonication had a greater effect on α-LA than on β-LG, and the properties of their mixtures differ significantly from the properties of each of the isolated proteins [Chandrapala et al. 2012].

Contradictory results to these obtained by Chandrapala et al. [2011] were reported by Stathopulos et al. [2004] who found that HIU increased the presence of the β structure, but decreased the α-helix structure in protein aggregates. Jin et al. [2015] in their research investigated the effect of sweep frequency and pulsed ultrasound (SFPU) and sequential double-frequency ultrasound (SDFU) on zein and glutelin. The pretreatment of SFPU had little effect on the secondary structure of zein, while SDFU reduced the β-sheet and increased the α-helix content. Both SFUP and SDFU increased the β-sheet and decreased the α-helix content of glutelin. Other studies of soybean β-conglycin showed that HIU did not change the secondary structure of 7S fraction in the Tris-HCl buffer [Hu et al. 2015]. In another report by Zhou et al. [2016] soybean glycinin was subjected to high intensity ultrasound (20 kHz, 80 W/cm^2, 0 to 40 min) at three ionic strengths (I = 0.06, 0.2 and 0.6) at pH 7.0. At all three ionic strengths, it was observed that the use of HIU increased the emulsion stability and reduced turbidity. In contrast, the particle size, solubility, index of emulsifying activity and surface hydrophobicity were different at the three ionic strengths. The results of the CD measurements showed that the HIU had only a minor effect on the secondary and tertiary structure of soybean glycinin. There was a slight increase in the content of β-sheet and a slight decrease in the content of β-turn. Similar observations have been reported by Jiang et al. [2014] who observed that high-intensity ultrasound increased the β-sheet content of black bean protein isolates. On the other hand,

Gülseren et al. [2007] noticed that the β-return content of bovine serum albumin decreased after the use of HIU. Many factors, such as the predominant type of protein secondary structure, the degree of denaturation and aggregation, conditions, as well as the type of the ultrasound used, might significantly influence the secondary structure of proteins.

Another type of modification that food proteins can be subjected to is a Maillard reaction. This reaction between proteins and polysaccharides is researched in order to improve functional properties, especially solubility and surface properties of proteins. Liu et al. [2012] investigated a dry-heated Maillard reaction between peanut protein isolate (PPI) and dextran (1:1 weight ratio) under controlled temperature and relative humidity conditions. The CD spectra showed that the Maillard reaction between PPI and dextran influenced the secondary structure of the peanut proteins, which was not only the result of biopolymer interactions but also thermal denaturation. Along with the course of the Maillard reaction, the α-helix structures were lost, with a simultaneous increase in the β-sheet content. Changes in the structure of PPI-dextran conjugates were mainly attributed to dextran modified conarachin and arachin (counting for 50% of peanut proteins) denatured by heat treatment. Moreover, in comparison with PPI, mixture and conjugates had more compacted tertiary conformation [Liu et al. 2012].

CD spectroscopy was also used to study the products of the Maillard reaction between whey protein isolate (WPI) and xylose (X), glucose (G) or sucrose (S) [Wang et al. 2013]. The CD spectra showed that the conjugates were characterized by a significant loss of secondary structure, which indicated a change in protein folding after the attachment of xylose and glucose to the WPI. The content of the β-sheet, β-turns and the random coil increased, while the α-helix decreased after the heat treatment of the aqueous solutions of the WPI-G and WPI-X systems. In the case of the CD spectra of the WPI-S conjugate, the change in the secondary structure of the proteins was not significant compared to the CD spectra of the initial WPI [Wang et al. 2013].

Another report describes the properties of conjugates of soy protein isolate (SPI) and dextran obtained by the Maillard reaction under macromolecular crowding out conditions [Zhuo et al. 2013]. The optimal reaction conditions determined experimentally were as follows: SPI to dextran ratio was 1:1 (w/w), a pH of 6.5, a temperature of 60°C, and a reaction time of 30 h. CD spectroscopy showed that the secondary and tertiary structures of the conjugate had changed significantly. The secondary structure of SDC (soy protein isolate-dextran conjugate) consisted mainly of β-sheets, with decreased α-helix content but with an increased content of disordered structures. The near-UV CD spectra showed that the SDC had a similar spectrum to SPI, but the intensity of all bands was lower

than that of SPI, indicating a significant loss of the tertiary conformation of the proteins in SDC [Zhuo et al. 2013].

Compared to the physical and chemical treatment, enzymatic modification is characterized by milder process conditions, easier reaction control, high modification efficiency and a lower amount of by-products formed. Gu et al. [2001] investigated protein-glutaminase (PG) modification of α-lactoglobulin (α-La). CD spectra showed that treatment of α-La with PG induced a change in its tertiary structure to a form close to a molten globule, while deamidation had no effect on the secondary structure of α-La. This molten globule-like form is closely related to the functional properties of food proteins such as gelling, emulsifying and foaming. Similar results were also obtained by Miwa et al. [2013] during analyzes of the effect of protein glutaminase (PG) on heat-induced conformational changes in whey protein isolate (WPI). The obtained CD spectra in the near-UV region allowed to observe that both heating and deamidation caused denaturation and loss of the tertiary structure of whey proteins. However, there were some differences in the CD spectra between the heat-treated or deamidated protein-glutaminase (PG) samples.

3.2. Investigation of the interaction of protein with ligand and determination of conformation changes as a result of ligand binding

Table 2 presents examples of application of CD spectroscopy to study the interaction of ligand-protein. Serum albumin (SA) is the most commonly used protein in binding studies of various ligands. SA is the main plasma protein, accounting for 60% of all plasma proteins. One of the basic functions of SA is the transport of various endogenous and exogenous compounds such as drugs, hormones or fatty acids [Reddy et al. 1999; Zsila et al. 2003].

Human serum albumin (HSA) is a globular protein that is composed of 3 homologous helical domains (I–III) that undergo conformational changes in response to pH modification or as a result of ligand binding [Bose 2016]. Each domain consists of 2 subdomains (A and B), containing 585 amino acid residues and stabilized by 17 disulfide bridges [Wu et al. 2015]. It was found that there are two ligand binding sites in the structure of HSA called the Sudlow I site and the Sudlow II site, located in subdomains IIA and IIIA [Wu et al. 2015]. Bovine serum albumin (BSA) is 76% homologous to human protein in its amino acid sequence but has three hydrophobic pockets. BSA consists of 582 amino acid residues constituting a single polypeptide organized into three homologous domains (I, II and III). Each

Table 2. Application of CD spectroscopy to study the interaction of ligand-protein (source: own elaboration)

Protein	Ligand	References
Human serum albumin	Curcumin	Reddy et al. [1999]; Zsila et al. [2003]
	Allura red AC	Wu et al. [2015]
	Kaempferol	Matei and Hillebrand [2010]
	Atrazine	Zhu et al. [2018]
	Carmoisine	Datta et al. [2013]
	Amaranth	Zhang and Ma [2013]
	(-)-epigallocatechin-3-gallate	Maiti et al. [2006]
Bovine serum albumin	2-tert-butylhydroquinone	Shahabadi et al. [2011]
	Quinoline	Shahabadi et al. [2012]
	Maltol	Zhang et al. [2012]
	(-)-epigallocatechin-3-gallate-copper complex	Zhang et al. [2019]
	Tea polyphenols	Bose [2016]
	Polyphenols	Skrt et al. [2012]
	Carmoisine	Datta et al. [2013]
Hemoglobin	Amaranth	Basu and Kumar [2015]
α-galactosidase	Cyclodextrins	Zou et al. [2017]

domain contains 10 helical segments and is divided in two subdomains (A and B) [Bose 2016; Zhang et al. 2019]. Binding of various compounds, including toxins, to serum albumin can have physiological effects. Serum albumin often modifies the solubility of hydrophobic compounds in plasma and modulates their delivery to cells. Absorption, distribution, metabolism, as well as the stability and toxicity of various compounds may be significantly changed as a result of their binding to serum albumin [Shahabadi et al. 2011; Zhang et al. 2012]. Therefore, studies of the interaction of these substances with serum albumin as the main proteins carrier

in plasma seems to be important for a better understanding of the metabolism and transport of these compounds, as well as to clarify the relationship between protein structure and function.

Food dyes are a group of food additives which main purpose is to improve the aesthetic value of food products. One of the dyes that have been tested for interaction with human serum albumin (HSA) by circular dichroism (CD) is curcumin. Curcumin is a compound found in turmeric rhizomes (*Curcuma longa*) and polyphenolic antioxidant that is believed to have anti-cancer, anti-inflammatory properties, and has been extensively studied for the prevention and inhibition of Alzheimer's disease [Reddy et al. 1999; Zsila et al. 2003]. The CD spectra of the curcumin-HSA complex changed significantly as the pH of the solution increased compared to the control spectrum at pH 7.4. The conformation alteration of HSA-bound curcumin is probably due to deprotonation of the phenolic OH group(s) of curcumin [Zsila et al. 2003]. The results of research showed that curcumin adopts different conformations, which may be of particular importance for the exertion of various pharmacological effects. Conformational change in the curcumin structure may significantly modify its biological activity [Zsila et al. 2003]. Earlier attempts to elucidate the physiological transport of curcumin, conducted and reported by Reddy et al. [1999], showed that curcumin does not change the conformation of the HSA protein. In addition, there are two types of curcumin binding sites in serum albumin, one with high affinity (with 1:1 binding stoichiometry) and the other with low affinity. Hydrophobic interactions are mainly involved in the formation of the curcumin-HSA complex [Reddy et al. 1999].

Quinoline yellow (Qy) is a synthetic dye used to color foods, medicines, and soft drinks. Excessive consumption of Qy with food can cause asthma, rash and hyperactivity [Shahabadi et al. 2012]. The results of CD studies showed that dye binding induced changes in the secondary structure of BSA. An increase in the α-helix content was observed from 36.60% in free BSA to 47.99% with the molar ratio of BSA to Qy of 1: 1.2 [Shahabadi et al. 2012]. Another azo dye which interaction with serum albumin has been studied is allura red AC [Wu et al. 2015]. Allura red AC is a food additive (E129), used to color beverages, cakes, sweets or powdered jelly. Like other azo dyes, allura red is suspected of causing allergies, especially in the presence of aspirin or benzoic acid intolerance. The results of a study by Wu et al. [2015] showed that allura red is bound by HSA protein at site I localized within the IIA subdomain. CD studies have shown that the binding of allura red to HSA induces a carbonyl rearrangement of the hydrogen bond network of the polypeptides, which alters the secondary structure of HSA. As the concentration of allura red increases, the content of α-helix, which is the domi-

nant secondary structure in HSA, decreases, the content of β-sheet also decreases, while the proportion of random coil and turn β increases.

Tert-butylhydroquinone (TBHQ) is used in food as an effective preservative of unsaturated vegetable oils as well as many edible animal fats and meat products [Shahabadi et al. 2011]. As a food additive, it is marked with the symbol E319. Shahabadi et al. [2011] investigated the interaction between TBHQ and bovine serum albumin (BSA) using several spectroscopic techniques. The obtained CD and FT-IR (Fourier Transform InfraRed) spectra indicate that the conformation of the BSA molecule is significantly altered in the presence of TBHQ. After ligand binding, the content of α-helical structure in BSA decreased. Hydrophobic interactions and hydrogen bonds play a major role in the binding of TBHQ [Shahabadi et al. 2011].

Maltol was another compound which interaction with serum albumin was investigated. This compound can be found in roasted malt, pine needles or larch tree bark. Maltol is a food additive (E636) mainly used as a flavor enhancer. However, excessive consumption of this compound can be potentially harmful, causing damage to, among others, kidneys. In a maltol-bovine serum albumin (BSA) interaction study, Zhang et al. [2012] used the methods of fluorescence, circular dichroism (CD) and FT-IR spectroscopy. The obtained results indicated that maltol was mainly bound in the subdomain IIA (Sudlow site I) of bovine serum albumin. Mainly hydrophobic interactions were involved in the interactions. The CD spectra confirmed that the secondary structure of BSA was changed in the presence of maltol. Compared to free BSA, with the maltol to BSA molar ratio of 10:1, the α-helix content decreased from 59.9% to 53.2%, while the β-sheet, β-coils and random coil content increased from 5.6% to 8.4%, from 12.4% to 13.5%, and from 22.1% to 24.9%, respectively [Zhang et al. 2012]. The obtained results describing the interaction of maltol with BSA were consistent with the results obtained earlier by Shahabadi et al. [2011] in TBHQ binding study.

Skrt et al. [2012] reported that the binding affinity to BSA was highest for the esterified catechins (epigallocatechin-3-gallate and epicatechin-3-gallate) and lowest for epigallocatechin. The structure of the polyphenols significantly influenced the binding process to BSA. It was noted that binding affinity decreased with glycosylation and lower number of hydroxyl groups in the second aromatic ring of catechins. The CD spectra showed that the (−)-epicatechin-3-gallate binding induced the greatest changes in the secondary structure of BSA.

Other studies have focused on the analysis of interactions of tea polyphenol such as: (−)-catechin (C), (−)-epicatechin (EC), (−)-epicatechin gallate (ECG), (−)-epigallocatechin (EGC) and (−)-epigallocatechin-3-gallate (EGCG), with bovine serum albumin (BSA) [Bose 2016]. The CD spectra revealed that the binding of the polyphenols resulted in a partial unfolding of the helical structure and an

increase in the content of β-sheet structure for most of the polyphenols used. Additionally, the CD spectra confirmed the increased efficiency of the galloyl moiety in inducing more pronounced structural changes in the protein [Bose 2016]. Therefore, the content of the α-helical structure in BSA decreased after interaction with the ECG to a greater extent than for the EC [Bose 2016]. Similarly, Maiti et al. [2006] noted that the α-helix content of HSA was reduced by 57% to 54% after binding to EGCG. At the same time, a slight increase in the β-sheet and the disordered structure of the protein was noticeable. It was also observed that the binding constants decreased with increasing temperature, indicating that temperature had a significant effect on HSA-EGCG binding [Bose 2016].

CD spectroscopy was also used to study the interaction between bovine serum protein (BSA) and the epigallocatechin-3-gallate (EGCG) copper complex under physiological conditions. EGCG is a polyphenol compound, a catechin derivative, present in the extract obtained from the leaves of *Camellia sinensis*. (−)-epigallocatechin-3-gallate is one of the most effective antioxidant compounds, showing antimutagenic and antitumor activity [Zhang et al. 2019]. The results of the experiment carried out by Zhang et al. [2019] showed that the binding of both EGCG and the EGCG-Cu complex to bovine serum protein (BSA) is accompanied by structural changes consisting in a decrease in the content of the α-helical structure [Zhang et al. 2019].

4. Advantages and limitations of circular dichroism spectroscopy

The most important spectroscopic techniques for studying the conformational changes of proteins in solutions are CD, FT-IR, Raman, fluorescence and UV spectroscopy. It should be noted that the CD method, like other spectroscopic techniques, should not be used alone and the information obtained from CD, is complemental to the data from other spectroscopic techniques. CD analysis has several important advantages, one of which is that it can be performed on small amounts of material in physiological buffers. CD spectroscopy is extremely sensitive to detecting protein conformational changes at a low concentrations (1 mg of protein). CD spectra in the far-UV region can provide useful information related to the protein's secondary structures, while CD spectra in the near-UV region allow to inference about the tertiary structure of the protein. CD spectroscopy is one of the best methods for monitoring any structural alterations that may result from changes in environmental conditions such as temperature, pH, and ionic

strength. Moreover, the technique is very useful in studies of protein-ligand interactions and protein denaturation. Disturbances in the native protein structure after ligand attachment, as well as these due to heat exposure or chemical agents, are visible as changes in the CD spectrum of the protein [Gopal et al. 2012]. It is also worth emphasizing that circular dichroism spectroscopy is a relatively simple and uncomplicated technique, and the CD measurements are fast [Choi and Ma 2007; Martin and Schilstra 2008].

The disadvantage of this technique can be quite complicated data analysis. The programs for estimating the content of secondary protein structures on the basis of data obtained from CD spectroscopy differ from each other in the calculation method used. The analysis of protein secondary structure largely depends on reference databases. CD spectrum processing software and computational approaches as well as more accurate reference databases are constantly being improved and refined.

In addition, only clear and highly diluted samples can be analyzed. Mostly, however, in diluted samples proteins are not in typical concentrations as they are in food products. Reliable assessment of protein conformational changes is possible only with high purity of the sample and under strictly defined environmental conditions. For some analyzes, protein solutions for CD measurement should have a purity of at least 95%. Furthermore, protein sample dissolution buffers must be transparent and contain no optically active substances. Disturbances in CD measurements due to the absorbance of various salts and buffering substances in the far-UV region limit the use of CD spectroscopy to study some effects of environmental conditions such as the presence of chaotropic salts or other factors disrupting the structure of proteins [Choi and Ma 2007]. When analyzing food, usually complex matrices are examined, containing not only proteins, but also a number of other components, including lipids, starch, dyes, etc. This complexity of real food systems might cause many difficulties in monitoring protein conformation. Moreover, it should be noted that the accuracy of this technique is highly dependent on reference databases verified by other techniques [Martin and Schilstra 2008].

5. Conclusion

Circular dichroism technique is an excellent method to determine the conformation of proteins in solution. CD measurements can be performed using small amounts of material in physiological buffers. Another important advantage is that

they allow the monitoring of structural changes in proteins resulting from modification in environmental conditions such as temperature, pH and ionic strength. However, CD spectroscopy, like other methods, has its limitations. It demands quite complicated data interpretation and very often measurement environment is far from the real one.

References

Anfinsen C.B. 1973. Principles that govern the folding of protein chains. Science, 181(4096), 223–230. https://doi.org/10.1126/science.181.4096.223

Basu A., Kumar G.S. 2015. Interaction of toxic azo dyes with heme protein: Biophysical insights into the binding aspect of the food additive amaranth with human hemoglobin. Journal of Hazardous Materials, 289, 204–209. https://doi.org/10.1016/j.jhazmat.2015.02.044

Berg J.M., Stryer L., Tymoczko J.L., Gatto G.J. 2018. Biochemia. Wydawnictwo Naukowe PWN, Warszawa.

Bhomi R., Trivedi V., Coleman N.J., Mitchell J.C. 2016. The thermal and storage stability of bovine haemoglobin by ultraviolet-visible and circular dichroism spectroscopies. Journal of Pharmaceutical Analysis, 6(4), 242–248. https://doi.org/10.1016/j.jpha.2016.02.004

Birnbaum M.D. 2018. A circular dichroism analysis of commercially available powdered whey protein structure. Journal of Nutrition and Food Sciences, 8, 1–3. https://doi.org/10.4172/2155-9600.1000690

Bose A. 2016. Interaction of tea polyphenols with serum albumins: A fluorescence spectroscopic analysis. Journal of Luminescence, 169(PartA), 220–226. https://doi.org/10.1016/j.jlumin.2015.09.018

Chandrapala J., Zisu B., Kentish S., Ashokkumar M. 2012. The effects of high intensity ultrasound on the structural and functional properties of α-lactalbumin, β-lactoglobulin and their mixtures. Food Research International, 48(2), 940–943. https://doi.org/10.1016/j.foodres.2012.02.021

Chandrapala J., Zisu B., Palmer M., Kentish S., Ashokkumar M. 2011. Effects of ultrasound on the thermal and structural characteristics of proteins in reconstituted whey protein concentrate. Ultrasonics Sonochemistry, 18(5), 951–957. https://doi.org/10.1016/j.ultsonch.2010.12.016

Choi S.M., Ma C.Y. 2007. Structural characterization of globulin from common buckwheat (Fagopyrum esculentum Moench) using circular dichroism and Raman spectroscopy. Food Chemistry, 102(1), 150–160. https://doi.org/10.1016/j.foodchem.2006.05.011

Datta S., Mahapatra N., Halder M. 2013. PH-insensitive electrostatic interaction of carmoisine with two serum proteins: A possible caution on its uses in food and pharmaceutical industry. Journal of Photochemistry and Photobiology B, 124, 50–62. https://doi.org/10.1016/j.jphotobiol.2013.04.004

Farrell H.M., Wickham E.D., Unruh J.J., Qi P.X., Hoagland P.D. 2001. Secondary structural studies of bovine caseins: Temperature dependence of β-casein structure as analyzed by circular dichroism and FTIR spectroscopy and correlation with micellization. Food Hydrocolloids, 15(4–6), 341–354. https://doi.org/10.1016/S0268-005X(01)00080-7

Frydenberg R.P., Hammershøj M., Andersen U., Greve M.T., Wiking L. 2016. Protein denaturation of whey protein isolates (WPIs) induced by high intensity ultrasound during heat gelation. Food Chemistry, 192, 415–423. https://doi.org/10.1016/j.foodchem.2015.07.037

Gopal R., Park J.S., Seo C.H., Park Y. 2012. Applications of circular dichroism for structural analysis of gelatin and antimicrobial peptides. International Journal of Molecular Sciences, 13(3), 3229–3244. https://doi.org/10.3390/ijms13033229

Greenfield N.J. 2006. Using circular dichroism spectra to estimate protein secondary structure. Nature Protocols, 1(6), 2876–2890. https://doi.org/10.1038/nprot.2006.202

Gu Y.S., Matsumura Y., Yamaguchi S., Mori T. 2001. Action of protein-glutaminase on α-lactalbumin in the native and molten globule states. Journal of Agricultural and Food Chemistry, 49, 5999–6005. https://doi.org/10.1021/jf010287z

Gülseren I., Güzey D., Bruce B.D., Weiss J. 2007. Structural and functional changes in ultrasonicated bovine serum albumin solutions. Ultrasonics Sonochemistry, 14(2), 173–183. https://doi.org/10.1016/j.ultsonch.2005.07.006

Han Y., Wang J., Li Y., Hang Y., Yin X., Li Q. 2015. Circular dichroism and infrared spectroscopic characterization of secondary structure components of protein Z during mashing and boiling processes. Food Chemistry, 188, 201–209. https://doi.org/10.1016/j.foodchem.2015.04.053

He R., He H.Y., Chao D., Ju X., Aluko R. 2014. Effects of high pressure and heat treatments on physicochemical and gelation properties of rapeseed protein isolate. Food Bioprocess Technology, 7(5), 1344–1353. https://doi.org/10.1007/s11947-013-1139-z

Hettiarachchy N.S., Sato K., Marshall M.R., Kannan A. 2012. Food Proteins and Peptides: Chemistry, Functionality, Interactions, and Commercialization. CRC Press, Boca Raton.

Hu H., Cheung I.W., Pan S., Li-Chan E.C. 2015. Effect of high intensity ultrasound on physicochemical and functional properties of aggregated soybean β-conglycinin and glycinin. Food Hydrocolloids, 45, 102–110. https://doi.org/10.1016/j.foodhyd.2014.11.004

Hu H., Wu J., Li-Chan E.C., Zhu L., Zhang F., Xu X., Fan G., Wang L., Huang X., Pan S. 2013. Effects of ultrasound on structural and physical properties of soy protein isolate (SPI) dispersions. Food Hydrocolloids, 30(2), 647–655. https://doi.org/10.1016/j.foodhyd.2012.08.001

Jiang L., Wang J., Li Y., Wang Z., Liang J., Wang R., Chen Y., Ma W., Qi B., Zhang M. 2014. Effects of ultrasound on the structure and physical properties of black bean protein isolates. Food Research International, 62, 595–601. https://doi.org/10.1016/j.foodres.2014.04.022

Jin J., Ma H., Wang K., Yagoub A., Owusu J., Qu W., He R., Zhou C., Ye X. 2015. Effects of multi-frequency power ultrasound on the enzymolysis and structural characteristics of corn gluten meal. Ultrasonics Sonochemistry, 24, 55–64. https://doi.org/10.1016/j.ultsonch.2014.12.013

Kuan Y.H., Bhat R., Patras A., Karim A.A. 2013. Radiation processing of food proteins – A review on the recent developments. Trends in Food Science & Technology, 30(2), 105––120. https://doi.org/10.1016/j.tifs.2012.12.002

Li H., Zhu K., Zhou H., Peng W. 2012. Effects of high hydrostatic pressure treatment on allergenicity and structural properties of soybean protein isolate for infant formula. Food Chemistry, 132(2), 808–814. https://doi.org/10.1016/j.foodchem.2011.11.040

Liu Y., Zhao G., Zhao M., Ren J., Yang B. 2012. Improvement of functional properties of peanut protein isolate by conjugation with dextran through Maillard reaction. Food Chemistry, 131(3), 901–906. https://doi.org/10.1016/j.foodchem.2011.09.074

Maiti T.K., Ghosh K.S., Dasgupta S. 2006. Interaction of (-)-epigallocatechin-3-gallate with human serum albumin: Fluorescence, Fourier transform infrared, circular dichroism, and docking studies. Proteins: Structure, Function and Genetics, 64(2), 355–362. https://doi.org/10.1002/prot.20995

Manderson G.A., Creamer L.K., Hardman M.J. 1999. Effect of heat treatment on the circular dichroism spectra of bovine beta-lactoglobulin A, B, and C. Journal of Agricultural and Food Chemistry, 47(11), 4557–4567. https://doi.org/10.1021/jf981291m

Martin S.R., Schilstra M.J. 2008. Circular Dichroism and its Application to the Study of Biomolecules. Methods in Cell Biology, 84, 263–293.

Matei I., Hillebrand M. 2010. Interaction of kaempferol with human serum albumin: A fluorescence and circular dichroism study. Journal of Pharmaceutical and Biomedical Analysis, 51(3), 768–773. https://doi.org/10.1016/j.jpba.2009.09.037

Matera-Witkiewicz A., Janicka-Kłos A. 2015. Technika dichroizmu kołowego – jej potencjał i znaczenie w badaniach biologicznych i farmaceutycznych. Farmacja Polska, 71(1), 28–33.

Miwa N., Yokoyama K., Nio N., Sonomoto K. 2013. Effect of enzymatic deamidation on the heat-induced conformational changes in whey protein isolate and its relation to gel properties. Journal of Agricultural and Food Chemistry, 61(9), 2205–2212. https://doi.org/10.1021/jf3047626

Ozuna C., Paniagua-Martínez I., Castaño-Tostado E., Ozimek L., Amaya-Llano S.L. 2015. Innovative applications of high-intensity ultrasound in the development of functional food ingredients: Production of protein hydrolysates and bioactive peptides. Food Research International, 77, 685–696. https://doi.org/10.1016/j.foodres.2015.10.015

Perreault V., Hénaux L., Bazinet L., Doyen A. 2017. Pretreatment of flaxseed protein isolate by high hydrostatic pressure: Impacts on protein structure, enzymatic hydrolysis and final hydrolysate antioxidant capacities. Food Chemistry, 221, 1805–1812. https://doi.org/10.1016/j.foodchem.2016.10.100

Qiu C., Xia W., Jiang Q. 2014. Pressure-induced changes of silver carp (Hypophthalmichthys molitrix) myofibrillar protein structure. European Food Research and Technology, 238, 753–761. https://doi.org/10.1007/s00217-014-2155-6

Ranjbar B., Gill P. 2009. Circular dichroism techniques: biomolecular and nanostructural analyses – A review. Chemical Biology & Drug Design, 74(2), 101–120. https://doi.org/10.1111/j.1747-0285.2009.00847.x

Reddy A.C.P., Sudharshan E., Rao A.G.A., Lokesh B.R. 1999. Interaction of curcumin with human serum albumin – A spectroscopic study. Lipids, 34, 1025–1029. https://doi.org/10.1007/s11745-999-0453-x

Rogers D.M., Jasim S.B., Dyer N.T., Auvray F., Réfrégiers M., Hirst J.D. 2019. Electronic circular dichroism spectroscopy of proteins. Chemistry, 5(11), 2751–2774. https://doi.org/10.1016/j.chempr.2019.07.008

Shahabadi N., Maghsudi M., Kiani Z., Pourfoulad M. 2011. Multispectroscopic studies on the interaction of 2-tert-butylhydroquinone (TBHQ), a food additive, with bovine serum albumin. Food Chemistry, 124(3), 1063–1068. https://doi.org/10.1016/j.foodchem.2010.07.079

Shahabadi N., Maghsudi M., Rouhani S. 2012. Study on the interaction of food colourant quinoline yellow with bovine serum albumin by spectroscopic techniques. Food Chemistry, 135(3), 1836–1841. https://doi.org/10.1016/j.foodchem.2012.06.095

Shen L., Tang C.H. 2012. Microfluidization as a potential technique to modify surface properties of soy protein isolate. Food Research International, 48(1), 108–118. https://doi.org/10.1016/j.foodres.2012.03.006

Skrt M., Benedik E., Podlipnik C., Ulrih N.P. 2012. Interactions of different polyphenols with bovine serum albumin using fluorescence quenching and molecular docking. Food Chemistry, 135, 2418–2424. https://doi.org/10.1016/j.foodchem.2012.06.114

Song C.L., Zhao X.H. 2014. Structure and property modification of an oligochitosan--glycosylated and crosslinked soybean protein generated by microbial transglutaminase. Food Chemistry, 163, 114–119. https://doi.org/10.1016/j.foodchem.2014.04.089

Stathopulos P.B., Scholz G.A., Hwang Y.M., Rumfeldt J.A., Lepock J.R., Meiering E.M. 2004. Sonication of proteins causes formation of aggregates that resemble amyloid. Protein Science, 13(11), 3017–3027. https://doi.org/10.1110/ps.04831804

Tomczyńska-Mleko M., Kamysz E., Sikorska E., Puchalski C., Mleko S., Ozimek L., Kowaluk G., Gustaw W., Wesołowska-Trojanowska M. 2014. Changes of secondary structure and surface tension of whey protein isolate dispersions upon pH and temperature. Czech Journal of Food Sciences, 32(1), 82–89. https://doi.org/10.17221/326/2012-CJFS

Tong P., Gao J., Chen H., Li X., Zhang Y., Jian S., Wichers H., Wu Z., Yang A., Liu F. 2012. Effect of heat treatment on the potential allergenicity and conformational structure of egg allergen ovotransferrin. Food Chemistry, 131(2), 603–610. https://doi.org/10.1016/j.foodchem.2011.08.084

Wang K., Sun D.W., Pu H., Wei Q. 2017. Principles and applications of spectroscopic techniques for evaluating food protein conformational changes: A review. Trends in Food Science & Technology, 67, 207–219. https://doi.org/10.1016/j.tifs.2017.06.015

Wang W., Bao Y., Chen Y. 2013. Characteristics and antioxidant activity of water-soluble Maillard reaction products from interactions in a whey protein isolate and sugars system. Food Chemistry, 139(1), 355–361. https://doi.org/10.1016/j.foodchem.2013.01.072

Wu D., Yan J., Wang J., Wang Q., Li H. 2015. Characterisation of interaction between food colourant allura red AC and human serum albumin: multispectroscopic analyses and docking simulations. Food Chemistry, 170, 423–429. https://doi.org/10.1016/j.foodchem.2014.08.088

Yan W., Xu B., Jia F., Dai R., Li X. 2016. The effect of high-pressure carbon dioxide on the skeletal muscle myoglobin. Food Bioprocess Technology, 9, 1716–1723. https://doi.org/10.1007/s11947-016-1747-5

Zhang B., Chi Y.J., Li B. 2014. Effect of ultrasound treatment on the wet heating Maillard reaction between β-conglycinin and maltodextrin and on the emulsifying properties of conjugates. European Food Research and Technology, 238(1), 129–138. https://doi.org/10.1007/s00217-013-2082-y

Zhang G., Ma Y. 2013. Mechanistic and conformational studies on the interaction of food dye amaranth with human serum albumin by multispectroscopic methods. Food Chemistry, 136(2), 442–449. https://doi.org/10.1016/j.foodchem.2012.09.026

Zhang G., Ma Y., Wang L., Zhang Y., Zhou J. 2012. Multispectroscopic studies on the interaction of maltol, a food additive, with bovine serum albumin. Food Chemistry, 133(2), 264–270. https://doi.org/10.1016/j.foodchem.2012.01.014

Zhang L., Liu Y., Wang Y. 2019. Interaction between an (-)-epigallocatechin-3-gallate-copper complex and bovine serum albumin: Fluorescence, circular dichroism, HPLC, and docking studies. Food Chemistry, 301, 125294. https://doi.org/10.1016/j.foodchem.2019.125294

Zhang Y., Zhong Q. 2012. Effects of thermal denaturation on binding between bixin and whey protein. Journal of Agricultural and Food Chemistry, 60(30), 7526–7531. https://doi.org/10.1021/jf3021656

Zhong J., Liu W., Liu C., Wang Q., Li T., Tu Z.C., Luo S.J., Cai X.F., Xu Y.J. 2012. Aggregation and conformational changes of bovine β-lactoglobulin subjected to dynamic high pressure microfluidization in relation to antigenicity. Journal of Dairy Science, 95(8), 4237–4245. https://doi.org/10.3168/jds.2012-5333

Zhou M., Liu J., Zhou Y., Huang X., Liu F., Pan S., Hu H. 2016. Effect of high intensity ultrasound on physicochemical and functional properties of soybean glycinin at different ionic strengths. Innovative Food Science and Emerging Technologies, 34, 205–213. https://doi.org/10.1016/j.ifset.2016.02.007

Zhu M., Wang L., Wang Y., Zhou J., Ding J., Li W., Xin Y., Fan S., Wang Z., Wang Y. 2018. Biointeractions of herbicide atrazine with human serum albumin: UV-Vis, fluorescence and

circular dichroism approaches. International Journal of Environmental Research and Public Health, 15(1), 116. https://doi.org/10.3390/ijerph15010116

Zhuo X.Y., Qi J.R., Yin S.W., Yang X.Q., Zhu J.H., Huang L.X. 2013. Formation of soy protein isolate-dextran conjugates by moderate Maillard reaction in macromolecular crowding conditions. Journal of Science of Food and Agriculture, 93(2), 316–332. https://doi.org/10.1002/jsfa.5760

Zou W., Wang M., Yao D., Zhu Z., Sun W., Cai H., Chen X., Li F., Shen W., Barba F.J., Zhang W. 2017. Fluorescence and circular dichroism spectroscopy to understand the interactions between cyclodextrins and α-galactosidase from green coffee beans. Food Bioscience, 20, 110–115. https://doi.org/10.1016/j.fbio.2017.09.002

Zsila F., Bikádi Z., Simonyi M. 2003. Unique, pH-dependent biphasic band shape of the visible circular dichroism of curcumin–serum albumin complex. Biochemical and Biophysical Research Communications, 301(3), 776–782. https://doi.org/10.1016/S0006-291X(03)00030-5

VIII ADVANCES IN APPLICATION OF ULTRASOUND IN FOOD PROCESSING AND ANALYZING

Angelika WOJTYŚ

Department of Analysis and Evaluation of Food Quality,
Faculty of Food Technology, University of Agriculture in Krakow,
Aleja Mickiewicza 21, 31-120 Krakow, Poland

angelika.wojtys@urk.edu.pl
ORCID: https://orcid.org/0000-0003-0593-6310

Abstract. Ultrasounds are mechanical waves, which originate from molecular movements oscillating in a propagation medium. The ultrasound waves are characterized by a frequency from 20 kHz to 1 MHz, that is beyond the range audible by humans. Depending on the frequency range, their applications in food processing, analysis, and quality control can be classified into two categories: low and high-power ultrasound. Low power ultrasound is used for monitoring the physical properties of food products, while high power ultrasound mainly supports many food processing operations (i.a. emulsification, extraction, drying, homogenization, pasteurization). This review summarizes the basic principles of the generation of ultrasounds and the main methods and applications of low and high-power ultrasound in food science and technology.

Keywords: ultrasound, application, food processing

1. Introduction

The type of sound wave depends on its frequency. The spectrum of sound, which represents the different frequencies present in the sound, is shown in Figure 1. Sound waves below the human hearing range are called infrasound. They are usually used by underwater sonars and whales. The frequency of sound for human hearing ranges from 20 Hz to 20 kHz. The audible signal can come from many sources, such as turbulence of gases or air, passage through fluids, and the impact of a solid against another solid. Sound is a natural phenomenon of waves therefore, it can contain either one frequency as a pure steady-state sine wave or complex frequencies (e.g. noise generated by multiple sources) [Arvanitoyannis et al. 2017; Mohammed and Alhajhoj 2019].

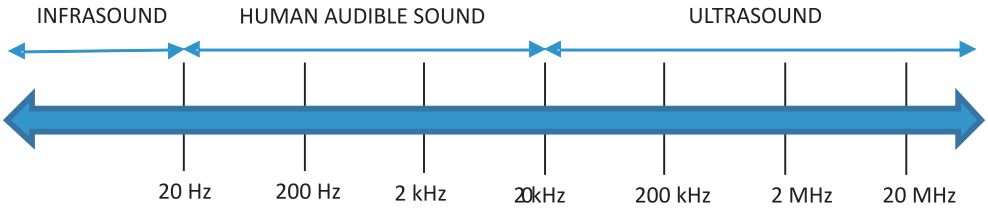

Fig. 1. Spectrum of the sound wave (source: based on Mohammed and Alhajhoj [2019])

The term ultrasound refers to sound waves beyond the range audible by humans, which is above 16 kHz. In practice, frequencies between 20 kHz and 10 MHz are usually used. Like audible waves, ultrasound is a mechanical wave in which the mechanical vibrations of medium particles around the equilibrium position propagate, in the medium, in the form of elastic waves. [Konopacka et al. 2015]. Depending on the angle at which the ultrasonic wave enters the material, three different types of waves can be generated: longitudinal waves, shear waves and surface waves (Figs 2A to 2C).

The longitudinal wave is generated as a result of applying the stress wave perpendicular to the surface materials, while the shear wave is generated by introducing a longitudinal wave parallel to the surface materials. The movement of molecules in the shear wave is perpendicular to the wave direction, so it has a lower speed and shorter wavelength than longitudinal waves of the same frequency. In turn, a surface wave (also called a Rayleigh wave) is generated when a longitudinal wave crosses surfaces at a critical angle of approximately 65° or more. These waves represent an oscillating motion that travels one wavelength across the material surface [Khairi et al. 2016].

Depending on the frequency range, ultrasound used in the food industry can be divided into two groups: low power ultrasound and high-power ultrasound. The first, ultrasound waves of low intensity (below 1 W/cm^2) and high frequency (above 100 kHz) are used as energy applicable in a non-invasive way, and are used to study the physicochemical properties of materials. The second one, high-intensity ultrasounds (above 1 W/cm^2, most often within the range from 10 to 1000 W/cm^2)

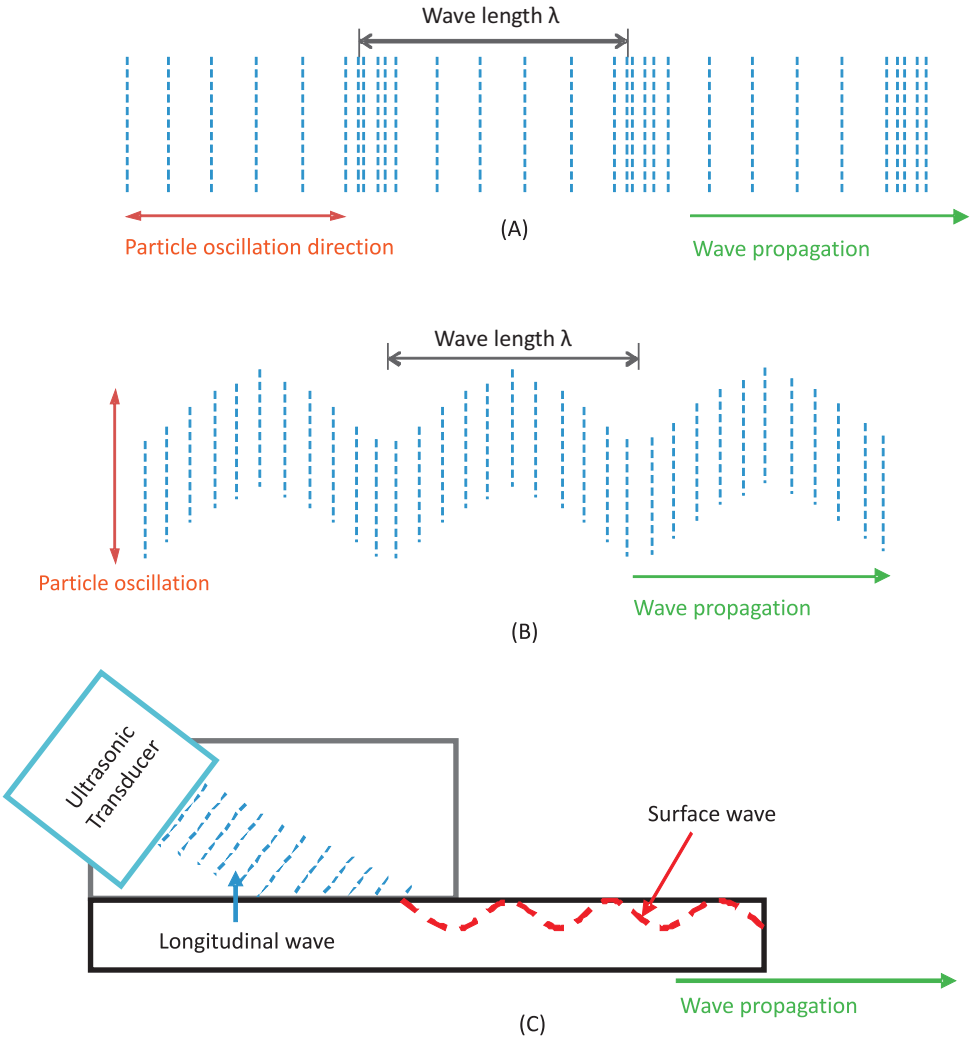

Fig. 2. Longitudinal wave (A), shear wave (B), surface wave (C) (source: based on Khairi et al. [2016])

and low frequency (usually within the range from 20 to 100 kHz), cause effects in the environment defined as secondary effects or even direct permanent changes after the passage of a harmonic wave, which can physically and chemically change the properties of materials [Awad et al. 2012; Konopacka et al. 2015].

The aim of this review is to summarize the basic principles of ultrasound and the main measurement methods used in food analysis and processing. In addition, the paper contains examples of the application of low and high power ultrasound in food analysis and processing over the last few years.

2. Ultrasound generation

The system generating ultrasonic waves consists of a generator, a transducer, and an application system. The purpose of the generator is to produce mechanical or electrical energy, while the transducer converts this energy into ultrasonic sound energy. The main types of transducers that are currently used are: fluid-driven, magnetostrictive transducers, and piezoelectric transducers [Khairi et al. 2016].

In fluid-driven transducers, the ultrasonic wave is produced by forcing liquid at high velocity to a thin metal blade, as usually used for homogenization or mixing. In essence, this type of transducer generates an ultrasonic wave when the kinetic energy of injected liquid causes the metal blade to vibrate [Ercan and Soysal 2013; Khairi et al. 2016].

Magnetostrictive transducers were the first to be used on an industrial scale to generate high power ultrasounds. In this type of transducer (Fig. 3A), the possibility of stimulating some solid bodies to vibrations through a magnetic field is used. The transducer is a rod made of a ferromagnetic material placed inside the wire coil, which is subjected to a magnetic field. The applied magnetic field, which arises when a current flows through the coil, causes a magnetic induction that in turn shortens or lengthens the rod. The rod returns to its' regular dimensions when the magnetic field is removed. This phenomenon is named magnetostriction. When the magnetic field is applied as a series of short pulses to a magnetostrictive material, it vibrates at the same frequency.

Materials with magnetostrictive properties include iron, nickel, cobalt, and many alloys of these metals, and a group of alum compounds called ferrites [Śliwiński 2001; Ercan and Soysal 2013].

The basis of piezoelectric transducers (Fig. 3B) is the piezoelectric phenomenon occurring in monocrystals with piezoelectric properties (quartz, tourmaline, lithium tantalate, lithium niobate, cadmium sulphide) and the electrostrictive phenomenon occurring in polycrystals composed of ferroelectric crystallites

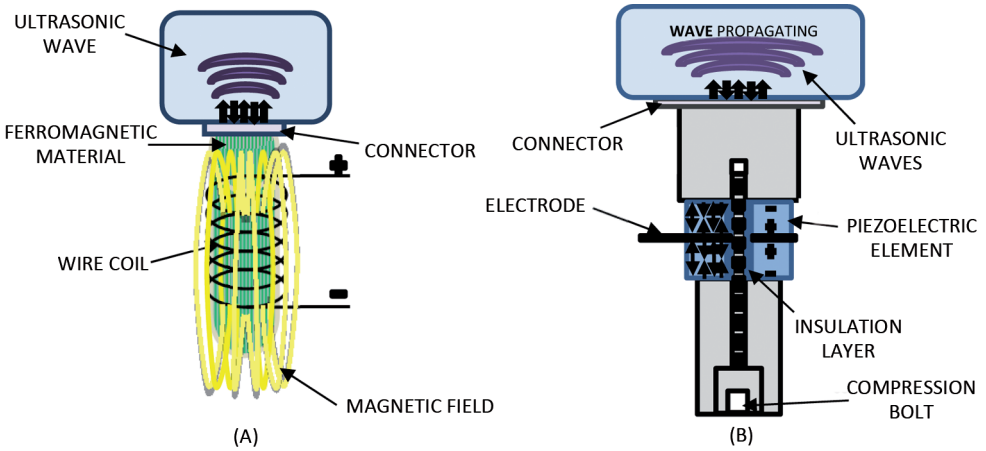

Fig. 3. Schema of magnetostrictive (A) and piezoelectric (B) transducers (source: based on Bhargava et al. [2021])

(barium titanate, barium zirconate). The piezoelectric phenomenon consists in the generation of an electric field in the material (the appearance of charges on its surface), which is subjected to external pressure. The intensity of the electric field is proportional to the mechanical stress. The most common form of a piezoelectrical transducer is a disk with a central hole. In practice, two piezoelectric discs are clamped between metal blocks which serve both to protect the delicate crystalline material and to prevent it from overheating. The resulting form provides a durable unit with doubled mechanical effect. This type of transducer is the most common device employed to generate ultrasound [Śliwiński 2001; Mulet 2003].

The application system is a coupler device which is used to transfer ultrasonic vibrations to the sample. This is generally obtained by probe system or ultrasonic bath. In ultrasonic baths, generally the transducers are fixed to the underside of the tank. Whereas, probe systems are used to transmit or to amplify the ultrasonic signal. Their lengths must be half the wavelengths, or multiple, to maintain the resonant conditions of the system. The amplitude gain of ultrasonic signal is defined by the probe shape [Ercan and Soysal 2013].

3. Low energy ultrasound in food processing

Passing an ultrasound wave through a substance, both solids, liquids and gases medium alters their structural and elasticity properties. When an ultrasonic transducer emits sound waves into a substance, the medium's molecules transfer mo-

tion to adjacent molecules and then return approximately to their original position [Mohammadi et al. 2014]. As a result of alternating compression and decompression cycles depending on the properties of the medium, the properties of ultrasonic waves (wavelength, velocity, amplitude, pressure, frequency and period) are changed. The parameters measured in majority studies are: ultrasonic velocity, attenuation coefficient and acoustic impedance [Awad et al. 2012; Dolas et al. 2019].

Ultrasonic velocity (c)

The main parameter in the ultrasonic sensor systems is ultrasonic velocity (c). It is sensitive to both the molecular system and intermolecular interactions. The velocity is calculated based on the distance propagated by ultrasonic waves in a unit of time as in the following equation:

$$c = \frac{d}{t} \tag{1}$$

where:

c – ultrasonic velocity,
d – distance,
t – time.

The ultrasonic velocity values depend on the medium (solid, liquid or gas) through which the wave travels. For a solid medium, a significant role in determining the output of the velocity have the density (ρ) and elastic (E) response of the material, which is affected by the oscillating pressure. The equation showing the correlation between these parameters depending on the size of the medium can be written by the formulas (plate and rod, respectively):

$$C = \sqrt{\frac{E}{\rho\left(1-\nu^2\right)}}; \quad C = \sqrt{\frac{E}{\rho}} \tag{2, 3}$$

The velocity of ultrasounds determination depends on the modulus of elasticity rather than density. It usually occurs because the differences in the modules of materials are higher than in density. The ultrasonic wave propagates faster into materials that are less dense or more resistant to deformation. Therefore, the wave velocity in the solid medium is faster than in liquid, even though it is less dense. The values of velocity for longitudinal waves in different types of medium are shown in Table 1. The following equation shows the modulus of elasticity for a solid medium that combines a volumetric modulus and a shear modulus:

$$E = K + \frac{4}{3} G \tag{4}$$

where:

K – bulk modules and

G – shear modulus.

Hence, the substitution of equation (4) into equation (3) results in the following formula:

$$C = \sqrt{\frac{K + \frac{4}{3} G}{\rho}} \tag{5}$$

In the case of liquid medium, which is characterized by homogeneous, compressible and isotropic characteristics, the shear modulus is not considered. Therefore, the equation is derived as follows [McClements and Gunasekaran 1997; Chandrapala 2015; Khairi et al. 2016; Firouz et al. 2019]:

$$C = \sqrt{\frac{B}{\rho}} \tag{6}$$

where:

B – adiabatic bulk modulus.

Table 1. The values of ultrasonic velocity in different materials measured at 20°C (based on McClements and Gunasekaran [1997])

Medium	Material	Velocity (m/s)
Solids	Glass	5560
	Aluminium	6400
	Steel	6000
Liquids	Water	1482
	Olive oil	1465
	Palm oil	1459
Gases	Air	330
	Oxygen	310
	Hydrogen	1300

Attenuation coefficient (α)

During the propagating of ultrasonic waves throughout the materials, their amplitude is reduced due to the attenuation phenomenon. The attenuation happens as a result of fluctuation produced by ultrasonic waves passing through the material that relates to its microscopic structure. The main factors that cause the attenuation phenomena are adsorptions and scattering. The absorption contribution is associated with a homogenous medium, whereas the scattering exists only in heterogeneous ones. The first factor occurs when the wave passes through a medium and is caused by a molecular process that converts the ultrasonic energy into thermal energy, reducing the initial amplitude of the wave signal. This process is called dissipation. In turn, scattering occurs when the ultrasonic wave strikes a discontinuity with dimensions larger than the wavelength (e.g. particles of medium) and is distracted in other directions than the incident wave (beyond the angular range of the ultrasonic transducer). In contrast to absorption, the energy is still transmitted as ultrasound, however the direction of propagation of the wave is changed, so it cannot be detected by a receiver in the forward direction. The attenuation coefficient (α) is determined by measuring the amplitude of a wave as a function of the distance propagated through a material and is defined by the following equation [McClements and Gunasekaran 1997; Chandrapala 2015; Khairi et al. 2016; Firouz et al. 2019]:

$$A = A_0 e^{-ax} \tag{7}$$

where:

A – amplitude of the wave,
x – distance traveled,
A_0 – initial (unattenuated) peak amplitude.

The attenuation coefficient is reported in the unit of Nepers per meter (Np/m) or decibels per meter (dB/m), where 1 Np = 8.686 dB [McClements and Gunasekaran 1997]. The parameter is used to quantify various materials based on how the amplitude of the transmitted ultrasound decreases as a function of frequency. A low value of the attenuation coefficient means that the medium is relatively transparent to the wave passing through it, while a high value means that the wave beam is quickly"weakened" as it passes through the medium [Chandrapala 2015].

Acoustic impedance (z)

Acoustic impedance (z) governs the proportion of transmission and reflectance of the ultrasound beam at the boundary between component phases. Simplified, it is the product of density (ρ) and ultrasonic velocity (c) passing through the boundary of material, which affects the reflection coefficients:

$$z = \rho c \tag{8}$$

Materials with different densities are characterized by different acoustic impedance, which results in reflections from the boundary between these materials. The SI unit of acoustic impedance is kg/m•s. This parameter is taken into account in cases where the ultrasonic wave travels from one medium to another (such as solid to liquid, gas to solid, liquid to gas, etc.) and is usually determined by measuring the fraction of an ultrasonic wave that is reflected from the material surface. Acoustic impedance is expressed by the following relationship [McClements and Gunasekaran 1997; Chandrapala 2015; Khairi et al. 2016; Dolas et al. 2019; Firouz et al. 2019]:

$$R = \frac{A_T}{A_t} = \frac{z_1 - z_2}{z_1 + z_2} \tag{9}$$

where:

R – a ratio of the amplitude of the reflected wave (A_T) to the incident wave (A_t), z_1 and z_2 – the acoustic impedances of two materials.

The sensitivity of ultrasound velocity to molecular organization and intermolecular interactions, makes, that this parameter measurement is suitable for determination of composition, structure, physical state, some molecular processes and detection of defects or foreign bodies in processed and packed food. In turn, the attenuation phenomenon depends on viscosity, compressibility, scattering, and absorption effects which can give information about some physical properties of food products, like phase composition, microstructure, bulk viscosity, rheology or size of the droplet, and stability in emulsions.

Moreover, this parameter is highly related to the way the analyzed material was produced, so it may be used in quality control assurance of various products. The application of the ultrasound velocity, attenuation coefficient, and acoustic impedance in different types of food analysis is summarized in Table 2.

Table 2. The application of ultrasonic parameters used in food analysis (source: own elaboration)

Parameter	Type of food analysis	References
Ultrasonic velocity (c)	Characterization of pork fat crystallization during cold storage	Corona et al. [2014]
	Evaluation of food-grade vegetable oils	Yan et al. [2019]
	Identification of meat types	Nowak [2015]
	Monitoring of changes of moisture and salt content during post-salting of meat	Contreras et al. [2021]
	Identification and investigation of mechanically separated meat (MSM)	Wieja et al. [2021]
	Evaluation of selected properties of a gelatinized potato starch colloid	Nowak and Markowski [2020]
Attenuation coefficient (α)	Determiantion of particle size distribution in diluted tomato paste	Ratajski et al. [2014]
	Determination of maturity and quality of tomato	Srivastava et al. [2014]
	Determination of fruit quality	Yildiz et al. [2019]
	Characterization of fresh pork loin of different feed system	González-Mohino et al. [2022]
	Online control of dough noodle quality	Kerhervé et al. [2019]
	Improvements yield during olive oil extraction	Amarillo et al. [2019]
Acustic impedance (z)	Evaluation of the quality of oranges	Morrison and Abeyratne [2014]
	Detection of dairy fouling	Wallhäußer et al. [2013]
	Estimation of coagulation time of milk	Derra et al. [2018]
	Monitoring of the cleaning of different food fouling materials	Escrig et al. [2019]

4. Ultrasound techniques in food analysis

For food analysis, pulse-echo, continuous-wave, and pitch-catch are the main techniques that are widely used in most ultrasound sensors. In these techniques, the transducers generate ultrasound pulses with a controlled frequency by transforming the electric current [Awad et al. 2012]. All of the above sensing modes can characterize the velocity, thickness, density, defects, and microstructure of the analyzed sample [Khairi et al. 2016].

Pulse-echo technique

Pulse-echo sensor mode is composed of a sample cell container, a signal generator, a transducer, and an oscilloscope (Fig. 4). The signal generator produces an electrical pulse which is converted to the ultrasound wave after passing through the transducer. The generated ultrasound pulse propagates through the sample and, after colliding with the wall of the sample, the container reflects to the transducer, which transforms it into the electric signals again. Then, the oscilloscope records the converted signal. The ultrasonic velocity and the attenuation coefficient can be calculated by analyzing the echoes received at the oscilloscope, due to the fact that each impulse is both partially transmitted and reflected. The ultrasonic parameters can be calculated as [Aboudaoud et al. 2012; Firouz et al. 2019]:

$$C = \frac{L}{\Delta T}; \qquad \alpha = \frac{1}{2L} \ln\left(\frac{A}{A_o}\right) \tag{10, 11}$$

where:

L – the cell thickness (m), ΔT – flight time of a sound wave (s), A and A_0 – amplitude of a sent and received ultrasound waves, respectively. The thickness of the sample cell (L) is half of the distance passed by ultrasonic pulse and can be calculated by referring to the material of known velocity.

The echo-pulse technique has found application in i.a. monitoring of yeast fermentation [Amer et al. 2015], characterization of maturity and quality of fruit [Morisson and Aeyratne 2014; Valente et al. 2013], estimation of coagulation time in cheese production [Derra et al. 2018] or comparison of milks, creams, and their dilutions [Yang et al. 2021].

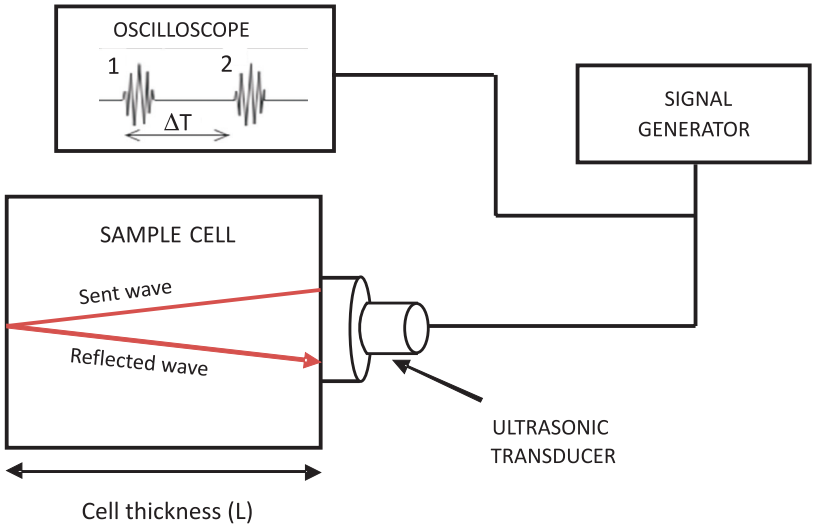

Fig. 4. A schematic diagram of ultrasonic pulse-echo technique (source: based on Firouz et al. [2019])

Continuous wave/through transmission technique

Continuous wave sensor mode is composed of two transducers located in front of each other (Fig. 5). The sample cell is equipped with two quartz X-cut transducers that are placed apart by a known distance (L). The pulse generator produces electrical continuous pulses with specific wavelength and frequency. The generated signal is fed to the first transducers (transmitter), where is converted to the ultrasound wave with the same frequency.

After passing through the sample cell, the generated ultrasonic wave is received by the second transducer (receiver), which converts it into the electrical signal. An oscilloscope, connected to both the generator and sample cell is used to record and monitor the original and final electrical pulses for comparison of the ultrasound parameters. Next, the recorded data is automatically transferred and stored in a connected computer. The ultrasonic velocity (c) and attenuation coefficient (α) can be calculated as follows [Kim et. al. 2009; Awad et al. 2012; Vasighi-Shojae et al. 2018; Firouz et al. 2019]:

$$C = \frac{L}{\Delta T}; \qquad \alpha = \frac{1}{L} \ln\left(\frac{A}{A_o}\right) \tag{12, 13}$$

where:

L – the cell length (m),
ΔT – time of flight (s),
A and A_0 – amplitude of the sent and received ultrasound waves, respectively.

Because the time needed for travelling of the initial pulse through the sample (time of flight) can be measured extremely precise, transmission techniques are widely used for applications, in which high accuracy is required [Mohammadi et al. 2014], such as improvement yield during olive oil extraction [Amarillo et al. 2019], evaluation of selected properties of a gelatinized potato starch colloid [Nowak and Markowski 2020] determining fruit quality and maturity [Yildiz et al. 2019] and monitoring process of milk curdling [Jiménez et al. 2017], or measuring acoustic properties without contact with the sample [Pallav et al. 2009].

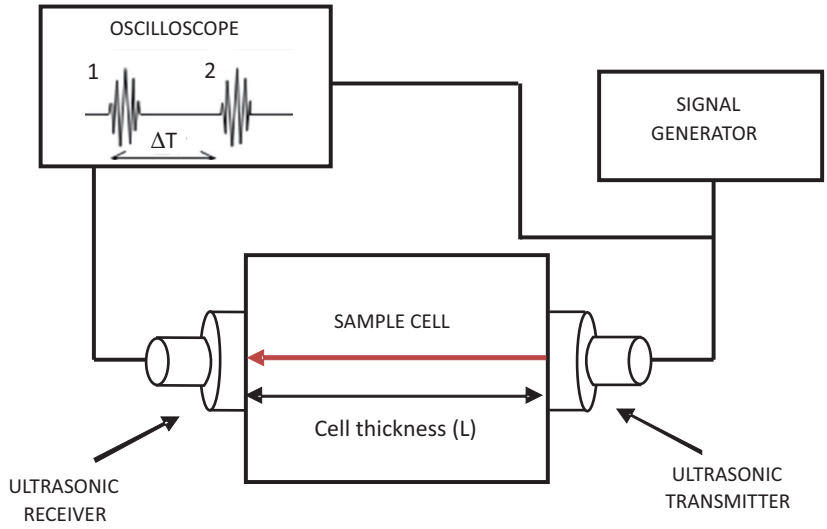

Fig. 5. A schematic diagram of ultrasonic continuous wave technique (source: based on Firouz et al. [2019])

Pitch-catch technique

Pitch-catch sensor mode is a modification of previously mentioned pulse-echo and continuous wave techniques. It is also composed of two transducers – transmitter and receiver, which are installed on the same side (Fig. 6). However, in this method, the ultrasonic pulse generated at a certain frequency passes through the sample and is reflected from the container wall back to the source of ultrasound.

Then, the receiving transducer converts the ultrasound pulse into the electrical signal [Khairi et al. 2016; Firouz et al. 2019].

The pitch-catch technique has found application in measurement of chilling injury in tomatoes [Verlinden et al. 2004] and evaluation of the hydration degree of the orange peel [Jiménez et al. 2012]. However, among the techniques mentioned, it is the least used in food analysis and processing.

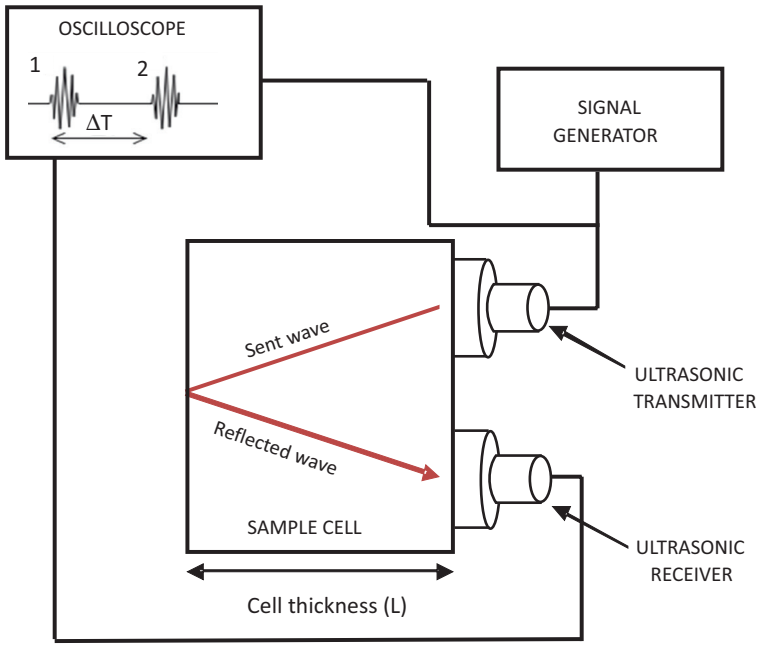

Fig. 6. A schematic diagram of ultrasonic pitch-catch technique (source: based on Firouz et al. [2019])

5. High power ultrasound in food processing

The main parameters affecting the power of ultrasound are energy, intensity, pressure, speed and temperature. When acoustic field is applied to a liquid the vibrations impose an acoustic pressure (P_a) additional to the ambient hydrostatic pressure (P_h) already present in the medium. The acoustic pressure is a sinusoidal wave dependent on time, frequency, and the maximum pressure amplitude of the wave; and it is represent by the following formula [Patist and Bates 2008]:

$$P_a = P_{a\max} \sin\left(2\pi f t\right) \tag{14}$$

where:

P_a – acoustic pressure,
t – time,
f – frequency,
P_{amax} – maximum pressure amplitude of the wave

The maximum pressure of the wave (P_{amax}) is directly related to the power input of the transducer.

The basic principle of high-power ultrasound is a cavitation phenomenon. A necessary condition for the occurrence of the phenomenon of cavitation in a solution is exceeding a certain intensity of ultrasound, called the cavitation threshold. The size of the cavitation threshold depends primarily on the physical state of the medium in which the waves propagate, its viscosity and density, and the process conditions (ultrasound intensity and frequency, temperature, pressure) [Konopacka et al. 2015]. Cavitation is the formation, growth and collapse of microbubbles within a solution as a result of pressure fluctuations caused the applied ultrasound field (Fig. 7). When the bubbles reach a critical size, they collapse during the compression cycle, creating a transient hotspot. As a result of the growth and rapid decomposition of gas bubbles, the temperature (to 5000 K) and pressure (up to 100 MPa) increase which causes waves with high shear force and turbulence [Chemat et al. 2017; Paniwnyk 2017; Alarcon-Rojo et al. 2019].

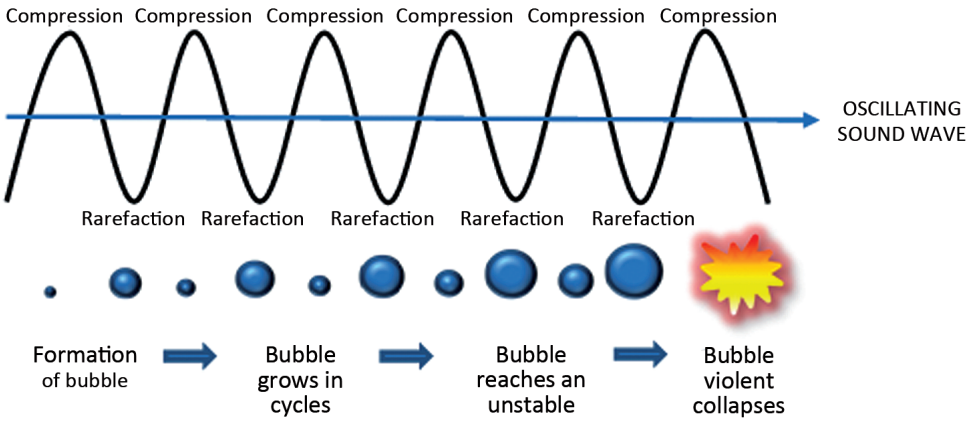

Fig. 7. Graphical summary of the bubble formation, growth, and subsequent collapse over several acoustic cycles (source: based on Leong et al. [2011])

The collapse of the bubbles generate high-speed jets of liquids into the surface which creates damages by shockwave. It effects in fragmentation of friable materials and localized erosion. Moreover, cavitation and shockwaves induce intense macroturbulence, micromixing and subsequently interparticle collisions. This affects the overall increased reactivity in the medium and mass transfer of solid particles due to the reduction of particle size [Chemat et al. 2017]. As previously mentioned, ultrasound depends on the process parameters. Firstly, the frequency is inversely proportional to the bubble size. Therefore, low-frequency ultrasound produces large cavitation bubbles. There are two types of cavitation during which microbubbles are created namely stable and transient cavitation. Stable cavitation is characterized by bubbles which oscillate in regular fashion for many acoustic cycles. In transient cavitation, bubbles formed undergo irregular oscillations creating regions of temperature and pressure. Secondly, a reduction in internal pressure causes a reduction in the number of cavitation bubbles because of increased cavitation. On the other hand, increasing the external pressure increases the pressure in the bulb as it collapses, causing a faster but abrupt collapse. As for the temperature, the higher the temperature, the lower the viscosity, which allows the microbubbles to collapse more rapidly. In addition, there is a direct relationship between the sonication intensity and the square of the ultrasonic source vibration amplitude. As a rule, increasing the intensity increases the sonochemical effects [Mohammadi et al. 2014; Jiménez et al. 2017; Dolas et al. 2019].

There are two known mechanisms for the formation of microbubbles or cavities. The first one includes pre-existing bubbles in the liquid, which are stabilized against dissolution because their surface is coated with contaminants. The second mechanism concerns solid particles (pollen) present in a liquid in which the gas is trapped in those particles where nucleation takes place [Leong et al. 2011]. Regardless of the phenomenon of cavitation, ultrasound generates various types of physical effects, e.g. vibrations (as a result of compression and decompression of the medium), resulting in chemical, mechanical, and thermal effects. Chemical transformations consist in the formation of free radicals in the form of H^+ and OH^- as a result of the decomposition of a water molecule in aqueous solutions. Moreover, chemical transformations include the transfer of a single electron in the cooling phase and the recombination of hydrogen atoms and hydroxyl radicals to produce hydrogen peroxide (H_2O_2), which is characterized by bactericidal properties. The thermal effects are caused by absorbing some of the ultrasonic energy and converting it into heat. In turn, the mechanical effects are caused by the generation of mechanical shocks that destroy the cell structure [Dolas et al. 2019].

In contrast to low-power ultrasound, high-intensity, low-frequency ultrasonic waves are destructive and thus have a significant influence on the physical, biochemical and mechanical properties of food products. They are widely used in emulsifying, defoaming, regulating microstructures, and modifying the textural properties of products, and also for sonocrystallization and modification of functional properties of food products. It also has significant applications in many unit operations of freezing, drying, softening, thickening, thawing, and osmodehydration [Bhargava et al. 2021]. Some applications of high-power ultrasound in various food processing are collected in Table 3.

Table 3. Examples of the application of high power ultrasound in food processing (source: own elaboration)

Applications	Products	Process parameters	Results	References
Drying – ultrasound pretreatment	Apple	Bath system Frequency = 21 and 35 kHz Intensity = 3 and 4 W/cm^2 Time = 30 min	The loss of dry matter, and the drying rate increased with increasing frequency.	Fijałkowska et al. [2016]
Enzyme inactivation	Grape juice	Bath system Frequency = 28 kHz Ultrasound Power = 420 W Time = 30 and 60 min	Inactivation of pectin methylesterase, peroxidase, and polyphenoloxidase by 91%, 90% and 89% at optimal conditions.	Aadil et al. [2015]
Extraction	Peanut seeds	Bath system Frequency = 20, 28, 40 and 60 kHz Ultrasound Power = 300 W Time = 30 min	The mechanism of ultrasonic cavitation on oil oxidation was studied. The best resonance frequency for the oil extraction was identified as 40 kHz according to the model results.	Zhang et al. [2017]
Fermentation	Sweet whey	Frequency = 20 kHz Ultrasound Power = 84 and 102 W Time = 75 and 150 s	The reduction of fermentation time and increasing the number of viable cell count at the end of fermentation.	Barukčić et al. [2015]

Table 3. cont.

Applications	Products	Process parameters	Results	References
Freezing	Apple, Potato, Radish	Frequency = 28 kHz Intensity = 0.62 W/cm^2 Time = 2 min (in 30 s cycles)	Ultrasound promoted the generation of ice nuclei during immersion freezing mainly leading to the shortening of the phase transition time and the improvement of the freezing rate. Ultrasound at 28 kHz resulted in the best firmness and lowest drip loss in a potato.	Zhu et al. [2018]
Homogenization	Milk	Frequency = 20 kHz Ultrasound Power = 80 W Time = 20, 60, 120, 300, 600 and 1200 s	Ultrasonic homogenization of milk reduces the size of its fat globules in relation to the exposure time.	Aernouts et al. [2015]
Pasterization	Peach juice	Bath system Frequency = 20 kHz Intensity 793.65 W/cm^2 Time = 0, 3, 6, 10 and 15 min	The improvement of the physical properties of peach juice, increase the stability against pulp sedimentation and serum cloudiness, maintaining or increasing the juice consistency, with insignificant color changes during the storage.	Rojas et al. [2016]
Tenderization	Beef meat	Bath system Frequency = 40 kHz Intensity = 11 W/cm^2 Time = 60 min	Ultrasound increased the tenderness and fragmentation of meat. The microstructure showed a visible reduction In a size of fascicles, greater interfibrillary spaces and thinner endomysium. Sonicated meat were characterized by more intense fresh smell and oily flavor.	Peña-Gonzales et al. [2018]

Applications	Products	Process parameters	Results	References
Diffusion/ Brining process	Pork meat	Ultrasound probe Frequency = 20 kHz Intensity = 5,09 W/cm^2 Ultrasound Power = 100 W	Ultrasound enhanced the NaCl diffusion into meat and resulted in microscopic pores on the surface of myofibers.	Visy et al [2021]
Cutting	Cheese	Frequency = 20 khZ Velocity = 40 mm/s	Ultrasound cutting reduced lipid peroxidation and decreased browning of analyzed cheeses. All cheese cut with ultrasound showed shiny and smooth surface appearance. Ultrasound cutting cheese were characterized by higher sensory quality parameters.	Yildiz et al. [2016]
Packaging	Cucumber	Frequency = 20 kHz Ultrasound Power = 400 W Intensity = 226 W/cm^2 Time = 5, 10, 15 min (pulse mode (10 s on and 5 s off)	Ultrasound treatment inhibited the growth of total number of colonies, mold and yeast in modified atmospheric packaged fresh-cut cucumber. Ultrasound treatment for 10 min had a good effect on the reduction of weight loss, firmness and maintenance of ascorbic acid content.	Fan et al. [2019]

6. Conclusion

Ultrasound turns up into an evolving technology in the practical world of food science and technology. Over the past few years, numerous studies have proven that low power intensity ultrasound provides simple methods for the monitoring of food quality (even online) and estimation of food composition, especially in fruit, meat and dairy technology. Moreover, ultrasound is being increasingly

used to enhance various processes in the food industry, supporting or replacing preexisting and conventional technologies. The conducted research has shown that ultrasound increases efficiency and reduce the time required for various processing operation, such as fermentation, drying or diffusion. The application of ultrasound in some food processing can not only improve the food quality, but also ensure a higher purity and safety of final products. Although there are many studies relating to ultrasonic application on a laboratory scale, the lack of knowledge, understanding, and reluctance to let go of traditional practices, prevents the implementation and commercialization of ultrasound at industrial levels.

References

Aadil R.M., Zeng X.A., Zhang Z.H., Wang M.S., Han Z., Jing H., Jabbar S. 2015. Thermosonication: A potential technique that influences the quality of grapefruit juice. International Journal of Food Science and Technology, 50(5), 1275–1282. https://doi.org/10.1111/ijfs.12766

Aboudaoud I., Faiz B., Aassif E., Moudden A., Izbaim D., Abassi D., Malainine M., Azergui M. 2012. The maturity characterization of orange fruit by using high frequency ultrasonic echo pulse method. IOP Conference Series Materials Science and Engineering, 42(1), 2881–2886. https://doi.org/10.1088/1757-899X/42/1/012038

Aernouts B., Van Beers R., Watté R., Huybrechts T., Jordens J., Vermeulen D., Van Gerven T., Lammertyn J., Saeys W. 2015. Effect of ultrasonic homogenization on the Vis/NIR bulk optical properties of milk. Colloids Surfaces B: Biointerfaces, 126, 510–519. https://doi.org/10.1016/j.colsurfb.2015.01.004

Alarcon-Rojo A.D, Carrillo-Lopez L.M., Reyes-Villagrana R., Huerta-Jimenez M., Garcia--Galicia I.A. 2019. Ultrasound and meat quality: A review. Ultrasonics Sonochemistry, 55, 369–382. https://doi.org/10.1016/j.ultsonch.2018.09.016

Amarillo M., Pérez N., Blasina F., Gambaro A., Leone A., Romaniello R., Xu X.Q., Juliano P. 2019. Impact of sound attenuation on ultrasound-driven yield improvements during olive oil extraction. Ultrasonic Sonochemistry, 53, 142–151. https://doi.org/10.1016/j.ultsonch.2018.12.044

Amer M.A., Novoa-Díaz D., Puig-Pujol A., Capdevila J., Chávez J.A, Turó A., García--Hernández M.J., Salazar J. (2015). Ultrasonic velocity of water–ethanol–malic acid–lactic acid mixtures during the malolactic fermentation process. Journal of Food Engineering, 149, 61–69. https://doi.org/10.1016/j.jfoodeng.2014.09.042

Arvanitoyannis I.S., Kotsanopoulos K.V., Savva A.G. 2017. Use of ultrasounds in the food industry – methods and effects on quality, safety and organoleptic characteristics of foods: A review. Critical Reviews in Food Science and Nutrition, 57(1), 109–128. https://doi.org/10.1080/10408398.2013.860514

Awad T., Moharram O., Shaltout O.E., Youssef M.M. 2012. Application of ultrasound in analysis, processing and quality of food: A review. Food Research International, 48, 410––427. https://doi.org/10.1016/j.foodres.2012.05.004

Barukčić I., Jakopović K.L., Herceg Z., Karlović S., Bożanić R. 2015. Influence of high intensity ultrasound on microbial reduction, physico-chemical characteristics and fermentation of sweet whey. Innovative Food Science and Emerging Technologies, 27, 94–101. https://doi.org/10.1016/j.ifset.2014.10.013

Bhargava N., Mor R.S., Kumar K., Sharanagat V.S. 2021. Advances in application of ultrasound in food processing: A review. Ultrasonics Sonochemistry, 70, 105293, 1–12. https://doi.org/10.1016/j.ultsonch.2020.105293

Chandrapala J. 2015. Low intensity ultrasound application on food systems. International Food Research Journal, 22(3), 888–895.

Chemat F., Rombaut N., Sicaire A.G., Meullemiestre A., Fabiano-Tixier A.S., Abert-Vian M. 2017. Ultrasound assisted extraction of food and natural products. Mechanisms, techniques, combinations, protocols and applications. A review. Ultrasonics Sonochemistry, 34, 540––560. https://doi.org/10.1016/j.ultsonch.2016.06.035

Contreras M., Benedito J., Garcia-Perez J.V. 2021. Ultrasonic characterization of salt, moisture and texture modifications in dry-cured ham during post-salting. Meat Science, 172, 108356. https://doi.org/10.1016/j.meatsci.2020.108356

Corona E., García-Pérez J.V., Santacatalina J.V., Ventanas S., Benedito J. 2014. Ultrasonic characterization of pork fat crystallization during cold storage. Journal of Food Science, 79, 828–838. https://doi.org/10.1111/1750-3841.12410

Derra M., Bakkali F., Amghar A., Sahsah H. 2018. Estimation of coagulation time in cheese manufacture using an ultrasonic pulse-echo technique. Journal of Food Engineering, 216, 65–71. https://doi.org/10.1016/j.jfoodeng.2017.08.003

Dolas R., Saravanan C., Kaur B.P. 2019. Emergence and era of ultrasonic's in fruit juice preservation: A review. Ultrasonics Sonochemistry, 58, 104609, 1–13. https://doi.org/10.1016/j.ultsonch.2019.05.026

Ercan S.S., Soysal C. 2013. Use of ultrasound in food preservation. Natural Science, 5(8B), 5–13. https://doi.org/10.4236/ns.2013.58A2002

Escrig J., Wolley E., Rangappa S., Simeone A., Watson N.J. 2019. Clean-in-place monitoring of different food fouling materials using ultrasonic measurements. Food Control, 104, 358–366. https://doi.org/.1016/j.foodcont.2019.05.013

Fan K., Zhang M., Jiang F. 2019. Ultrasound treatment to modified atmospheric packaged fresh-cut cucumber: Influence on microbial inhibition and storage quality. Ultrasonics Sonochemistry, 54, 162–170. https://doi.org/10.1016/j.ultsonch.2019.02.003

Fijałkowska A., Nowacka M., Wiktor A., Dadan M., Witrowa-Rajchert D. 2016. Ultrasound as a pretreatment method to improve drying kinetics and sensory properties of dried apple. Journal of Food Process Engineering, 39, 256–265. https://doi.org/10.1111/jfpe.12217

Firouz M.S., Farahmandi A., Hosseinpour S. 2019. Recent advances in ultrasound application as a navel technique in analysis processing and quality control of fruits, juices and dairy products industries: A review. Ultrasonics Sonochemistry, 57, 73–88. https://doi.org/10.1016/j.ultsonch.2019.05.014

González-Mohino A., Jiménez A., Rufo M., Paniagua J.M., Antequera T., Perez-Palacios T. 2022. Ultrasound parameters used to characterize Iberian fresh pork loins of different feeding systems. Journal of Food Engineering, 314, 110795. https://doi.org/10.1016/j.jfoodeng.2021.110795

Jiménez N., Picó R., Camarena F., Redondo J., Roig B. 2012. Ultrasonic evaluation of the hydration degree of the orange peel. Postharvest Biology and Technology, 67, 130–137. https://doi.org/10.1016/j.postharvbio.2011.12.020

Jiménez A., Rufo M., Paniagua J.M., Crespo A.T., Guerrero M.P., Riballo M.J. 2017. Contribiutions to ultrasound monitoring of the proces of milk curdling. Ultrasonics, 76, 192–199. https://doi.org/10.1016/j.ultras.2017.01.007

Kerhervé S.O., Guillermic R.M., Strybulevych A., Hatcher D.W., Scanlon M.G., Page J.H. 2019. Online non-contact quality control of noodle dough using ultrasound. Food Control, 104, 249–357. https://doi.org/10.1016/j.foodcont.2019.04.024

Khairi M.T.M., Ibrahim S., Yunus M.A.M., Faramarzi M. 2016. Contact and non-contact ultrasonic measurement in the food industry: A review. Measurement Science and Technology, 27, 012001. https://doi.org/10.1088/0957-0233/27/1/012001

Kim K.B., Lee S., Kim M.S., Cho B.K. 2009. Determination of apple firmness by nondestructive ultrasonic determination. Postharvest Biology and Technology, 52, 44–48. https://doi.org/10.1016/j.postharvbio.2008.04.006

Konopacka D., Płocharski W., Siucińska K. 2015. Możliwości zastosowania ultradźwięków w przemyśle owocowo-warzywnym. Przemysł Fermentacyjny i Owocowo-Warzywny, 4, 16–21. https://doi.org/10.15199/64.2015.4.2

Leong T., Ashokkumar M., Kentish S. 2011. The fundamentals of power ultrasound – A review. Acoustic Australia, 39(2), 43–52.

McClements D.J., Gunasekaran S. 1997. Ultrasonic characterization of foods and drinks: Pronciples, methods, and applications. Critical Reviews in Food Science and Nutrition, 37(1), 1–46.

Mohammadi V., Ghasemi-Varnamkhasti M., Ebrahimi R., Abbasvali M. 2014. Ultrasonic techniques for the milk production industry. Measurement, 58, 93–102. https://doi.org/10.1016/j.measurement.2014.08.022

Mohammed M.E.A, Alhajhoj M.R. 2019. Importance and applications of ultrasonic technology to improve food quality. [In:] Food Processing. Eds. R.A. Marc, A.V. Diáz, G.D.P Izquierdo. IntechOpen, London, United Kingdom, 1–17. https://doi.org/10.5772/intechopen.88523

Morrison D.S., Abeyratne U.R. 2014. Ultrasonic techniques for non-destructive quality evaluation of oranges. Journal of Food Engineering, 141, 107–112. https://doi.org/10.1016/j.jfoodeng.2014.05.018

Mulet A., Cárcel J.A., Sanjuán N., Bon J. 2003. New food drying technologies – Use of ultrasound. Food Science and Technology International, 9(3), 2015–221. https://doi.org/10.1177/1082013203034641

Nowak K.W. 2015. Identification of meat types by ultrasonic methods. Technical Science, 18(2), 79–84.

Nowak K.W, Markowski M. 2020. Evaluation of selected properties of a gelatinized potato starch colloid by an ultrasonic method. Measurement, 158, 107717. https://doi.org/10.1016/j.measurement.2020.107717

Pallav P., Hutchins D.A., Gan T. 2009. Air-coupled ultrasonic evaluation of food materials. Ultrasonic, 49, 244–253. https://doi.org/10.1016/j.ultras.2008.09.002

Paniwnyk L. 2017. Applications of ultrasound in processing of liquid foods: A review. Ultrasonics Sonochemistry, 38, 704–806. https://doi.org/10.1016/j.ultsonch.2016.12.025

Patist A., Bates D. 2008. Ultrasonic innovations in the food industry: From the laboratory to commercial production. Innovative Food Science & Emerging Technologies, 9, 147––145.

Peña-Gonzalez E., Alarcon-Rojo A.D., Garcia-Galicia I., Carrillo-Lopez L., Huerta--Jimenez M. 2019. Ultrasound as a potential process to tenderize beef: Sensory and technological parameters. Ultrasonic-Sonochemistry, 53, 134–141. https://doi.org/10.1016/j.ultsonch.2018.12.045

Ratajski A., Mikš-Krajnik M., Białobrzewski I. 2014. The use of ultrasonic measurements for the determination of particle size distribution in diluted tomato paste. International Journal of Food Science & Technology, 49, 288–293. https://doi.org/10.1111/ijfs.12265

Rojas M.L., Leite T.S., Cristianini M., Alvim I.D., Augusto P.E.D. 2016. Peach juice processed by the ultrasound technology: Changes in its microstructure improve its physical properties and stability. Food Research International, 82, 22–33. https://doi.org/10.1016/j.foodres.2016.01.011.

Śliwiński A. 2001. Ultradźwięki i ich zastosowanie. Wydawnictwo WNT, Warszawa.

Srivastava S., Vassadl S., Sadistap S. 2014. Non-contact ultrasonic based stiffness evaluation system for tomatoes during shelf-life-storage. Journal of Nutrition & Food Science, 4(3), 1–6. https://doi.org/10.4172.2155-9600.1000273

Vasighi-Shojae H., Gholami-Parashkouhi M., Mohammadzamani D., Soheili A. 2018. Ultrasonic based determination of apple quality as a nondestructive technology. Sensing and Bio-Sensing Research, 21, 22–26. https://doi.org/10.1016/j.sbsr.2018.09.002

Wieja K., Kiełczyński P., Szymański P., Szalewski M, Balczarzak A., Ptasznik S. 2021. Identification and investigation of mechanically separated meat (MSM) with an innovative ultrasonic method. Food Chemistry, 348, 128907. https://doi.org/10.1016/j.foodchem.2020.128907

Valente M., Prades A., Laux D. 2013. Potential use of physical measurements including ultrasound for a better mango fruit quality characterization. Journal of Food Engineering, 116, 57–64. https://doi.org/10.1016/j.jfoodeng.2012.11.022

Verlinden B.E., De Smedt V., Nicolaï B.M. 2004. Evaluation of ultrasonic wave propagation to measure chilling injury in tomatoes. Postharvest Biology and Technology, 32, 1, 109–113. https://doi.org/10.1016/j.postharvbio.2003.11.006

Visy A., Jonas G., Szakos D., Horvath-Mezofi Z., Hidas K.I., Barko A., Friedrich L. 2021. Evaluation of ultrasound and microbubbles effect on pork meat during brining process. Ultrasonics Sonochemistry, 75, 105589. https://doi.org/10.1016/j.ultsonch.2021.105589

Wallhäußer E., Hussein W.B., Hussein M.A., Hinrichs J., Becker T. 2013. Detection of dairy fouling: Combining ultrasonic measurements and classification methods. Engineering of Life Science, 13(3), 292–301. https://doi.org/10.1002/elsc.201200081

Yan J., Wright W.M., Roos Y., Van Ruth S.M. 2019. Evaluation of food-grade vegetable oils using ultrasonic velocity measurment and fatty acid composition. [In:] 2019 IEEE International Ultrasonics Symposium (IUS), 2435–2438.

Yang Y., Wright W.M.D., Hettinga K.A., van Ruth S.M. 2021. Exploration of an ultrasonic pulse echo system for comparison of milks, creams, and their dilutions. Lebensmittel--Wissenschaft & Technologie, 136, 110616. https://doi.org/10.1016/j.lwt.2020.110616

Yildiz F., Ozdemir A.T., Uluıs S. 2019. Evaluation Performance of Ultrasonic Testing on Fruit Quality Determination. Journal of Food Quality, 6810865, 1–7. https://doi.org/10.1155/2019/6810865

Yildiz G., Rababah T.M., Feng H. 2016. Ultrasound-assisted cutting of cheddar, mozzarella and Swiss cheeses – Effects on quality attributes during storage. Innovative Food Science and Emerging Technologies, 37, 1–9. https://doi.org/10.1016/j.ifset.2016.07.013

Zhang L., Zhou C., Wang B., Yagoub A.E.A., Ma H., Zhang X., Wu M. 2017. Study of ultrasonic cavitation during extraction of the peanut oil at varying frequencies. Ultrasonics Sonochemistry, 37(7), 106–113. https://doi.org/10.1016/j.ultsonch.2016.12.034

Zhu Z., Chen Z., Zhou Q., Sun D.W., Chen H., Zhao Y., Zhou W., Li X., Pan H. 2018. Freezing efficiency and quality attributes as affected by voids in plant tissues during ultrasound--assisted immersion freezing. Food and Bioprocess Technology, 11(9), 1615–1626. https://doi.org/10.1007/s11947-018-2103-8/

IX APPLICATION OF SPECTROFLUOROMETRIC METHODS IN FAT QUALITY ASSESSMENT

Magdalena MICHALCZYK, Joanna BANAŚ

Department of Biotechnology and General Technology of Food,
Faculty of Food Technology, University of Agriculture in Krakow,
Aleja Mickiewicza 21, 31-120 Krakow, Poland

magdalena.michalczyk@urk.edu.pl
ORCID: https://orcid.org/0000-0002-7962-8196

joanna.banas@urk.edu.pl
ORCID: https://orcid.org/0000-0002-1354-0765

Abstract. The assessment of the composition and quality of fats is a complex issue and can be conducted using various analytical techniques. These often involve certain restrictions concerning the information obtained or requirements related to the equipment or reagent utilization. This study presents possible applications of fluorescent spectroscopy both in the assessment of fat oxidative changes and detection of fat adulteration. This method is relatively sensitive and enable the reduction of the utilized reagents, however, often need to be combined with a mathematical analysis.

Keywords: spectrofluorimetry, fat adulteration, fat quality

1. Introduction

Fats in food products perform multiple functions. They affect the assessment of food texture, for example, tenderness and juiciness of meat [Amaral et al. 2018]. Fats are the solvent for some vitamins; many bioactive compounds, such as carotenoids, including lutein, coenzyme Q10, and cholesterol; steroid hormones; and aromatic substances. Moreover, they themselves are also a source of fragrances. In the body, lipids function both as an energy-supplying and building component as well as a precursor of regulatory substances. From a nutritional point of view, n-3 and n-6 polyunsaturated fatty acids are particularly valuable. They are, among others, precursors to bioactive mediators and should be provided in the diet in appropriate proportions [Lands 2012]. Despite some controversy regarding the nutritionally optimal composition and amount of fat intake [Calder and Deckelbaum 2011; Twenefour and Shields 2020], the assessment of uncontrolled fat oxidation products occurring in food products is unequivocal. Another possible problem connected with fats is their adulteration, especially of those more expensive.

2. Qualitative changes in fats requiring assessment and monitoring in food products. The problem of adulteration

Due to fat importance for the functioning of the human body and health-related aspects, fats provided with the diet should be of appropriate composition and quality. The selection of a right fat composition in a diet can be hampered not only by difficulties in meeting individual body needs, availability of proper fat types, but also by fat adulteration and a quality loss resulting from products' processing and storage. In stored raw materials and products, fats undergo processes generally defined as rancidity that includes both hydrolysis and oxidation. Fat hydrolysis, being a part of the ripening process of fermented meat products (e.g., ham, sausages) and cheeses, is an important factor influencing the final organoleptic evaluation of product. Apart from water content, the rate of hydrolysis in raw ripening meat products is influenced by, i.a. temperature, starter culture used and active acidity [Wójciak and Dolatowski 2012]. Nevertheless, the products of triacylglycerol hydrolysis may also affect adversely the fat odour. Depending on the concentration and the presence of other aroma constituents, this may refer

to, for example, butyric acid. The appearance of free fatty acids due to undergoing hydrolysis during high-temperature heat treatment of water-rich products, lowers also the smoking point of frying fat [Dana and Saguy 2001]. As free fatty acids are oxidized more rapidly, they may also contribute to the freeze-induced protein denaturation in frozen meat products. However, the mere presence of free fatty acids in food products does not have an adverse effect on consumer health. Nevertheless, products of uncontrolled, non-enzymatic oxidation occurring in stored food products or those formed during high-temperature processing of fats are already harmful. These products include, i.a., hydroperoxides, peroxides, aldehydes and oxysterols as well as products of cholesterol oxidation [Domínguez et al. 2019]. In contrast, controlled oxidation of fats and cholesterol taking place in organisms due to action of enzymes such as lipoxygenases, cyclooxygenases or cytochrome P450, leads to the formation of steroid hormones, hormone-like mediators, bile acids and other important substances regulating the proper functioning of the body [Hajeyah et al. 2020; Lands 2012]. Lipoxygenases contained in plant raw materials, presumably involved in plant responses to stress factors, are also engaged, for example, in the formation of both desirable and undesirable aromatic substances. These enzymes oxidize polyunsaturated fatty acids and esters (containing cis, cis-1,4-pentadiene system) and take part in the formation of compounds of plant hormone-like nature [Baraniak and Szymanowska 2006].

Oxidation of the fat present in food products leads to both changes in its smell, taste, colour and nutritional value, and the formation of components harmful to health. Secondary oxidation products of unsaturated fatty acids can have both negative and beneficial effect on the odour. For example, 2-E-hexenal is considered to be the basic tomato aroma compound [Baraniak and Szymanowska 2006]. In turn, in meat products, the onset of oxidative changes probably occurs already during the animal's life and intensifies at the time of slaughter, when due to molecular oxygen, unsaturated fatty acids are converted into peroxides. The phospholipids are oxidized most quickly. These transformations are accelerated by the presence of iron, salts and enzyme activity. Another step that intensifies fat oxidation is heat treatment, which causes a relatively rapid development of undesirable odour of thus-treated meat during its further refrigerated storage [Amaral et al. 2018]. Oxidation occurring in food products can take place with the participation of lipoxygenase enzyme; under the influence of light, mainly ultraviolet radiation; and in the presence of oxygen and sensitizers [Amaral et al. 2018]. Its most important type – autooxidation, is a typical chain reaction involving radical species.

Radical chain reactions involved in fat oxidation have three main phases: initiation, propagation and termination. In the first phase the radical of fatty

acid is formed, removing a hydrogen atom from it. During propagation, the peroxyl radicals, formed after attaching the oxygen atom to the alkyl radical, convert subsequent molecules into alkyl radicals and form hydroperoxides which are the primary products of fat oxidation. In the phase of termination, the chain reaction is finishing, two free radicals react with each other to form a non-radical adduct. Hydroperoxides are converted to a number of compounds, including aldehydes, hydrocarbons, alcohols, and furans [Wójciak and Dolatowski 2012; Amaral et al. 2018].

In the case of high-temperature heat treatment, the process of oxidative fat decomposition is similar. In the first stage, due to atmospheric oxygen, hydroperoxides of unsaturated fatty acids are formed at high temperature. The second stage involves the decomposition of hydroperoxides. As a result, secondary breakdown products such as carbonyls (e.g. aldehydes and ketones), alcohols and acids are formed. In the third stage, secondary products undergo polymerization, which changes the colour and viscosity of the fried oils [Dana and Sanguy 2001]. During frying, besides polymerization resulting from oxidation, non-oxidation-related polymerization also occurs, the extent of which depends on the temperature and frying time. In addition to polymers, the resulting products include, i.a. cyclic fatty acids monomers, dimers, carboxylic acids, aldehydes and ketones [Dana and Sanguy 2001]. As reported by Dana and Sanguy [2001], cyclic monomers are highly harmful and are formed during high-temperature processing (around 200°C), mainly from linolenic and linoleic acids.

Moreover, both stored and heated products contain many other compounds that can affect the rate of fat oxidation and, under the action of the fat rancidity products, can undergo transformations that change the characteristics and lower the products' quality. Free radicals formed in these processes may influence the oxidation of other important bioactive constituents, such as vitamins, proteins or pigments [Baraniak and Szymanowska 2006].

Adulteration may be considered with regard to different fat types like, for example, fish oils, butter, olive oil or vegetable oils [Rohman et al. 2021]. This is a problem that may relates to various characteristics of fat declared on the packaging, for example, the addition of cheaper fats from other plant or animal species or false information about the declared place of origin of the product. In the case of vegetable oils, besides their adulteration with oil extracted from another plant species, adulteration of cold-pressed oils with refined equivalents may also be practiced [Jamwal et al. 2021]. Vegetable oils may also be adulterated, for example, with lard. In consequence, their nutritional value may change; this may also be a problem for vegetarians or vegans. Fat adulteration may be detected by the assessment of the profile of triacylglycerols and other additional fat constitu-

ents such as, e.g. campesterol, stigmasterol, and tocotrienols, and using the DNA analysis. Another group of methods are those that comprehensively assess the fat profile [Meenu et al. 2019].

3. Classic methods of fat quality assessment and their limitations

The measurement of the extent of undesirable changes in fats, due to the large variety of products, is often based on the analysis of indicators. The assessment may concern products formed at various stages of fat transformation. Acid value is one of the commonly used indicators of hydrolytic changes, while peroxide value enables determination of the primary products of fat oxidation. In turn, commonly used indicators for secondary rancidity products are anisidine value, thiobarbituric acid reactive substances (TBARS) value, and total polar compounds; although, carbonyl value and conjugated diene value are also used. At present, the Kreis test is the less commonly used method. In addition, the content of such secondary oxidation products as hexanal, nonanal or 2-pentylfuran can be determined by gas chromatography methods.

Acid value characterise the content of free fatty acids, thus describing the range of hydrolytic changes in fat. It is determined by dissolving fat and titrating free fatty acids with KOH solution [AOCS Cd 3d-63 method; AOCS 2004]. This value is sometimes used to assess the quality of frying oil. For example in Japan, its acceptable upper limit is 2.5 mg/g of fat [Hara et al. 2006]. Dana and Saguy [2001] report however that the most commonly used values of this indicator are between 5 and 25 mg/g, depending on the fried product. Among the disadvantages of this indicator, Kuselman et al. [1998] mentioned the time-consuming nature of the analysis itself. Therefore, the authors propose a modification involving a few-minute extraction of free fatty acids themselves from the sample, using special reagents, and pH-metric measurement of this value.

Peroxide value determines the content of peroxides and hydroperoxides, which are unstable intermediate products that undergo further transformation. It is expressed as active oxygen milliequivalents per kilogram of fat. Its determination is based on the oxidation of potassium iodide by sample peroxides. The liberated iodine is then estimated by titration with sodium-thiosulphate solution [AOCS Cd 8b-90 method; AOCS, 2004]. Skiera et al. [2012] claim that the results obtained for this indicator may be significantly affected by reducing and oxidizing of compounds present in the examined fats, such as, for example, thymoqui-

none or hydroxytyrosol. Moreover the results of peroxide number determination may depend on factors, such as time of reaction, access to both light and oxygen and temperature [Tsiaka et al. 2013]. Various studies provide contradictory conclusions concerning the correlation between the results of the TBARS test and the peroxide value, depending, for example, on the types of assessed food products [Fernández et al. 1997]. Other limitation of peroxide value is that it is rather not suitable for evaluating fats used for high-temperature frying, since peroxides are volatile under such conditions [Dana and Saguy 2001].

One of the most common indicators of the range of changes caused by fat oxidation is thiobarbituric acid reactive substances (TBARS) value. It is primarily used to determine malondialdehyde (MDA), but other substances can also react with this acid. Malondialdehyde (MDA) is formed by autooxidation of unsaturated aldehydes in the second stage of fat oxidation processes and the substrates in this process are fatty acids with at least three double bonds. This compound is highly harmful [Dana and Saguy 2001]. Small amounts of MDA can also be produced from other substrates [Fernández et al. 1997]. TBARS indicator, expressed as milligrams MDA per kilogram of a product, allows the determination of both malondialdehyde and other substances reacting with 2-thiobarbituric acid (TBA), including, for example, other aldehydes, like furfural. This indicator is determined both by extraction and distillation method. Extraction allows that either a solution of malondialdehyde is obtained or its complex with 2-thiobarbituric acid is formed in the product sample. The distillation method is recommended for the samples containing sugar. In one of its stages, the malondialdehyde is distilled from the sample [Salih et al. 1987; Ganhão et al. 2011]. For the extraction method, it is recommended to perform an absorbance scan from 400 to 600 nm, in order to find the maximum absorbance and exclude errors due to the presence of other absorbing substances near the TBA-MDA complex. The maximum absorbance of the described complex is in the nearby 532 nm. MDA itself may also be determined by the HPLC method after its prior distillation from the sample. However, heating the samples during distillation may affect to some extent the results obtained, for example, by increasing the oxidation rate of the sample and raising the aldehyde content in it. On the other hand, the phenomenon of turbid filtrate can occur in the extraction method, due to high fat content or transformation caused by the activity of microorganisms (peptides, amino acids) [Salih et al. 1987]. In addition, pigments, even anthocyanins from plant components, or products of browning reactions present in the sample, can also affect the value of the readings. The application of additional filtration is not always sufficiently effective. On the other hand, incubation at room temperature extends its length to even more

than dozen hours [Ganhão et al. 2011]. The results obtained in this test will also depend on the fatty acid composition of the examined fat. Malondialdehyde, which is determined in the TBARS test, is also characterized by instability as undergoes further oxidative transformations leading to the formation of alcohols and acids. This, in turn, limits its usefulness as an indicator of fat quality [Fernández et al. 1997].

The anisidine value, like TBARS value, describes the content of non-volatile carbonyls in fat [Ye et al. 2020]. P-anisidine value gives the content of aldehydes, including primarily unsaturated 2,4-dienals and 2-alkenals in fat [Tompkins and Perkins 1999]. The principle of this method is based on the measurement of the coloured Schiff base formed after the reaction of p-anisidine with the carbonyl group [Skiera et al. 2012]. The anisidine value is a commonly used indicator of the frying fats quality, since it correlates with the results of sensory evaluation [Dana and Sanguy 2001]. Tompkins and Perkins [1999] found relatively high values of correlation coefficients between the anisidine value and the content of hexanal, t-2-octenal, t,t,-2,4-decadienal in partially hydrogenated soybean oil used for frying potatoes. However, as noted by Zuo et al. [2017], this value does not reflect the content of saturated aldehydes. Furthermore, Ye et al. [2020] claim that flavouring agents may influence this values. For example, according to their studies chocolate-vanilla and lemon flavours increase the anisidine value in fish oils.

The total polar compounds (PC) is another quality indicator of the frying fat. This indicator can be determined, for example, by HPLC or near-infrared spectroscopy (NIR) methods. Polar compounds include, among others, aldehydes, ketones, alcohols, acids, free fatty acids, partial glycerides, and oxidized polymers [Gu et al. 2020]. In EU countries, the value of this indicator was set at a level below 10–25% for frying oil [Hara et al. 2006, Dana and Sanguy 2001]. Frying fats can also be characterized by polymer content [Dana and Sanguy 2001]. In addition, other useful indicators for frying fats are: carbonyl value, conjugated dienes value, anisidine value, acid value, and TBARS [Dana and Sangui 2001].

Conjugated dienes are determined spectrophotometrically by measuring the absorbance of the dissolved fat sample at 233 nm. In turn, conjugated triene content can be determined at the range of 268-278 nm [Kim and LaBella 1987]. According to these authors, as the fat oxidation process progresses, both the conjugated diene value and TBARS decreases during the storage. Therefore, they stated that these indicators, when used separately, are not sufficient to assess the extent of oxidative changes in this raw material.

4. Spectrofluorimetric methods in fat quality assessment

As mentioned previously, there are various objections regarding different methods of fat quality assessment. They concern ecological issues, like for example, utilization of reagents and reactants that pollute the environment, costs, the need to have expensive equipment, time-consuming and laborious nature of analyses, and the results themselves. The values of the fat rancidity indicators may depend on fatty acid composition, presence of other compounds in the sample, stage of oxidative changes in the fat, and assumed assay conditions. Some analyses are considered to be, for example, too little specific or there are objections to their sensitivity. This leads to a constant search for better methods of fat quality assessment as well as to modifications of existing ones. Among the methods that can provide an alternative to classical indicators are those based on fluorescence.

Fluorescence describes a phenomenon of photon emission by the molecules excited under radiation. The emission takes place in an excited state, in which the electron spin is kept the same as in the ground state (both states have the same multipletion). Such a transition is spin-allowed and runs at a relatively high speed, in the order of 10^8 s^{-1} [Lakowicz 2006]. The radiation emitted has less energy associated with longer wavelength than the absorbed radiation, characterized by shorter wavelength [Andrade-Eiroa et al. 2013]. In order to excite molecules, visible, ultraviolet or near infrared radiation can be used. The fluorescence quantum yield (φ) determines the probability of returning the excited molecule to its ground state by means of fluorescence. Andrade-Eiroa et al. [2013] note that quantum yield of chromophore, defined as the quotient of the number of quanta emitted as fluorescence and total number of quanta absorbed, depends on the solvent used and the presence of other dissolved components. The value of this parameter for a single fluorophore does not depend on wavelength. The higher the quantum yield value, the stronger the fluorescence of a given compound. Apart from the concentration of the fluorophore and its quantum yield, the excitation radiation also has an effect on the fluorescence intensity. In practice, medium power sources (Hg and Xe lamps) are used. In addition to the above-mentioned factors, the fluorescence intensity is also affected by the temperature, pH and colour of the examined sample. Darker-coloured samples can reabsorb more fluorescent radiation than bright ones [Karoui and Blecker 2011].

Among the fluorescent techniques used to evaluate food products are excitation-emission spectrofluorimetry and synchronous spectrofluorimetry. In the first group there are two types of spectra, emission and excitation, associated with

the fluorescence phenomenon. In the first case, the fixed excitation wavelength is used and the emission wavelength changes. In contrast, in the other case, emission wavelength remains the constant [Andrade-Eiroa et al. 2013]. However, for complex systems, single emission or excitation spectra are in many cases insufficient to analyse them accurately. The total luminescence spectrum, otherwise referred to as the excitation-emission matrix, provides more detailed information. It can be obtained by recording emission spectra at different wavelengths of exciting radiation. The total luminescence spectra are presented, for example, in three-dimensional space as the dependence of fluorescence intensity as a function of excitation and emission wavelength [Sikorska et al. 2012].

The synchronous spectrofluorimetry principle is based on simultaneous scanning of the selected range of excitation and emission wavelengths. Synchronous spectrofluorimetry can be performed as constant-wavelength synchronous luminescence (CWSL), constant-energy synchronous luminescence (CESL), and variable-angle synchronous fluorescence spectrometry. In CWSL, spectra are recorded with maintaining a constant difference or increment between the excitation wavelength and the emission wavelength. The CESL spectra are achieved at a constant difference between the energy of excitation monochromators and emission monochromators. In the last technique, in turn, different scan speeds for emission and excitation monochromators are applied [Andrade-Eiroa et al. 2010]. Synchronous spectrofluorimetry can be applied for examining complex mixtures of fluorophores. Their advantage is the simplification of spectra and their fast obtaining. However, compared to the emission-excitation matrix, less information is obtained [Sikorska et al. 2008, 2012]. The simplification of the spectra results from the preferential enhancement of strong fluorescence bands [Poulli et al. 2009; Cao et al. 2017].

The fluorescence measurement methods include front-face and right-angle sampling geometry. Right-angle fluorescence spectroscopy involves the use of right-angle radiation to the surface of the sample. Classic geometry (right-angle) can only be used for liquid samples and solutions which absorbance does not exceed 0.1; hence, analysing dark or solid samples is impossible [Karoui and Becker 2011].

Figure 1 sets together emission spectra recorded in the right-angle geometry for cold-pressed rapeseed oil. One of them was obtained for the undiluted product, while the other for its 1% (v/v) solution in hexane.

As can be seen, during the preparation of solution, almost all information is lost about the contents of chlorophylls and pheophytins, the fluorescence of which can be observed in the wavelength range 650–700 nm, as well as about changes in them, occurring, e.g. during storage [Sikorska et al. 2008]. As for the solution

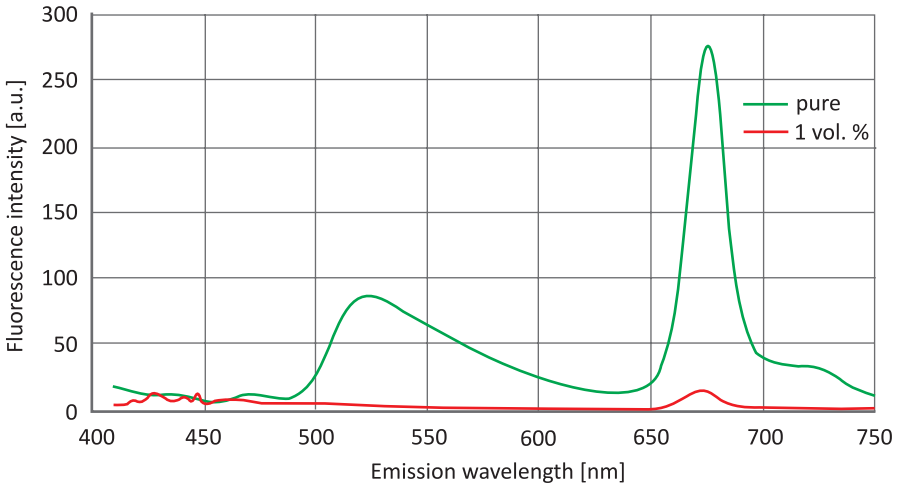

Fig. 1. Emission spectra of undiluted cold-pressed rapeseed oil and its 1% v/v solution in hexane, measured in right-angle geometry (source: own research)

spectrum, the fluorescence band of carotenoids is practically invisible (range 500––600 nm) [Lai et al. 2007]; its intensity in the undiluted sample is relatively high. The smallest differences can be observed in the range corresponding to the fluorescence of secondary fat oxidation products (400–500 nm) [Veberg et al. 2006]; although, also in this case the observed bands have a slightly different shape.

When using the right-angle geometry, the problems with the band broadening should also be taken into account. This is due to the overlapping of spectra of individual components, light scattering and its reflection [Karoui and Becker 2011]. The application of front-face geometry solves some of the problems that arise in classical spectrophotometry. This geometry uses a different value of the angle between the sample and the detector. The most commonly used angle is 56°, at which the so-called inner-filter effect may be eliminated [Sádecká and Tóthová 2007]. The front-face geometry also enables the analysis of solid and liquid samples, where the absorbance exceeds 0.1 [Karoui and Becker 2011].

Spectra presenting the fluorescence of a given product consist of bands corresponding to the wavelengths of excitation and emission radiation, characteristic for the compounds constituting such a product. Compounds with the relatively strong fluorescent properties comprise, among others, those having conjugated double bond systems or showing an aromatic character [Sikorska 2012]. Substances that may be a component of fat products and exhibit chemoluminescence include, among others vitamins A and E, chlorophylls and pheophytins, products of fat oxidation or phenolic compounds [Sikorska et al. 2008, 2012; Sikorska et al. 2012].

The combination of spectrofluorimetry and statistical methods such as Principal Component Analysis, Linear Discriminate Analysis, Partial Least Squares, Hierarchical Cluster Analysis, Common Components and Specific Weight Analysis, Discriminate Partial Least Squares Regression, Parallel Factor Analysis and others, allow, i.a. identification or grouping samples with different properties, quantity analysis of examined compounds, and indication of samples with similar properties [Sádecká and Tóthová 2007; Andrade-Eiroa et al. 2010; Sikorska 2012].

As Andrade-Eiroa et al. [2010] pointed out, spectrofluorimetry is an exceptionally sensitive technique and can be used for the analysis of a very wide spectrum of substances, and in the case of using synchronous spectrofluorimetry is also a technique with satisfactory selectivity. Other advantages of these techniques are: relatively short analysis time, the absence of a destructive effect on the examined sample, the small quantities needed for analysis, and the relative simplicity of determinations and their low cost, including the relatively low cost of the spectrofluorimeter [Karoui et al. 2006; Andrade-Eiroa et al. 2013]. Spectrofluorimetric techniques can be used both to assess storage- and heat-induced changes in fats, to detect fat impurities and adulteration, and to confirm the declared region of origin.

Of the many applications of spectrofluorimetry in food research, its use in determination of oxidative changes in fats and fat-containing products during storage under various conditions, is one of the most important. Figure 2 presents the emission spectra recorded at an excitation wavelength of 382 nm in the emission wavelength range of 400–750 nm, which were registered for in-shell peanuts stored at 20°C in darkness. The selected spectral range makes it possible to track changes in the fluorescence intensity of secondary products of fat oxidation, mainly malondialdehyde (MDA). In addition, changes in chlorophylls and pheophytin and carotenoids may also be analysed, as already mentioned in the discussion of Figure 1.

The storage of the examined product at 20°C significantly intensified oxidative changes in the fat phase, which is visible as a substantial increase in the intensity of the fluorescence band in the emission wavelengths of 400–500 nm after just three-week storage and an even greater rise in the content of fat oxidation products after the next three weeks of storage.

In turn, the emission spectra shown in Figure 3 illustrate the effect of light on the range of oxidative changes in cold-pressed mustard oil. Apart from the determination of the scope of such changes, the application of fluorimetry makes it possible to find out the influence of other substances present in the product.

Storage of the examined oil in the dark resulted in slight oxidative changes combined with a little decrease in chlorophyll content. In turn, LED irradiation of

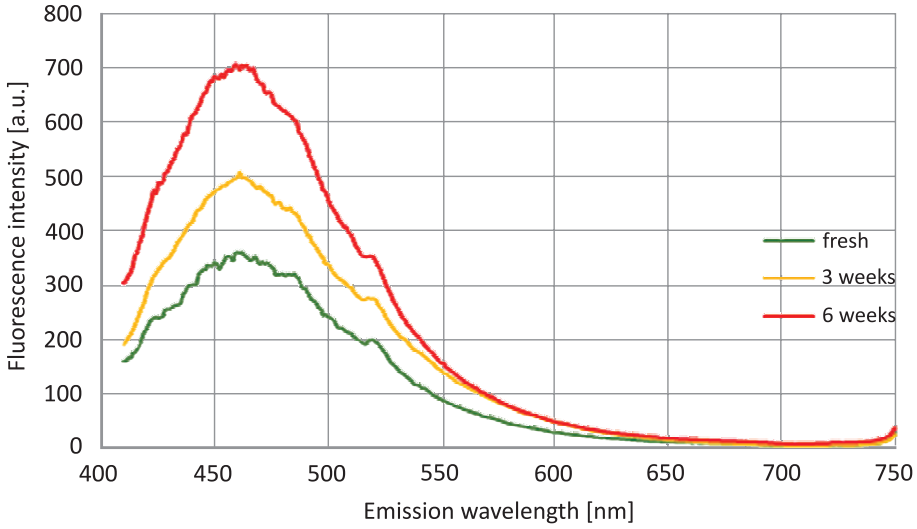

Fig. 2. Emission spectra recorded for in-shell peanuts stored at 20 ± 1 °C, in darkness (source: own research)

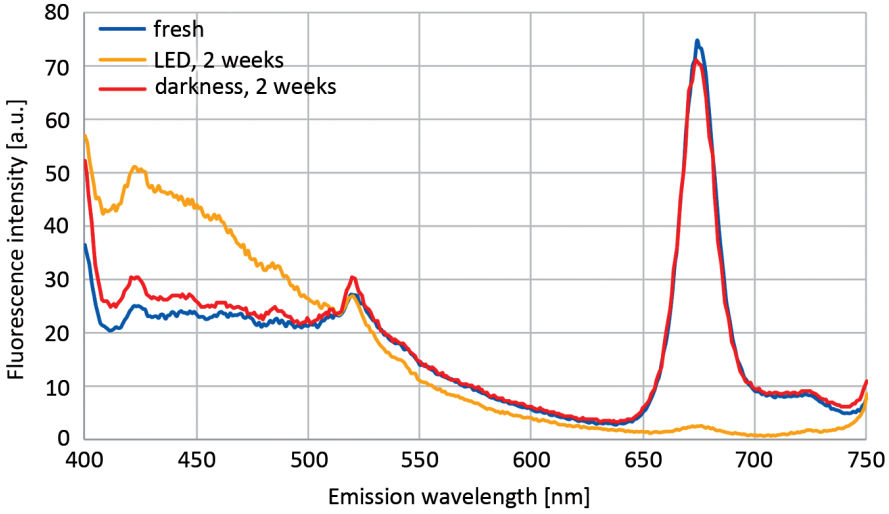

Fig. 3. Emission spectra of fresh cold-pressed mustard oil and the product after two-week storage at 20°C in the dark, under LED illumination (source: own research)

this oil, when combined with the presence of chlorophylls in a product acting as photosensibilisers under such conditions, accelerated significantly fat oxidation and caused almost complete chlorophyll decomposition.

The possible applications of fluorescence analysis in determining the extent of fat oxidative were also investigated, among others, by Kyriakidis and Skarkalis [2000], Sikorska et al. [2008], Poulli et al. [2009], Tena et al. [2009], and Domínguez Manzano et al. [2019]. For example, Kyriakidis and Skarkalis [2000], who examined corn, cotton, sunflower and soybean oils and registered their fluorescent spectra at excitation wavelength of 365 nm, found a strong fluorescence band at 430–450 nm. With regard to extra virgin olive oil, the authors observed 3 bands: doubled at 440 and 445 nm, at 525 nm, and at 680 nm (chlorophyll), which allows extra virgin olive oil to be distinguished from the other mentioned fats. According to the authors, heating of virgin olive oil at 70°C caused a decay of green colour, which was accompanied by, among others, a decreasing peak at 680 nm and decreasing intensity of peak at 440 nm. As for the peak recorded at 445 nm, the authors noted an increase in its fluorescence intensity due to heating of the oil samples, which they ascribed to the resulting oxidation products. In the remaining vegetable oils, the intensity of this peak was also greater than in unheated olive oils, which the authors attribute to the higher content of polyunsaturated fatty acids susceptible to oxidation processes. Poulli et al. [2009] also claimed that the use of synchronous fluorescence spectroscopy in combination with mathematical analysis (PCA) can be used in monitoring olive oil oxidised under UV radiation and heated at 80°C. Similar studies were conducted by Domínguez Manzano et al. [2019], who oxidized the olive oil at up to 80°C, under sunlight and UV radiation. In their studies, the authors applied the parallel factor analysis supervised by linear discriminant analysis (LDA-PARAFAC). According to them, the front face fluorescence combined with mathematical analysis can be applied in real time quality control of virgin olive oil. Spectra regions related to polyphenol and chlorophyll compounds were important in mentioned work.

Tena et al. [2009] used higher temperatures for olive oil heating. They heated virgin olive oil at 190°C for up to 94 h, in 8-hour cycles per day. Both undiluted and diluted in hexane samples were evaluated. Observations were performed in the right-angle system. In the authors' opinion, the results obtained are promising and enable the use of this quick and simple method to evaluate the extent of oil oxidation under frying, especially since there is a relationship between percentage of polar compounds and wavelengths where spectra maximum appears. The values of more than 25% of total polar compounds corresponded to the maximum of the spectrum with a wavelength greater than 486 nm.

5. The use of spectrofluorimetry in authenticity tests and detection of fat adulteration

As in the case of the analysis of the type and extent of oxidative fat changes, spectrofluorimetry has also been widely used in the detection of adulteration of fats such as extra virgin olive oil and butter. The adulterants added can modify the intensity or location of individual fluorescence bands or cause the appearance of new ones. Figure 4 presents synchronous spectra recorded for extra virgin olive oil (EV) samples with increasing amount of adulterants added in the form of pomace oil (P), at the excitation wavelengths in range of 280–700 nm and $\Delta\lambda$ = 30 nm.

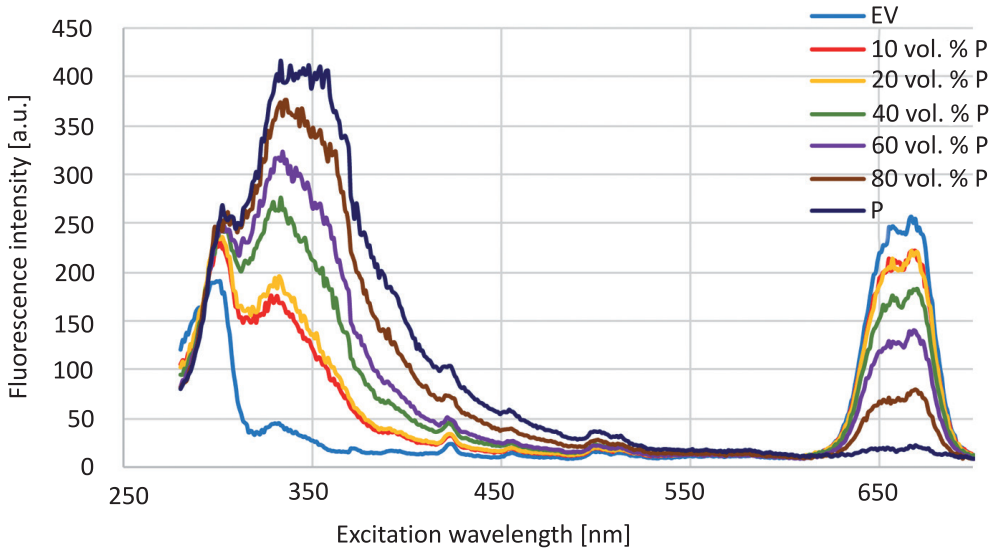

Fig. 4. Synchronous spectra ($\Delta\lambda$ = 30 nm) registered for extra virgin olive oil (EV) with a different addition of pomace oil (P) (source: own research)

The effect of the quantity of the added adulterant is visible as a gradual decrease in the fluorescence intensity of chlorophylls and pheophytins (630–680 nm) as well as tocopherols (280–320 nm). In addition, there is a gradual increase in band intensity in the range of 320–480 nm, attributed to the fluorescence of polyphenols and Maillard reaction products. Such compilation is used for the development of adulteration detecting methodology by means of spectrofluorimetry. On the basis of the registered intensity of the fluorescence bands of substances

characteristic for a given product and their changes related to the amount of the adulterant added, a calibration curve can be drawn up that is useful for the detection of potential sample adulteration. Figure 5 compares synchronous spectra registered for commercial olive oil samples with the calibration samples.

With regard to the sample A, its similarity to the calibration olive EV is relatively high, except for the fluorescence intensity of chlorophylls. These differences may be due to natural fluctuations in the content of these compounds. In the sample D, although the fluorescence intensity of chlorophylls and pheophytins was more similar to the EV sample, presence of a band in the range of 320–380 nm of much greater intensity and similar to the spectrum of sample P, may indicate the sample adulteration with pomace oil.

A precise analysis of the type and quantity of the added adulterant can be performed by means of various chemometric methods. Spectrofluorimetry most often combined with mathematical analysis was used in studies on the adulteration of fats such as butter or olive oil. Dankowska et al. [2014] applied a synchronous fluorescence spectroscopy combined with multivariate data analysis to evaluate butter with the addition of palm and coconut oils. The authors set the lowest limit of adulteration detectability at 5.5%. A similar 5% limit was reported by Ntakatsane et al. [2013] for detecting butterfat adulteration with canola, sunflower, maize and rice bran oils. The authors stated that due to butterfat adultera-

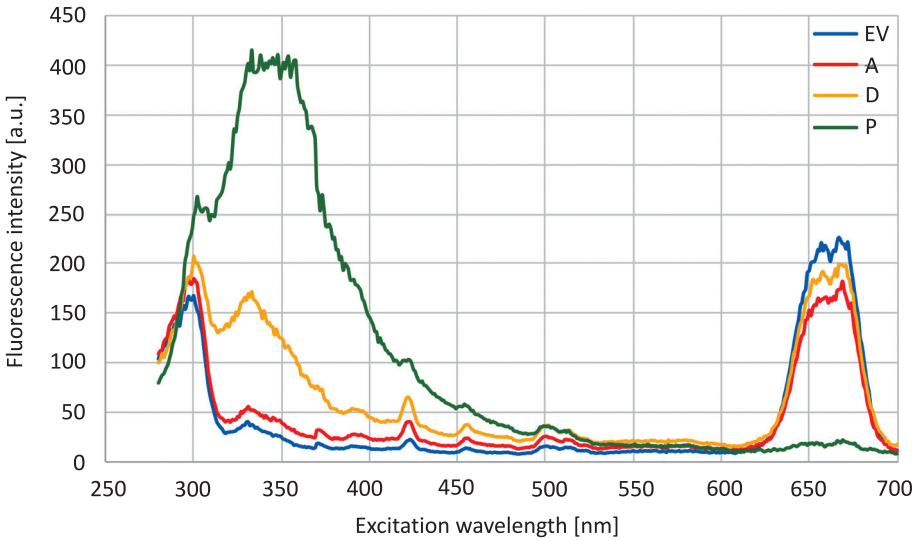

Fig. 5. Synchronous spectra (Δλ = 30 nm) of commercial olive oil samples (A, D) and calibration samples (EV and P) (source: own research)

tion with rice bran and maize oils its spectra changed very significantly; whereas, the detection of adulteration with canola and sunflower oils required the use of a principal component analysis to be detected. For the spectra obtained, the concentration of vitamin A, decreasing with the addition of oils to butterfat, was important.

Oil adulteration may include the addition of other vegetable oils as well as the addition of less expensive types of oil, for example, olive-pomace oil or refined olive oil. Guimet et al. [2005] applied excitation-emission fluorescence spectroscopy in detection of adulteration of extra virgin olive oil with the 5% addition of olive-pomace oil. The authors used excitation wavelengths of 300–390 nm and emission wavelengths of 415–600 nm. Among the tested methods of mathematical analysis, the discriminant N-PLS analysis was found to be the best in detecting adulterations. Dankowska et al. [2013], who applied synchronous fluorescence spectroscopy to examine extra virgin olive oil with the addition of soybean, sunflower and rapeseed oils, using 30 nm intervals between excitation and emission wavelengths, identified the lowest limit of adulteration detectability at 2.5%. The excitation wavelengths were in the range of 240–700 nm.

Synchronous fluorescence combined with PLS1 (Partial Least-Squares Regression) allowed Dupuy et al. [2005] to separate, with satisfactory results, virgin olive oil samples obtained from five French registered designation of origins. The authors identified, among others, bands referring to chlorophylls *a* and *b*, pheophytins *a* and *b*, α, β, γ-tocopherols and phenolic compounds. Synchronous spectra were measured at wavelengths of 250–700 nm, maintaining a 30 nm difference between the emission and excitation wavelengths.

Li et al. [2015] presented another example of the fluorescence spectroscopy application in assessing oil quality. When determining adulteration of walnut oil with soybean oil, the authors compared two methods: Fourier transform infrared and fluorescence spectroscopy combined with a mathematical analysis. They found that the spectrofluorometric method allowed the detection of a 5% addition of soybean oil without use of a mathematical analysis. The application of Fourier transform infrared method combined with soft independent modelling of class analogies (SIMCA), caused that the classification limit of added soybean oil was 10%. The authors used excitation wavelengths of 360 nm and recorded emission at 370 to 700 nm. Fluorescence spectroscopy was also used, with satisfactory effect, by Dogruer et al. [2021] to detect adulteration of cold pressed oils from sesame, pumpkin seed, grape seed, and black cumin. The adulterant agent was sunflower oil.

On the other hand, Ntakatsane et al. [2014] proposed using front face fluorescence spectroscopy combined with partial least squares regression (PLSR)

analysis to distinguish the origin of vegetable and animal fats. They concluded that there were no significant differences between fatty acids profiles (saturated and unsaturated fatty acids) predicted on the basis of fluorescence spectra and those obtained by gas chromatography. The authors, based on their research, predict that the mentioned technique may be used, for example, for detecting adulteration of milk fat with vegetable oils.

6. Conclusion

The aforementioned examples of the applications of spectrofluorometric techniques indicate that despite certain limitations and, often, the need to combine them with mathematical analysis, they are a useful tool for the relatively quick analysis of adulterations and oxidative changes in fat products. Moreover, their advantages include high sensitivity and selectivity and the fact that in most cases they do not require a complicated procedure of sample preparation.

Acknowledgements

This research was financed by the Ministry of Science and Higher Education of the Republic of Poland.

References

Amaral A.B., da Silva M.V., da Silva Lannes S.C. 2018. Lipid oxidation in meat: Mechanisms and protective factors – A review. Food Science and Technology, Campinas, 38(Suppl. 1), 1–15. https://dx.doi.org/10.1590/fst.32518

Andrade-Eiroa Á., de-Armas G., Estela J.M., Cerdà V. 2010. Critical approach to synchronous spectrofuorimetry. I. Trends in Analytical Chemistry, 29(8), 885–901. https://dx.doi.org/10.1016/j.trac.2010.04.010

Andrade-Eiroa Á., Canle M., Cerdá V. 2013. Environmental applications of excitation--emission spectrofluorimetry: An in-depth review I. Applied Spectroscopy Reviews, 48, 1–49. https://dx.doi.org/10.1080/05704928.2012.692104

AOCS. 2004. Official Methods and Recommended Practices of the AOCS. AOCS Press, Champaign.

Baraniak M.B., Szymanowska U. 2006. Lipooksygenaza w żywności pochodzenia roślinnego. Żywność. Nauka. Technologia. Jakość, 2(47), 29–45.

Calder P.C., Deckelbaum R.J. 2011. Harmful, harmless or helpful? The n-6 fatty acid debate goes on. Current Opinion in Clinical Nutrition and Metabolic Care, 14, 113–114. https://dx.doi.org/10.1097/MCO.0b013e328343d895

Cao J., Li C., Liu R., Liu X.R., Fan Y., Deng Z.Y. 2017. Combined application of fluorescence spectroscopy and chemometrics analysis in oxidative deterioration of edible oils. Food Analytical Methods, 10, 649–658. https://dx.doi.org/10.1007/s12161-016-0587-2

Dana D., Saguy I.S. 2001. Frying of nutritious foods: Obstacles and feasibility. Food Science Technology Research, 7(4), 265–279. https://dx.doi.org/10.3136/fstr.7.265

Dankowska A., Małecka M., Kowalewski W. 2013. Zastosowanie fluorymetrii synchronicznej do wykrywania zafałszowania oliwy z oliwek wybranymi olejami z nasion. Żywność. Nauka. Technologia. Jakość, 2(87), 106–115.

Dankowska A., Małecka M., Kowalewski W. 2014. Application of synchronous fluorescence spectroscopy with multivariate data analysis for determination of butter adulteration. International Journal of Food Science and Technology, 49, 2628–2634. https://dx.doi.org/10.1111/ijfs.12594

Dogruer I., Uyar H.H., Uncu O., Ozen B. 2021. Prediction of chemical parameters and authentication of various cold pressed oils with fluorescence and mid-infrared spectroscopic methods. Food Chemistry, 345, 128815. https://dx.doi.org/10.1016/j.foodchem.2020.128815

Domínguez R., Pateiro M., Gagaoua M., Barba F.J., Zhang W., Lorenzo J.M. 2019. A comprehensive review on lipid oxidation in meat and meat products. Antioxidants, 8, 429. https://dx.doi.org/10.3390/antiox8100429

Domínguez Manzano J., Muñoz de la Peña A., Durán Merás I. 2019. Front-face fluorescence combined with second-order multiway classification, based on polyphenol and chlorophyll compounds, for virgin olive oil monitoring under different photo- and thermal-oxidation procedures. Food Analytical Methods, 12, 1399–1411. https://doi.org/10.1007/s12161-019-01471-1

Dupuy N., Le Dréau Y., Ollivier D., Artaud J., Pinatel C., Kister J. 2005. Origin of French virgin olive oil registered designation of origins predicted by chemometric analysis of synchronous excitation-emission fluorescence spectra. Journal of Agricultural and Food Chemistry, 53(24), 9361–9368. https://dx.doi.org/10.1021/jf051716m

Fernández J., Pérez-Álvarez J.A., Fernández-López J.A. 1997. Thiobarbituric acid test for monitoring lipid oxidation in meat. Food Chemistry, 59(3), 345–353. https://dx.doi.org/10.1016/S0308-8146(96)00114-8

Ganhão R., Estévez M., Morcuende D. 2011. Suitability of the TBA method for assessing lipid oxidation in a meat system with added phenolic-rich materials. Food Chemistry, 126, 772–778. https://dx.doi.org/10.1016/j.foodchem.2010.11.064

Gu H., Huang X., Sun Y., Chen Q., Wei Z., Lv R. 2020. Intelligent evaluation of total polar compounds (TPC) content of frying oil based on fluorescence spectroscopy and low-field NMR. Food Chemistry, 342, 128242. https://dx.doi.org/10.1016/j.foodchem.2020.128242

Guimet F., Ferré J., Boqué R. 2005. Rapid detection of olive-pomace oil adulteration in extra virgin olive oils from the protected denomination of origin "Siurana" using excitation--emission fluorescence spectroscopy and three-way methods of analysis. Analytica Chimica Acta, 544, 143–152. https://doi.org/10.1016/j.aca.2005.02.013

Hajeyah A.A., Griffiths W.J., Wang Y., Finch A.J., O'Donnell V.B. 2020. The biosynthesis of enzymatically oxidized lipids. Frontiers in Endocrinology, 11, 591819. https://dx.doi.org/10.3389/fendo.2020.591819

Hara S., Ogawa E., Totani Y. 2006. Evaluation of heat-deteriorated oils. I. TLC-FID method for determining polar compounds content. Journal of Oleo Science, 55(4), 167–172. https://dx.doi.org/ 10.5650/jos.55.167

Jamwal R., Amit, Kumari S., Sharma S., Kelly S., Cannavan A., Singh D.K. 2021. Recent trends in the use of FTIR spectroscopy integrated with chemometrics for the detection of edible oil adulteration. Vibrational Spectroscopy, 113, 103222. https://dx.doi.org/10.1016/j.vibspec.2021.103222

Karoui R., Blecker C. 2011. Fluorescence spectroscopy measurement for quality assessment of food systems – A review. Food Bioprocess Technology, 4, 364–386. https://dx.doi.org/10.1007/s11947-010-0370-0

Karoui R., Thomas E., Dufour E. 2006. Utilisation of rapid technique based on front-face fluorescence spectroscopy for differentiating between fresh and frozen-thawed fish fillets. Food Research International, 39, 349–355. https://dx.doi.org/10.1016/j.foodres.2005.08.007

Kim R.S., LaBella F.S. 1987. Comparison of analytical methods for monitoring autoxidation profiles of authentic lipids. Journal of Lipid Research, 28(9), 1110–1117. https://dx.doi.org/10.1016/S0022-2275(20)38624-7

Kuselman I., Tur'Yan Y.I., Bourenko T., Goldfeld I., Shenhar A. 1998. PH-metric determination of the acid value of vegetable oils without titration. Journal of AOAC International, 81(4), 873–879. https://dx.doi.org/10.1093/jaoac/81.4.873

Kyriakidis N.B., Skarkalis P. 2000. Fluorescence spectra measurement of olive oil and other vegetable oils. Journal of AOAC International, 83(6), 1435–1439. https://doi.org/10.1093/jaoac/83.6.1435

Lai A., Santangelo E., Soressi G.P., Fantoni R. 2007. Analysis of the main secondary metabolites produced in tomato (Lycopersicon esculentum, Mill.) epicarp tissue during fruit ripening using fluorescence techniques. Postharvest Biology and Technology, 43, 335–342. https://dx.doi.org/10.1016/j.postharvbio.2006.09.016

Lakowicz J.L. 2006. Principles of Fluorescence Spectroscopy. Springer, Singapore.

Lands B. 2012. Consequences of essential fatty acids. Nutrients, 4, 1338–1357. https://dx.doi.org/10.3390/nu4091338

Li B., Wang H., Zhao Q., Ouyang J., Wu Y. 2015. Rapid detection of authenticity and adulteration of walnut oil by FTIR and fluorescence spectroscopy: A comparative study. Food Chemistry, 181, 25–30. https://dx.doi.org/10.1016/j.foodchem.2015.02.079

Meenu M., Cai Q., Xu B. 2019. A critical review on analytical techniques to detect adulteration of extra virgin olive oil. Trends in Food Science & Technology, 91, 391–408. https://dx.doi.org/10.1016/j.tifs.2019.07.045

Ntakatsane M.P., Liu X.M., Zhou P. 2013. Rapid detection of milk fat adulteration with vegetable oil by fluorescence spectroscopy. Journal of Dairy Sciences, 96(4), 2130–2136. https://dx.doi.org/10.3168/jds.2012-6417

Ntakatsane M.P., Liu X., Zhou P., Mothibe K.J., Adegoke G.O., Odenya W.O. 2014. Characterization of fatty acid profile by EFFS. Journal of Food Measurements and Characterization, 8, 1–8. https://dx.doi.org/10.1007/s11694-013-9158-z

Pedersen D.K., Munck L., Engelsen S.B. 2002. Screening for dioxin contamination in fish oil by PARAFAC and N-PLSR analysis of fuorescence landscapes. Journal of Chemometrics, 16, 451–460. https://dx.doi.org/10.1002/cem.735

Poulli K.I., Mousdis G.A., Georgiou C.A. 2009. Monitoring olive oil oxidation under thermal and UV stress through synchronous fluorescence spectroscopy and classical assays. Food Chemistry, 117, 499–503. https://dx.doi.org/10.1016/j.foodchem.2009.04.024

Rohman A., Putri A.R., Irnawati W.A., Nisa K., Lestari L.A. 2021. The employment of analytical techniques and chemometrics for authentication of fish oils: A review. Food Control, 124, 107864. https://dx.doi.org/10.1016/j.foodcont.2021.107864

Sádecká J., Tóthová J. 2007. Fluorescence spectroscopy and chemometrics in the food classification – A review. Czech Journal of Food Sciences, 25(4), 159–173. https://dx.doi.org/10.17221/687-CJFS

Salih A.M., Smith D.M., Price J.F., Dawson L.E. 1987. Modified extraction 2-thiobarbituric acid method for measuring lipid oxidation in poultry. Poultry Science, 66, 1483–1488. https://dx.doi.org/10.3382/ps.0661483

Sikorska E. 2012. Metody fluorescencyjne w ocenie jakości żywności. Fluorescence methods in food quality assessment. Zeszyty Naukowe, Uniwersytet Ekonomiczny w Poznaniu, 234, 59–75.

Sikorska E., Khmelinskii I.V., Sikorski M., Caponio F., Bilancia M.T., Pasqualone A., Gomes T. 2008. Fluorescence spectroscopy in monitoring of extra virgin olive oil during storage. International Journal of Food Science and Technology, 43, 52–61. https://dx.doi.org/10.1111/j.1365-2621.2006.01384.x

Sikorska E., Khmelinskii I., Sikorski M. 2012. Analysis of olive oils by fluorescence spectroscopy: Methods and applications. [In:] Olive Oil – Constituents, Quality, Health Properties And Bioconversions. Ed. D. Boskou. IntechOpen, Croatia. https://dx.doi.org/10.5772/30676

Skiera C., Steliopoulos P., Kuballa T., Holzgrabe U., Diehl B. 2012. ^{1}H NMR approach as an alternative to the classical p-anisidine value method. European Food Research Technology, 235, 1101–1105. https://dx.doi.org/10.1007/s00217-012-1841-5

Tena N., García-González D.L., Aparicio R. 2009. Evaluation of virgin olive oil thermal deterioration by fluorescence spectroscopy. Journal of Agricultural and Food Chemistry, 57, 10505–10511. https://doi.org/10.1021/jf902009b

Tompkins C., Perkins E.G. 1999. The evaluation of frying oils with the p-Anisidine value. Journal of the American Oil Chemists' Society, 76(8), 945–947. https://dx.doi.org/10.1007/s11746-999-0111-6

Tsiaka T., Christodouleas D.C., Calokerinos A.C. 2013. Development of a chemiluminescent method for the evaluation of total hydroperoxide content of edible oils. Food Research International, 54, 2069–2074. https://dx.doi.org/10.1016/j.foodres.2013.08.036

Twenefour D., Shields E. 2020. Saturated fats and the management of diabetes: The debates, controversies and consensus. Practical Diabetes, 37(4), 115–120. https://dx.doi.org/10.1002/pdi.2283

Veberg A., Vogt G., Wold J.P. 2006. Fluorescence in aldehyde model systems related to lipid oxidation. LWT – Food Science and Technology, 39, 562–570. https://dx.doi.org/10.1016/j.lwt.2005.03.009

Wójciak K.M., Dolatowski Z.J. 2012. Oxidative stability of fermented meat products. Acta Scientiarum Polonorum. Technologia Alimentaria, 11(2), 99–109.

Ye L., Harris E., Budge S.M., Sullivan R.J. 2020. Flavors' decreasing contribution to p-Anisidine value over shelf life may invalid the current recommended protocol for flavoured fish oils. Journal American Oil Chemical Society, 97, 1335–1341. https://dx.doi.org/10.1002/aocs.12435

Zuo W., Hu X., Yang Y., Jiang L., Ren L., Huang H. 2017. Development of an improved method to determine saturated aliphatic aldehydes in docosahexaenoic acid-rich oil: A supplement to p-Anidisine value. European Journal of Lipid Science and Technology, 119, 1700243. https://dx.doi.org/10.1002/ejlt.201700243

X THE PRINCIPLE OF THE FLOW CYTOMETRY TECHNIQUE AND ITS APPLICABILITY

Katarzyna PETKA-PONIATOWSKA

Department of Plant Products Technology and Nutrition Hygiene,
Faculty of Food Technology, University of Agriculture in Krakow,
Aleja Mickiewicza 21, 31-120 Krakow, Poland

katarzyna.petka-poniatowska@urk.edu.pl
ORCID: https://orcid.org /0000-0002-8286-2485

Abstract. Flow cytometry (FC) is an analytical technique that allows to quickly enumerate and distinguish various types of cells on the basis of the measurement of scattered light or the fluorescence emitted by properly irradiated cells. It allows the quantification and biological evaluation of cells as well as some of their components: nuclei, mitochondria and chloroplasts. FC was discovered as an improvement to the fluorescence microscopy and is characterized by efficiency that allows to analyze in a short time various parameters of a large number of cells without losing data about the properties of a single cell, and the obtained results can be analyzed statistically. Every year new methods and procedures are developed that use this technique for research in various scientific disciplines.

Keywords: flow cytometry, fluorochrome, immunology, microbiology, genetics

1. Introduction

The beginnings of flow cytometry date back to 1934, when an article was published in the Science journal describing the possibility of using a photoelectric sensor to count cells flowing through a capillary. This type of cytometer could

detect only one parameter – the size of cells [Adan et al. 2017]. The author of this idea Andrew Moldavan never implemented his innovative project. It was not until 1947 when the first report on the cytofluometric detection of bacterial aerosols was published. The research was sponsored by US Army and was invented to quickly identify bacteria in the air in case of biological weapon use [Baran 2008]. Until 1970, there were only two companies in the cytometric market: Bio/Physics Systems (America) producing the Cytograph and Cytofluorograph and Phywe AG (Germany) distributing the Impulscytophotometer (IPC). Then, Technicon launched in the first of a series of flow hematological counters differentiating the leukocyte population [Baran 2008].

In the early 1980s, thanks to the simultaneous use of two types of fluorescently labeled antibodies, it became possible to analyze several types of proteins (antigens) simultaneously. Following this lead, three large companies: Becton-Dickinson, Coulter and Ortho introduced laser flow cytometers to their offer, that enabled the separation of the studied molecules (cells). Other improvements in sorting efficiency and data processing were also gradually introduced [Baran 2008].

2. Construction of a flow cytometer

There are two basic types of flow cytometers. One group consists of typical *analyzers* that are used in research laboratories to evaluate the expression of surface or intracellular proteins and antigens (e.g. surface receptors, cytokines, hormones), enzyme activity (e.g. kinases, caspases) or to assess the gene expression and mRNA transcription for various cell products (FISH technique) [Álvarez-Barrientos et al. 2000; Adan et al. 2017]. Another group are *cell sorters* having the ability not only to collect and analyze data about flowing cells, but also to sort cells based on their properties. They are able to deflect flowing particles according to differences in their electric potential and collect them in separate tubes [Cossarizza 2019]. This allows for additional evaluation of some functional parameters. The degree of purity of isolation of cells that meet certain (selected by scientist) criteria is over 99%. Due to their high efficiency, sorters are used to isolate very rare cells, such as cancer cells suspended in the blood, fetal erythrocytes or genetically modified cells. These devices have also found application in transplantation and *in vitro* fertilization [Álvarez-Barrientos et al. 2000; Adan et al. 2017; Cossarizza 2019]. There are also cytometers that are designed for specific tasks, such as detecting, characterizing and counting microorganisms suspended in water or somatic and bacterial cells in milk.

A typical flow cytometer consists of [Skotny and Pucińska 2013; Adan et al. 2017; Cossarizza 2019; Vembadi et al. 2019; Bio-Rad 2021]:

- ***the fluidics system*** – a stream of liquid (so called *sheath fluid*) surrounding the suspension of analyzed cells sucked from test tube, which are in such way transported to the laser beam for interrogation (Fig. 1). The passing through the point of measurement (part called *flow cell*) should be conducted at the appropriate speed, which can be controlled (and changed) by the cytometer operator. The role of sheath fluid is to keep the cells flowing inside the stream separate and focus them in the center of the sample core;
- ***the optic system***, that consist of excitation optics and collection optics;
- ***the electronics system*** converting the detected light signals into electronic impulses, that can be processed and analyzed by computer;
- ***the data analysis syste****m*, that is appropriate software allowing for statistical processing of the obtained results.

The excitation optics consist of source of light that illuminates tested particles. Usually an air-cooled argon laser (blue laser with the length beam of 488 nm) is used, however in some cytometers a diode laser (red diode laser ~635 nm length beam) can be an option. The laser beam is shaped by special lenses and focused on the cells that flow within the fluidic stream (Fig. 1) [Adan et al. 2017]. The collecting optics are set of lenses, mirrors and filters. Lenses collect light emitted from the interaction between tested cell and laser beam, while mirrors split the light signal to various optical detectors: the photomultiplier tubes (PMTs) or a photodiode. The photodiode is less sensitive detector, so it is used to detect the stronger forward-scatter light (FSC) signal. PMTs are used to detect the weaker signals generated by side-scattered light (SSC) and fluorescence (FL). The specificity of a detector for a particular fluorescent dye results from a type of filter placed in front of the PMTs, which allows to cut off a narrow range of wavelengths which finally reaches the detector. When cells or particles in a fluid stream pass through the laser beam light signals are generated. Detectors convert the light signal to electronic signals (voltage pulse) proportionally to their intensity (strength). Signals can be amplified, but finally each voltage pulse is assigned a digital value by the Analog-to-Digital Converter (ADC) representing 0–1,000 mV channels. The particular channel numbers (separately for FSC, SSC and up to 4 fluorescence signals) are transferred to the computer and data produced by all the light signals generated, by one cell flowing through the laser beam, are stored by computer system as a set of data characterizing this measuring point (i.e., one cell). Such data can be then processed, graphically displayed and statistically analyzed in

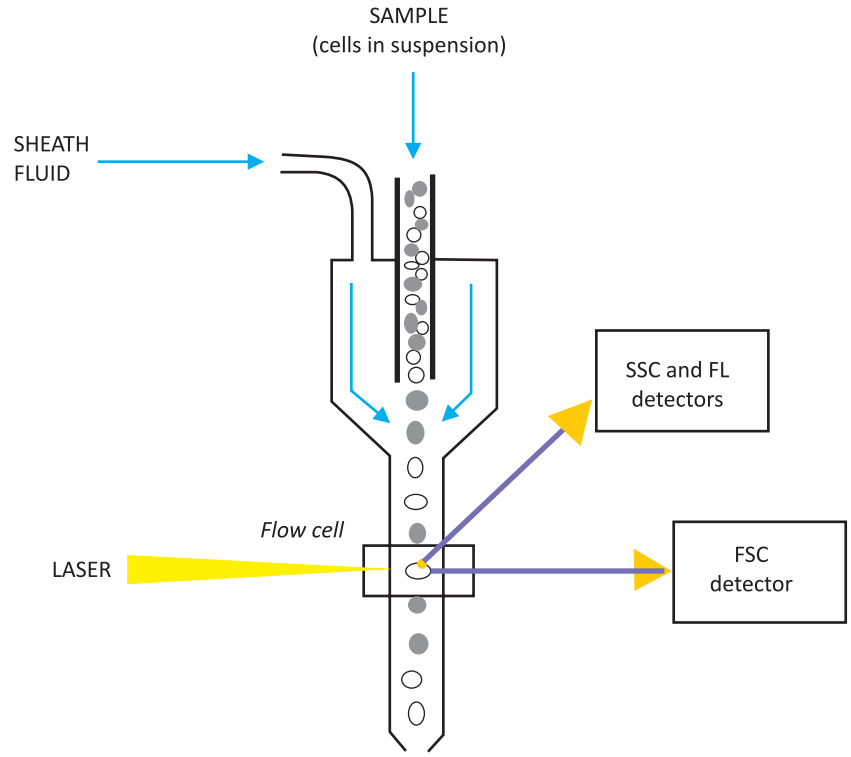

Fig. 1. The principle of creating a sample stream surrounded by sheath fluid and its flow through the flow cell – the point of interaction between single cell and incident laser light (source: based on Adan et al. [2017])

various ways [Ormerod 2008; Skotny and Pucińska 2013; Adan et al. 2017; Cossarizza 2019; Vembadi et al. 2019].

The electronic system is also important for proper adjusting the flow cytometer before analysis. For example, an electronic threshold can be used to limit the number of events that the flow cytometer acquires. A threshold is the value of selected, defined by the user, one parameter. Only those signals that have an intensity greater than or equal to the threshold value are processed and sent to the computer. For example threshold set on FSC allows to eliminate cell debris. Consequently, only whole cells are collected and then analyzed. It is important especially in situation when cytometer is programmed to collect a specific number of cells (e.g., 10 000) or has to test a given volume of suspension (e.g., 50 µl) [Ormerod 2008; Adan et al. 2017].

3. The principle of operation of the flow cytometer

The majority of flow cytometers allows the analysis of particles or cells from 0.2 to 150 μm in size. When cells are not labelled with fluorescent stains usually only 2 parameters can be achieved by interaction with laser beam – the signals generated by forward-scattered (FSC) and side-scattered (SSC) light. Light scattering occurs when a particle deflects incident laser light (Fig. 2). FSC correlates with the amount of light that is scattered in the forward direction (along the same axis the laser beam is travelling) and its intensity is attributed to cell-surface area or size. The laser light that is scattered at 90° to the axis of the laser path is detected as SSC and is proportional to the internal complexity (granularity) of the cells, because cell's membrane, nucleus, inclusions and any granular material inside the cell disperse the light [Beckton and Dickinson 2002; Ormerod 2008; Adan et al. 2017; Bio-Rad 2021].

Based on the correlated measurement of FSC (size) and SSC (cellular complexity) the differentiation between various cell types in heterogenous population can be done. For example, when the peripheral blood sample was analysed and then FSC data are plotted on the x-axis, while SSC data on the y-axis (Fig. 3),

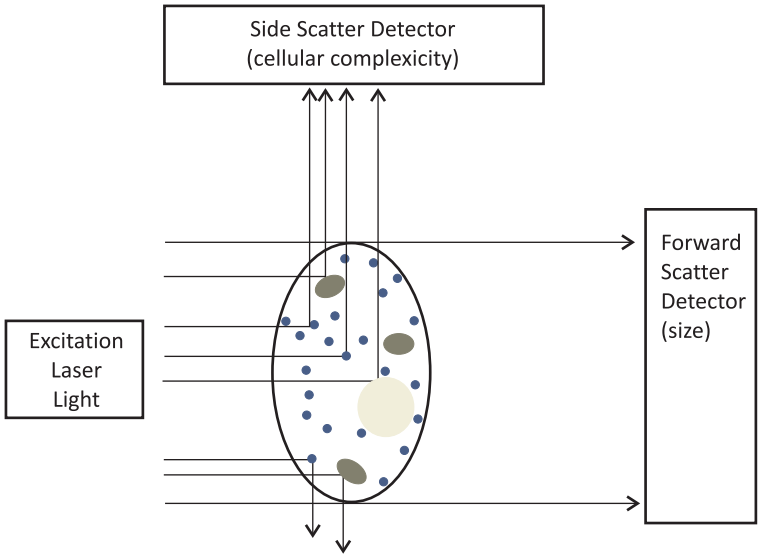

Fig. 2. The scattering of light: FSC is proportional to cell size, while SSC is proportional to cell granularity or internal complexity (source: based on Beckton and Dickinson [2002] and Adan et al. [2017])

the populations of lymphocytes, monocytes and neutrophils can be distinguished and further analyzed without their physical isolation. FC software allows to gate selected subpopulation (gate G1 at Fig. 3) and to analyse cell within gate without previous cells separation.

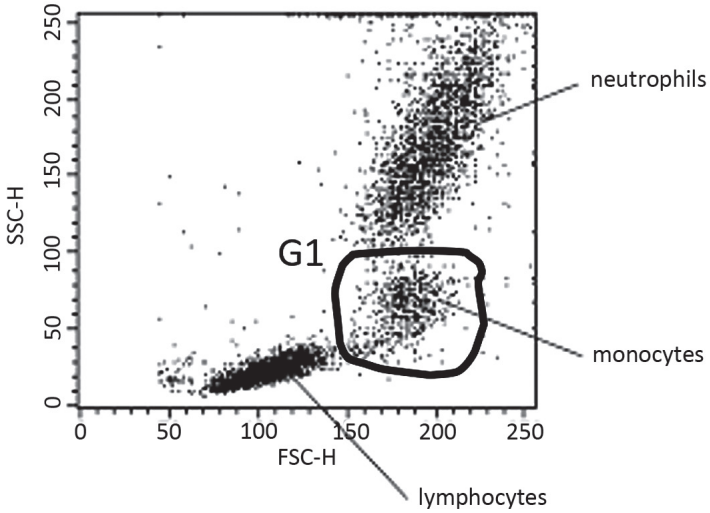

Fig. 3. The example of SSC vs. FSC analysis of peripheral blood sample (white cells). Each dot represents an individual cell analysed by the flow cytometer. G1 – gate set on monocytes subpopulation (source: Beckton and Dickinson [2002], p. 11)

Much more information can be achieved when cells are fluorescently stained. There are several types of fluorochromes (fluorophores) that absorb light energy of a specific wavelength (excitation) and re-emit light (emission) at a longer wavelength. When labeled cells pass through the flow cell, every single particle is irradiated with a focused laser beam. The light is scattered, but at the same time it excites the fluorochromes attached to the cells or inside it. The resulting signals are measured with appropriate detectors, converted into electrical impulses, amplified and sent to a computer for further processing, storage and analysis. Therefore, if the analysis or distinguishing between cells with similar size and granularity is demanded, it is necessary to fluorescently label whole cells or their elements. This can be accomplished by the use of fluorescent molecules alone (e.g., cellular dyes) or fluorophore-labeled antibodies or DNA probes. There are many fluorophores used in FC, they differ with wavelengths of maximum absorption (≈ excitation) and emission (Tab. 1) [Davey and Kell 1996].

Table 1. Cellular parameters measured by flow cytometry and examples of fluorochromes used for staining (source: besed on Davey and Kell [1996]; McCarthy [2007]; Kim and Sederstrom [2015])

Determinant/ cellular parameter	Stain	Excitation (max) wavelength [nm]	Emission (max) wavelength [nm]
DNA	Ethidium bromide (EthBr)	510	595
	Bis Benzimide (Hoechst 33342)	350	461
	2'-(4-Hydroxyphenyl)-5-(4-methyl-1-piperazinyl)-2,5'-bi(1H-benzimidazole) trihydrochloride (Hoechst 33258)	343	540
	Nuclear yellow (Hoechst S769121)	355	495
	7-aminoactinomycin D (7-AAD)	546	647
	TO-PRO-3 Iodide	642	661
	4',6-diamidino-2-phenylindole (DAPI)	358	461
	1, 5-bis{[2-(di-methylamino)ethyl]amino}-4, 8-dihydroxyanthracene-9, 10-dione (DRAQ5)	646	665
	1, 5-bis{[2-(di-methylamino)ethyl]amino}-4, 8-dihydroxyanthracene-9, 10-dione (DRAQ7)	644	681
Nucleic acids	Propidium iodide (PI)	365,535	617
	Thiazole orange (TO)	509	525
	Pyronin Y	497	563
Protein	Fluorescein isothiocyanate (FITC)	490	530
	Phycoerythrin (PE)	490	570
Antibodies	Allophycocyanin (APC)	650	660
Proliferation	Carboxyfluorescein succinimidyl ester (CFSE)	495	519
	Oregon Green 488	496	524
Transmembrane potential	Oxonol-V	610	639

Table 1. cont.

Determinant/ cellular parameter	Stain	Excitation (max) wavelength [nm]	Emission (max) wavelength [nm]
Fats	Nile Red	550	640
Apoptosis	Annexin V Alexa Fluor® 488	495	519
Ca^{2+} concentration	1H-Indole-6-carboxylic acid (INDO-1)	400	475
pH	Seminaphthorhodafluor dye (SNARF®-1)	548	579
	BCECF Acid (2',7'-Bis-(2-Carboxyethyl)-5-(and-6)-Carboxyfluorescein)	490	535

It is important to select fluorochromes properly. They should have the same length of excitation light, but different emission light length. The argon ion laser, which is the most commonly used in cytometry, emits a light of 488 nm length and can excite many fluorochromes. Among the most widely used fluorochromes fluorescein isothiocyanate (FITC) and phycoerythrin (PE) can be mentioned (Fig. 4). Both have absorption peak spectra at approximately 490 nm, so can be

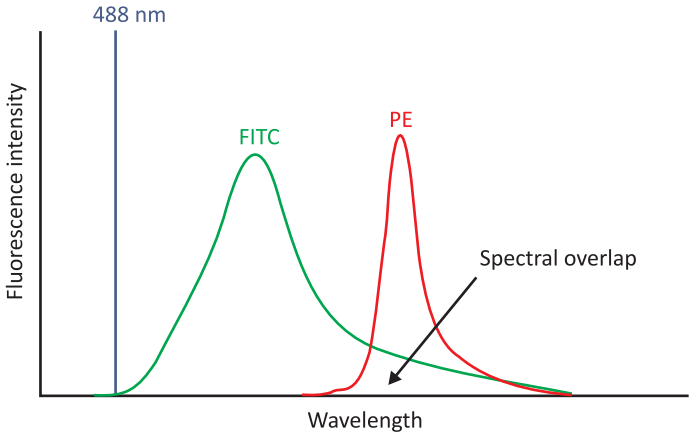

Fig. 4. Fluorescence emission spectra for FITC and PE showing the overlap in emission for the two fluorochromes (488 nm – argon laser wavelength) (source: based on Davies and Allen [2007])

easily excited by the argon lasers. However, the peak emission wavelengths of FITC and PE are distant enough (530 nm and 570 nm, respectively) to be picked up by different detectors. Table 1 presents selected cellular parameters and examples of fluorochromes applied to detect their behavior in flow cytometry analysis.

Fluorochromes used in FC differ in their mode of action. Some of them emit a signal only after attaching to specific cellular components: proteins (FITC), nucleic acids (PI) or fats (Nile Red). Another group are the so-called fluorogenic substrates, the activity of which depends on the presence of appropriate enzymes. There are also markers related to the physiological parameters of the cell (pH, membrane potential, Ca^{2+} concentration etc.) and fluorochromes attached to antibodies or nucleotide probes that serve to directly detect antigens and DNA or RNA sequences [Davey and Kell 1996; Álvarez-Barrientos et al. 2000; McCarthy 2007; Skotny and Pucińska 2013; Errante 2015; Kim and Sederstrom 2015].

4. The results standardization and presentation

Due to the fixed optics and digital electronics, the cytometer allows the simultaneous multi-color analysis of up to 4-6 fluorescent markers and two scattering parameters (FSC and SSC). Although it creates great analytical possibilities, it also carries the risk of error and causes difficulties in comparing the obtained data [Álvarez-Barrientos et al. 2000; Errante 2015]. For this reason, the course of the experiment should be each time described in detail. Such a report should take into account, inter alia, procedures used for the preparation of the test material and a description of the reagents used, i.e., enzymes, buffers, dyes, including the data of their suppliers, catalog numbers and clone designations. This information is essential for control purposes and ensures a high degree of reproducibility of the results. The type of test sample is also important, which can be, for example, isolated live cells from peripheral blood, bone marrow, tissue biopsy, lymph node, saliva, cerebrospinal fluid, alveolar-bronchial lavage, body fluids from body cavities, as well as samples of water, wine, beer and other liquid food products. The research sample and reagents should not be frozen, and the method of their storage should be included in the description [Álvarez-Barrientos et al. 2000].

The parameters of the flow cytometer itself are equally important. The methodology should include cytometer model, type of software used and manufacturer's data. The laser lines and emission filters used with the appropriate fluorescent reagents should also be listed. What is important, the use of multiple fluorochromes increases the risk of interference that results from overlapping individual spectra (see Fig. 4). This can be avoided by properly conducted calibration

and by using so-called compensation, i.e., narrowing the detection spectrum to a very narrow wavelength range. This function is set in the cytometer during data collection and should be included in the description of the experiment, as well as sample size, statistical data, the threshold value and method of its determination [Álvarez-Barrientos et al. 2000; Skotny and Pucińska 2013].

The results obtained after cytometric analysis can be presented in several ways. Typically, they are illustrated as one-dimensional (histograms), two-dimensional (dot density, contour plot) or three-dimensional (perspective) plots (Fig. 5).

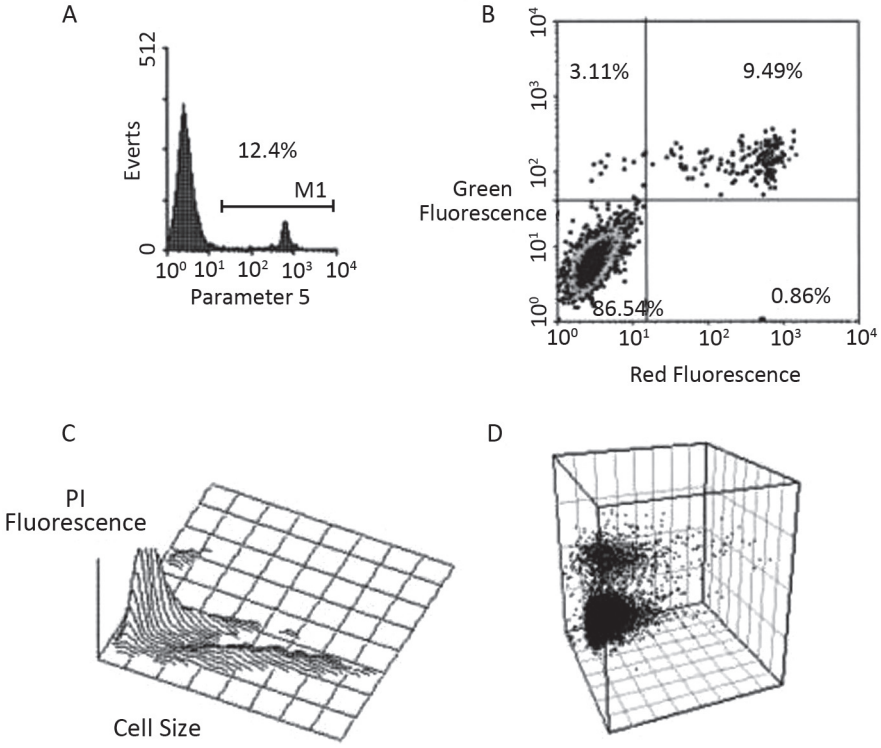

Fig. 5. Different ways of presenting flow cytometry data: one-dimensional histogram showing the ratio of the selected parameter (X axis) to the number of cells tested (Y axis) (A), the two-dimensional graph shows the scattered cells depending on the intensity of the emitted signal in relation to the two selected parameters; cells in the upper left corner are positive for the Y axis parameter, cells in the upper right corner – for both parameters, in the lower left corner – double negative, and those in the lower right corner of the chart are positive for the X axis parameter (B), less common three-dimensional plots can take into account various parameters on the Z axis, such as the number of cells or the fluorescence signal (C and D) (source: Álvarez-Barrientos et al. [2000], p. 171)

There are many publications that contain protocols of pre-analytical cell preparation, analysis methods and procedures of adequate staining. Cossarizza et al. [2019] present the guidelines for FC usage in the broad area of immunology and hematology, providing the theory and key practical aspects of flow cytometry.

5. Applications of flow cytometry

Flow cytometry can be applied in many areas of science and research such as immunology, microbiology, biotechnology, molecular biology, genetics, clinical and environmental sciences and many more [Davey and Kell 1996; Brown and Wittwer 2000; Betters 2015; Wilkinson 2015].

5.1. Immunology

Flow cytometry enables the qualitative and quantitative assessment of the cell population and subpopulations, their morphological features and functional states. The emergence of the technology of producing monoclonal antibodies and their combination with fluorescent dyes made it possible to quickly assess the phenotype associated with the presence of antigens located on the surface of the cell membrane. In its simplest form, the *immunophenotyping* experiment involves the examinations of the cells stained with fluorochrome-coupled antibodies that are directed against cell surface antigens typical for particular population of cells, e.g., distinguishing between CD4 and CD8 populations of T cells [McKinnon 2018].

The cells immunophenotyping has found application in the diagnosis of, among others, acute and chronic leukemias, myelodysplastic syndromes, lymphomas, hematologic neoplasms, myelodysplastic and myeloproliferative syndromes, tumors of the bones, head and neck [Orfao et al. 2004; Craig and Foon 2008]. Its use often allows the correct selection of the therapy required, determining the degree of re-emission and detecting the so-called minimal residual disease (MRD), i.e., small amounts of cancer cells that remain in the body and cause disease recurrences. Flow cytometry detects residual blasts in patients who appear to be completely remitted according to morphological criteria. It is also possible to evaluate various cytoplasmic and nuclear antigens using FC technique, labelled specific antibodies and by increasing the permeability of the cytoplasmic membranes (so-called permeabilization).

Flow cytometry can be applied for studying the measurement of antigen specific responses which is widely used in vaccine research or for analysis of intracel-

lular cytokine production [McKinnon 2018]. FC has also been used in the diagnosis of some autoimmune, rheumatic, respiratory, and gastrointestinal diseases, as well as for monitoring the host immune response to infection or the diagnosis of immunodeficiencies [Marrone 2009; Soloski and Chrest 2013; Mortaz et al. 2015; Fleisher et al. 2016; Kanegane et al. 2018; Cabral-Marques et al. 2019; Madkaikar et al. 2019; Rawat et al. 2019; Flores-Gonzalez et al. 2020].

In *transplantology*, the flow cytometry technique is used to determine human leukocyte antigens (HLA) on the surface of donor and recipient cells and in the so-called crossmatch [Tait 2016], i.e., the assessment of the presence of cytotoxic antibodies against the donor's cells in the recipient's serum. Control studies of the lymphocyte subpopulation in a patient after transplantation provide data on the state of his immune system and allow to determine the effectiveness of the immunosuppressive therapy. It means that FC plays a well-established role in the pre-transplant crossmatching as well as in monitoring the health and immunological responses in transplant recipient [Maguire et al. 2014; Hutchinson 2015].

In *allergology*, it is used to assess the effectiveness of desensitization therapy based on cytofluorimetric analysis of the level of Th1 and Th2 helper lymphocytes or by assessing the degree of basophil degranulation [Yabu et al. 2016].

5.2. Molecular biology and genetics

Analysis of cell proliferation, cell cycle, apoptosis and necrosis, signal transduction pathways as well as the expression of various proteins and nucleic acids can be assessed by FC. Cell proliferation can be measured by FC using several assays and different markers. Methods such as: incorporation of thymidine analogues (BrdU) into replicating DNA, generation tracing of hereditary persistent dyes (CFSE), and expression of proliferation related antigens (Ki67, PCNA) can be used [McKinnon 2018].

Cell cycle analysis assays involve DNA staining with a saturating amount of DNA-binding dye (see Table 1). DNA-binding dyes include PI, 7-AAD, Hoechst 33342, 33258 and S769121, TO-PRO-3, DAPI, DRAQ5™ and DRAQ7™ or Pyronin Y [Pożarowski and Darzynkiewicz 2004; Kim and Sederstrom 2015; McKinnon 2018]. Thanks to the FC the mitotic cycle of neoplastic cells with the assessment of DNA ploidy and the breakdown of certain proteins, e.g., cyclins, can be studied [Heiden et al. 2000; Pożarowski and Darzynkiewicz 2004; Davies and Allen 2007]. There are 4 procedures usually used to analyze the cell cycle by flow cytometry. The first two are based on univariate analysis of cellular DNA content

following cell staining with either PI or DAPI and deconvolution of the cellular DNA content frequency histograms. This approach reveals distribution of cells in three major phases of the cycle (G1 vs S vs G2/M) and makes it possible to detect apoptotic cells with fractional DNA content. The third approach is based on the bivariate analysis of DNA content and proliferation-associated proteins. The expression of cyclin D, cyclin E, cyclin A, or cyclin B1 vs DNA content is presented as an example. This approach allows to distinguish, for example, G0 from G1 cells, identify mitotic cells, or relate expression of other intracellular proteins to the cell cycle position. The fourth procedure relies on the detection of 5'-bromo-2'-deoxyuridine (BrdU) incorporated to label the DNA-replicating cells [Pożarowski and Darzynkiewicz 2004; Kim and Sederstrom 2015].

Apoptosis (programmed cell death) serves to maintain homeostasis of the immune system by removing cells without causing an inflammatory response. Detection of apoptosis by flow cytometry uses multiple targets along the cascade of apoptotic events [Wlodkowic et al. 2011; Nalbant 2018]. Moreover, FC allows to discriminate between apoptosis and necrosis [Wlodkovic et al. 2011; Pietkiewicz et al. 2015]. There are also commercial kits (e.g., Annexin V-FITC kit from Sigma-Aldrich or Alexa Fluor® 488 Annexin V/Dead Cell Apoptosis Kit from ThermoFisher Scientific) that allow fluorescent detection of annexin V (protein implicated in apoptotic mechanism in cells) in apoptotic cells and quantitative determination by flow cytometry. Mentioned above kits use annexin V conjugated with FITC or Alexa Fluor® 488 dye to label phosphatidylserine sites on the membrane surface. The kit includes also PI to label the cellular DNA in necrotic cells, where the cell membrane has been totally compromised. This combination allows the differentiation among early apoptotic cells (annexin V positive, PI negative), necrotic cells (annexin V positive, PI positive), and viable cells (annexin V negative, PI negative).

Since its introduction, the propidium iodide flow cytometric assay has been widely used for the evaluation of apoptosis in various experimental models. It is based on the principle that apoptotic cells, among other typical features, are characterized by DNA fragmentation and, consequently, loss of nuclear DNA content. Use of a fluorochrome, such as PI, that is capable of binding and labeling DNA makes it possible to obtain a rapid (the protocol can be completed in about 2 h) and precise evaluation of cellular DNA content by flow cytometric analysis, and subsequent identification of hypodiploid cells (Fig. 6) [Riccardi and Nicoletti 2006].

In most cases of apoptosis, the caspase signaling pathway is activated and it can be also analyzed by flow cytometry [Telford et al. 2002]. For this, intracellular staining and antibodies specific for the active form of caspase 3 are used.

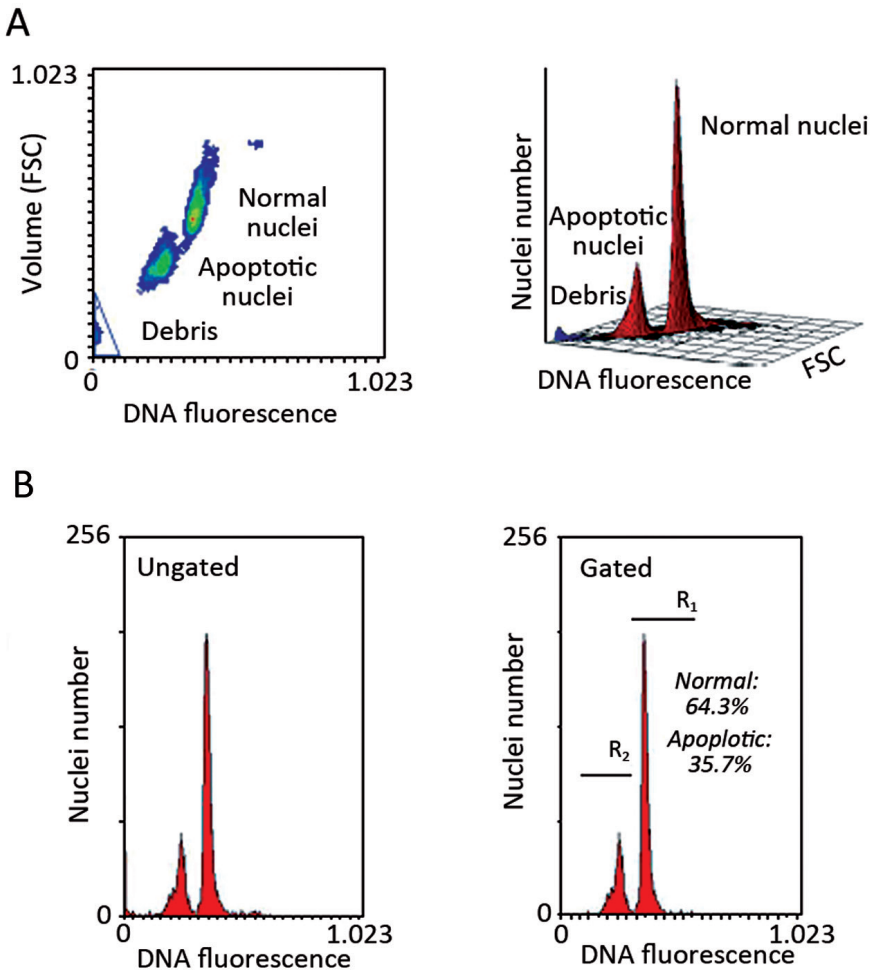

Fig. 6. Measurements of apoptotic thymocytes: Dot-plot analysis of thymocytes undergoing apoptosis. Debris and residuals of necrotic cells (the bulk of which has been eliminated during acquisition with the flow cytometer) can be recognized (and gated-off by eliminating the corresponding region) by the lower diameter (FSC) and reduced DNA fluorescence compared to apoptotic thymocytes. The right panel shows a 3D representation of the peaks corresponding to normal nuclei apoptotic nuclei and debris (A), A precise and reproducible estimate of the percentage of normal and apoptotic nuclei can be obtained by analysis of the DNA histogram after elimination of residual debris (B) (source: Riccardi and Nicoletti [2006], p. 1460)

There are additional tests that use fluorogenic substrates which, when exposed to caspase, are cleaved and then emit fluorescence [McKinnon 2018].

For studying signaling pathways in various cells populations by FC the antibodies to resting and phosphorylated signaling molecules such as pERK, pp38, pJNK, pSTAT1, pSTAT5, and pSTAT6, MAP-kinases etc. are used [Chow et al. 2001; Krutzik and Nolan 2003; Goldeck et al. 2013; Davies and Allen 2007; Marsman et al. 2020].

Flow cytometry combined with fluorescence in situ hybridization (FISH) can be used to detect RNA expression along with protein expression at a level of a single-cell [Arrigucci et al. 2017].

Fluorescent proteins (GFP, mCherry, YFP, mRuby, etc.) are used as markers for protein expression. Typically, cells are transferred with a plasmid that contains the promoter sequence and encodes the gene of interest along with the fluorescent protein. Expression of a fluorescent protein is used as an indicator of the expression of the selected gene. It is used in the control of transplanted cells *in vivo*, bacterial and viral infections [Errante 2015].

Not only information about the presence or absence of a specific molecule is important, but also data on its density on the cell surface. This type of analysis is performed by comparing the fluorescence intensity of the particles with the glow intensity of the microspheres (beads) coupled to various known amounts of the fluorochrome. Flow cytometry set new directions of research in medicine, mainly in immunology and oncology [Almeida Santiago et al. 2016].

5.3. Microbiology

One of the earliest applications of flow cytometry is to analyze the autofluorescence of microorganisms present in water (river, lakes, seas, oceans). The autofluorescence of photosynthetic pigments such as chlorophylls, phycoerythrin, phycocyanin, and allophycocyanin, can be used for algae identification [Davey and Kell 1996]. However, flow cytometry can be used to distinguish not only aquatic microorganisms. It can be applied for drinking water analysis as well as the analysis of wastewater treatment [Wilkinson 2015]. Basing on the autofluorescence signal and different SSC and FSC it is possible to "isolate" various subpopulations and analyze the cells without the need to culture them. When light scattering signals and autofluorescence are insufficient, particular microorganisms can be stained, for example the whole DNA present in cell can be stained with specific dyes. In order to distinguish biological from nonbiological particles, nucleic acids staining is the most suitable. Traditionally, ethidium bromide or propidium iodide are used most often.

As in other research areas the fluorescently labelled antibodies (for example with FITC, DAPI, phycoerythrin (PE), PE-cyanine7, PE-cyanine5.5, allophycocyanin (APC), APC-cyanin5.5, APC-cyanin 7, Alexa Fluor™, Brilliant Violet™ 421, Vio667, VioGreen, VioBlue, Amine Aqua, Pacific Orange, Pacific Blue), can be used, thus enabling the enumeration of surface antigens on the target cells or the detection of a given cell type in a mixed population [Pitsillides et al. 2011; Hunka et al. 2020]. A particular additional benefit of the approach is that the cells do not have to be cultured. Using specific antibodies against particular microorganism, they can be identified in various fluids, such as blood samples, spinal fluid, drinking water and various liquid foodstuff. Flow cytometry is used for microbiological control of many alcoholic and non-alcoholic drinks, such as beer, wine, fruit juices, pasteurized milk. It can also be used to the technological process monitoring (e.g., the number of yeasts in beer or wine) or for detection of pathogens (*Salmonella*, *E. coli*, *Listeria monocytogenes*, *Yersinia*, *Staphylococcus aureus*, *Bacillus* etc.) [Davey and Kell 1996; Álvarez-Barrientos et al. 2000; Malacrinò et al. 2001; Davey and Guyot 2020; Herrero et al. 2006; Novak et al. 2007; Salma et al. 2013; Wang et al. 2014; Betters 2015; Wilkinson 2015; Kinsinger et al. 2017; Longin et al. 2017; Props et al. 2018]. Flow cytometry allows for yeast budding analysis [Porro et al. 2009] as well as to study sporeforming bacteria [Wilkinson 2015]. When fluorescently labeled probes specific to 16S rRNA (bacteria) or 18S rRNA (yeasts) are used the phylogenetic studies can be conducted as well as species, strains, serotypes can be identified without microorganism cultivation [Amann et al. 1990; Fernández-Lago et al. 2000; Props et al. 2018; Sharma et al. 2020].

Flow cytometry can also be used for assessment of viability of bacteria and yeasts [Boyd et al. 2003; Herrero et al. 2006; Quiros et al. 2007; Salma et al. 2013; Davey and Guyot 2020]. Viable cells can be detected by their ability to cleave a nonfluorescent precursor to release a fluorochrome (intracellularly). There are also commercial kits enabling distinguishing and count live and dead bacteria or yeasts. It should be added that flow cytometry has an advantage over cultivating methods as is much quicker (result in less than 1h instead of some days of culturing in plate) and – which is more important – it can detect also bacteria at viable but non-culturable (VBNC) state [Divol and Lonvaud-Funel 2005; Herrero et al. 2006; Quiros et al. 2007, 2009]. Thanks to that the impact of various disinfectants or bacteriostatic/bactericidal compounds can be assessed [Frohling and Schulter 2015].

Among fluorochromes that are usually used for distinguishing live/dead cell are: acridine orange (AO), DAPI, EthBr, PI, Hoechst 33258/33342, SYTO-9, and thiazole orange (TO) that specifically bind to nucleic acids. Some of them,

such as Hoechst 33342, SYTO-9, or TO cross an intact plasma membrane, which results in viable cells staining [Robertson 2019]. On the other side, intact membranes in live cells are impermeable to some of mentioned dyes (e.g., PI, Eth Br) so they are not allowed into the live cell, and they stain only dead cells [Chitarra and Van den Bulk 2003, Quiros et al. 2007, Davey and Guyot 2020]. Beside the cell viability, flow cytometry allows also to examine the metabolic activity (enzymes, pathways), mitochondrial activity, membrane integrity and plasma membrane potential, production of reactive oxygen species as well as intracellular pH (using BCECF) or Ca^{2+} concentration (using INDO-1) [McCarthy 2007; Wilkinson 2015].

Finally, flow cytometry technique can also be used for absolute cell counting. There are commercially available special fluorescent beads of known concentration (e.g. BD Liquid Counting Beads from BD Biosciences, CountBright™ Absolute Counting Beads for flow cytometry from ThermoFisher Scientific), which are collected together with the sample and then the sample is analyzed and the gated cell number for the population of interest is compared with the number of beads that had pass through the laser beam in the same sample to calculate the absolute cells number per milliliter [McKinnon 2018].

6. Conclusion

Despite the fact that flow cytometry is a method with several decades of tradition, modifications are still being developed that allow for new applications in various fields of science. Flow cytometers can be found in hospitals, industry, research laboratories and university classrooms. With the development of knowledge, there are more and more new ideas to use this technique to quickly identify important microorganisms, rare types of cells, or mutations. The best example is COVID-19, a new disease entity. Flow cytometry allowed for development a method for the rapid detection of anti-SARS-CoV-2 antibodies [Lapuente et al. 2020; Soni et al. 2020]. It can be assumed that cytometry can find many new applications.

References

Adan A., Alizada G., Kiraz Y., Baran Y., Nalbant A. 2017. Flow cytometry: Basic principles and applications. Critical Reviews in Biotechnology, 37(2), 163–176. https://doi.org/10.3109/07388551.2015.1128876

Almeida Santiago M., Paula Fonseca e Fonseca B., Silva Marques C.F., Silva E.D, Bertho A.L., Almeida Nogueira A.C. 2016. Flow cytometry as a tool for quality control of fluorescent conjugates used in immunoassays. PLOS ONE, 11(12), e0167669. https://doi.org/10.1371/journal.pone.0167669

Al-Mukhalafi Z., Pyle R., Al-Hussein K. 2001. Monitoring immune responses in organ recipients by flow cytometry. Saudi Journal of Kidney Diseases and Transplantation, 12(1), 32–41.

Álvarez-Barrientos A., Arroyo J., Cantón R., Nombela C., Sánchez-Pérez M. 2000. Applications of flow cytometry to clinical microbiology. Clinical Microbiology Reviews, 13(2), 167––195. https://doi.org/10.1128/cmr.13.2.167-195.2000

Amann R., Binder B.J., Olson R.J., Chisholm S.W., Devereux R., Stahl D.A. 1990. Combination of 16S rRNA-targeted oligonucleotide probes with flow cytometry for analysing mixed microbial populations. Applied and Environmental Microbiology, 56(6), 1919–1925. https://doi.org/10.1128/AEM.56.6.1919-1925.1990

Arrigucci R., Bushkin Y., Radford F., Lekehal K., Vir P., Pine R., Martin D., Sugarman J., Zhao Y., Yap G.S., Lardizabel A.A., Tyagi S., Gennaro M.L. 2017. FISH-Flow, a protocol for the concurrent detection of mRNA and protein in single cells using fluorescence in situ hybridization and flow cytometry. Nature Protocols, 12, 1245–1260. https://doi.org/10.1038/nprot.2017.039

Baran J. 2008. New time of flow cytometry – Applications of contemporary cytometers. Postępy Biologii Komórki, 35(24), 3–15.

Becton, Dickinson and Company 2002. Introduction to Flow Cytometry: A Learning Guide. BD Biosciences, San Jose, CA, USA.

Betters D.M. 2015. Use of flow cytometry in clinical practice. Journal of the Advanced Practitioner in Oncology, 6(5), 435–440. https://doi.org/10.6004/jadpro.2015.6.5.4

Bio-Rad 2021. Flow cytometry guides. https://info.bio-rad.com/Flow-Cytometry-Guides-LP.html [accessed: March 23, 2021].

Boyd A.R., Gunasekera T.S., Attfield P.V., Simic K., Vincent S.F., Veal D.A. 2003. A flow--fytometric method for determination of yeast viability and cell number in a brewery. FEMS Yeast Research, 3, 11–16. https://doi.org/10.1111/j.1567-1364. 2003.tb00133.x

Brown M., Wittwer C. 2000. Flow cytometry: Principles and clinical applications in hematology. Clinical Chemistry, 46,8(B), 1221–1229. https://doi.org/10.1093/clinchem/46.8.1221

Cabral-Marques O., Schimke L.F., de Oliveira E.B., El Khawanky N., Ramos R.N., Al-Ramadi B., Segundo G.R., Ochs H.D., Condino-Neto A. 2019. Flow cytometry contributions for

the diagnosis and immunopathological characterization of primary immunodeficiency diseases with immune dysregulation. Frontiers in Immunology, 10, 2742. https://doi.org/10.3389/fimmu.2019.02742

Chitarra L.G., van den Bulk R.W. 2003. The application of flow cytometry and fluorescent probe technology for detection and assessment of viability of plant pathogenic bacteria. European Journal of Plant Pathology, 109, 407–417. https://doi.org/10.1111/j.1364-3703.2011. 00711.x

Chow S., Patel H., Hedley D.W. 2001. Measurement of MAP kinase activation by flow cytometry using phospho-specific antibodies to MEK and ERK: Potential for pharmacodynamic monitoring of signal transduction inhibitors. Cytometry, 46, 72–78. https://doi.org/10.1002/cyto.1067

Cossarizza A. 2019. Guidelines for the use of flow cytometry and cell sorting in immunological studies. European Journal of Immunology, 49(10), 1457–1973. https://doi.org/10.1002/eji.201970107

Craig F.E., Foon K.A. 2008. Flow cytometric immunophenotyping for hematologic neoplasms. Blood, 111(8), 3941–3967. https://doi.org/10.1182/blood-2007-11-120535

Davey H.M, Guyot S. 2020. Estimation of microbial viability using flow cytometry. Current Protocols in Cytometry, 93(1), e72. https://doi.org/10.1002/cpcy.72

Davey H.M, Winson M.K. 2003. Using flow cytometry to quantify microbial heterogeneity. Current Issues in Molecular Biology, 5(1), 9–15. https://doi.org/10.21775/cimb.005.009

Davey H.M., Kell D.B. 1996. Flow cytometry and cell sorting of heterogeneous microbial populations: The importance of single-cell analyses. Microbiology Reviews, 60(4), 641–696.

Davies D., Allen P. 2007. DNA analysis by flow cytometry. [In:] Flow Cytometry: Principles And Applications. Ed. M.G. Macey. Humana Press Inc., Totowa, NJ, 165–180.

Divol B., Lonvaud-Funel A. 2005. Evidence for viable but nonculturable yeasts in botrytis--affected wine. Journal of Applied Microbiology, 99, 85–93. https://doi.org/10.1111/j.1365-2672.2005.02578

Errante P.R. 2015. Flow cytometry: A literature review. Periódicos da UFBA. https://doi.org/10.13140/RG.2.1.2461.0969

Fernández-Lago L., Vallejo F.J., Trujillano I., Vizcaíno N. 2000. Fluorescent whole-cell hybridization with 16S rRNA-targeted oligonucleotide probes to identify Brucella spp. by flow cytometry. Journal of Clinical Microbiology, 38(7), 2768–2771. https://doi.org/10.1128/JCM.38.7.2768-2771.2000

Fleisher T.A., Madkaikar M., Rosenzweig S.D. 2016. Application of flow cytometry in the evaluation of primary immunodeficiencies. Indian Journal of Pediatrics, 83(5), 444–449. https://doi.org/10.1007/s12098-015-2011-0

Flores-Gonzalez J., Cancino-Díaz J.C., Chavez-Galan L. 2020. Flow cytometry: From experimental design to its application in the diagnosis and monitoring of respiratory diseases. International Journal of Molecular Sciences, 21(22), 8830. https://doi.org/10.3390/ijms21228830

Frohling A., Schulter O. 2015. Flow cytometric evaluation of physico-chemical impact on Gram-positive and Gram-negative bacteria. Frontiers in Microbiology, 6, 939. https://doi.org/10.3389/fmicb.2015.00939

Goldeck D., Low I., Shadan N.B., Mustafah S., Pawelec G., Larbi A. 2013. Multi-parametric phospho-flow cytometry: A crucial tool for T lymphocyte signaling studies. Cytometry Part A, 83(3), 265–272. https://doi.org/10.1002/cyto.a.22252

Heiden T., Castaños-Vélez E., Andersson L., Biberfeld P. 2000. Combined analysis of DNA ploidy, proliferation, and apoptosis in paraffin-embedded cell material by flow cytometry. Laboratory Investigation, 80, 1207–1213. https://doi.org/10.1038/labinvest.3780128

Herrero M., Quiros C., Garcia A., Diaz M. 2006. Use of flow cytometry to follow the physiological states of microorganisms in cider fermentation processes. Applied and Environmental Microbiology, 72(10), 6725–6733. https://doi.org/10.1128/AEM.01183-06

Hunka J., Riley J.T., Debes G.F. 2020. Approaches to overcome flow cytometry limitations in the analysis of cells from veterinary relevant species. BMC Veterinary Research, 16(1), 83. https://doi.org/10.1186/s12917-020-02299-2

Hutchinson J.A. 2015. Flow cytometry in transplantation. Transplantation, 99(7), 1308–1309. https://doi.org/10.1097/TP.0000000000000818

Kanegane H., Hoshino A., Okano T., Yasumi T., Wada T., Takada H., Okada S., Yamashita M., Yeh T., Nishikomori R., Takagi M., Imai K., Ochs H.D., Morio T. 2018. Flow cytometry--based diagnosis of primary immunodeficiency diseases. Allergology International, 67(1), 43–54. https://doi.org/10.1016/j.alit.2017.06.003

Kim K.H., Sederstrom J.M. 2015. Assaying cell cycle status using flow cytometry. Current Protocols in Molecular Biology, 111, 28.6.1–28.6.11. https://doi.org/10.1002/0471142727.mb2806s111

Kinsinger N.M., Mayton H.M., Luth M.R., Walker S.L. 2017. Efficacy of post-harvest rinsing and bleach disinfection of E. coli O157:H7 on spinach leaf surfaces. Food Microbiology, 62, 212–220. https://doi.org/10.1016/j.fm.2016.10.019

Krutzik P.O., Nolan G.P. 2003. Intracellular phospho-protein staining techniques for flow cytometry: Monitoring single cell signaling events. Cytometry Part A, 55(2), 61–70. https://doi.org/10.1002/cyto.a.10072

Lapuente D., Maier C., Irrgang P., Hübner J., Peter A.S., Hoffmann M., Ensser A., Ziegler K., Winkler T.H., Birkholz T., Kremer A.E., Steininger P., Korn K., Neipel F., Überla K., Tenbusch M. 2020. Rapid response flow cytometric assay for the detection of antibody responses to SARS-CoV-2. European Journal of Clinical Microbiology & Infectious Diseases, 40, 751–759. https://doi.org/10.1007/s10096-020-04072-7

Longin C., Petitgonnet C., Guilloux-Benatier M., Rousseaux S., Alexandre H. 2017. Application of flow cytometry to wine microorganisms. Food Microbiology, 62, 221e231. https://doi.org/10.1016/j.fm.2016.10.023

Madkaikar M.R., Shabrish S., Kulkarni M., Aluri J., Dalvi A., Kelkar M., Gupta M. 2019. Application of flow cytometry in primary immunodeficiencies: Experience from India. Frontiers in Immunology, 10, 1248. https://doi.org/10.3389/fimmu.2019.01248

Maguire O., Tario J.D., Shanahan T.C., Wallace P.K., Minderman H. 2014. Flow cytometry and solid organ transplantation: A perfect match. Immunological Investigations, 43(8), 756–774. https://doi.org/10.3109/08820139.2014.910022

Malacrinò P., Zapparoli G., Torriani S., Dellaglio F. 2001. Rapid detection of viable yeasts and bacteria in wine by flow cytometry. Journal of Microbiological Methods, 45, 127–134. https://doi.org/10.1016/S0167-7012(01)00243-3

Marrone B.L. 2009. Flow cytometry: A multipurpose technology for a wide spectrum of global biosecurity applications. Journal of the Association for Laboratory Automation, 14(3), 148–156. https://doi.org/10.1016/j.jala.2009.03.001

Marsman C., Jorritsma T., Brinke T., van Ham M.S. 2020. Flow cytometric methods for the detection of intracellular signaling proteins and transcription factors reveal heterogeneity in differentiating human B cell subsets. Cells, 9(12), 2633. https://doi.org/10.3390/cells9122633

McCarthy D.A. 2007. Fluorochromes and fluorescence. [In:] Flow Cytometry: Principles and Applications. Ed. M.G. Macey. Humana Press Inc., Totowa, NJ, 59–110.

McKinnon K.M. 2018. Flow cytometry: An overview. Current Protocols in Immunology, 120, 5.1.1–5.1.11. https://doi.org/10.1002/cpim.40

Mortaz E., Gudarzi H., Tabarsi P., Adcock I.M., Masjedi M.R., Jamaati H.R., Garssen J., Akbar Velayati A., Redegeld F.A. 2015. Flow cytometry applications in the study of immunological lung disorders. Iran Journal of Allergy and Asthma and Immunology, 14(1), 12–18.

Nalbant A. 2018. Use of flow cytometry for detection of apoptotic cell death in Th17 cells. Proceedings, 2(25), 1560. https://doi.org/10.3390/proceedings2251560

Novak J., Basarova G., Teixeira J.A., Vincente A. 2007. Monitoring of brewing yeast propagation under aerobic and anaerobic conditions employing flow cytometry. Journal of The Institute of Brewing, 113(3), 249–255. https://doi.org/10.1002/j.2050-0416.2007.tb00284. x

Orfao A., Ortuño F., de Santiago M., Lopez A., San Miguel J. 2004. Immunophenotyping of acute leukemias and myelodysplastic syndromes. Cytometry Part A, 58(1), 62–71. https://doi.org/10.1002/cyto.a.10104

Ormerod M.G. 2008. Flow Cytometry – A Basic Introduction. https://flowbook.denovo-software.com/ [accessed: March 23, 2021].

Pietkiewicz S., Schmidt J.H., Lavrik I.N. 2015. Quantification of apoptosis and necroptosis at the single cell level by a combination of imaging flow cytometry with classical annexin V/propidium iodide staining. Journal of Immunological Methods, 423, 99–103. https://doi.org/10.1016/j.jim.2015.04.025

Pitsillides C.M., Runnels J.M., Spencer J.A., Zhi L., Wu M.X., Lin C.P. 2011. Cell labeling approaches for fluorescence-based in vivo flow cytometry. Cytometry Part A, 79(10), 758–765. https://doi.org/10.1002/cyto.a.21125

Porro D., Vai M., Vanoni M., Alberghina L., Hatziz C. 2009. Analysis and modeling of growing budding yeast populations at the single cell level. Cytometry Part A, 75(2), 114–120. https://doi.org/10.1002/cyto.a.20689

Pożarowski P., Darzynkiewicz Z. 2004. Analysis of cell cycle by flow cytometry. Methods in Molecular Biology, 281, 301–311. https://doi.org/10.1385/1-59259-811-0:301

Props R., Rubbens P., Besmer M., Buysschaert B., Sigrist J., Weilenmann H., Waegeman W., Boon N., Hammes F. 2018. Detection of microbial disturbances in a drinking water microbial community through continuous acquisition and advanced analysis of flow cytometry data. Water Research, 145, 73–82. https://doi.org/10.1016/j.watres.2018.08.013

Quiros C., Herrero M., Garcia A., Diaz M. 2007. Application of flow cytometry to segregated kinetic modeling based on the physiological states of microorganisms. Applied and Environmental Microbiology, 73(12), 3993–4000. https://doi.org/10.1128/AEM.00171-07

Quiros C., Herrero M., Garcia A., Diaz M. 2009. Quantitative approach to determining the contribution of viable-but-nonculturable subpopulations to malolactic fermentation processes. Applied and Environmental Microbiology, 75(9), 2977–2981. https://doi.org/10.1128/AEM.01707-08

Rawat A., Arora K., Shandilya J., Vignesh P., Suri D., Kaur G., Rikhi R., Joshi V., Das J., Mathew B., Singh S. 2019. Flow cytometry for diagnosis of primary immune deficiencies. A tertiary center experience from North India. Frontiers in Immunology, 10, 2111. https://doi.org/10.3389/fimmu.2019.02111

Riccardi C., Nicoletti I. 2006. Analysis of apoptosis by propidium iodide staining and flow cytometry. Nature Protocols, 1(3), 1458–1461. https://doi.org/10.1038/nprot.2006.238

Robertson J., McGoverin C., Vanholsbeeck F., Swift S. 2019. Optimisation of the protocol for the LIVE/DEAD BacLight bacterial viability kit for rapid determination of bacterial load. Frontiers in Microbiology, 10, 801. https://doi.org/10.3389/fmicb.2019.00801

Salma M., Rousseaux S., Sequeira-Le Grand A., Divol B., Alexandre H. 2013. Characterization of the viable but nonculturable (VBNC) state in Saccharomyces cerevisiae. PLOS ONE, 8(10), e77600. https://doi.org/10.1371/journal.pone.0077600

Sharma A., Lee S., Park Y.S. 2020. Molecular typing tools for identifying and characterizing lactic acid bacteria: A review. Food Science and Biotechnology, 29(10), 1301–1318. https://doi.org/10.1007/s10068-020-00802-x

Skotny A., Pucińska J. 2013. Modern flow cytometry. Acta Bio-Optica et Informatica Medica. Inżynieria Biomedyczna, 19(1), 3–11.

Soloski M., Chrest F. 2013. Disease mechanisms in rheumatology – tools and pathways: Multiparameter flow cytometry for discovery of disease mechanisms in rheumatic diseases. Arthritis & Rheumatism, 65(5), 1148–1156. https://doi.org/10.1002/art.37847

Soni N., Pai P., Kumar G., Prasad V., Dasgupta S., Bhadra B. 2020. Application of flow--virometry for large-scale screening of COVID 19 cases. Future Virology, 15(18), 525–532. https://doi.org/10.2217/fvl-2020-0141

Tait B.D. 2016. Detection of HLA antibodies in organ transplant recipients – Triumphs and challenges of the solid phase bead assay. Frontiers in Immunology, 7, 570. https://doi.org/10.3389/fimmu.2016.00570

Telford W.G., Komoriya A., Packard B.Z. 2002. Detection of localized caspase activity in early apoptotic cells by laser scanning cytometry. Cytometry, 47(2), 81–88. https://doi.org/10.1002/cyto.10052

Vembadi A., Menachery A., Qasaimeh M.A. 2019. Cell cytometry: Review and perspective on biotechnological advances. Frontiers in Bioengineering and Biotechnology, 7, 147. https://doi.org/10.3389/fbioe.2019.00147

Wang C., Esteve-Zarzoso B., Mas A. 2014. Monitoring of Saccharomyces cerevisiae, Hanseniaspora uvarum, and Starmerella bacillaris (synonym Candida zemplinina) populations during alcoholic fermentation by fluorescence in situ hybridization. International Journal of Food Microbiology, 191, 1–9. https://doi.org/10.1016/j.ijfoodmicro.2014.08.014

Wilkinson M. 2015. Flow cytometry in microbiology technology and applications. Caister Academic Press, Ireland. https://doi.org/10.21775/9781910190111

Wlodkowic D., Telford W., Skommer J., Darzynkiewicz Z. 2011. Apoptosis and beyond: Cytometry in studies of programmed cell death. Methods in Cell Biology, 103, 55–98. https://doi.org/10.1016/B978-0-12-385493-3.00004-8

Yabu J.M., Siebert J.C., Maecker H.T. 2016. Immune profiles to predict response to desensitization therapy in highly HLA sensitized kidney transplant candidates. PLOS ONE, 11(4), e0153355. https://doi.org/10.1371/journal.pone.0153355

XI GUT-ON-CHIP AS A POWERFUL NEW TOOL FOR ANALYSIS OF BIOACTIVE FOOD INGREDIENTS

Małgorzata PIERZCHALSKA

Department of Biotechnology and General Technology of Foods,
Faculty of Food Technology, University of Agriculture in Krakow,
Aleja Mickiewicza 21, 31-120 Krakow, Poland

malgorzata.pierzchalska@urk.edu.pl
ORCID: https://orcid.org/0000-0002-6830-5842

Abstract. Cell culture techniques have served as a powerful tool in food sciences for many decades. Our knowledge of food bioavailability, functionality and safety have been broadened significantly as the result of testing food or food specific ingredients in experiments employing human cell lines, of which enterocytes-like Caco-2 cells are the best example.

The field of intestinal cell culture was recently revolutionized by the development of intestinal organoid-type culture. Intestinal organoids are small spheres of a few hundred micrometers in diameter. The empty lumen of organoids is covered by the unicellular layer of epithelial cells. They originate from human and model animals' intestinal crypts or stem cells, creating in less than 10 days three-dimensional structures comprising the stem cells niche and all differentiated cells of intestinal epithelium. The next step was to create a miniaturized cell culture where epithelial cells are grown in microchannels and can be constantly perfused and subjected to periodical stretch emulating peristaltic movement of the gut.

Although various gut-on-chip models mimic accurately many functions of intestinal epithelium, their use requires skillful researchers, sophisticated equipment and is also costly. Nevertheless, gut-on-chip technology allows the fast, robust, and relatively quick testing of many food ingredients or food samples at the same

time. It creates a new perspective to study an influence of food on the intestinal cell biology and provides an automatic platform for assessing many aspects of cell physiology, such as proliferation, gene expression and metabolism.

Keywords: gut, cell culture, chip, food testing

1. Introduction

The *in vitro* modelling is a very important part of investigations in the field of food sciences. Food ingredients passing through gastrointestinal tract are not only fragmented, digested and absorbed but also come into close contact with cells comprising intestinal mucosa and with gut microbiota. These types of interactions are often responsible for both positive (cancer prevention, immunity boosting, etc.) and negative (toxicity, allergies, cancerogenesis) influence of food ingredients on human health. These interactions could be effectively studied in simplified *in vitro* models employing intestinal cell culture.

The cell culture methodology allows keeping cells and tissue alive after separation from a source organism. This powerful experimental tool, although widely used in food studies for decades, is incessantly refined. Its contribution to the development of our knowledge of active food ingredients could not be overestimated [Fois et al. 2019]. Nevertheless, due to the complexity of time and work-consuming procedures of the cell lines propagation and primary epithelial intestinal cells isolation, the cell culture techniques have not been broadly employed in routine food testing. This situation may change in the near future as a result of two recent technical breakthroughs: the introduction of human intestinal organoid culture systems [Sato and Clevers 2013] and the development of microfluidic organ-on-chip (i.e. OOC) methodology [Xiang et al. 2020].

2. Intestinal organoids

Routinely, most types of animal cells are cultured attached to the glass or plastic surfaces of the bottom of a culture dish where they spread and divide as long as they cover all accessible area forming a monolayer. This type of cell culture is called two-dimensional (2D) as the cells lack the ability to create multilayer structures characteristic for tissues of origin. As a consequence not all fea-

tures and functions of cells *in vivo* could be emulated in monolayers. This fact has led to the development of three-dimensional (3D) cell culture techniques where the tissue-like environment is introduced along with the thick layer of gel-forming substances (e.g. extracellular matrix proteins or other natural and synthetic hydrogels) serving as scaffolds of various mechanical properties on which the cells can grow, move and aggregate in the three- dimensional space [Kaur et al. 2021].

The development of 3D culture techniques has had special impact on the studies on primary intestinal cells – the most important cells in the context of investigations concerning food ingredients – intestinal mucosa interaction. In 3D culture conditions many noncancerous types of epithelial cells form conglomerates with fluid-filled lumens (spheres), called spheroids. It is also the case of Caco-2 cells which, although isolated from colon tumour, spontaneously change into enterocytes-like cells in prolonged, dense culture (Caco-2 cell line is the most popular type of cells in the field of food sciences). Most tumour cells, however, in such an environment, tend to form solid ball-shaped aggregates (i.e. micro-tumours) [Gunti et al. 2021].

The intestinal epithelium of vertebrates is a one-layer of cells covering both villi and crypts of Lieberkühn, with proliferation restricted to small area of crypts' bottom. The intestinal crypts form a niche for scarce stem cells and consist of progenitors of all types of cells present in intestinal epithelium. The brush border area contains millimetre-long protrusions, i.e. villi. In the villus base, the progenitors differentiate into absorptive enterocytes or other non-absorptive cell types (such as goblet and enteroendocrine cells, producing mucus and hormones). Differentiated cells migrate upwards to the villus tip, where they undergo apoptosis, and are constantly shed to the lumen. As a result, "new" epithelial cells replace the "old" ones with a speed incomparable to any other tissue of the body. The differentiation and migration cycle on the crypt-villus axis determines the proper function of the intestine as an organ of absorption, as an efficient barrier to the external world, and an immunological response modulator [Chin et al. 2018]. This unique organization is a reason why, to maintain the primary intestinal epithelial cell culture for a long time, it is not enough to provide cells with a proper mixture of chemical factors. It has been for many years a substantial challenge to obtain a normal two-dimensional culture of enterocytes. To keep such cultures alive and to preserve the stemness of some cells present in the initial preparation, one also needs to create the 3D environment with special biophysical properties. In other words, it is necessary to mimic the natural stem cell niche of intestinal crypts to keep proliferation and differentiation of enterocytes going.

A breakthrough came with the publication by Toshiro Sato et. al. [2009] who got an idea to embed isolated murine intestinal crypts in protein gel consisting of extracellular matrix proteins produced by Engelbreth-Holm-Swarm mouse sarcoma, composed of 60% laminin, 30% collagen IV, and 8% entactin (i.e. Matrigel™) – known to support spheroid cultures. When such cultures were fed with media containing special factors promoting stemness and sustaining proliferation in epithelium (i.e. R-spondin-1, Noggin, and Epidermal Growth Factor), spheroids were shortly formed and, after two or three days of growing, the ball-shaped aggregates transformed into structures containing both crypt-like protrusions and villus-like areas between them [Sato and Clevers 2013]. Such structures are called enteroids, and they can now be obtained from small and large intestines of human, rodent or farm animals, new-borns, or adults. Moreover, enteroids were also successfully cultured from murine [Mustata et al. 2013] and chicken [Pierzchalska et al. 2016] embryonic tissue and from human induced pluripotent stem cells [Finkbeiner et al. 2012]. In the last case, it is possible to create organoids consisting not only of epithelial, but also mesenchymal cells. Such organoids, called induced human intestinal organoids (iHIOs) [Finkbeiner and Spence 2013], resemble the most late embryonic intestinal tissue [Wells and Spence 2014]. Organoids were recently used as an *in vitro* model system in studies on intestinal regeneration, transformation, metabolism, and intestinal cells – pathogens or commensal microorganisms interactions [Finkbeiner et al. 2012; Zhang et al. 2014; Karve et al. 2017; Ranganathan et al. 2020]. Even though many new data were obtained with the use of intestinal organoids, the researchers point out at some disadvantages of the new method. The media, Matrigel and cell culture vessels are expensive. The procedure of organoid development is time-consuming and complex. It requires skilful researchers as some methods of routine cell analysis, like protein and mRNA expression studies, are more complicated than 2D cell cultures analysis due to difficulties in releasing organoids from the protein matrix (Fig. 1).

As a result of the polarization of enteroids (the inside-directed brush border face the lumen of the closed bulbs) the inside is not easily accessible for applying factors which physiologically stimulate intestinal epithelial cells from apical side (e.g. active food ingredients, drugs, gut bacteria or viruses).

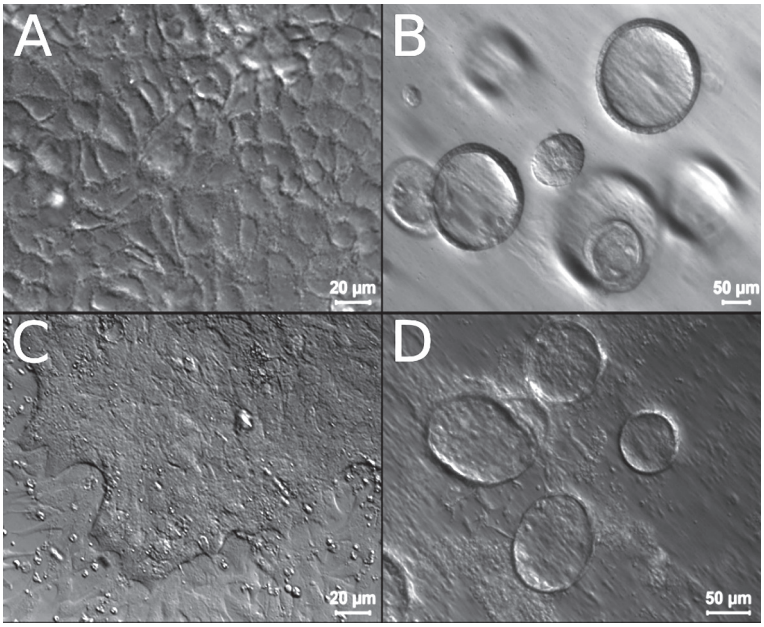

Fig. 1. Cell lines and primary cells derived from intestinal tissue or intestinal tumours are used in the *in vitro* modelling of intestinal epithelium. They can be cultured on solid substrate (A, C) or as spheroids/organoids in Matrigel matrix (B, D): Caco-2 human cell line derived from colon carcinoma differentiated *in vitro* into enterocyte-like cells (A, B); primary intestinal epithelial cells (IEC, derived from 19-days old chicken embryo; C, D) (source: own unpublished data)

3. Human gut-on-chip

Most types of cells respond to both chemical and mechanical signals by changing the expression of many genes but for some cells the importance of mechanical stimuli is more evident in comparison to others [Janmey and McCulloch 2007]. The endothelial cells and the cells in intestinal epithelium are subjected to pulsative fluid shear stress caused by the blood flow or the flow of gut contents, respectively. The cells of pulmonary origin are adapted to continuous stretching and relaxation accompanying breathing movements and gut mucosa cells are subjected to similar forces in the rhythm of peristaltic waves. The attachment to very stiff glass or plastic surfaces does not mimic the situation *in vivo*, and in consequence the two-dimensional cell culture does not emulate the crucial environmental factors encountered by cells in the tissue due to the lack of physiological mechani-

cal stimuli. The lack of the flow factor and the proper geometry of scaffolds are probably a reason why intestinal organoids do not develop proper mature villus compartment (the villus-like areas resemble more the organization of foetal villi). All these shortcomings of organoids system were the rationale for seeking more relevant cellular models better mimicking all aspects of intestinal physiology, i.e. tissue stiffness, geometry and biochemistry, assuming that all these factors are critical for emulation of biological processes [Steinway et al. 2020]. These needs can be fulfilled by microfabrication and microfluidic technologies. In microfluidic devices the net of carefully designed microchannels (tubes with micrometric diameter) are trapped into some solid material like glass or polymer. They are connected to external flow system (e.g. syringes or pumps) by input and output holes allowing to perform various laboratory protocols in microscale (lab-on-chip technology). In the case of cell-culture on chip some part of the channel is transformed into the micro cell culture surface of desired shape and properties.

3.1 Gut-on-chip in 2D

The typical chip used for an organ culture is a type of cell culture vessel which has a shape of a flat cuboid block about 40 mm long, 20 mm wide and a few mm high – so the two dimensions of the chip make it comparable to the glass bottom microscopic slide, although it is higher. Cells are grown on the much smaller area of small tubules' walls or in small round chambers created by microfabrication technology inside of a solid material from which the chip is made. In most cases, the organisation of the chips' space allows a direct observation of growing cells under the inverted microscope and their incubation in custom cell culture incubators. Frequently the docking to an external platform permits the continuous, easily programmed, and automatic exchange of cell culture media. Generally, polydimethylsiloxane (PDMS) – clear-transparent, gas-permeable, and flexible rubber – is used as a basic chip component. In some gut-on-chip platforms the cell culture chamber is divided by the porous membrane separating the space into two compartments – like in classical transwell systems where the apical part of the insert is separated from the well by polyethylene terephthalate (PET) or polycarbonate (PC) porous membrane with holes of 0.4 μm diameter. The simplest gut-on-chip models are generally 2D cultures of human Caco-2 cells but miniaturized and enriched with the factor of fluid flow (Figs 2A and 2B). The last can be realized by input valves being connected to cell culture medium reservoirs and external peristaltic pumps – (physiologically-relevant pump-driven flow systems, PDFS) or by putting the chip on gently rocking platform – (bidirectional

gravity-driven flow systems, BGDF) [Xiang et al. 2020]. It was recently shown by whole transcriptome analysis that there are substantial differences in gene transcription between Caco-2 cells cultured in static and fluidic conditions (from 29635 genes studied the expression of 5927 were substantially changed in cells kept on-chip with continuous flow of medium in both upper and lower chambers with the speed of 100 µl/h as compared to static culture) [Kulthong et al. 2021]. In some devices, like in organ-on-chip designed by Donald Ingber and co-workers from Harvard's Wyss Institute, the peristaltic movement of the gut is mimicked by adding two lateral vacuum chambers and the application of vacuum to the side chambers under computer control exert cyclic mechanical strain to the cells in monolayer [Hyun et al. 2012]. The same platform can be used for culture of the primary intestinal cells of human origin [Kasendra et al. 2018] (Fig. 2C).

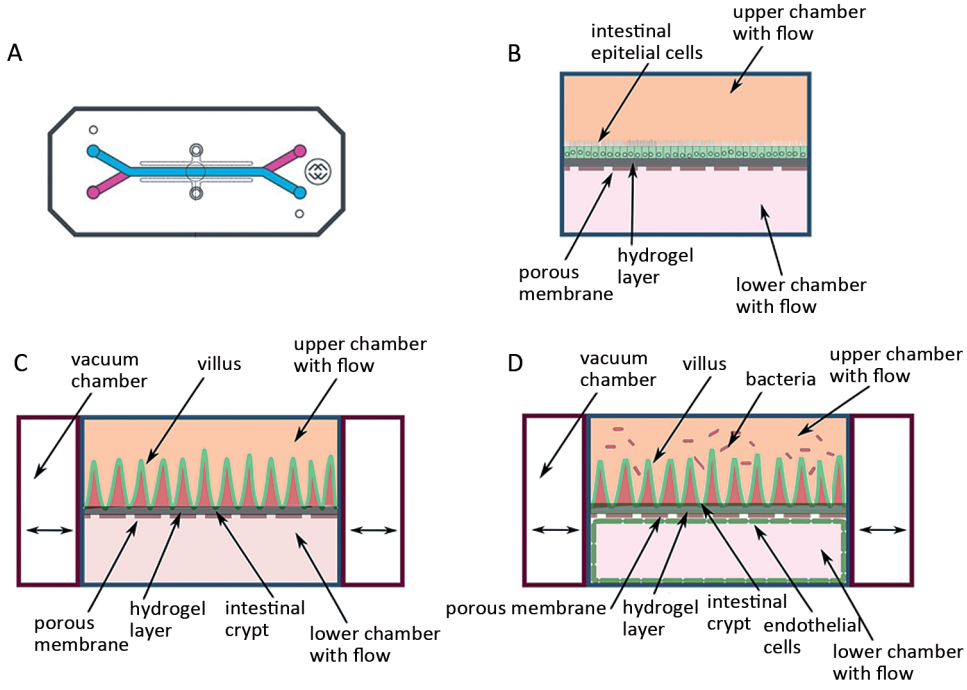

Fig. 2. Schematic representation of a gut chip, including its top view showing: the upper (blue) and lower (pink) cell culture microchannels as seen from above (A), the vertical section of typical 2D-gut-on-chip model (B), or 3D-gut-on-chip model with vacuum chambers allowing periodic mechanical stretching of the cells on chip (C), and microbiom-gut co-culture model on chip with endothelial cells cultured on lower chamber walls forming microvessel (D) (source: scheme in A part of the panel according to Kasendra et al. [2020], with own modification; schemes B, C, D – own elaboration)

3.2. Gut-on-chip in 3D

The construction of real "mini-guts" representing almost all functionalities of an intestine requires two important steps. First, epithelial cells should form an open tubule separating an empty lumen which can be perfused to get rid of dead epithelial cells. It can be done with the use of commercially available organ-on--chip platforms (e.g. OrganoPlate® from Mimetas) when the cells can be grown on the microchannels walls covered by extracellular matrix proteins [Naumovska et al. 2020]. Secondly, the separated crypts and villi regions should have a chance to be formed. This possibility can be created on chip platforms by various technological means. The presence of peristaltic stretch and strain motions causes a spontaneous restoration of villi-crypts axis when cells are seeded on porous membrane covered by ECM (mixture of type I collagen and Matrigel) [Kim et al. 2016], but in such case the tubules are not formed. This problem can be overcome by another microchip construction in which the main chamber of the chip is connected to two medium reservoirs, but it is also filled with hydrogel (collagen I and Matrigel mixture). In this scaffold a microchannel with 150 μm diameter is laser-light ablated with microdissection method. This channel contains microcavities (170 μm high and 70-50 μm wide) that mimic the geometry of the native crypts in the small intestine. When intestinal stem cells were introduced into such a device, a structure with the stem proliferating cells located in the "crypts" and the other differentiated cells of intestinal epithelium inhabiting other parts of the channel, is spontaneously formed. The culture established in this way has a potential of self-renewal and can be kept alive for many weeks [Nikolaev et al. 2020].

4. Gut-on-chip in food analysis

Nowadays, there is the growing interest in the human OOC coming from the pharmacological industry which perceives this new technology as a promising tool in drug testing procedures and personalized medicine strategies. It is generally believed that these methods are going to bridge the gap between animal and human studies, saving a profound number of human lives and the huge amount of money, currently lost in unsuccessful clinical trials. But the food industry is also planning to use gut-on-chips for food testing and safety analysis and many such experimental approaches have been already undertaken successfully.

One of the first attempts to employ microchip technology to food analysis was the Swiss *Nutrichip* project aimed at the development of a standardized method for assessing the immunomodulatory properties of food ingredients. In the one published study Caco-2 and THP-1 (monocytes) human cell lines co-culture on a chip was used to assess the immunomodulatory properties of milk [Vergères et al. 2012; Ramadan et al. 2013].

Another problem studied recently with the gut-on-chip model is the probiotic bacteria – intestinal mucosa interaction (Fig. 2D). To study this complicated issue, one must create the conditions emulating closely the *in vivo* gut environment encountered by physiological or pathological microflora – an anaerobic condition and flow of fluid. These factors are generally missing in the traditional transwell systems. Such environment was created in so called HuMiX model consisted of long spiral-shaped chambers (a microbial chamber separated by the mucin-covered nanoporous membrane from an epithelial cell chamber which is subsequently separated by microporous membrane from a perfusion chamber) with controlled fluid flow, oxygen level and automatic measurement of transepithelial resistance (TEER) of epithelial layer (Fig. 3B). The optimized protocol for the co-culture of human epithelial cells with gastrointestinal microbes with the use of this device was also developed and tested in the studies on transcriptional and metabolic changes induced in human cells following their co-culture with *Lactobacillus rhamnosus* GG or *Bacteroides caccae* or the mixture of both [Shah et al. 2016]. In the more complicated system a mitigating role of *Lactobacillus rhamnosus* presence on the inflammation caused by an opportunistic strain of *Candida albicans* was investigated by another group that used a multilayer chip inhabited by differentiated intestinal epithelial cells (Caco-2 cells), endothelial cells (Huvec) and human peripheral blood mononuclear cells (PBMC) differentiated *in vitro* into primary macrophages [Maurer et al. 2019]. In another system of glass micro-chip the mixture of 17 dioxin congeners (7 polychlorinated dibenzo-p-dioxins and 10 polychlorinated dibenzofurans) were applied to Caco-2 cell monolayers and during 24 hours the absorption of these toxic, food-born compounds were assessed by gas chromatography – high resolution mass spectrometry [Kulthong et al. 2021].

There are also some studies on interaction between food ingredients and gut biology in which primary gut epithelial cells on chip are used. It was shown that both epithelial cells derived from human small intestine and from colon can be successfully cultured on chips along with endothelial and immune cells of the intestinal mucosa [Kasendra et al. 2018; Kasendra et al. 2020]. To establish colon-on-chip culture, colonic organoids obtained from biopsies taken from various area of patients' colon were formed in Matrigel™ and cultured for one week, then organoids were dissociated into fragments and seeded on S-1 commercially

available chips (Emulate Inc., Boston, MA, USA). With the use of this type of gut model it was proven that some human milk oligosaccharides obtained in the process of milk fermentation by adult gut microbiota can beneficially modulate gut barrier function and enhance immunity [Šuligoj et al. 2020].

It is now possible to buy commercially available platforms allowing to create gut-on-chip models, well-suited to specific research goals, from several suppliers located in USA and EU (e.g. Zoë® from Emulate Inc, USA; Humimic™ from TissUse GmbH, Germany; inCHIPit™ from Biond Solution B.V, Netherlands). These state-of-art systems, however, are relatively expensive and need very special equipment (pumps, incubators, software etc.) dedicated to them and produced by the same company. The alternative approach was recently presented by Winkler et al. [2020] who described the organ-on-chip based on double-sided medical-grade adhesive tapes. The gut-on-tape was characterized and tested in experiments evaluating the influence of a common food compounds (chili pepper-derived capsaicinoids) on epithelial barrier created by Caco-2 cells. As the authors have suggested, in their analysis, the price of one organ-on-chip in the form of tape can be as low as 0.5 €. In contrast to that, the price of PDMS chip is estimated at 100 € per organ [Winkler et al. 2020].

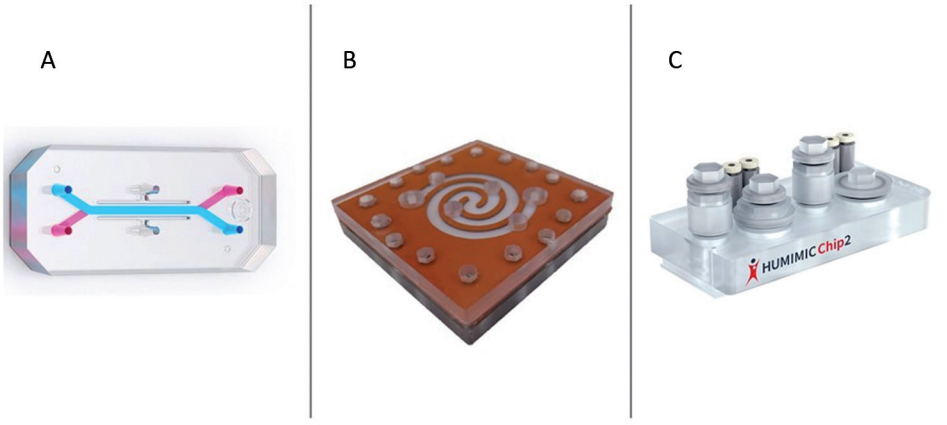

Fig. 3. Macroscopic view of various organ-on-chip devices used for mini-gut models formation:
Chip-S1, Emulatebio, Inc, https://emulatebio.com/products-services/ [accessed: September 1, 2022] (A),
HuMix, https://www.fnr.lu/university-luxembourg-announces-breakthrough-humix-model--nature-communications/ [accessed: September 1, 2022] (B),
Humimic Chip2, **TissUse GmbH,** https://www.tissuse.com/en/humimic/chips/humimic-chip2/ [accessed: September 1, 2022] (C)

5. Conclusion

The OOC is a relatively new but dynamically developing technology. This type of cell culture is charachterized by many important features, like miniaturization, the better emulation of *in vivo* environment, robustness and repeatability. It is particularly suitable for culturing cells originated from gut due to special requirements of these cells that are difficult to fulfill when using traditional methods.

It is very likely that the efforts undertaken in many research laboratories to standardize the gut-on-chip models and to develop some robust and cheap platforms will popularize the use of the gut-on-chip technology in food testing in the near future.

References

Chin A.M., Hill D.R., Aurora M., Spence J.R. 2018. Morphogenesis and maturation of the embryonic and postnatal intestine. Seminar in Cell and Developemental Biology, 66, 81–93. https://doi.org/10.1016/j.semcdb.2017.01.011.Morphogenesis

Finkbeiner S.R., Spence J.R. 2013. A gutsy task: Generating intestinal tissue from human pluripotent stem cells. Digestive Diseases Sciences, 58(5), 1176–1184. https://doi.org/10.1007/s10620-013-2620-2

Finkbeiner S.R., Zeng X.L., Utama B., Atmar R.L., Shroyer N.F., Estesa M.K. 2012. Stem cell--derived human intestinal organoids as an infection model for rotaviruses. mBio, 3(4), 1–6. https://doi.org/10.1128/mBio.00159-12

Fois C.A.M., Le T.Y.L., Schindeler A., Naficy S., McClure D.D., Read M.N., Valtchev P., Khademhosseini A., Dehghani F. 2019. Models of the gut for analyzing the impact of food and drugs. Advanced Healthcare Materials, 8(21), 1–23. https://doi.org/10.1002/adhm.201900968

Gunti S., Hoke A.T.K., Vu K.P., London N.R.. 2021. Organoid and spheroid tumor models: Techniques and applications. Cancers, 13(4), 1–18. https://doi.org/10.3390/cancers13040874

Hyun B., Kim J., Huh D., Hamilton G., Ingber D.E. 2012. Human gut-on-a-chip inhabited by microbial flora that experiences intestinal peristalsis-like motions and flow. Lab on a Chip, 12, 2165–2174. https://doi.org/10.1039/c2lc40074j

Janmey P.A., McCulloch C.A. 2007. Cell mechanics: Integrating cell responses to mechanical stimuli. Annual Review of Biomedical Engineering, 9, 1–34. https://doi.org/10.1146/annurev.bioeng.9.060906.151927

Karve S.S., Pradhan S., Ward D.V, Weiss A.A. 2017. Intestinal organoids model human responses to infection by commensal and Shiga toxin producing Escherichia coli. PLOS One, 12(6), e017896. https://doi.org/10.1371/journal.pone.0178966

Kasendra M., Luc R., Yin J., Manatakis D.V, Kulkarni G., Lucchesi C., Sliz J., Apostolou A., Sunuwar L., Obrigewitch J., Jang K.J., Hamilton G.A., Donowitz M., Karalis K. 2020. Duodenum Intestine-Chip for preclinical drug assessment in a human relevant model. eLife, 450, 1–23. https://doi.org/10.7554/eLife.50135

Kasendra M., Tovaglieri A., Sontheimer-Phelps A., Jalili-Firoozinezhad S., Bein A., Chalkiadaki A., Scholl W., Zhang C., Rickner H., Richmond C.A., Li H., Breault D.T., Ingber D.E. 2018. Development of a primary human Small Intestine-on-a-Chip using biopsy-derived organoids. Scientific Reports, 8(1), 1–14. https://doi.org/10.1038/s41598-018-21201-7

Kaur S., Kaur I., Rawal P., Tripathi D.M., Vasudevan A. 2021. Non-matrigel scaffolds for organoid cultures. Cancer Letters, 504, 58–66. https://doi.org/10.1016/j.canlet.2021.01.025

Kim H.J., Li H., Collins J.J., Ingber D.E. 2016. Contributions of microbiome and mechanical deformation to intestinal bacterial overgrowth and inflammation in a human gut-on-a--chip. Proceedings of the National Academy of Sciences of the United States of America, 113(1), E7–E15. https://doi.org/10.1073/pnas.1522193112

Kulthong K., Hooiveld G.J.E.J., Duivenvoorde L., Miro Estruch I., Marin V., van der Zande M., Bouwmeester H. 2021. Transcriptome comparisons of in vitro intestinal epithelia grown under static and microfluidic gut-on-chip conditions with in vivo human epithelia. Scientific Reports, 11(1), 1–13. https://doi.org/10.1038/s41598-021-82853-6

Maurer M., Gresnigt M.S., Last A., Wollny T., Berlinghof F., Pospich R., Cseresnyes Z., Medyukhina A., Graf K., Gröger M., Raasch M., Siwczak F., Nietzsche S., Jacobsen I.D., Figge M.T., Hube B., Huber O., Mosig A.S. 2019. A three-dimensional immunocompetent intestine-on-chip model as in vitro platform for functional and microbial interaction studies. Biomaterials, 220, 119396. https://doi.org/10.1016/j.biomaterials.2019.119396

Mustata R.C., Vasile G., Fernandez-Vallone V., Strollo S., Lefort A., Libert F., Monteyne D., Pérez-Morga D., Vassart G., Garcia M.I. 2013. Identification of Lgr5-Independent spheroid-generating progenitors of the nouse fetal intestinal epithelium. Cell Reports, 5(2), 421–432. https://doi.org/10.1016/j.celrep.2013.09.005

Naumovska E., Aalderink G., Valencia C.W., Kosim K., Nicolas A., Brown S., Vulto P., Erdmann K.S., Kurek D. 2020. Direct on-chip differentiation of intestinal tubules from induced pluripotent stem cells. International Journal of Molecular Sciences, 21(14), 4964. https://doi.org/10.3390/ijms21144964

Nikolaev M., Mitrofanova O., Broguiere N., Geraldo S., Dutta D., Tabata Y., Elci B., Brandenberg N., Kolotuev I., Gjorevski N., Clevers H., Lutolf M.P. 2020. Homeostatic mini-intestines through scaffold-guided organoid morphogenesis. Nature, 585(7826), 574–578. https://doi.org/10.1038/s41586-020-2724-8

Pierzchalska M., Panek M., Czyrnek M., Grabacka M. 2016. The three-dimensional culture of epithelial organoids derived from embryonic chicken intestine. Methods in Molecular Biology, 1576, 135–144. https://doi.org/10.1007/7651_2016_15

Ramadan Q., Jafarpoorchekab H., Huang C., Silacci P., Carrara S., Koklü G., Ghaye J., Ramsden J., Ruffert C., Vergeres G., Gijs M.A.M. 2013. NutriChip: Nutrition analysis meets microfluidics. Lab on a Chip, 13(2), 196–203. https://doi.org/10.1039/c2lc40845g

Ranganathan S., Smith E.M., Foulke-Abel J.D., Barry E.M. 2020. Research in a time of enteroids and organoids: How the human gut model has transformed the study of enteric bacterial pathogens. Gut Microbes, 12(1), 1795389. https://doi.org/10.1080/19490976.2020.1795389

Sato T., Clevers H. 2013. Growing self-organizing mini-guts from a single intestinal stem cell: Mechanism and applications. Science, 340(6137), 1190–1194. https://doi.org/10.1126/science.1234852

Sato T., Vries R.G., Snippert H.J., Van De Wetering M., Barker N., Stange D.E., Van Es J.H., Abo A., Kujala P., Peters P.J., Clevers H. 2009. Single Lgr5 stem cells build crypt-villus structures in vitro without a mesenchymal niche. Nature, 459(7244), 262–265. https://doi.org/10.1038/nature07935

Shah P., Fritz J.V., Glaab E., Desai M.S., Greenhalgh K., Frachet A., Niegowska M., Estes M., Jäger C., Seguin-Devaux C., Zenhausern F., Wilmes P. 2016. A microfluidics-based in vitro model of the gastrointestinal human-microbe interface. Nature Communications, 7, 11535. https://doi.org/10.1038/ncomms11535

Steinway S.N., Saleh J., Koo B.K., Delacour D., Kim D.H. 2020. Human Microphysiological models of intestinal tissue and gut microbiome. Frontiers in Bioengineering and Biotechnology, 8, 725. https://doi.org/10.3389/fbioe.2020.00725

Šuligoj T., Vigsnæs L.K., Van den Abbeele P., Apostolou A., Karalis K., Savva G.M., Mcconnell B., Juge N. 2020. Effects of human milk oligosaccharides on the adult gut microbiota and barrier function. Nutrien, 12(9), 2808. https://doi.org/10.3390/nu12092808

Vergères G., Bogicevic B., Buri C., Carrara S., Chollet M., Corbino-Giunta L., Egger L., Gille D., Kopf-Bolanz K., Laederach K., Portmann R., Ramadan Q., Ramsden J., Schwander F., Silacci P., Walther B., Gijs M. 2012. The NutriChip project-translating technology into nutritional knowledge. British Journal of Nutrition, 108(5), 762–768. https://doi.org/10.1017/S0007114512002693

Wells J.M., Spence J.R. 2014. How to make an intestine. Development (Cambridge), 141(4), 752–760. https://doi.org/10.1242/dev.097386

Winkler T.E., Feil M., Stronkman E.F.G.J., Matthiesen I., Herland A. 2020. Low-cost microphysiological systems: Feasibility study of a tape-based barrier-on-chip for small intestine modeling. Lab on a Chip, 20(7), 1212–1226. https://doi.org/10.1039/d0lc00009d

Xiang Y., Wen H., Yu Y., Li M., Fu X., Huang S. 2020. Gut-on-chip: Recreating human intestine in vitro. Journal of Tissue Engineering, 11, 2041731420965318. https://doi.org/10.1177/2041731420965318

Zhang Y.G., Wu S., Xia Y., Sun J. 2014. Salmonella-infected crypt-derived intestinal organoid culture system for host-bacterial interactions. Physiological Reports, 2(9), e12147. https://doi.org/10.14814/phy2.12147

XII MODERN METHODS OF RAPID IDENTIFICATION OF PATHOGENS IN FOOD

Iwona DROŻDŻ

Department of Fermentation Technology and Microbiology,
Faculty of Food Technology, University of Agriculture in Krakow,
Aleja Mickiewicza 21, 31-120 Krakow, Poland

iwona.drozdz@urk.edu.pl
ORCID: https://orcid.org/0000-0003-2359-3155

Abstract. Food of various origins can be a reservoir of numerous pathogens. Therefore, it is important to diagnose those microorganisms quickly. Until now, identification has been based on breeding methods which are laborious and time-consuming. However, they cannot be completely abandoned as they may yield preliminary results. Modern methods of identifying pathogens use molecular biology techniques, including genotyping, which is based on PCR, hybridization and sequencing. In addition, phagotyping and spectrophotometric methods are used. Molecular techniques are fast and precise. However, due to the consistently high prices of equipment, reagents and the need for experience of personnel, it takes time to make them available to a greater extent in food industry plants.

Keywords: genotyping, phagotyping, spectrophotometric methods, pathogens in food

1. Introduction

Food and drink, as sources of many organic compounds and nutrients, provide a good medium for the development of microorganisms, including pathogens. Pathogenic microorganisms can cause food poisoning which is dangerous to the health and life of consumers. The factors that cause poisoning are microorganisms or their toxins, as well as viruses. Annual reports of the WHO indicates 600 milion cases of foodborne diseases and 420 000 deaths [Wojtatowicz 2009; WHO 2015]. Therefore, the priority is to ensure the microbiological safety of food, which is also regulated by law.

Controlling the microbiological quality of food is a very important part of its processing. There are many tools that allow such control. These include the HACCP system (Hazard Analysis and Critical Control Point), based on the effective control of critical points of a given production process determined on the basis of a hazard analysis [Kołożyn-Krajewska 2013]. Procedures for the Hazard Analysis and Critical Control Points (HACCP) system and guidelines for their application are also provided in the Codex Alimentarius. This document standardizes quality control procedures, guidelines, standards and other recommendations for food hygiene at the international level. Such procedures should be implemented in each country.

Health safety of food and beverages, in terms of microbiological quality, is defined as the absence of pathogens and their toxins in a given amount of food product [Kołożyn-Krajewska 1995]. The quality and quantity of microorganisms in food and beverages results from the observance of hygiene at every stage of production, from the raw material and the thermal treatments used. Treatments allowing to minimize the number of microorganisms may sometimes be insufficient or insufficient, which increases the number of microorganisms in food, including pathogens. The food product becomes a source of pathogens, enters our body, and then the gastrointestinal tract, mucous membranes and the lymphatic system of the throat become the gate of infection. Quality control and rapid identification of pathogens are therefore essential to reduce food poisoning.

Initially, the methods used to identify microorganisms (pathogens) were based on culture studies, macroscopic and microscopic analysis, as well as biochemical and physiological properties. Such studies were labor-intensive and time-consuming [Hać-Szymańczuk 2012]. Over time, it was possible to miniaturize biochemical and biophysical tests, which shortened the time of analyzes and gave faster results. Identification kits in the form of plates were created and the systems enabling computer analysis of results were automated. Finally, with

the advancement of molecular biology, there has been another breakthrough in microbiological diagnostics. Molecular analyzes are used to quickly and directly detect pathogens in clinical samples and food. According to EU standards, depending on the food or drink, various pathogens are analyzed in them, e.g. *Listeria monocytogenes*, pathogenic strains of *Escherichia coli, Salmonella* sp., *Enterobacter sakazaki* or enterotoxins *Staphylococcus aureus* and others. Molecular biology techniques allow for the rapid identification of pathogens and allow the detection of microorganisms that are difficult to cultivate on plates. Molecular biology-based tests for the detection of pathogens should be sensitive to obtain reliable results, easy to perform, should allow the identification of the genus, species and strain of the pathogen, and allow the determination of phylogenetic relatedness [Palka 2007; Walczak et al. 2009]. The demand for rapid diagnostic tests based on molecular methods is very high. Thanks to them, especially in highly developed countries, pathogens can be detected quickly and easily [Słomski 2008; Buchowicz 2009; Kondak 2009].

2. Techniques of molecular biology – genotyping

Molecular biology methods are based on the determination and analysis of nucleic acid sequences. Each organism has a specific nucleotide sequence that can be compared to a known pattern and identifies the organism and/or the degree of phylogenetic relatedness. In the diagnosis of pathogens, the sequences coding the ribosomal RNA of both ribosome subunits or the rRNA itself, e.g. 16S rRNA, 16-23S rRNA is most often analyzed. The molecular techniques that enable such analysis are based on the amplification of DNA by the polymerase chain reaction (PCR) method. Based on the amplification, restriction analysis is also used [Pizzigella et al. 1993]. In addition, hybridization techniques with DNA probes [Palka 2007; Olejnik-Schmidt et al. 2009], as well as sequencing are used. Microorganisms can also be identified by resistance-coding genes or bacterial plasmids [Kondak 2009; Hać-Szymańczuk 2012; Szemraj and Szemraj 2013].

The information obtained on the identified microorganism depends on the selection of the molecular method used in microbiological diagnostics. This information concerns the classification of microorganisms in terms of taxonomy, i.e. belonging to a specific family, genus, species and, above all, strain [Olejnik-Schmidt et al. 2009].

2.1. Polymerase chain reaction and its modifications

In the PCR method (polymerase chain reaction), a DNA fragment is used for amplification, most often with a size of 0.2 to 40 Kb. Ideal amplicon length/size depends on many variables and design preferences. For standard PCR scientists generally design amplicons to be between 200–1000 bp. For quantitative PCR, standard amplicons range from 75–150 bp. PCR is a cyclic reaction (approx. 30 cycles). After each cycle, the number of copies of the amplified DNA fragment doubles and increases exponentially after amplification. Amplification consists of several steps: denaturation, binding of primers and synthesis of DNA strands by a thermostable polymerase [Słomski 2008; Harwood and Wipat 2011]. PCR amplification uses template DNA (e.g. genomic DNA), a DNA thermostable polymerase, set of appropriate primers for the desired target gene or DNA segment to be amplified, deoxynucleotides (dNTPs: dATP, dCTP, dGTP, dTTP), for the specific DNA polymerase, and Mg^{2+} ions. The specificity of the PCR reaction is ensured by primers, which are single-stranded DNA fragments of about 20 nucleotides in length. The primers attach to a specific fragment of DNA by hybridization. The condition for the exact matching of primers is the appropriate process temperature. The amplification process begins with the denaturation of the double-stranded template DNA at about 95°C for 45–60 seconds. After the temperature is lowered, the hybridization reaction of the single-stranded DNA templates with the oligonucleotide primers begins. The temperature required for this reaction depends on the length and the G + C base content of the primers and is about 50–60 C. The reaction takes 30 to 120 seconds. The last stage is elongation, i.e. the synthesis of a DNA strand complementary to the template. This process takes place at a temperature of about 72°C and is catalyzed by the thermostable DNA polymerase from the 3 'end on both templates. This stage takes 30-180 seconds. Increasing the temperature to 95°C restarts the entire PCR cycle. The *in vitro* amplification process is possible thanks to thermocyclers, which allow for a rapid temperature change. After the reaction is complete, the number of copies of the DNA fragments produced is very high, depends on the amount of starting DNA and the efficiency of the reaction. The amplification products are identified by e.g. ethidium bromide or fluorescent dyes, which binds to the DNA molecule and is excited by UV after an agarose gel electrophoresis process. It is also possible to measure the fluorescence of the resulting complex of DNA with a fluorescent dye [Słomski 2008; Kondak 2009; Harwood and Wipat 2011].

The development of molecular biology techniques made it possible to modify the traditional PCR procedure depending on the needs of microbiological di-

agnostics [Kadri 2019]. In the last few years, many methods of identifying microorganisms based on the polymerase chain reaction have been developed that improve the efficiency and specificity of the reaction. Such methods include multiplex PCR, nested PCR, RT-PCR, touchdown PCR, Hot Start PCR, PCR-DGGE, PCR-PFGE, PCR-RFLP, PCR-RAPD, Real-time PCR and others.

The multiplex PCR process uses sets of specific primers, thanks to which it is possible to amplify many DNA fragments during the same reaction. The resulting DNA fragments of different lengths are separated using gel electrophoresis. Multiplex PCR is often used to detect the presence of harmful microbes in food, and is also used in laboratories carrying out routine microbiological diagnostics [Kondak 2009; Walczak et al. 2009; Szemraj and Szemraj 2013].

Two pairs of primers with different species specificities are used in nested PCR. It is intended to reduce non-specific binding in products due to the amplification of unexpected primer binding sites. In a first step, spanning 15–20 cycles, the primary amplification of the desired DNA stretch takes place with a first pair of low specificity primers. The second step uses a pair of high specificity primers, and the template is the DNA produced in the first step of the reaction [Walczak et al. 2009; Szemraj and Szemraj 2013]. This technique is used to detect and identify microorganisms and viruses [Binduga-Gajewska et al. 1999; Chołuj and Przewodowski 2014], but also in human genetics and forensics.

Touchdown PCR (Multiple Touchdown PCR) is a method that uses a very high initial annealing temperature of primers to complementary sequences, which is lowered in subsequent cycles. In this method, primers do not amplify non-specific sequences. Lowering the temperature increases the specificity of the PCR reaction [Green and Sambrook 2018; Walczak et al. 2009]. The technique allows for quick and specific results in the identification of microorganisms and in clinical samples [Lai 2017].

A typical reaction will start with a one minute denaturation at 94°C. Any longer than 3 minutes may inactivate the DNA polymerase, destroying its enzymatic activity. One method, known as hot-start PCR, drastically extends the initial denaturation time from 3 minutes up to 9 minutes. With hot-start PCR, the DNA polymerase is added after the initial exaggerated denaturation step is finished. This protocol modification avoids likely inactivation of the DNA polymerase enzyme [Walczak et al. 2009].

RT-PCR (reverse transcriptase PCR) is a PCR reaction with reverse transcriptase in which is able to the synthesis of cDNA fragments resulting from the transcription of mRNA information into cDNA during the process of reverse transcription. This reaction is catalyzed by reverse transcriptase. In microbiological diagnostics, this method is used to detect pathogens whose genetic material is

RNA, but also allows the discrimination of live and dead microorganisms [Kondak 2009; Szemraj and Szemraj 2013].

PCR-DGGE (denaturing gradient gel electrophoresis) is a method that enables the detection of differences between DNA fragments of the same size but with different sequences. DNA fragments are separated during a gel gradient in denaturing conditions. Double-stranded DNA under the influence of denaturing agents (urea or formamide) melts in regions called melting domains, which vary for specific sequences (specific melting point). Therefore, DNA fragments of the same length and different sequences can be separated in the gel during electrophoresis. As a result of electrophoretic separation, a specific bacterial "DNA imprint" is obtained, i.e. a characteristic pattern of bands – a DNA pattern for each analyzed sample, which corresponds to a specific microorganism in the sample [Ercolini 2004]. The PCR-DGGE method can be used to identify microorganisms in environmental, medical and food microbiology, for screening tests, in forensics [Ziembińska-Buczyńska and Kraśnicki 2016; Łyszcz and Gałązka 2017].

PCR-PFGE (Pulsed-Field Gel Electrophoresis) is electrophoresis in a pulsed electric field. This method is used for the analysis of large segments of DNA fragments from 30–2000 Kb. The technique is based on the use of short electrical pulses oriented in a direction different than the corresponding migration of nucleic acid fragments, and the fragment separation is based on the time when a single DNA molecule changes direction again in the electric field and can last more than 24 hours. PFGE is used to differentiate species such as *Listeria monocytogenes* and *Listeria innocua*, and to distinguish between strains of one microbial species [Olejnik-Schmidt et al. 2009; Harwood and Wipat 2011].

PCR-RFLP (Restriction Fragments Length Polymorphism) consists in digesting genomic DNA, isolated from the tested strain and amplified during PCR reaction, with specific restriction enzymes. The resulting restriction fragments of different lengths are separated by agarose gel electrophoresis. For each microorganism, a characteristic pattern of bands (pattern) is obtained, i.e. DNA fragments of different molecular weight. This imprint is compared with the restriction pattern of the genomic DNA of other microbial strains. RFLP is used for the classification of microbial strains, in the diagnosis of microbiology and genetic diseases [Palka 2007; Włodarczyk 2007; Olejnik-Schmidt et al. 2009].

PCR-RAPD is a method of randomly amplifying polymorphic DNA fragments. This method uses a single, 5-15 nucleotide long oligonucleotide primer that anneals at multiple sites on both DNA strands. As a result, many DNA amplification products are produced. With the help of RAPD, it is possible to diagnose and differentiate many organisms, as well as to determine phylogenetic relationships between them [Robak et al. 2005].

Real-Time PCR, or real-time polymerase chain reaction, is a technique that allows to determine the number of copies of a replicated nucleic acid fragment in a sample. It combines the classic PCR reaction and the detection of the obtained product thanks to the use of dyes or fluorescent probes. The concentration of the PCR product is monitored by measuring the fluorescence, which increases in proportion to the amount of DNA during the PCR reaction. The dyes used in Real-Time PCR are dyes that bind either non-specifically or specifically to a DNA molecule. SYBR Green I is a dye that binds unspecifically to double-stranded DNA. Fluorescent probes labeled with fluorescent dyes are also used, which bind complementarily to the nucleic acid sequence tested, therefore they hybridize with internal sequences of the amplified fragment (e.g. Molecular Beacons probe with a hairpin structure, which contains a reporter dye at the 3' and 5' ends and quencher molecule or the TaqMan probe) [Słomski 2008; Kondak 2009; Olszewska 2013]. Quantitative analysis of the product, using the phenomenon of dye fluorescence or hybridization with a probe labeled with a fluorescent dye, gives a graph showing the increase in the fluorescence signal depending on the increase in the amount of the product in the subsequent PCR cycles. The Real-Time PCR method is a faster and more sensitive method than classic PCR, it enables qualitative and quantitative analysis, therefore it is used in medical diagnostics and food analysis [Słomski 2008; Szemraj and Szemraj 2013], for example: *Salmonella* detection meat samples [Delibato et al. 2011], *Listeria monocytogenes* in foods [Junge et al. 2012] or *E. coli* O157:H7, *L. monocytogenes/ivanovii, S. enterica*, *V. parahaemolyticus*, β*Streptococcus hemolyticus*, *Yersinia enterocolitica*, *E. faecalis*, *Shigella* spp., *Proteus mirabilis*, *Vibrio fluvialis*, *S. aureus* and *Campylobacter jejuni* in food and drinking water [Liu et al. 2019].

2.2. Hybridization techniques

Hybridization is one of the most important methods used in molecular microbiological diagnostics. Nucleic acid hybridization consists in joining together nucleotides according to the principle of complementarity. In the case of DNA, it is necessary to denature the nucleic acid into two single strands. Denaturation takes place in a strongly alkaline environment or under the influence of high temperature. The single-stranded DNA section required for hybridization to the target nucleic acid fragment of the pathogen (DNA or RNA) is obtained by restriction digestion from the bacterial strain or by synthesis on the matrix of bacterial genetic material. This single-stranded nucleic acid segment labeled with radioisotopes or other non-radioisotope techniques acts as a molecular probe. Radioisotope labeling consists

in inserting ^{32}P or ^{35}S radioisotope in place of non-radioactive phosphorus atoms [Creager 2009]. After hybridization, autoradiography is used, which enables the detection of signals. Non-radioisotope labeling consists in linking the nucleic acid with fluorescent tags or natural heptanes, biotin (vitamin) or digoxigenin (a steroid isolated from the *Digitals purpurea* plant), which are detected with the help of antibodies [Węgleński and Golik 2006; Słomski 2008; Kondak 2009].

Hybridization with a molecular probe takes place in several steps. In the first step, denatured DNA or RNA is immobilized on solid supports. Next, incubation takes place in the molecular probe solution, during which the probe hybridizes with complementary nucleic acid fragments. After rinsing the non-hybridized probes, detection of the resulting hybrids is performed using radioisotope or non-radioisotope methods [Słomski 2008].

We distinguish several hybridization methods depending on the type of nucleic acids [Cooper 2000]. Northern hybridization is the binding of RNA molecules separated during denaturing gel electrophoresis with a molecular probe. Prior to hybridization, restriction fragments are transferred to a nylon filter. After hybrid formation, detection of the molecular probe signal is performed. The northern technique is used in the analysis of gene expression and allows the study of the quantity detection of mRNA in the cell [Węgleński and Golik 2006; Słomski 2008].

Southern blot hybridization allows the identification of DNA fragments. It involves hybridization of the probe with complementary DNA fragments. Initially, the DNA is cut by restriction enzymes, then separated by electrophoresis, denatured and transferred to a nylon or nitrocellulose filter. The labeling of probes that hybridize to the DNA immobilized on the filter can be very different. Typically, phosphorus (^{32}P, ^{33}P) radioisotopes or ligands which are detected by enzyme immunoreaction, or biotin or digoxigenin, detected by immunochemical reactions or colorimetry, are used to label the probes. Highly specific probes determine the sensitivity of the Southern method and allow the detection of very small amounts of DNA [Słomski 2008; Szemraj and Szemraj 2013].

An interesting solution is the fluorescent in situ hybridization (FISH), which is used to detect the sought DNA or RNA sequences directly in the cells. A molecular probe, labeled with fluorochromes or with a nucleotide linked to the tag, hybridizes to a complementary nucleic acid sequence. After formation of the hybrid, the signal of the bound probe is detected either directly or indirectly. Due to its high speed, the FISH technique is widely used in medical diagnostics, in research on transgenic animals, in food analysis (for example: non-*Saccharomyces* yeast species [Xufre et al. 2006] or *Listeria monocytogenes* [Rocha et al. 2019]) and in chromosome mapping [Bottari et al. 2006; Słomski 2008; Olszewska 2013; Szemraj and Szemraj 2013].

2.3. Sequencing

Sequencing revealed the full genomic sequences of many organisms and created databases to identify organisms by comparison with the sequences in different databases. There are several first, second and third generation sequencing methods [Kotowska and Zakrzewska-Czerwińska 2011; Artyszuk and Wołkowicz 2018]. First generation sequencing includes methods based on DNA chain termination. The most widely used sequencing technique is the Sanger method. This method is based on the synthesis of various lengths of labeled DNA fragments. The process is catalyzed by a polymerase that replicates the DNA. The reaction uses labeled dideoxynucleotides that inhibit the step of extending the amplified DNA [Sanger et al. 1977]. After performing PCR-like labeling reactions, material is obtained in the form of DNA fragments of various lengths (single nucleotide difference) terminated with differently labeled fluorescently labeled dideoxynucleotides. High voltage capillary electrophoresis is used to read the sequencing reaction. With this method, relatively long DNA fragments, up to 1 Kb, can be obtained. It can be also verified by the readings obtained by analyzing the chromatograms [Słomski 2008; Harwood and Wipat 2011; Artyszuk and Wołkowicz 2018].

An alternative sequencing technique to the Sanger method is the technique developed by Allan Maxam and Walter Gilbert in 1976–1977. In this method, both DNA strands are labeled first at the 5' end. The DNA molecule is then denatured and separated by gel electrophoresis. The next step is to purify a given DNA fragment from the gel and divide it into four parts. Each part is labeled separately with reagents specific to a specific nucleotide. The modified nitrogen base is detached from the sugar residue. The addition of piperidine (the second reagent) cuts the DNA where there is no nitrogen base. Labeled DNA fragments of various lengths are created. The DNA fragments are separated again by gel electrophoresis and visualized by autoradiography. Patterns of DNA bands with different molecular weights allow the determination of DNA sequences. However, this method is not very popular [Słomski 2008; Artyszuk and Wołkowicz 2018].

First generation sequencing methods are constantly being modified and improved. The introduction of the automatic sequencing method and fluorescent tags allowed for Sanger sequencing and separation of DNA fragments in one reaction and real-time sequence analysis [Prober et al. 1987].

In 1995, an analysis of the genome of *Haemophilus influenzae* and *Mycoplasma genitalium* was carried out, using the "shotgun" method (blind shot) [Fleischmann et al. 1995; Fraser et al. 1995] became a breakthrough in sequencing. The

method involves breaking the genome into a collection of small DNA fragments that are sequenced individually. A computer program looks for overlaps in the DNA sequences and uses them to place the individual fragments in their correct order to reconstitute the genome. In the shotgun method, DNA is fragmented by sonication or nuclease digestion. The fragments are separated by gel electrophoresis, isolated and ligated into a plasmid vector. The bacteria are transformed with the vector with the cloned fragment, which is amplified and sequenced. A DNA library is created that is used to sequence the bacterial genome. Characteristic for this type of sequencing is the use of computer techniques, thanks to which the obtained fragments of the genome can be assembled and stored in the so-called contigs – contiguous sequences of different parts of the genome that make up the entire genome [Fleischmann et al. 1995; Brown 2012].

Modern sequencing methods rely on the shotgun method because they take advantage of the production of a large number of short and random reads that make up the entire genome. These new sequencing techniques were created in 2005 and are called the next-generation sequencing era – NGS (Next-generation Genome Sequencing) [Margulies et al. 2005]. In second generation sequencing methods, a single strand of DNA is replicated on a solid support and subjected to the sequencing process. The appropriately modified DNA fragments are sequenced and assembled into contigs during the readings. With second generation techniques, library preparation and sequencing processes are streamlined and more efficient [Pareek 2014]. Thanks to miniaturization and automation, sequencers have been created that enable the simultaneous sequencing of up to a million DNA fragments. On the other hand, the achievements of nanotechnology enable direct reading of the sequence from a single DNA molecule (SMS – Single Molecule Sequencing) without the need for its amplification – 3rd generation sequencing [Satyr and Żmieńko 2020]. However, the division of NGS methods into the second and third generation is rather conventional and collectively referred to as WGS (Whole Genome Sequencing) techniques.

2.4. The use of genotyping to identify pathogens in food

There are many scientific publications on the use of genetic engineering techniques in scientific research, broadly understood laboratory diagnostics, to obtain new microbial strains for biotechnological purposes (Tab. 1). Food and drink are also an area where genotyping can be used. Thanks to the techniques described above, microbial contamination in food can be detected quickly. In contrast to the classic, labor-intensive and time-consuming methods, genotyping methods

are fast, ensuring quality and food safety [Misiewicz and Goncerzewicz 2013; Zadernowska et al. 2014].

RAPD-PCR can be used to detect *Bacillus cereus*. Thanks to this method, it is possible to study the phylogenetic relationship between bacteria. Lee et al. [2011] observed that with a constant primer sequence all *Bacillus* species amplified 500 bp DNA fragments, *B. cereus* strains additionally 910 bp products, and *B. subtilis* 880 bp.

RAPD-PCR can identify and differentiate *Listeria monocytogenes* in food (poultry, pork, beef, milk and cheese) using a primer HLWL 74 [Park et al. 2012], and in other studies S1F and S1R to amplify the 460 bp fragment and S2F and S2R for the 890 bp fragment [Paillard et al. 2003]. The genetic diversity of *Escherichia coli* O157:H7 was identified and analyzed [Radu et al. 2001] in beef tenderloin and chicken burgers. The analyzes were performed using the GEN15001 primer. Usually, in order to confirm the results obtained in the RAPD-PCR method, another method is used, e.g. in this case PFGE. In this way, *Campylobacter jejuni* and *C. coli* in poultry meat were identified [Silva et al. 2015]. In other studies, primers OPQ-01 - OPQ-20 that identify *Escherichia coli* O157: H7/NM were designed and tested. The OPQ-3 primer was particularly useful for detection [Lin i Lin 2007]. In this experiment, additionally pathogenic *E. coli* strains were sequenced. *L. monocytogenes* isolates from avocado fruit from South Africa with primers were identified and typed by RFLP-PCR: seq01 and seq02 [Strydom et al. 2013]. According to Kołakowska and Madajczak [2011], the most effective methods of intra-species typing of *L. monocytogenes* are REA-PFGE and ribotyping, while rep-PCR (repetitive element palindromic PCR) and ERIC-PCR (Enterobacterial Repetitive Intergenic Consensus PCR) methods are important in the standard diagnostics of these bacteria.

Campylobacter jejuni and *Escherichia coli* in food can be identified by RFLP-PCR. The flaA gene (1700 bp) was split into smaller sequences ranging from 120 to 900 bp. The band patterns of the analyzed bacteria were compared with the reference strains of *C. jejuni* and *C. coli* strains. As a result, 3 different *C. jejuni* strain profiles and 2 *C. coli* profiles were obtained [Wieczorek and Osek 2005]. *Campylobacter* was identified by the AFLP-PCR (Amplified Fragment Length Polymorphism PCR) method, which also uses restriction enzymes and phylogenetic relatedness on the basis of polymorphisms [Dium et al. 2001], *Listeria monocytogenes* [Lomonaco et al. 2011].

Campylobacter jejuni bacteria isolated from poultry were identified by RFLP-PCR [Nebola and Steinhauserova 2006]. Strain identification was performed by analyzing the 23S rRNA sequence, and for subtyping strains, the flagellin gene (*fla*-RFLP) was analyzed.

Identification of *Listeria* in fruits and vegetables is also possible thanks to multiplex PCR. *Listeria* bacteria amplify products with a size of 938 bp, while the very dangerous pathogen *Listeria monocytogenes*, apart from the above-mentioned product, also amplifies the product with a size of 287 bp. In the experiment of Szymczak et al. [2011], all strains of bacteria isolated from organic fruit and vegetables contained *Listeria monocytogenes*. The multiplex PCR method has also been used to test the microbiological purity of production lines used in the food industry and to analyze water and soil in terms of microbiological contamination [Kaczmarek et al. 2008]. Multiplex real-time PCR is used to identify different species of *Salmonella* spp., *E. coli* O157:H7 and *L. monocytogenes* [Garrido et al. 2013]. Real-time PCR is a good tool to identify Shiga toxins produced by pathogenic *E. coli* O157: H7 strains in food [Di and Tumer 2010].

Listeria monocytogenes is the cause of listeriosis. The bacteria can contaminate cheese, dairy products, especially raw milk, fish, fresh meat and untreated food. *Listeria* bacteria are resistant to preservatives, multiply easily at low temperatures and have effective defense mechanisms against food sterilization methods. All this is a significant problem in maintaining the microbiological purity of food and ensuring its good quality and safety. For molecular methods of rapid identification of *Listeria*, among others, serotyping. *L. monocytogenes* has 12 serotypes, of which three serotypes: 1/2α, 1/2*b* and 4b, are responsible for 90% of listeriosis in humans and animals. The infectious agents of *Listeria* are Hly encoded by the *hly* virulence gene, which encodes the protein listeriosin O (hemolysin), the InlA and InlB proteins encoded by the internalin *inl*A and *inl*B genes, the *iap* infectivity gene which encodes the extracellular protein p60 and whose internal fragment is species specific *Listeria* bacteria. It is also used to identify them in the PCR technique (ADIAFOOD method, BAX System, GeneDisc *Listeria monocytogenes*) and Real-Time PCR (IQ-Check *Listeria monocytogenes* kit) [Wróblewska and Misiewicz 2009; Nowak and Ołtuszak-Walczak 2012]. This species can also be identified by the method of hybridization of the 16S rRNA region with a specific oligonucleotide molecular probe. Several alternative hybridization methods have been developed to rapidly detect the presence of *L. monocytogenes* in food: LumiProbe 24 *Listeria monocytogenes* and AccuProbe *Listeria monocytogenes* kits [Nowak and Ołtuszak-Walczak 2012].

The source of *Salmonella* bacteria are meat products, especially poultry and pork, dairy products, eggs, fruit, vegetables and fodder. The most frequently identified pathogen of this type is *Salmonella enterica*, which is responsible for food poisoning. To perform PCR, specific primers based on gene fragments encoding ribosomal RNA (rDNA) are used: 18S rDNA, 28S rDNA and 5.8S rDNA characteristic for *Salmonella* sp. gene sequences *fim*A i *inv*A. Another method for

the rapid identification of *Salmonella* in meat is Real-time PCR [Misiewicz and Goncerzewicz 2013].

Bacteria of this type can also be identified using in situ hybridization. However, the use of this method for effective detection of pathogens in food requires optimal conditions for the preparation of the tested samples, because the tested food sample may contain other pathogens. And this may produce erroneous results. Therefore, it is important to select the appropriate probe for specific species of microorganisms. It is also important to determine the optimal conditions for preparing samples for further molecular analysis [Zadernowska et al. 2014]. So *Salmonella* sp., in food is measured in 25 g of the product. Typically, for the detection of *S. enterica* in poultry by the FISH method, an oligonucleotide Sal3 probe is used, which is labeled with fluorescent dyes at the 5' ends. Before testing, the cells should be separated from the protein and fat molecules present in the meat. In the first stage, the microorganism is multiplied in a non-selective medium. Skipping this step may result in false-negative results. The detection limit of the FISH method is approximately 10^3 cfu/g, and the pre-propagation step significantly increases the sensitivity. The parameters of bacterial cell permeabilization should also be properly established, thanks to which molecular probes can easily penetrate the cell interior. Penetration of probes into cells is hindered by their large size, as well as the fixation of cells [Zadernowska et al. 2014]. Other oligonucleotide probes for detecting *S. enterica* by FISH are labeled with Cy5 and Cy3 fluorescent dyes at the 5' ends (EUB_{338} – Cy5, NON_{338} – Cy5 i Sal3 – Cy3). The complete coverage of the signals that was observed indicates a well-performed permeabilization of *Salmonella* sp. The tests of mixed cultures confirmed the specificity of the probes described for this bacterium. The NON_{338} probe was used in the negative control, allowing the detection of nonspecifically bound probes. The FISH technique was used to diagnose the presence of *Salmonella* sp. in all infected samples, which confirms its high specificity and reliability. This technique significantly shortens the analysis time, which is important when testing food products with a short shelf life [Zadernowska et al. 2014].

One of the methods of genotyping, not described earlier, are DNA microarrays using hybridization (DNA *microarray*, DNA *chip, gene array*). DNA microarrays are used in food as one of the ways to identify food pathogens. With this technique, pathogens in minced meat can be identified: *Listeria monocytogenes* A and B, *Salmonella*, *Campylobacter* [Murawska et al. 2004]. The advantages of cDNA microarrays include: the possibility of identification and comparing the expression of many genes in one experiment, no need to know the sequence of the studied genes, the possibility of analyzing various types of microarrays in one reader, there is also the possibility of modifying the obtained sets of genes, which

Table 1. Review of diagnostic techniques of selected food pathogens (source: own elaboration)

Pathogens	Identification method	Literature
Bacillus cereus	RAPD-PCR	Lee et al. 2011
Listeria monocytogenes	RAPD-PCR	Park et al. [2012]; Paillard et al. [2003]
	RFLP-PCR	Strydom et al. [2013]
	REA-PFGE	Kołakowska and Madajczak [2011]
	Ribotyping	Kołakowska and Madajczak [2011]
	AFLP-PCR	Lomonaco et al. [2011]
	Multiplex PCR	Szymczak et al. [2011]; Kaczmarek et al. [2008]
	Multiplex real-time PCR	Garrido et al. [2013]
	Serotyping	Wróblewska and Misiewicz [2006]; Nowak and Ołtuszak-Walczak [2012]
	PCR	Wróblewska and Misiewicz [2006]; Nowak and Ołtuszak-Walczak [2012]
	Real-time PCR	Wróblewska and Misiewicz [2006]; Nowak and Ołtuszak-Walczak [2012]
	Hybridization	Nowak and Ołtuszak-Walczak [2012]
	DNA miccroarray	Murawska et al. [2004]
Escherichia coli O157:H7	RAPD-PCR	Radu et al. [2001]; Silva et al. [2015]; Lin and Lin [2007]
	RFLP-PCR	Wieczorek and Osek [2005]
	Multiplex real-time PCR	Garrido et al. [2013]
	Real-time PCR	Di and Tumer [2010]
Campylobacter jejuni	RAPD-PCR	Silva et al. [2015]
	RFLP-PCR	Wieczorek and Osek [2005]; Nebola and Steinhauserova [2006]
	AFLP-PCR	Dium et al. [2001]
	DNA miccroarray	Murawska et al. [2004]
Salmonella sps.	Multiplex real-time PCR	Garrido et al. [2013]
	PCR	Misiewicz and Goncerzewicz [2013]
	Real-time PCR	Misiewicz and Goncerzewicz [2013]
	Hybridization *in situ*	Zadernowska et al. [2014]
	Hybridization FISH	Zadernowska et al. [2014]
	DNA miccroarray	Murawska et al. [2004]

means that the research is not dependent on commercial products [Ziarno 2007]. Like microarrays, DNA chips allow the analysis of a large number of genes in one test (quantitative measurements). In addition, the tests are easy and reliable thanks to the automation of the staining process, it is also possible to enclose the plate with its own hybridization chamber. DNA chips also have their disadvantages: the use of chips depends on commercial sources, the reading is adequate to the method (it is not adapted to the cDNA matrix reading). The use of oligonucleotide microarrays is associated with high costs, and the methods used are characterized by low flexibility [Ziarno 2007].

3. Phagotyping methods

Phagotyping is a technique that can distinguish bacteria. It is mainly used in epidemiological studies to identify and characterize the strains causing an epidemic [Schofield et al. 2012]. The basis of the method is the ability of bacteria to infect bacteria by bacterial viruses, bacteriophages that infect only a specific group of bacteria. Phage contain genetic material (DNA or RNA) encased in a protein or lipidoprotein coat or capsid. The virus must infect bacteria because it lacks a set of genes for energy production and ribosomes for protein production. Due to the life cycle, bacteriophages can be divided into lytic (virulent) and lysogenic (moderate). In the lytic cycle, the bacterial cell is lysed and the phages are released. In the lysogenic cycle, the bacteriophage genome is dormant, integrated into the bacterial genome (profage). It is replicated and passed down from generation to generation, but under certain conditions the prophage can become virulent [Kutter and Sulakvelidze 2004].

Bacteriophages can infect different kinds, species, strains, and even the highly specialized serotypes of bacteria. The ability to infect depends on bacterial surface receptors that phages recognize. The phagotyping method involves growing an unknown culture in a petri dish and then adding a small amount of different bacteriophages. The appearance of phage plaques, i.e. transparent zones after the lysis of bacterial cells, indicates infection. By observing the occurrence of an infection caused by a specific bacteriophage, the investigated bacterial colony is identified. The phagotyping method can identify most pathogens, even up to serotypes and serogroups. Unlike genetic or serological methods, bacterial cells must be alive where living objects cannot be distinguished from dead [Scheper et al. 2010].

Viral biosensors, such as bacteriophages, play an important role in the detection of pathogens in food. Bacteriophages are biological entities that are actively

used as probes for the detection and recognition of pathogens. A promising variant of phagotyping for the identification of *Salmonella typhimurium* LT2 is the use of a fluorescent dye to label the bacteriophage (P22 phage bound to the SYBR gold dye). After viruses have infected cells, the emission of fluorescent phage DNA inside the cell allows for detection with a fluorescence microscope. Thanks to this, it is possible to observe their shape and size [Mossier-Boss et al. 2003].

Phagotyping methods are used to distinguish *Salmonella*, including the most common in Poland serotype *Salmonella* Enteritidis [Dera-Tomaszewska and Tokarska-Pietrzak 2012]. Phagotyping is also used to identify soil bacteria of the genus *Bacillus* that can be a source of food contamination [Shah Mahmud et al. 2017].

4. Spectrophotometric methods

4.1. Mass spectrometry method

Mass spectrometry is a new, very fast method used to identify microorganisms. One of the most popular methods of mass spectrometry is MALDI-ToF (Matrix-Assisted Laser Desorption /Ionization – Time of Flight) – laser desorption and matrix-assisted ionization. It allows you to quickly and accurately study the protein profile (proteome). The analysis of proteins – products of gene expression allows the classification of the microorganism into species and strains. The protein composition of the cell is influenced by time, the change in the composition of the medium, fluctuations in pH and temperature of the culture, as well as the cell type and the growth phase [Szczepańska and Robak 2013; Mielko and Młynarz 2020]. Therefore, in this method, proteins specific for a given microorganism are determined, which will not change despite changing cultivation conditions.

The test organisms should come from 18–24 hours of pure culture. Cells undergo preliminary chemical protein extraction. The obtained analyte is applied to a metal plate. After drying, the matrix is applied. The plate, dried at room temperature, is placed in the MALDI Biotyper measuring chamber. The laser beam ionizes the proteins that begin to migrate in the electric field. It is the measurement of the time of flight of molecules that is the basis for creating a unique microbial profile. The molecular weights and the charge of the migrating elements are also analyzed. The spectra made by the spectrometer are compared with the databases [Kosikowska et al. 2015].

MALDI-ToF is widely used in the food industry for the identification of microorganisms. Therefore food safety control is ensured, hygienic conditions of work in production plants can be improved, and pathogens responsible for food poisoning can be identified [Czyrko et al. 2015]. That's why MALDI-ToF, it is possible to recognize strains from the same species because they have the same m/z ratio (mass of ion to ion charge), but different intensity. [Szczepańska and Robak 2013]. The method allows to obtain results faster than in classical tests, provides a large number of results, and the procedure is not complicated. The disadvantage is the cost of purchasing an analytical camera. Of course, the analyzes allow to obtain reliable results if the biological material is pure culture [Żabicka and Literacka 2013; Czyrko et al. 2015].

4.2. Fatty acid analysis

In addition to a specific protein profile, microorganisms also have a unique fatty acid profile that allows them to be identified. These compounds can be analyzed qualitatively, focusing on the specific components of lipids and the quantity of individual acids, as well as their mutual quantitative relations in the examined microorganism. The diversity of lipid compounds is due to the presence of carbon chains of various lengths, non-permanent cis-trans conformations, the presence of substituents, aromatic rings and branching. The measurement is influenced by the culturing conditions (pH, nutrient solution, temperature) which must be standardized [Bzducha 2007]. A method that allows the analysis of fatty acid profiles to identify the microorganism is MIDI-FAME combined with gas chromatography. A characteristic system of fatty acids with a chain length of 9 to 20 carbon atoms is obtained [Sekora et al. 2009].

A pure culture of 18–24 h of culture should be prepared for the analyzes. The appropriate number of cells is saponified (cell lysis and the release of fatty acids from it, which, after reaction with sodium hydroxide, transform into sodium salts). The next step consists in bathing the samples in a boiling water bath, and then cooling the sample and mixing it with appropriate reagents. The sample is returned to the 80 ° C bath for the formation of volatile fatty acid methyl esters (FAME). The next step – extraction with appropriate reagents - transfers the FAMEs to the organic phase from the aqueous phase of the sample. The last step is to transfer the upper phase and add more reagents to get an emulsion and get rid of unmethylated acids. The upper phase with fatty acids is transferred to the vessels intended for chromatographic analyzes [Biedroń et al. 2013]. The databases used by software such as Sherlock Microbial Identification System by MIDI, Inc. are used to identify bacteria

on the basis of fat profiles. The method is especially useful in the case of problems with sample identification by biochemical methods [Buyer 2002].

4.3. The use of spectrometric methods to identify pathogens in food

In the food industry, thanks to biophysical methods, e.g. MALDI-ToF or MIDI-FAME, it is possible to quickly identify pathogens (*Pseudomonas aeruginosa*, *Escherichia coli*, *Staphylococcus aureus*), control the safety of food products, and improve production hygiene [Buyer 2002; Welker 2011].

Clostridium perfringens anaerobic bacilli can cause food poisoning and contaminated food can be a reservoir of the pathogen. Identification of *C. perfringens* strains was carried out using the MALDI-TOF method, and to verify the results, also sequencing of 16S rRNA and the *cpa* gene [Brodzik et al. 2016]. *E. coli* [Calvano et al. 2016; Randall et al. 2017; Zurita et al. 2019], *Staphylococcus* w tym *S. aureus* [Böhme et al. 2012; Tajdar et al. 2019], *Enterococcus faecalis* and *E. faecium* [Lindenstrauß et al. 2011; Ledina et al. 2018] bacteria or serotypes of *Salmonella* spp. [Ojima-Kato et al. 2017] can be identified in food with MALDI-ToF. Also based on the lipid profiles of these bacteria [Shu et al. 2012].

5. Conclusion
Advantages and disadvantages of identifying pathogens with molecular techniques

Molecular techniques that are increasingly used to detect pathogens in food have many advantages and disadvantages. The development of molecular techniques has reduced the identification of microorganisms by classical methods. Molecular methods will not completely replace traditional methods. Classic methods, which are often faster and cheaper, can extend and supplement diagnostics with molecular methods [Olszewska 2013; Szemraj and Szemraj 2013]. The advantages of molecular biology diagnostics are: acceleration of the procedure and faster detection of microorganisms, heir quantity and reduction of the analysis time, which allows to obtain results faster. Due to the high sensitivity of molecular methods, the obtained results are more reliable. Molecular techniques make it possible to detect microorganisms that are difficult to cultivate and pathogens that cannot be cultured in vitro. The use of these techniques enables the diagnosis of related bac-

terial species, the differentiation of specific strains, as well as the degree of relatedness between them. The disadvantages of molecular biology methods include the high purchase costs of equipment, appropriate reagents, primers, molecular probes, which may limit their use, especially in small food industry plants. Proper preparation of samples for testing may also be a problem, because food, as a matrix, is characterized by quite a significant complexity, which makes it difficult to extract bacterial cells [Olszewska 2013].

PCR-based techniques are specific, sensitive and selective. They are distinguished by a simple procedure and relatively low reaction costs. It is possible to automate the reaction process, which is associated with the reduction of the test duration. The biggest advantage of PCR methods, however, is the possibility of using them to identify non-cultivable microorganisms or bacteria whose cultivation takes time [Osek 2005; Szemraj and Szemraj 2013]. In addition, in the case of real-time PCR, quantitative measurements can be made and the amount of tested microorganisms can be determined. The disadvantages of this method may be the exponential increase of the amplification product and the number of variants obtained with subsequent cycles of the PCR reaction, as well as the risk of obtaining false positive results [Palka 2007; Kondak 2009]. An important feature of the RT-PCR method is the ability to distinguish living cells from dead ones and identifying microorganisms that have RNA [Kondak 2009]. Hybridization techniques, on the other hand, are sensitive and results are obtained quickly. Their main advantage is high sensitivity and relatively short hybridization time. Thanks to hybridization, you can map the genomes (Southern method), or examine the level of gene expression and identify the type of RNA in the cells (*northern* analysis) [Słomski 2008]. The technique of fluorescence *in situ* hybridization FISH, in addition to the previously mentioned advantages, allows you to monitor the biodiversity of the bacterial flora in food and difficult to remove biofilms that arise on technological lines and packaging. Unfortunately, the test sample must contain a large number of cells, otherwise there is a possibility of false negative results [Olszewska 2013; Szemraj and Szemraj 2013; Zadernowska et al. 2014].

Molecular methods should be widely used to detect the presence and amount of pathogens in food. Good knowledge of molecular biology techniques has a positive effect on the durability of the product, contributes to the optimization and modernization of technological processes and, above all, guarantees high quality and safety of food products. All this leads to an increasing use of molecular methods in microbiological diagnostics of food. Nevertheless, the limitations of molecular methods mean that their widespread use will only be possible in the distant future [Olszewska 2013].

References

Artyszuk D., Wołkowicz T. 2018. Zastosowanie sekwencjonowania pełnogenomowego do genotypowania bakterii. Postępy Mikrobiologii, 57(2), 179–193. https://doi.org/10.21307/PM-2018.57.2.179

Biedroń I., Wasilkowski D., Traczewska T.M. 2013. Metody identyfikacji mikroorganizmów bytujących w biofilmach sieci wodociągowej. [In:] Interdyscyplinarne zagadnienia w inżynierii i ochronie środowiska. Praca zbiorowa. T. 3. Eds. T.M. Traczewska. Oficyna Wydawnicza Politechniki Wrocławskiej, Wrocław, 51–59.

Binduga-Gajewska I., Gut W., Wielkopolska A., Jarząbek Z. 1999. Zastosowanie metody RT--PCR i nested-PCR do wykrywania zakażeń enterowirusami. Medycyna Doświadczalna i Mikrobiologia, 51 (3-4), 375–381.

Böhme K., Morandi S., Cremonesi P., Fernández No I.C., Barros-Velázquez J., Castiglioni B., Brasca M., Cañas B., Calo-Mata P. 2012. Characterization of Staphylococcus aureus strains isolated from Italian dairy products by MALDI-TOF mass fingerprinting. Electrophoresis, 33, 2355–2364. https://doi.org/10.1002/elps.201100480

Bottari B., Ercolini D., Gatti M., Neviani E. 2006. Application of FISH technology for microbiological analysis: Current state and prospects. Mini-Review. Applied Microbiology and Biotechnology, 73, 485–494. https://doi.org/10.1007/s00253-006-0615-z

Brodzik K., Augustynowicz E., Korzeniowska-Kowal A., Lutyńska A. 2016. Zastosowanie metody MALDI-TOF do identyfikacji szczepów Clostridium perfringens. Medycyna Doświadczalna i Mikrobiologia, 68, 13–21.

Brown T.A. 2012. Genomy. Wydawnictwo Naukowe PWN, Warszawa.

Buchowicz J. 2009. Odkrycia leżące u podstaw współczesnej biotechnologii. [In:] Biotechnologia molekularna. Modyfikacje genetyczne, postępy, problemy. Ed. J. Buchowicz. PWN, Warszawa, 11–39.

Buyer J.S. 2002. Identification of bacteria from single colonies by fatty acid analysis. Journal of Microbiological Methods, 48, 259–265. https://doi.org/10.1016/s0167-7012(01)00327-x

Bzducha A. 2007. Szybkie metody identyfikacji mikroorganizmów w żywności. Medycyna Weterynaryjna, 63(7), 773–778.

Calvano C.D., Picca R.A., Bonerba E., Tantillo G., Cioffi N., Palmisano F. 2016, MALDI--TOF mass spectrometry analysis of proteins and lipids in Escherichia coli exposed to copper ions and nanoparticles. Journal of Mass Spectrometry, 51, 828–840. https://doi.org/10.1002/jms.3823

Chołuj J., Przewodowski W. 2014. Technika PCR i jej modyfikacje w identyfikacji patogenów ziemniaka. Ziemniak Polski, 3, 40–45.

Cooper G.M. 2000. Detection of nucleic acid and proteins. [In:] The Cell. A Molecular Approach. 2nd Edition. Sinauer Associates, Sunderland (MA).

Creager A.N.H. 2009. Phosphorus-32 in the phage group: Radioisoopes as historical tracers of molecular biology. Studies in History and Philosophy of Biological and Biomedical Sciences. 40(1), 29–42. https://doi.org/10.1016/j.shpsc.2008.12.005

Czyrko J., Bruś D.M., Mykhailiv O. 2015. Technika MALDI nowoczesna metoda analityczna. Przemysł Spożywczy, 69(2), 32–35. https://doi.org/10.15199/65.2015.4.4

Dera-Tomaszewska B., Tokarska-Pietrzak E. 2012. Typowanie bakteriofagowe w diagnostyce pałeczek Enteritidis występujących w Polsce. Postępy Mikrobiologii, 51(4), 323–329.

Delibato E., Fiore A., Anniballi F., Auricchio B., Filetici E., Orefice L., Losio M.N., De Medici D. 2011. Comparison between two standardized cultural methods and 24 hour duplex SYBR green real-time PCR assay for Salmonella detectionin meat samples. New Microbiology, 34(3), 299–306.

Di R., Tumer N.E. 2010. Real-time reverse transcription PCR detection of viable shigatoxin--producing Escherichia coli O157:H7 in food. Journal of Food Safety, 30, 51–66. https://doi.org/10.1111/j.1745-4565.2009.00189.x

Dium B., Vandamme P.A.R., Rigter A., Laevens S., Dijkstra J.R., Wagenaar J.A. 2001. Differentiation of Campylobacter species by AFLP fingerprinting. Microbiology, 147(10), 2729–2737. https://doi.org/10.1099/00221287-147-10-2729

Ercolini D. 2004. PCR-DGGE fingerprinting: Novel strategies for detection of microbes in food. Journal of Microbiological Methods, 56, 297–314. https://doi.org/10.1016/j.mimet.2003.11.006

Fleischmann I.R.D., Adams M.D., White O., Clayton R.A., Kirkness E.F., Kerlavage A.R., Bult C.J., Tomb J.F., Dougherty B.A., Merrick J.M. 1995. Whole-genome random sequencing and assembly of Haemophilus influenzae. Science, 269, 496–512. https://doi.org/10.1126/science.7542800

Fraser C.M., Gocayne J.D., White O., Adams M.D., Clayton R.A., Fleischmann R.D., Bult C.J., Kerlavage A.R., Sutton G., Kelley J.M., Fritchman R.D., Weidman F., Small K.V., Sandusky M., Fuhrmann J., Nguyen D., Utterback T.R., Saudek D.M., Phillips C.A., Merrick J.M., Tomb J.F., Dougherty B.A., Bott K.F., Hu P.C., Lucier T.S., Peterson S.N., Smith H.O., Hutchison 3rd C.A., Venter J.C. 1995. The minimal gene complement of Mycoplasma genitalium. Science, 270, 397–403. https://doi.org/10.1126/science.270.5235.397

Garrido A., Chapela M.J., Román B., Fajardo P., Vieites J.M., Cabado A.G. 2013. In-house validation of a multiplex real-time PCR method for simultaneous detection of Salmonella spp., Escherichia coli O157 and Listeria monocytogenes. International Journal of Food Microbiology, 164(1), 92–98. https://doi.org/10.1016/j.ijfoodmicro.2013.03.024

Green M.R., Sambrook J. 2018. Touchdown polymerase chain reaction (PCR). Cold Spring Harbol Protocols, 5. https://doi.org/10.1101/pdb.prot095133

Hać-Szymańczuk E. 2012. Tradycja i nowoczesność w identyfikacji drobnoustrojów. Gospodarka Mięsna, 64(10), 28–30.

Harwood C.R., Wipat A. 2011. Zarządzanie genomem i jego analiza: Prokaryota. [In:]Podstawy biotechnologii. Eds. C. Ratledge, B. Kristiansen. PWN, Warszawa, 60–61, 64–65, 72–73.

Junge B., Grönewald C., Berghof-Jäger K. 2012. BIOTECON diagnostics foodproof Listeria monocytogenes Detection Kit, 5' nuclease in combination with the foodproof ShortPrep II kit. Journal of AOAC International. 95(1), 92–99. https://doi.org/10.5740/jaoacint.11-0096

Kaczmarek M., Hoppe-Gołębiewska J., Słomski R. 2008. PCR multipleks. [In]: Analiza DNA. Teoria i praktyka. Ed. W. Uchman. Wydawnictwo Uniwersytetu Przyrodniczego w Poznaniu, Poznań, 220–224.

Kadri K. 2019. Polymerase chain reaction (PCR): Principle and applications. [In:] Synthetic Biology – New Interdisciplinary Science. Eds. M.L. Nagpal, O.M. Boldura, C. Baltă, S. Enany. IntechOpen London. https://doi.org/10.5772/intechopen.86491

Kołakowska A., Madajczak G. 2011. Genetyczne metody typowania pałeczek Listeria monocytogenes. Przegląd Epidemiologiczny, 65, 421–427.

Kołożyn-Krajewska D. 1995. Gwarantowana jakość mikrobiologiczna żywności a metody predyktywne. Żywność. Technologia. Jakość, 2(3), 53–54.

Kołożyn-Krajewska D. 2013. Metody i systemy zapewniania i zarządzania jakością. [In:] Higiena produkcji żywności. Ed. D. Kołożyn-Krajewska. Wydawnictwo SGGW, Warszawa, 48–61.

Kondak K. 2009. Molekularne metody diagnostyki mikrobiologicznej. Diagnostyka Laboratoryjna, 45(4), 325–331.

Kosikowska U., Stępień-Pyśniak D., Pietras-Ożga D., Andrzejczuk S., Juda M., Malm A. 2015. Zastosowanie spektrometrii masowej MALDI-TOF MS w identyfikacji bakterii izolowanych z materiałów klinicznych od ludzi i zwierząt. Diagnostyka Laboratoryjna, 51(1), 23–30.

Kotowska M., Zakrzewska-Czerwińska J. 2010. Kurs szybkiego czytania DNA – nowoczesne techniki sekwencjonowania. Biotechnologia, 4(91), 24–38.

Kutter E., Sulakvelidze A. 2004. Bacteriophages: Biology and Applications. CRC Press, Boca Raton.

Lai J. 2017. Multiple Touchdown PCR (MT-PCR): A new application of PCR for better precision and stability. www.blue-raybio.com [accessed: September 12, 2019].

Lee J., Gun-Hee K., Jae-Young P., Cheon-Seok P., Dae Young K., Jinkuy L., Jong Sang K., Jeong Hwan K. 2011. A RAPD-PCR method for the rapid detection of Bacillus cereus. Journal of Microbiology and Biotechnology, 21(3), 274–276. https://doi.org/10.4014/jmb.1008.08031

Ledina T., Golob M., Djordjevic J., Magas V., Colovic S., Bulajic S. 2018. MALDI-TOF mass spectrometry for the identification of Serbian artisanal cheeses microbiota. Journal of Consumer Protection and Food Safety, 13, 309–314. https://doi.org/10.1007/s00003-018-1164-y

Lin Ch.K., Lin J.Ch. 2007. Development of PCR primers based on a fragment from randomly amplified polymorphic DNA for the detection of Escherichia coli O157:H7/NM. Molecular and Cellular Probes, 21, 182–189. https://doi.org/10.1016/j.mcp.2006.11.001

Lindenstrauß A.G., Pavlovic M., Bringmann A., Behr J., Ehrmann M.A., Vogel R.F. 2011. Comparison of genotypic and phenotypic cluster analyses of virulence determinants and possible role of CRISPR elements towards their incidence in Enterococcus faecalis and Enterococcus faecium. Systematic and Applied Microbiology, 34, 553–560. https://doi.org/10.1016/j.syapm.2011.05.002

Liu Y., Cao Y., Wang T., Dong Q., Li J., Niu C. 2019. Detection of 12 common food-borne bacterial pathogens by TaqMan Real-Time PCR using a single set of reaction conditions. Frontiers Microbiology, 10, 222. https://doi.org/10.3389/fmicb.2019.00222

Lomonaco S., Nucera D., Parisi A., Normanno G., Botteo M.T. 2011. Comparison of two AFLP methods and PFGE using strains of Listeria monocytogenes isolated from environmental and food samples obtained from Piedmont, Italy. International Journal of Food Microbiology, 149, 177–182. https://doi.org/10.1016/j.ijfoodmicro.2011.06.012

Łyszcz M., Gałązka A. 2017. Genetyczne metody różnicowania mikroorganizmów w systemie gleba – roślina. Postępy Mikrobiologii. 56, 3, 341–352 https://doi.org/10.21307/PM-2017.56.3.341

Margulies M., Egholm M., Altman W.E., Attiya S., Bader J.S., Bemben L.A., Berka J., Braverman M.S., Chen Y.J., Chen Z., Dewell S.B., Du L., Fierro J.M., Gomes X.V., Goodwin B.C., He W., Helgesen S., Ho C.H., Irzyk G.P., Jando S.C., Alenquer M.L.I., Jarvie T.P., Jirage K.B., Kim J.B., Knight J.R., Lanza J.R., Leamon J.H., Lefkowitz S.M., Lei M., Li J., Lohman K.L., Lu H., Makhijani V.B., McDade K.E., McKenna M.P., Mers E.W., Nickerson E., Nobile J.R., Plant R., Puc B.P., Ronan M.T., Roth G.T., Sarkis G.J., Simons J.F., Simpson J.W., Srinivasan M., Tartaro K.R., Tomasz A., Vogt K.A., Volkmer G.A., Wang S.H., Wang Y., Weiner M.P., Yu P., Begley R.F., Rothberg J.M. 2005. Genome sequencing in open microfabricated high density picoliter reactors. Nature, 437, 376–380. https://doi.org/10.1038/nature03959

Maxam A.M., Gilbert W. 1977. A new method for sequencing DNA. Proceedings of the National Academy of Sciences of the USA, 74, 560–564. https://doi.org/10.1073/pnas.74.2.560

Mielko K.A., Młynarz P. 2020. Biotypowanie mikroorganizmów za pomocą spektrometrii mas oraz spektrometrii NMR. Wiadomości Chemiczne, 74(1–2), 57–70.

Misiewicz A., Goncerzewicz A. 2013. Wykrywanie bakterii Salmonella metodami molekularnymi w produktach żywnościowych. Zeszyty Problemowe Postępów Nauk Rolniczych, 573, 3–11.

Mossier-Boss P.A., Lieberman S.H., Andrews J.M., Rohwer F.L., Wegley L.E., Breitbart M. 2003. Use of fluorescently labeled phage in the detection and identification of bacterial species. Applied Spectroscopy, 57, 1138–1144. https://doi.org/10.1366/00037020360696008

Murawska A., Tyburski J., Budzyński T., Jarkiewicz-Tretyn J., Donderski W., Tretyn A. 2004. Zastosowanie techniki mikromacierzy (czipów) DNA w badaniu bakteriologicznym produktów spożywczych. Medycyna Weterynaryjna, 60(5), 481–484.

Nebola M., Steinhauserova I. 2006. PFGE and PCR/RFLP typing of Campylobacter jejuni strains from poultry. British Poultry Science, 4(47), 456–461. https://doi.org/10.1080/00071660600829159

Nowak A., Ołtuszak-Walczak E. 2012. Listeria monocytogenes w żywności – metody wykrywania i oznaczania. Przemysł Spożywczy, 66(11), 30–33.

Ojima-Kato T., Yamamoto N., Nagai S., Shima K., Akiyama Y., Ota J., Tamura J. 2017. Application of proteotyping Strain Solution™ ver. 2 software and theoretically calculated mass database in MALDI-TOF MS typing of Salmonella serotype. Applied Microbial and Cell Physiology, 101, 8557–8569. https://doi.org/10.1007/s00253-017-8563-3

Olejnik-Schmidt A., Broniarczyk J., Schmidt M. 2009. Genetyczne metody identyfikowania, klasyfikacji i różnicowania mikroorganizmów. Przemysł Spożywczy, 63, 2, 12–16.

Olszewska M. 2013. Metody biologii molekularnej w mikrobiologii żywności. Przemysł Spożywczy, 67(2), 10–14.

Osek J., Kowalczyk A., Wieczorek K. 2005. Molekularne metody wykrywania i identyfikacji chorobotwórczych bakterii w żywności. Medycyna Weterynaryjna, 61(1), 5–9.

Paillard D., Dubois V., Duran R., Nathier F., Guittet C., Caumette P., Quentin C. 2003. Rapid identification of Listeria Species by using restriction fragment length polymorphism of PCR-amplified 23S rRNA gene fragments. Applied and Environmental Microbiology, 69(11), 6386–6392. https://doi.org/10.1128/aem.69.11.6386-6392.2003

Palka R. 2007. Zastosowanie osiągnięć biologii molekularnej w mikrobiologii żywności. Przemysł Spożywczy, 61(2), 6–8.

Pareek C.S. 2014. An overview of next-generation genome sequencing platforms. [In:] Next-Generation Sequencing: Current Technologies and Applications. Ed. J. Xu. Caister Academic Press, United Kingdom, 1–24.

Park S., Jung J., Choi S., Oh Y., Lee J., Chae H., Ryu S., Jung H., Park G., Choi S., Kim B., Kim J., Chae Y.Z., Jung B., Lee M., Kim H. 2012. Molecular characterization of Listeria monocytogenes based on the PFGE and RAPD in Korea. Advances in Microbiology, 2, 605–616. https://doi.org/10.4236/aim.2012.24079

Pizzighella S., Rassu M., Piacentini I., Maschera B., Palú G. 1993. Polymerase chain reaction amplification and restriction enzyme typing as an accurate and simple way to detect and identify human papillomaviruses. Journal of Medical Microbiology, 39(1), 33–38. https://doi.org/10.1099/00222615-39-1-33. PMID: 8392107

Prober J.M., Trainor G.L., Dam R.J., Hobbs F.W., Robertson C.W., Zagursky R.J., Cocuzza A.J., Jensen M.A., Baumeister K. 1987. A system for rapid DNA sequencing with fluorescent chain-terminating dideoxynucleotides. Science, 238, 336–341. https://doi.org/10.1126/science.2443975

Radu S., Ling O.W., Rusul G., Karim M.I., Nishibuchi M. 2001. Detection of Escherichia coli O157:H7 by multiplex PCR and their characterization by plasmid profiling, antimicrobial resistance, RAPD and PFGE analyses. Journal of Microbiological Methods, 46(2), 131–139. https://doi.org/10.1016/s0167-7012(01)00269-x

Randall L.P., Lodge M.P., Elviss N.C., Lemma F.L., Hopkins K.L., Teale C.J., Woodford N. 2017. Evaluation of meat, fruit and vegetables from retail stores in five United Kingdom regions as sources of extended-spectrum beta-lactamase (ESBL)-producing and carbapenem-

-resistant Escherichia coli. International Journal of Food Microbiology, 241, 283–290. https://doi.org/10.1016/j.ijfoodmicro.2016.10.036

Robak M., Baranowska K., Barszczewski W., Wojtatowicz M. 2005. RAPD jako metoda różnicowania i identyfikacji drożdży. Biotechnologia, 71(4), 142–155.

Rocha R., Sousa J.M., Cerqueira L., Vieira M.J., Almeida C., Azevedo N.F. 2019. Development and application of Peptide Nucleic Acid Fluorescence in situ Hybridization for the specific detection of Listeria monocytogenes. Food Microbiology, 80, 1–8. https://doi.org/https://doi.org/10.1016/j.fm.2018.12.009

Sanger F., Nicklen S., Coulson A.R. 1977. DNA sequencing with chain-terminating inhibitors. Proceedings of the National Academy of Sciences of the USA, 74, 5463–5467. https://doi.org/10.1073/pnas.74.12.5463

Satyr A., Żmieńko A. 2020. Sekwencjonowanie nanoporowe i jego zastosowanie w biologii. Postępy Biochemii, 66(3), 193–204. https://doi.org/10.18388/pb.2020_328

Scheper T., Belkin S., Gu M.B. 2010. Whole cell sensing systems II. Springer, Berlin.

Schofield D.A., Sharp N.J., Westwater C. 2012. Phage-based platforms for the clinical detection of human bacterial pathogens. Bacteriophage, 2(2), 105–283. https://doi.org/10.4161/bact.19274

Sekora N.S., Lawrence K.S., Agudelo P., van Santen E., McInroy J.A.2009. Using FAME analysis to compare, differentiate, and identify multiple nematode species. The Journal of Nematology, 41(3), 163–173.

Shah Mahmud R., Garifulina K.I., Ulyanova V.V., Evtugyn V.G., Mindubaeva L.N., Khazieva L.R., Dudkina E.V., Vershinina V.I., Kolpakov A.I., Ilinskaya O.N. 2017. Bacteriophages of soil bacilli: A new multivalent phage of Bacillus altitudinis. Molecular Genetics, Microbiology and Virology, 32(2), 87–93. https://doi.org/10.3103/S0891416817020082

Silva D.T., Tejada T.S., Blum-Menezes D., Dias P.A., Timm C.D. 2015. Campylobacter species isolated from poultry and humans, and their analysis using PFGE in southern Brazil. International Journal of Food Microbiology, 217, 189–194. https://doi.org/10.1016/j.ijfoodmicro.2015.10.025

Słomski R. 2008. Analiza DNA. Teoria i praktyka. Wydawnictwo Uniwersytetu Przyrodniczego w Poznaniu, Poznań.

Strydom A., Bester I.M., Cameron M., Franz C.M.A.P., Witthuhn R.C. 2013. Subtyping of Listeria monocytogenes isolated from a South African avocado processing facility using PCR-RFLP and PFGE. Food Control, 31(2), 274–279. https://doi.org/10.1016/j.foodcont.2012.10.029

Shu X., Li Y., Liang M., Yang B., Liu C., Wang Y., Shu J. 2012. Rapid lipid profiling of bacteria by online MALDI-TOF mass spectrometry. International Journal of Mass Spectrometry, 321–322, 71–76. https://doi.org/10.1016/j.ijms.2012.05.016

Szczepańska E., Robak M. 2013. Proteomika w badaniu drobnoustrojów. Acta Scientiarum Polonorum. Biotechnologia, 12, 4, 25–40.

Szemraj J., Szemraj M. 2013. Metody oparte na identyfikacji kwasów nukleinowych obecne w rutynowej diagnostyce mikrobiologicznej. [In:] Diagnostyka bakteriologiczna. Ed. E.M. Szewczyk. PWN, Warszawa, 383–393.

Szymczak B., Sawicki W., Bogusławska-Wąs E., Koronkiewicz A., Dąbrowski W. 2011. Występowanie L. monocytogenes w świeżych owocach i warzywach pochodzących z upraw ekologicznych województwa zachodniopomorskiego. Żywność. Nauka. Technologia. Jakość, 75(2), 67–75.

Tajdar M., Reynders M., Van Praet J., Argudín M.A., Vandecasteele S.J., Nulens E.A. 2019. A case of a surgical-site infection with Staphylococcus condimenti. Infection, 47, 853––856. https://doi.org/10.1007/s15010-019-01276-8

Walczak P., Ołtuszak-Walczak E., Merlak D. 2009. Zastosowanie metody PCR do wykrywania patogenów w żywności. Przemysł Spożywczy, 63(12), 12–15.

Welker M. 2011. Proteomics for routine identification of microorganisms. Proteomics, 11, 3143–3153. https://doi.org/10.1002/pmic.201100049

Węgleński P., Golik P. 2006. Inżynieria genetyczna. [In:] Genetyka molekularna. Ed. P. Węgleński. PWN, Warszawa, 132–140.

Wieczorek K., Osek J. 2005. Przydatność wybranych technik PCR w różnicowaniu termotolerancyjnych szczepów Campylobacter. Żywność. Nauka. Technologia. Jakość, 45(4), 132–138.

Włodarczyk M. 2007. Pozycja filogenetyczna bakterii i zasady ich taksonomii. [In:] Biologia molekularna bakterii. Eds. J. Baj, Z. Markiewicz. PWN, Warszawa, 16–17.

Wojtatowicz M. 2009. Żywność jako środowisko rozwoju drobnoustrojów. [In:] Teoria i ćwiczenia – mikrobiologia żywności. Eds. M. Wojtatowicz, R. Stempniewicz, B. Żarowska. Uniwersytet Przyrodniczy we Wrocławiu, Wrocław, 11–16.

World Health Organization. 2015. WHO estimates of the global burden of foodborne diseases: Foodborne disease burden epidemiology reference group 2007–2015. http://www.who.int/foodsafety/publications/foodborne_disease/fergreport/en/ [accessed: August 25, 2018].

Wróblewska S., Misiewicz A. 2006. Wykrywanie i identyfikacja L. monocytogenes w żywności. Prace Instytutów i Laboratoriów Badawczych Przemysłu Spożywczego, 61, 91–101.

Xufre A., Albergaria H., Inácio J., Spencer-Martins I., Gírio F. 2006. Application of fluorescence in situ hybridisation (FISH) to the analysis of yeast population dynamics in winery and laboratory grape must fermentations. International Journal of Food Microbiology, 108 (3), 376–384. https://doi.org/10.1016/j.ijfoodmicro.2006.01.025

Zadernowska A., Chajęcka-Wierzchowska W., Kłębukowska L. 2014. Fluorescencyjna hybrydyzacja in situ jako alternatywna metoda oznaczania obecności pałeczek Salmonella sp. w mięsie drobiowym. Żywność. Nauka. Technologia. Jakość, 92(1), 92–102.

Ziembińska-Buczyńska A., Kraśnicki K. 2016. Zastosowanie metody PCR-DGGE w mikrobiologii sądowej. Problemy Kryminalistyki, 292(2), 15–21. https://doi.org/10.34836/pk.2016.292.2

Ziarno M. 2007. Osiągnięcia technologii molekularnej stosowane w analizie żywności. Przemysł Spożywczy, 61(11), 33–35.

Zurita J., Yanez F., Sevillano G., Ortega-Paredes D., Pazy Mino A. 2019. Ready-to-eat street food: A potential source fordissemination of multidrug-resistant Escherichia coli epidemic clones in Quito, Ecuador. Letters in Applied Microbiology, 70, 203–209. https://doi.org/10.1111/lam.13263

Żabicka D., Literacka E. 2013. Nowoczesne metody wykrywania i identyfikacji bakterii. Forum Zakażeń, 4(1), 65–72. https://dx.doi.org/10.15374/fz2013009

XIII EVALUATION OF RESEARCH ON GLYCEMIC INDEX OF CARBOHYDRATE FOOD

Dorota LITWINEK

Department of Carbohydrate Technology and Cereal Processing,
Faculty of Food Technology, University of Agriculture in Krakow,
Aleja Mickiewicza 21, 31-120 Krakow, Poland

dorota.litwinek@urk.edu.pl
ORCID: https://orcid.org/0000-0001-7263-1061

Abstract. The term glycemic index (GI) is often used in practical applications by consumers and nutritionists, despite some criticism mainly related to methodology for designation its value. Over the past 40 years, numerous papers have been published worldwide on the methodology of glycemic index indication. The aim of this work is to present the *in vivo* and *in vitro* methods used for determining glycemic index value. The advantages and disadvantages of their use are presented.

The research concerning the concept of starch digestibility and bioavailability is a controversial issue due the different methods applied to study this subject. Although many years have passed, since the introduction of the glycemic index concept, its impact on human health and the prevention of chronic diseases is still in the research phase, and the number of publications in this area has increased significantly. This is related both to the unclear effects on human health of a low glycemic index diet and to methodologies that leave many uncertainties, both for *in vivo* and *in vitro* methods.

The introduction of the International Standard [ISO 26642:2010] for glycemic index determination permits a wide range of choices for researchers when designing a GI testing plan, rather than a single standardized protocol, which can significantly affect the GI results obtained. Despite the advent of the International Organization for Standardization (ISO) method, *in vivo* testing can be difficult to interpret, espe-

cially when comparing results between laboratories due to different standards, different methods of blood glucose analysis (from sample collection to the final result). But with a well-designed test report, inter-laboratory results can give good similarity. Enzyme-kinetic parameters obtained from high-throughput *in vitro* amylolysis assays therefore have potential for rapid prediction of GI for starch-rich foods. Currently, there are no international standards for *in vitro* starch digestibility tests, and methods vary widely. This paper presents the key differences between the most popular methods. It is pointed out that some methods seem to be more suitable for the evaluation of specific foods than others. Therefore, there is a certain necessity to compare results only within samples tested in the same way, which significantly limits the possibility of wide practical use of these analytical methods. A great potential for the use of *in vitro* methods is when testing completely new food products.

Keywords: glycemic index, carbohydrate food, starch digestibility

1. Introduction

Carbohydrates are polyhydroxy aldehydes, ketones, alcohols, acids, their simple derivatives and their polymers having linkages of the acetal type [FAO 1998]. Terminology and classification of carbohydrates remain a difficult issue. The Scientific Update endorsed the primary classification, recommended by the 1997 Expert Consultation, based on chemical form, while acknowledging that classification of carbohydrates based on chemistry should also have dimensions of physical effects (food matrix), functional/physiological effects and health outcomes [Cummings and Stephen 2007]. The chemical classification provides a practical basis for measurement and labeling, but does not allow a simple translation into nutritional effects. Each chemical class of carbohydrate has overlapping physiological properties and health effects. As a result several terms have been used to describe their functional properties [Mann et al. 2007].

The term glycemic index (GI) is often used in practical applications by consumers and nutritionists, despite some criticism mainly in relation to research methodology [Vrolix and Mensink 2010; Wolever 2013; Flavel et al. 2021].

Over the past 40 years, numerous papers have been published worldwide on the methodology of glycemic index determination using both *in vitro* and *in vivo* methods. While the *in vivo* glycemic index method has been standardized and unified by the International Organization for Standardization (ISO), the *in vitro* method is still under development. The aim of this work is to present the *in vivo* and *in vitro* methods used for determining glycemic index value.

2. The idea of the glycemic index

The concept of glycemic index (GI) was introduced in 1981 by Jenkins et al., as a means of classifying different sources of carbohydrate and foods containing carbohydrates, according to their effect on postprandial glycemia. The GI is defined as the postprandial incremental glycemic area after a test meal, expressed as the percentage of the corresponding area after equi-carbohydrate portion of a referenced food [Jenkins et al. 1981].

Dietary carbohydrates are digested and absorbed at different rates and to different extents in the human small intestine, depending on their botanical sources and physical form of the food [Englyst et al. 1999; Bello-Perez et al. 2020]. GI indicates the extent to which the available carbohydrate of a food raises blood glucose level in relation to an equal weight of glucose. It was reasoned that, by expressing the results as a percentage of orally taken with food glucose, any differences between subjects would be normalized; that is, the GI of a food would have the same value in nearly everyone [Wolever 2013].

Hundreds of foods have been tested for GI with the aim of ranking foods within and between food categories. A GI classification system is in common use with which foods are categorized as having low (<55), medium (55–69) or high GI (>70) [Brand-Miller et al. 2003; Atkinson et al. 2008; ISO 26642:2010]. Based on clinical trials conducted shortly after the GI concept was introduced by Jenkins et al. [1981]. FAO/WHO Expert suggested that the concept of GI might provide a useful means to help of the selection of the most appropriate carbohydrate-containing foods for the maintenance of health and the treatment of several diseases [FAO 1998]. Low GI diets have been suggested to protect against diabetes, heart disease, cancer, acne and improve cognition, endurance exercise, weight loss and eye function [Wolever 2013; Flavel et al. 2021]. Not surprisingly, in the last 20 years there has been an abundance of papers related to both the assessment of the impact of a low GI diet on health and the prevention of chronic disease, as well as methods to assess the GI of foods.

Nowadays it is acknowledged that choice of carbohydrate-containing foods should not be based solely on GI since low-GI foods may be energy dense and contain substantial amounts of sugars, fat or undesirable fatty acids that contribute to the diminished glycemic response but not necessarily to good health outcomes. Despite these reservations it does appear that distinguishing between foods with appreciable differences in the indices may produce some benefit in terms of glycemic control in diabetes and lipid management. The benefits demonstrated in randomized-controlled trials are smaller than those conferred by other

dietary and lifestyle changes especially those which facilitate weight loss in the overweight and obese [Mann et al. 2007; Venn and Green 2007]. Nevertheless, new research in this area is still being published and the results are not conclusive [Gangwisch et al. 2020; Vlachos at al. 2020; Toh at al. 2020; Li et al. 2021].

3. Determination of the glycemic index according to ISO 26642:2010 (*in vivo*)

Until 2010, most of glycemic index studies were conducted based on the Jenkins et al. [1981] study and the requirements outlined in the FAO/WHO [1997] report. Although there have been publications aimed at systematizing the methodology [Wolever et al. 1991; Brouns et al. 2005; Venn and Green 2007], but none of them has become permanent. The development of International Standard [ISO 26642:2010] originated from a recognized need to standardization the determination of glycemic index of food for practice and research purposes, particularly with its increasing use as a nutrition claim, illustrating the importance of GI in human nutrition.

The International Standard [ISO 26642:2010] is based on a Joint FAO/WHO Expert Consultation [1998] and the research presented by Wolever et al. [2003, 2008] and Brouns et al. [2005].

The International Standard defines the concept of GI as a "property of the carbohydrate of different foods, specifically the blood glucose-raising ability of the digestible carbohydrates in a given food", noting that GI of food is incremental area under the (blood glucose response) curve (IAUC) after consumption of the carbohydrate portion of a test food expressed as a percentage of the average IAUC response to the same amount of carbohydrate form a reference food taken by the same subject on a separate occasion. Carbohydrate portion mean portion of food containing either 50g of glycemic carbohydrate or if the portion size is unreasonable large 25g of glycemic carbohydrate. The IAUC should be calculated geometrically by applying the trapezoid rule [ISO 26642:2010].

Glycemic index analysis should be performed on products/meal that contain available carbohydrates in an amount that has a significant effect on the blood glucose-raising, the minimum amounts is specified as 10 g or more of glycemic carbohydrate per serving. The GI of heterogeneous food must be tested by the International Standard, not determined by mathematical calculation of GI of individual ingredients or food items. Similarly, re-testing is necessary if the macronutrient composition composition changed as a result changed formulation, and

also when processing method changed concentration, osmolality, acidity or other physical or chemical factor.

Conducting a study requires considerable preparation for the analysis, which is connected with obtaining the appropriate permits from ethical committees available in the country, in addition, subject should be informed of all the details and risks involved in participation and should sign an informed consent form prior to testing. Adequate preparation of the place where: products/meals will be prepared and consumed and blood will be taken.

The International Standard clearly specifies how subjects should be selected (what conditions they should fulfill and what causes their exclusion from the group) that the test should be conducted with a minimum of 10 healthy individuals. Subjects in the study may include people with no known food allergies or intolerances and who are not taking any medication known to affect glucose tolerance. Excluded are people who have known history of diabetes mellitus or use of antihyperglycaemic drugs or insulin, undergone medical or surgical event within 3 months, patients with digestive and nutrient absorption disorders, and those using steroids, protease inhibitors or antipsychotics. However, when planning the study, one should take into account that some subjects may be eliminated at the stage of calculating the results. It happens when singular values are inconsistent with other in the group (GI value for a particular subject that falls outside the range of $\bar{I}_G \pm 2s$; where: $\bar{I}_G$ is the mean value of GI and s is the standard deviation, of a group of all subject).

Although some part of the methodology is very clearly defined, some of the parameters (Table 1) must be selected by the researcher, based on guidelines.

The International Standards recommend a classification of foods as low, medium or high GI, for which respectively GI is less or equal than 55, greater than 55 and less or equal than 70, and greater than 70. This classification is appropriate to food or food items, not for mixed meals.

3.1. Experimental procedure

The period for glycemic index testing should be no longer than 3 months. During this period, the reference food should be tested three times in addition to the foods being tested (tested once); it is acceptable to test the reference food twice. All tests must be conducted on separate days. Tested foods should be in the physical state in which they are normally consumed, in an amount dependent on their glycemic carbohydrate content. When the product is available in various flavor (identical macronutrient composition) it is allowed to testtwo flavors within one group of subjects (at last five subjects test each flavor), but if the two flavors pro-

duce statistically different GI values ($p < 0,05$), the individual flavors should be tested in 10 or more subjects.

Subject in the day of test shall be in the fasting state. They should take no food or drink for 10 h or more, prior to the test. Alcohol intake on the previous evening and vigorous exercise on the morning of the test are prohibited. First, fasting glucose is measured, and this measurement should be taken at least 2 times at a maximum interval of 5 minutes. The average of the values obtained will constitute the baseline blood glucose concentration.

After testing the blood glucose levels, subjects consume a properly prepared product (test food or reference food), it is important that the product is consumed within 12–15 minutes each time (drinking is acceptable (Tab. 1)). Blood samples should be taken at 15, 30, 45, 60 and 120 minutes after consumption of the product. During the 2 hour analysis subject should rest, physical activity is not permitted.

Table 1. Variable parameters in the methodology ISO 26642:2010 (source: own elaboration)

Parameters to selected	Guidelines	Note
Portion of tested and reference food	Portion containing 50 g of glycemic carbohydrate	The smaller portion of carbohydrate can be used for food with lower concentration of carbohydrates, because the portion of the meal that should have been consumed at the time of the test was too large.
	Portion containing 25 g of glycemic carbohydrate	
Referenced food	Anhydrous glucose powder (50 g) dissolved in 250 ml of water and refrigerated	Use of alternative reference food is acceptable provided its content of glycemic carbohydrate is standardized and its GI relative to glucose has been established and verified as consistent by the laboratory using it. Final GI values obtained using reference foods other than glucose shall always be expressed relative to glucose.
	Dextrose (glucose monohydrate, 55 g)	
	Commercial solution used for oral glucose tolerance test containing glucose (50 g)	
	White bread or other specific carbohydrate food of consistent composition and GI, as alternative reference food	

Parameters to selected	Guidelines	Note
Drinks serve with test food	Water	Drinks shall be served in quantities of 250–500 ml for all performed test, always in the same way.
	Coffee	
	Tea (with 30 ml milk and non-nutritive sweetener, if desire)	
Blood samples	Capillary blood (finger prick)	Capillary blood is preferred because of rapid changes in blood glucose immediately after a meal may be identified at finger sites better than at venous whole blood or plasma. GI results derived from capillary blood glucose have been found to be less variable than those obtained via venous sampling.
	Venous whole blood	
	Plasma	
Analysis of blood glucose	Spectrophotometry	Very important is that the laboratory's inter-assay CV (coefficient of variation) on standard solution should be <3,6%. Glucometer devices used for self-blood glucose monitoring have analytical CVs above 3,6 and are therefore not suitable for GI testing.
	Electrochemical detection--coupled enzyme systems	

3.2. Calculation of glycemic index

The results obtained should be worked out individually for each subject and product. Only the average of the GI values of at least 10 subjects constitutes a valid result. Test data shall be analyzed geometrically by applying the trapezoid rule to calculation of incrementally area under the curve (IAUC – area under the curve as the incremental area under blood glucose response curve, ignoring the area beneath the fasting concentration). First, the IAUC of the reference product for each replicate is calculated as the sums of the areas of the triangles and trapezoids, than the mean IAUC of the three repetitions standard deviation and coefficient of variation – CV (as a percentage the ratio of the standard deviation to mean) is calculated. The subject CV for the reference food for the group of subjects tested shall be ≤ 30%, if the mean CV is greater one outlying result for the reference test in each subject can be deleted, if reference food was testing tree times.

For each individual subject, the GI of the test food ($I_{G,t}$) is calculated by:

$$I_{G,t} = \frac{A_t}{\bar{A}_{ref}} \times 100 \quad (1)$$

where A_t is the IAUC of the test food, obtained by the trapezoidal method. The final *GI* of the test food is expressed as the mean *GI* value of 10 or more subjects ±standard error of the mean, as a nearest whole number.

A useful instrument in interpreting the results can also be the analysis of the average blood glucose response curve calculated from the average blood glucose concentration of all subjects at each time point or blood glucose response curve calculated as the absolute blood glucose values or the change in blood glucose values from the fasting values on the ordinate. An important point of the analyzed method is to indicate what exactly should be included in the final test report, because as the international standard indicates, apart from calculating the basic values it is necessary to present the details of the methodology. It is important to show, the amount and content of carbohydrates in the tested product and in the reference product as well as the method of their determination, the portion size and the way of preparing meals and drinks. All these parameters can directly influence the results obtained.

4. *In vitro* digestibility of starch and estimated glycemic index

The number of studies related to *in vitro* GI determination has steadily increased each year. Although the first reports on the possibility of relating the rate of starch digestion to the glycemic index of foods date back to 1992 [Englyst et al. 1992], the real interest in prediction glycemic index based on *in vitro* assays has occurred in the last decade (Fig. 1).

Following an intense period of analytical controversy, a European Concerted Action (EURESTA) was undertaken, confirming that a significant fraction of starch in foods is not digested and absorbed in the small intestine, reaching the colon, where it is fermented to variable extent by the microbiome. This fraction was called resistant starch (RS) [Asp and Björck 1992; Englyst et al. 1992; Bello-Perez et al. 2020]. From that moment, many research groups were interested in the classification of RS types [Englyst et al. 1992; Bello-Perez et al. 2020], methods to determine RS [Goñi et. al. 1996; McCleary et al. 2015]. Starch digestibility is

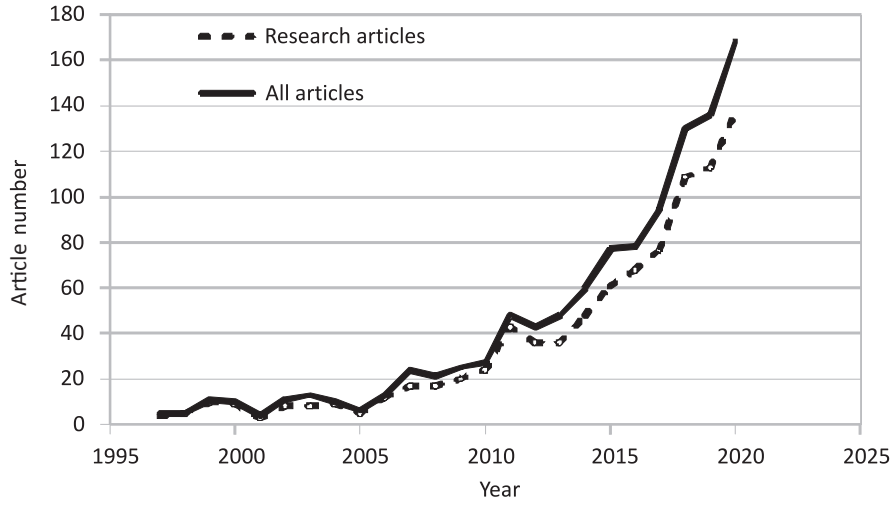

Fig. 1. The increasing number of articles related to glycemic index *in vitro* method (based on Elsevier database)

associated with the proportion of starch that is absorbed in the small intestine. The kinetic component of starch digestion is mainly associated with so-called glycemic index (GI), which has a strong influence on postprandial metabolism. The GI is used to quantify the postprandial blood glucose response to starchy foods and it is a tool for their characterization and classification in terms of the physiological response they elicit [Goñi et al. 1997; Germaine et al. 2008].

Despite the fact that all *in vitro* starch hydrolysis analyses boil down to digestion with appropriately selected enzymes of the tested food product, the way of interpreting the results varies. Analysis of *in vitro* starch digestibility data varies between publications, with some using the percent starch hydrolysis directly like Englyst et al. [1992, 1999] whereas others have selected specific time points in the starch hydrolysis curves [Goñi et al. 1997; Zhang at al. 2019] to predict GI. One approach used to compare starch digestibility curves with *in vivo* results is the hydrolysis index (HI).

4.1. Interpretation of *in vitro* glycemic index by Englyst [1992, 1996, 1999]

The *in vitro* methodology for determination of the rapidly digestible starch (RDS), slowly digestible starch (SDS) and resistant starch (RS) of carbohydrate digestibility fractions was developed and further validated in conjunction with

a series of *in vivo* studies on the rate and extent of starch digestion in the human small intestine [Englyst et al. 1992, 1996, 1999]. This method quantifies the carbohydrate digestibility fractions through enzymatic hydrolysis and measurement of the glucose released. Samples are analyzed "as eaten" with a food matrix fragmentation representative of chewing, followed by an initial acid-protease treatment to simulate gastric conditions. The subsequent amylolytic hydrolysis phase was designed to use an excess of pancreatic enzymes, overcoming variability introduced by enzyme activity or sample amount. Conforming to these principles ensures reproducible measures of: RDS as the glucose release after incubation for 20 min adjusted for any sugar glucose present; SDS as the additional glucose release by 120 min incubation; and RS as the remaining starch [Englyst et al. 1992, 1999].

On the basis of these data, Englyst et al. [1992] proposed to calculate the Starch Digestible Index (SDI) (% fast digestible starch to total starch) as a measure of relative rate of starch digestion:

$$SDI = \frac{RDS}{TotalStarch} \times 100 \tag{2}$$

At the same paper, they showed a significant correlation between the SDI and GI determined by the *in vivo* method. This approach seems to be fully justified in the case of analysis of high-starch products, which contain little simple sugars. Therefore, the next step in the analysis of the effect of consumed carbohydrates on postprandial blood glucose concentration was the determination of rapidly available glucose (RAG) as the glucose measured after 20 min incubation with pancreatin, amyloglucosidase and invertase. RAG represents the actual amount of glucose that will be rapidly assimilated by the body, this value is determined in g/100g food [Englyst et al.1999]. Since the RAG value relates to the food as eaten and includes both RDS and free sugar glucose, it should be a better indicator of blood glucose and insulin response than SDI. The great advantage is that this parameter can be successfully used to analyze foods rich in such sugars as fruits and vegetables containing in their composition; there are very often large amounts of precisely glycemic carbohydrates. Moreover, this value is even better correlated with high-starch products than SDI itself.

Like the glycemic index, the SDI reflects the rate of digestion of the starch present in the food, but it does not give any information about actual amount of glucose likely to be rapidly available from the food. The RAG appears to be a simple-to-use indicator of the amount of glucose rapidly available, and it may be a useful adjunct to the GI results determined *in vivo* and an important tool in

the management of diabetic patients and dietitians [Englyst et al. 1999]. Thus, it is not entirely explainable that for products containing significant amounts of sugars, it is more common to determine only the SDI [Zhang at al. 2019; Muttagi and Ravindra 2020; Rajkumar et al. 2020] and not the SDI and RAD [Srigiripura at al. 2019] to determine the body's response to the product consumed.

4.2. Interpretation of *in vitro* glycemic index by Goñi et al. [1997]

A non-linear model established by Goñi et al. [1997] is applied to describe the kinetics of starch hydrolysis. The first order equation has the form:

$$C = C_{\infty}\left(1 - e^{-kt}\right) \tag{3}$$

where: C corresponds to the percentage of starch hydrolyzed at time t, C_{∞} is the equilibrium percentage of starch hydrolyzed after 180 min, k is the kinetic constant and t is the time (min). The parameters C_{∞} and k were estimated for each food products and each treatment based on the data obtained from the *in vitro* hydrolysis procedure. The *AUC* was calculated as the integral of the kinetic equation, and used to obtain the HI for each food. The HI is calculated as the area under the hydrolysis curve (*AUC*) for the test food, as a percentage of the corresponding area under the curve (AUC_{ref}) for reference wheat bread.

Goñi et al. [1997] showed this hydrolysis index to be a good predictor of glycemic response. Expected GI was thus estimated using the model:

$$GI = 39.71 + (0.549\ HI) \tag{4}$$

In this model, the linear correlation between *in vivo* glycemic response and *in vitro.* Hydrolysis Index (HI) was 0.894 ($p \leq 0.05$), but the best correlated value with *in vivo* glycemic responses was the percentage of starch hydrolysis at 90 min (0.909, $p \leq 0.05$) estimated using the model:

$$GI = 39.21 + 0.803\ (H_{90}) \tag{5}$$

where: H_{90} is percentage of total starch hydrolyzed at 90 min.

4.3. Experimental procedure

There are currently no international standards for *in vitro* starch digestibility testing and methods vary widely. Key differences between published methods include variations in the initial preparation of food, amounts and types of enzymes used and incubation using non-restricted (test tube) versus restricted (dialysis) systems. Method of determination of sugars, reporting of results and predicted glycemic response also varies (Tab. 2). Of these methods, some appear more appropriate for evaluating specific food types than others.

Despite recent advances in developing *in vitro* methods to assess carbohydrate digestibility, there is an obvious need to design a standardized batch gastrointestinal digestion method based on physiologically relevant conditions. The use of mammalian digestive enzymes should be prioritized over the use of microbial enzymes since the former better reflect the carbohydrase activities of enzymes of the human gastrointestinal tract [Hernandez-Hernandez et al. 2019].

5. Advantages and disadvantages of *in vitro* and *in vivo* studies

Glycemic index testing is one of the better known one analytical methods to determine the effects of food on the human body. However, it should be recognized that these methods are not fully standardized despite their great popularity [Wolever et al. 2008; Yu et al. 2018; Hernandez-Hernandez et al. 2019]. The introduction of the International Standard [2010] for glycemic index determination permits a wide range of choices for researchers when designing a GI testing plan, rather than a single standardized protocol, which can significantly affect the GI results obtained. That suggests the international standard has assisted with framing the general parameters of GI testing, further standardization of testing procedures is still required to ensure the continued relevance of the GI to clinical nutrition [Flavel et al. 2021].

More inaccuracies arise in the determination of starch digestibility and *in vitro* prediction of GI. With the development of enzyme-based methods [Hernandez-Hernandez et al. 2019], it seems necessary to systematize this analysis as soon as possible, which would certainly make it possible to definitively confirm or negate the relationship between these methods. Since the current state of knowledge is not clear and require further research [Ferrer-Mairal et al. 2012; Bellmann et al. 2018; Bohn et al. 2018].

Table 2. Variable parameters in the *in vitro* starch digestibility methodology (source: own elaboration)

Parameters to selected	Applied solutions	References
Sample preparation	Homogenized in liquid medium	Goñi et al. [1997]
	Breakdown using chewing	Holm and Björck [1992]; Germaine et al. [2008]
	Mincing	Englyst et al. [1992, 1996, 1999]; Germaine et al. [2008]; Regand et al. [2011]; Muttagi and Ravindra [2020]
	Mincing with amylase	Germaine et al. [2008]
	Rotary mixer with PBS	Edwards et al. [2019]
	Not presented	Zhang et al. [2020]
Amounts and type of enzyme	Pepsin, α-amylase (type VIB)	Goñi et al. [1997]
	Pepsin, amylase (type XIII-A)-during mincer, pancreatic amylase (Type I-A) – during incubation	Germaine et al. [2008]
	Pepsin, Porcine pancreatin, amyloglucosidase	Regand et al. [2011]
	Amyloglucosidase, invertase, pancreatin, pullulanase	Englyst et al. [1992, 1999]; Muttagi and Ravindra [2020]; Zhang et al. [2020]
	porcine pancreatic α-amylase	Edwards et al. [2019]
Incubation method	Shaking water bath, inactivation enzyme at 100°C – 5 minut	Goñi et al. [1997]; Germaine et al. [2008]
	Restricted system, inactivation enzyme at 100°C – 5 minut	Germaine et al. [2008]
	Shaking water bath with glass beads, inactivation enzyme with ethanol	Regand et al. [2011]
	Shaking water bath with glass beads and guar gum, inactivation enzyme with ethanol	Englyst eta al. [1992, 1999]; Muttagi and Ravindra [2020]; Zhang et al. [2020]
	Rotary mixer, 0.3 M inactivation enzyme with Na_2CO_3, pH 9	Edwards et al [2019]

Table 2. cont.

Parameters to selected	Applied solutions	References
Method for the determination of sugars	The glucose oxidase-peroxidase assey	Goñi et al. [1997]; Englyst et al. [1992]; Regand et al. [2011]; Zhang et al. [2019]; Muttagi and Ravindra [2020]
	3,5-dinitrosalicyclic method	Germaine et al. [2008]
	HPLC	Englyst et al. [1999]
	PAHBAH assay	Edwards et al. [2019]
The way of interpreting the results	HI and predicted GI	Goñi et al. [1997]; Germaine et al. [2008]; Edwards et al. 2019
	Starch Digestible Index (SDI)	Englyst et al. 1992, 1999; Regand et al. 2011; Muttagi and Ravindra [2020]; Zhang et al. [2019]

Even if similar trends in the rate of starch digestion are observed [Ferrer-Mairal et al. 2012], it should be taken into account that a range of intrinsic and extrinsic factors that alter the rate of gastrointestinal motility, digestion, and absorption also influence the GI, and these cannot always be predicted using an *in vitro* model [Jenkins 2007].

Measurement of GI requires the use of human subjects for evaluation of the 2 h blood glucose response after food intake. This resource intensive, physiological test is not suitable for new food product development or quality assurance. *In vitro* testing has been proposed as a faster, more cost effective method of screening food products for their predicted GI during product development, prior to selection of optimized products for *in vivo* GI testing [Brand-Miller and Holt 2003; Jenkins 2007; Bellmann et al. 2018].

6. Conclusion

The research concerning the concept of starch digestibility and bioavailability is a controversial issue due the different methods applied to study this subject. Although 40 years have passed since the introduction of the glycemic index concept, its impact on human health and the prevention of chronic diseases is still in the research phase, and the number of publications in this area has increased

significantly. This is related both to the unclear effects on human health of a low-GI diet and to methodologies that leave many uncertainties, both for *in vivo* and *in vitro* methods.

Despite the advent of the ISO method, *in vivo* testing can be difficult, especially when comparing results between laboratories due to different standards, different methods of blood glucose analysis (from sample collection to the final result). But with a well-designed test report, inter-laboratory results can give good similarity.

Enzyme-kinetic parameters obtained from high-throughput *in vitro* amylolysis assays therefore have potential for rapid prediction of GI for starch-rich foods. However, the methodology should be standardized internationally. At present, there is a certain necessity to compare results only within samples tested at the same time, which significantly limits the possibility of wide practical use of these analytical methods.

References

Asp N.G., Björck I. 1992. Resistant starch. Trends in Food Science and Technology, 3, 111–114. https://doi.org/10.1016/0924-2244(92)90153-N

Atkinson F.S., Foster-Powel K., Brand-Miller J.C. 2008. International tables of glycemic index and glycemic load values: 2008. Diabetes Care, 31(12), 2281–2283. https://doi.org/10.2337/dc08-1239

Bellmann S., Minekus M., Sanders P., Bosgra S., Havenaar R. 2018. Human glycemic response curves after intake of carbohydrate foods are accurately predicted by combining in vitro gastrointestinal digestion with in silico kinetic modeling. Clinical Nutrition Experimental, 17, 8–22. https://doi.org/10.1016/j.yclnex.2017.10.003

Bello-Perez L.A., Flores-Silva P.C., Agama-Acevedo E., Tovar J. 2020. Starch digestibility: past, present, and future. Journal of the Science of Food and Agriculture, 100(14), 5009–5016. https://doi.org/10.1002/jsfa.8955

Bohn T., Carriere F., Day L., Deglaire A., Egger L., Freitas D., Dupont D. 2018. Correlation between in vitro and in vivo data on food digestion. What can we predict with static in vitro digestion models? Critical Reviews in Food Science and Nutrition, 58(13), 2239–2261. https://doi.org/10.1080/10408398.2017.1315362

Brand-Miller J.C., Thomas M., Swan V., Ahmad Z.I., Petocz P., Colagiuri S. 2003. Physiological validation of the concept of glycemic load in lean young adults. The Journal of Nutrition, 133(9), 2728–2732. https://doi.org/10.1093/jn/133.9.2728

Brouns F., Bjorck I., Frayn K.N., Gibbs A.L., Lang V., Slama G., Wolever T.M.S. 2005. Glycaemic index methodology. Nutrition Research Reviews, 18(1), 145–171. https://doi.org/10.1079/NRR2005100

Cummings J.H., Stephen A.M. 2007. Carbohydrate terminology and classification. European Journal of Clinical Nutrition, 61 (Suppl. 1), S5–S18. https://doi.org/10.1038/sj.ejcn.1602936

Edwards C.H., Cochetel N., Setterfield L., Perez-Moral N., Warren F.J. 2019. A single-enzyme system for starch digestibility screening and its relevance to understanding and predicting the glycaemic index of food products. Food & Function, 10(8), 4751–4760. https://doi.org/10.1039/C9FO00603F

Englyst H.N., Kingman S.M., Cummings J.H. 1992. Classification and measurement of nutritionally important starch fractions. European Journal of Clinical Nutrition, 46, S33–S50.

Englyst H.N., Veenstra J., Hudson G.J. 1996. Measurement of rapidly available glucose (RAG) in plant foods: A potential in vitro predictor of the glycaemic response. British Journal of Nutrition, 75(3), 327–337. https://doi.org/10.1079/BJN19960137

Englyst K.N., Englyst H.N., Hudson G.J., Cole T.J., Cummings J.H. 1999. Rapidly available glucose in foods: An in vitro measurement that reflects the glycemic response. The American Journal of Clinical Nutrition, 69(3), 448–454. https://doi.org/10.1093/ajcn/69.3.448

FAO 1998. Carbohydrates in Human Nutrition. Report of a Joint FAO/ WHO Expert Consultation (FAO Food and Nutrition Paper 66). Food and Agriculture Organization, Rome.

Ferrer-Mairal A., Penalva-Lapuente C., Iglesia I., Urtasun L., De Miguel-Etayo P., Remón S., Moreno L.A. (2012). In vitro and in vivo assessment of the glycemic index of bakery products: Influence of the reformulation of ingredients. European Journal of Nutrition, 51(8), 947–954. https://doi.org/10.1007/s00394-011-0272-6

Flavel M., Jois M., Kitchen B. 2021. Potential contributions of the methodology to the variability of glycaemic index of foods. World Journal of Diabetes, 12(2), 108. https://dx.doi.org/10.4239/wjd.v12.i2.108

Gangwisch J.E., Hale L., St-Onge M.P., Choi L., LeBlanc E.S., Malaspina D., Lane D. 2020. High glycemic index and glycemic load diets as risk factors for insomnia: analyses from the Women's Health Initiative. The American Journal of Clinical Nutrition, 111(2), 429–439. https://doi.org/10.1093/ajcn/nqz275

Germaine K.A., Samman S., Fryirs C.G., Griffiths P.J., Johnson S.K., Quail K.J. 2008. Comparison of in vitro starch digestibility methods for predicting the glycaemic index of grain foods. Journal of the Science of Food and Agriculture, 88(4), 652–658. https://doi.org/10.1002/jsfa.3130

Goñi I., Garcia-Diz L., Mañas E., Saura-Calixto F. 1996. Analysis of resistant starch: A method for foods and food products. Food Chemistry, 56(4), 445–449. https://doi.org/10.1016/0308-8146(95)00222-7

Goñi I., Garcia-Alonso A., Saura-Calixto F. 1997. A starch hydrolysis procedure to estimate glycemic index. Nutrition Research, 17(3), 427–437. https://doi.org/10.1016/S0271-5317(97)00010-9

Hernandez-Hernandez O., Olano A., Rastall R.A., Moreno F.J. 2019. In vitro digestibility of dietary carbohydrates: Toward a standardized methodology beyond amylolytic and microbial enzymes. Frontiers in Nutrition, 6, 61. https://doi.org/10.3389/fnut.2019.00061

Holm J., Björck I. 1992. Bioavailability of starch in various wheatbased bread subjects and rate and extent of in vitro starch digestion. The American Journal of Clinical Nutrition, 55, 420–429. https://doi.org/10.1093/ajcn/55.2.420

ISO 26642:2010. Food Products – Determination of the glycaemic index (GI) and recommendation for food classification.

Jenkins A.L. 2007. The glycemic index: Looking back 25 years. Cereal Foods World, 52(2), 50–53. https://dx.doi.org/10.1094/CFW-52-1-0050

Jenkins D.J.A., Wolever T.M.S., Taylor R.H., Barker H., Fielden H., Baldwin J.M., Goff D.V. 1981. Glycemic index of foods: A physiological basis for carbohydrate exchange. The American Journal of Clinical Nutrition, 34(3), 362–366. https://doi.org/10.1093/ajcn/34.3.362

Li M., Cui Z., Meng S., Li T., Kang T., Ye Q., Meng H. 2021. Associations between dietary glycemic index and glycemic load values and cardiometabolic risk factors in adults: Findings from the China health and nutrition survey. Nutrients, 13(1), 116. https://doi.org/10.3390/nu13010116

Mann J., Cummings J.H., Englyst H.N., Key T., Liu S., Riccardi G., Wiseman M. 2007. FAO/WHO scientific update on carbohydrates in human nutrition: Conclusions. European Journal of Clinical Nutrition, 61(1), S132–S137. https://doi.org/10.1038/sj.ejcn.1602943

McCleary B.V., Sloane N., Draga A. 2015. Determination of total dietary fibre and available carbohydrates: A rapid integrated procedure that simulates in vivo digestion. Starch--Stärke, 67(9–10), 860–883. https://doi.org/10.1002/star.201500017

Muttagi G.C., Ravindra U. 2020. Effect of storage on in vitro starch digestibility of functional foods. European Journal of Nutrition & Food Safety, 87–97. https://doi.org/10.9734/ejnfs/2020/v12i830273

Rajkumar P.S., Suriyamoorthy P., Moses J.A., Anandharamakrishnan C. 2020. Mass transfer approach to in vitro glycemic index of different biscuit compositions. Journal of Food Process Engineering, 43(12), e13559. https://doi.org/10.1111/jfpe.13559

Regand A., Chowdhury Z., Tosh S.M., Wolever T.M., Wood P. 2011. The molecular weight, solubility and viscosity of oat beta-glucan affect human glycemic response by modifying starch digestibility. Food Chemistry, 129(2), 297–304. https://doi.org/10.1016/j.foodchem.2011.04.053

Srigiripura C.V., Kotebagilu N.P., Urooj A. 2019. In vitro starch and protein digestibility of disease specific nutrition formulations. Current Research in Nutrition and Food Science Journal, 7(1), 66–74. https://dx.doi.org/10.12944/CRNFSJ.7.1.07

Toh D.W.K., Koh E.S., Kim J.E. 2020. Lowering breakfast glycemic index and glycemic load attenuates postprandial glycemic response: a systematically searched meta-analysis of randomized controlled trials. Nutrition, 71, 110634. https://doi.org/10.1016/j.nut.2019.110634

Venn B.J., Green T.J. 2007. Glycemic index and glycemic load: Measurement issues and their effect on diet–disease relationships. European Journal of Clinical Nutrition, 61(1), S122––S131. https://doi.org/10.1038/sj.ejcn.1602942

Vlachos D., Malisova S., Lindberg F.A., Karaniki G. 2020. Glycemic index (GI) or glycemic load (GL) and dietary interventions for optimizing postprandial hyperglycemia in patients with T2 diabetes: A review. Nutrients, 12(6), 1561. https://dx.doi.org/10.3390%2Fnu12061561

Vrolix R., Mensink R.P. 2010. Variability of the glycemic response to single food products in healthy subjects. Contemporary Clinical Trials, 31(1), 5–11. https://doi.org/10.1016/j.cct.2009.08.001

Wolever T.M.S. 2013. Is glycaemic index (GI) a valid measure of carbohydrate quality? European Journal of Clinical Nutrition, 67(5), 522–531. https://doi.org/10.1038/ejcn.2013.27

Wolever T.M., Brand-Miller J.C., Abernethy J., Astrup A., Atkinson F., Axelsen M., Zhang J. 2008. Measuring the glycemic index of foods: Interlaboratory study. The American Journal of Clinical Nutrition, 87(1), 247S–257S. https://doi.org/10.1093/ajcn/87.1.247s

Wolever T.M., Jenkins D.J., Jenkins A.L., Josse R.G. 1991. The glycemic index: Methodology and clinical implications. The American Journal of Clinical Nutrition, 54(5), 846–854. https://doi.org/10.1093/ajcn/54.5.846

Wolever T.M.S., Vorster H.H., Björck I., Brand-Miller J., Brighenti F., Mann J.I., Wu X. 2003. Determination of the glycaemic index of foods: Interlaboratory study. European Journal of Clinical Nutrition, 57(3), 475–482. https://doi.org/10.1038/sj.ejcn.1601551

Yu W., Tao K., Gilbert R.G. 2018. Improved methodology for analyzing relations between starch digestion kinetics and molecular structure. Food Chemistry, 264, 284–292. https://doi.org/10.1016/j.foodchem.2018.05.049

Zhang Y., Zhang Y., Li B., Wang X., Xu F., Zhu K., Li S. 2019. In vitro hydrolysis and estimated glycemic index of jackfruit seed starch prepared by improved extrusion cooking technology. International Journal of Biological Macromolecules, 121, 1109–1117. https://doi.org/10.1016/j.ijbiomac.2018.10.075

XIV DIFFICULTIES IN OBJECTIVE COMPARISON OF ANTIOXIDANT ACTIVITY RESULTS

Joanna KAPUSTA-DUCH

Department of Human Nutrition and Dietetics,
Faculty of Food Technology, University of Agriculture in Krakow,
Aleja Mickiewicza 21, 31-120 Krakow, Poland

joanna.kapusta-duch@urk.edu.pl
ORCID: https://orcid.org/0000-0003-3882-2483

Abstract. An extensive use of assays for the evaluation of antioxidant activity of food products, caused that DPPH, ABTS, ORAC, CUPRAC, TRAP, DMPD, CBA, LPIC, CRA and FRAP acronyms are today commonly used words in scientific publications, papers and internet websites. These methods are characterized by great diversity and none of the methods developed so far has been recognized as the standard method. This study compares the basic methods for the determination of antioxidant activity. The advantages and disadvantages of each of them are also presented, as well as the main causes of difficulties in their standardization. There is huge potential in this research field to develop novel analytical methods to determine the antioxidant capacity in foods products, but also in material of biological origin.

Keywords: determination of antioxidant activity, oxidative stress, *in vitro* and *in vivo* assays, HAT (hydrogen atom transfer) mechanism, SET (single electron transfer) mechanism

1. Introduction

In the etiopathogenesis of many diseases, including cancer, an important role is attributed to the damage caused by reactive oxygen species (ROS), reactive nitrogen species (RNS) and other free radicals. According to the chemoprevention principle, it is assumed that the use of compounds with antioxidant properties may prevent the development of cancer at the initiation and promotion stages. Antioxidants can be defined as reducing and/or anti-radical substances that counteract ROS-induced damage in cells. The role of antioxidants is not limited to inactivation of free radicals, but also involves mechanisms of induction of cytoprotective proteins in the cell, including antioxidant enzymes, enzymes catalyzing glutathione synthesis, and others involved in repair of oxidative damage [Matschke et al. 2019; Sies and Jones 2020].

Reactive oxygen species are defined as products of incomplete reduction of an oxygen molecule, both neutral molecules or ions and oxygen free radicals. A radical is a group of atoms that behave as a single entity, whereas a free radical is an atom or molecule that can exist by itself and has one or more unpaired electrons [Ifeanyi et al. 2018]. Reactive oxygen species are necessary for the proper body functioning. They act as signal transmitters, regulate cellular repair processes and gene expression as well as take part in metabolic processes, redox reactions in the respiratory chain, regeneration of high-energy compounds (ATP), and oxygen transport by haemoglobin. They also activate cytochrome P450 and phagocytosis of microorganisms [Bou-Fakhredin et al. 2021]. However, they can also exert harmful effect [Ali et al. 2020]. Excess ROSs cause a state of oxidative stress leading to damage to cell components and cell dysfunction, including oxidation of low molecular compounds (glutathione, ascorbate), collagen degradation, depolymerization of hyaluronic acid, oxidation of haemoglobin, and inactivation of enzymes and transport proteins. This also results in damage of DNA and chromosomes, peroxidation of cell membrane lipids, erythrocyte degradation, disorders of intracellular Ca^{2+} ion homeostasis, modification of antigenic properties of cells, platelet aggregation, changes in cell morphology, mutation formation, and neoplastic cell transformation. The effect of reactive oxygen species on cells depends to a large extent on their concentration and exposure time [Galadari et al. 2017]. Low concentration of ROSs has physiological functions, while higher concentration leads to cell damage and the development of many diseases. As a result of oxidative modification of lipids, proteins and DNA, homeostasis is disturbed leading to cellular death through apoptosis or necrosis [Ali et al. 2020].

2. Characteristics of basic methods for the determination of antioxidant activity

In food analysis, many analytical methods are used to provide information about the antioxidant properties in foods [Durazzo 2017]. *In vitro* studies employ the ability of antioxidants to deactivate free radicals. These reactions may follow mechanisms:

- hydrogen atom transfer (HAT),
- single electron transfer (SET).

However, taking into account the measurement system used, these methods can be divided into:

- additive,
- post-additive.

Using additive methods, the delay in the onset of the oxidant action on the indicator antioxidant is determined. The delay is due to the earlier, easier, competitive oxidation of the sample antioxidants. Its magnitude is an indicator of the magnitude of antioxidant activity. These methods mimic the protective processes taking place in living organisms.

Post-additive methods determinate activity by measuring the change in concentration of the test reagent or a product as a result of a direct chemical or radical reaction between an oxidant (molecular or radical) and antioxidants present in the sample [Grajek 2007; Cybul and Nowak 2008; Capanoglu et al. 2018].

3. Basic differences between various methods

3.1. Methods using SET-type mechanism

In the SET-type methods, the antioxidants activity or capacity is determined spectrophotometrically by their ability to reduce a fluorescent or colored probe (oxidizing agent/ oxidant/substrate) [Siddeeg et al. 2021]. The change in absorbance as a function of the concentration of antioxidant in the sample is a linear relationship, while the slope of the line reflects the reducing ability of the antioxidant present in the sample. Generally, the antioxidant reactivity during the SET assay depends mainly on two major antioxidant functional group preterits namely, the ionization and deprotonation potentials. Under acidic pH, the protonation

on the antioxidant is increased leading to a decrease in the ionization potential and so suppressing the overall antioxidant reducing abilities. The results obtained are often converted into Trolox equivalents, as TEAC (Trolox Equivalent Antioxidant Capacity). In these analyses, Trolox, which is a synthetic, water-soluble vitamin E derivative with high antioxidant activity, serves as a reference material [Arts et al. 2004; Cybul and Nowak 2008; Moharram and Youssef 2014].

3.1.1. DPPH Assay

The DPPH methods depend on measuring the scavenging potential of certain antioxidants by using the synthetic-free radical generator, DPPH (2,2-diphenyl-1-picrylhydrazyl) [Prior et al. 2005]. DPPH is a relatively long-lasting free radical and can therefore be easily prepared for the analysis. Upon reacting with the H^+donating antioxidant, the reduction in DPHH to hydrazine leads to a reduction in the absorbance of the reaction as measured at 515–517 nm [Kedare and Singh 2011]. The reaction also results in an obvious discoloration from purple to yellow. The degree in the absorbance decrease, as well as, in discoloration correlates with the H^+-donating abilities, concentration, and activity of the antioxidant in the sample. At the practical levels, the DPPH assay is conducted by mixing certain volumes of the samples with a certain volume DPPH solution followed by incubation at room temperature and reading the tubes at 515–517 nm. The reaction medium for this assay should preferably be alcoholic (ethanol or methanol) to avoid processes of aggregation of the stable radical. [Grajek 2007; Cybul and Nowak 2008; Siddeeg et al. 2021]. In order to facilitate the interpretation of the results, the efficient concentration (EC_{50}) has been introduced, which is defined as the concentration of antioxidant required to obtain a 50% antioxidant effect. The percentage of remaining unreduced DPPH radical is inversely proportional to the antioxidant concentration in the sample. In turn, the time needed to reduce the value of the initial DPPH radical concentration by 50% is graphically determined from the curve reflecting kinetics of reaction and is referred to as the T_{EC50} parameter [Molyneux 2004; Bartoń et al. 2005; Grajek 2007; Cybul and Nowak 2008].

The DPPH assay is a fast, simple, accurate, comparable and reproducible method. It proved to be effective in evaluating the antioxidant properties of lithium, sodium, potassium, rubidium and cesium alkali metal salts complexed with chlorogenic acid. This method is widely used to measure the antioxidant capacity of natural raw materials and food; metal-based nanocomposites for applications as nano-antioxidants and several metal complexes. It is particularly often used to determine the antioxidant properties of phenolic compounds

[Nenadisand Tsimidou 2002; Cybul and Nowak 2008; Frezzini et al. 2019; Marchi et al. 2022].

The main limitation to the method lies in the absorption range of the DPPH radical, which occurs in a visible region where several antioxidants also absorb, possibly hindering detection of the end of the reaction between DPPH and the antioxidant [Marchi et al. 2022]. During measurements, the access of light and oxygen to the sample should be limited, and the pH and solvent should be carefully selected, as all these factors are responsible for a decrease in the absorbance of the DPPH solution [Kedare and Singh 2011]. Another limitation is that DPPH dissolves only in organic solvents that does not allow the determination of hydrophilic antioxidants [Yeo and Shahidi 2019; Cybul and Nowak 2008].

3.1.2. ABTS Assay

The use of the ABTS [2,2'-azino-bis(3-ethylbenzothiazoline-6-sulfonic acid)] reagent enables the measurement of the total antioxidant activity of samples. It has a broad range of tested materials, including body fluids and food samples. The ABTS assay is a test that directly measures the quantity of H_2O_2 in the sample or to reflect the activity of H_2O_2-producing enzymes [Roginsky and Lissi 2005]. At the practical levels, an ABTS working reagent is prepared by mixing equal quantities of freshly prepared 7 mM ABTS solution with 2.45 mM potassium persulphate solution [Siddeeg et al. 2021]. The oxidation of ABTS occurs immediately. The maximum absorbance and full stability of the radical are obtained after 6 hours. The radicals generated during the reaction are blue-green in color and show maximum absorbance at several wavelengths: 417, 645, 734 and 815 nm. Antioxidants reduce the cation radical to a degree depending on the length of the reaction, the concentration of the antioxidant and its activity [Cybul and Nowak 2008]. The solution becomes discolored and decrease in color intensity is proportional to the antioxidants content in the solution) (expressed as the number of Trolox equivalents per unit volume or mass of the sample). This method also enables the measurement of reaction kinetics based on lag time. This is the time delay in the initiation of the ABTS radical oxidation by the addition of an antioxidant. The length of the lag time is proportional to the concentration of the examined antioxidant. The radical scavenging potential (activity) of ABTS in the sample (percent of inhibition) is evaluated from the standard curve [Osman et al. 2006; Grajek 2007; Cybul and Nowak 2008; Marchi et al. 2022].

The $ABTS^+$ is a stable radical that produces colored green solutions that rapidly react with the antioxidants [Marchi et al. 2022]. The ABTS assay performance makes it a routine and simple analysis used to determine the antioxidant capacity

of both hydrophobic and hydrophilic antioxidant samples. Additional advantages are high rate of the reaction between ABTS cation radical and antioxidants as well as the ABTS solubility, both in water buffers (with various pH) and in organic solvents [Cybul and Nowak 2008].

The result depends on the reaction time; the reaction must be kept in the dark to avoid false values [Marchi et al. 2022]. During the reaction of ABTS with flavonoids (such as luteolin and chrysin) products are formed with stronger antioxidant properties and faster reacting with the radical than the parent compounds. The Trolox equivalent antioxidant capacity is then the sum of the activity of the examined substance and the products of its reaction with the radical and this may cause falsification of analytical results due to overestimation of the antioxidative properties [Arts et al. 2004; Cybul and Nowak 2008].

3.1.3. DMPD Assay

The method using the N,N-dimethyl-ρ-phenylenediamine (DMPD) compound is also classified under discoloration methods, i.e. methods based on the measurement of the degree of discoloration of a reagent solution [Cybul and Nowak 2008]. In the availability of Fe^{3+} and under acidic conditions, DMPD produces a highly reactive radical, $DMPD^{+}$ radical that has a stable purple color which can be detected at 514 nm. This radical can scavenge the antioxidant in the sample (AOH) which transfers an electron to the $DMPD^{+}$ radical, thus decoloring the solution. Therefore, the decrease in the light intensity (absorbance) is correlated negatively with the concentration of the antioxidant in the sample [Siddeeg et al. 2021].

The proposed initial concentration of 1 mM DMPD solution with absorbance values in the range of 0.8–1.0 guarantees high sensitivity of the measurements as well as the optimal range of oxidant inhibition. The analyzed sample is added after the free radicals are formed. Antioxidants quench the color that results in, proportional to their amount and activity in the sample, discoloration of the solution. The antioxidant capacity of the samples is driven by the Trolox standard curve [Grajek 2007; Cybul and Nowak 2008; Siddeeg et al. 2021].

However, since the plasma contains high levels of Fe^{3+}, this method is not recommended to detect the antioxidant capacity in this blood fraction The disadvantage of this method is its low specificity [Siddeeg et al. 2021].

3.1.4. FRAP Assay

Ferric reducing antioxidant power (FRAP) assay is a widely used method that uses antioxidants as reductants in a redox-linked colorimetric reaction, wherein Fe^{3+} is reduced to Fe^{2+}. Ferric (Fe^{3+}) to ferrous (Fe^{2+}) ion reduction at low pH causes

formation of a colored ferrous-probe complex from a colorless ferric-probe complex. As a result, color of the substrate changes and the colorless reagent converts to intensely blue product with an absorption maximum at 593–595 nm. The sample antioxidant capacity is determined by comparing the change in absorbance of the analyzed sample with the value of the Fe^{2+} standard solution. Absorbance is changing linearly over a wide range and the determined value of the sample is directly proportional to the antioxidant concentration [Firuzi et al. 2005; Cybul and Nowak 2008].

This method is highly reproducible, sensitive, rapid and lowcost. It can measure the combined activity of redox-active antioxidants in a food, or in plasma or urine following ingestion of a food [Marchi et al. 2022].

The pH assay requires acidic conditions (pH 3.6) and the antioxidants with redox potential lower than that of the redox pair Fe^{3+}/Fe^{2+} can reduce the Fe^{3+}, leading to a false result [Marchi et al. 2022]. FRAP results might vary depending on the analysis time as observed for the reaction between antioxidants and Fe^{3+}, which ranged from several minutes to several hours. Therefore, a single-point absorption end point may not represent a complete reaction, since different antioxidants require different reaction times for detection [Prior et al. 2005; Pastor et al. 2020].

3.1.4.1. CRA Assay

The copper reduction assay (CRA) and CUPRAC (the cupric ion reducing antioxidant capacity) are the variants of the FRAP method. The difference is that instead of iron, another ions are reduced. Due to the presence of antioxidants in the sample, the Cu^{2+} complex is reduced to a colored copper Cu^{+1} complex and its absorption is then measured. In this method the bathocuproine (2,9-dimethyl-4,7-diphenyl-1,10-phenanthroline) is used, which forms an orange complex with copper Cu^{+1}. This complex is a chromophore with a maximum absorbance at 490 nm [Apak et al. 2004; Cybul and Nowak 2008].

3.1.4.2. CUPRAC Assay

The cupric ion reducing antioxidant capacity (CUPRAC) measures the antioxidant potential of a sample by measuring the rate of conversion of Cu^{+2} to Cu^{+1} in the presence of neocuproine (Nc) or athocuproine (BC) (chelating agents). In the test, the chelators complex with the Cu^{+1} containing compound to yield a stable color that can be read at 450 nm [Siddeeg et al. 2021]. The sample antioxidant capacity is expressed as uric acid equivalents and the graph is drawing expressing the dependence of the Cu^{+1} complex absorbance, which has a rectilinear course

in the uric acid concentration range of 0.05-2 mM [Apak et al. 2005; Cybul and Nowak 2008].

There are stable and rapid methods. Cupric ion reducing antioxidant capacity (CUPRAC) is one of the best tests to measure the antioxidant potential of the thiolgroup and plasma antioxidants like AA, β-carotene, bilirubin, tocopherols and albumin. The Cu^{2+} ion has a redox potential (0.16 V) lower than that of the Fe^{3+} ion, which makes the CUPRAC reaction more selective than the FRAP reaction. Unlike FRAP, CUPRAC method is performed in aqueous solution with neutral variety of antioxidants with hydro- or lipo-soluble chemical structures. In addition, CRA and CUPRAC measurement methods has been applied to assess the antioxidant capacity of Mo^{6+}, Ru^{2+}, Oxovanadium^{4+}, Co^{2+}, Pd^{2+}, Cu^{2+}, Fe^{2+} and Mn^{2+} [Siddeeg et al. 2021; Marchi et al. 2022].

In CUPRAC method only hydrophilic antioxidants are suitable and it is difficult to set an appropriate reaction time [Marchi et al. 2022].

3.2. Mechanism of hydrogen atom transfer (HAT)

In the HAT process, the antioxidant neutralizes the radical species by donating a hydrogen atom, H. The reactivity of this mechanism is dependent on the pH of the solution, the environment, and the bond dissociation energy (BDE) of the O–H bond, which is correlated to BDE value [Marchi et al. 2022]. An antioxidant present in the analyzed sample and the model antioxidant of known concentration, called a "molecular probe" compete with each other for the opportunity to react with the peroxyl radical. In these methods, measurement of antioxidant activity is based on monitoring the course of these competing reactions [Grajek 2007; Cybul and Nowak 2008].

3.2.1. ORAC Assay

Analyses based on this mechanism include a method of determining the oxygen radical absorbance capacity (ORAC). This assay measures the decrease in the fluorescence of the fluorescein probe which detects peroxy radicals generated by 2,2'-Azobis(2-amidinopropane) dihydrochloride (AAPH) due to free radicals scavenging by the antioxidant in the presence of free radical scavengers. The decrease in fluorescence is linear. This test is usually performed in commercially available 96-well polypropylene fluorescence plates and the decreases are fluorescence is read at excitation/emission 485/520 nm every 1 min for 35 min. Different concentrations of Trolox are used as standards and the antioxidant activity (concentration) is calculated from the standard curve or the area under the curve

[Price et al. 2006; Cybul and Nowak 2008; Prior 2005; Siddeeg et al. 2021; Marchi et al. 2022].

This method is more sensitive than the FRAP one. In this method, oxidative activity is determined by integrating the area between the fluorescence curves for the test sample and the blank. This assay enables the determination of the activity of fat- or water-soluble compounds with antioxidant properties. At present, in the ORAC method, among others, fluorescein or dichlorofluorescein are used as molecular probes. The method belongs to those of high precision and sensitivity [Osman et al. 2006; Cybul and Nowak 2008].

The antioxidant capacity estimation requires the integration of the area under curve (AUC) of the fluorescence curves for the examined sample and the reference sample. Photobleaching of the probe and control reaction conditions (temperature and oxygen) are also disadvantages of this method [Cybul and Nowak 2008; Marchi et al. 2022].

3.2.2. TRAP Assay

The total radical-trapping antioxidant parameter (TRAP) method is based on the continuous formation of lipid or peroxyl radicals under aerobic conditions, and is detected by fluorescence. This method measures the ability of an antioxidant to scavenge ROO in the presence of a molecular probe [Marchi et al. 2022]. The TRAB method relies on preserving the decomposition of fluorescence of the R-phycoerythrin (R-PE) by azo compound 2,2'-azobis(2-amidinopropane) dihydrochloride (AAPH) (a radical generator). The antioxidant activity of the extract is proportional to the decoloration of the product. Antioxidants react ca. 100 times faster with radicals than R-PE and due to this, they are able to break the chain of free radical-induced reactions. When the lag phase period of reaction is over, i.e. when the antioxidants have completely reacted, the R-PE protein oxidation begins and a gradual fluorescence decay of the mixture is observed. This method is carried out at 37 °C and the reactants are soluble in phosphate pH buffer pH 7.4. TRAP may be either directly measured by a fluorescence-based method (TRAPm) or calculated (TRAPc) by a mathematical formula, considering the serum levels of four natural antioxidants. The quantitative determination of the antioxidant activity in the analyzed sample is based on determining the lag times for the sample and for the known amount of Trolox, during the oxidation process [Grajek 2007; Cybul and Nowak 2008; Dresch et al. 2009; Santos-Sánchez et al. 2019].

TRAP is the best test to be used for plasma samples. Its advantage is great simplicity [Siddeeg et al. 2021].

This is a complicated method that requires a long time of equipment use and an expert experimenter; in addition, TRAP also uses an aqueous solution, which is not necessarily a physiological medium, to mimic and generate lipid peroxyl radicals [Marchi et al. 2022].

3.2.3. LPIC Assay

The lipid peroxidation inhibition capacity (LPIC) method measures the ability of both lipophilic and hydrophilic antioxidants to protect a lipophilic fluorescent probe 4, 4-difluoro-5-(4-phenyl-1,3-butadienyl)-4-bora-3a,4a-diaza--s-indacene-3-undecanoic acid, incorporated in the membrane, from 2,2'-azobis(2-amidinopropane)hydrochloride generated radicals in the surrounding aqueous solution [Zhang et al. 2006]. This assay is based on the estimation of the ability of antioxidants occurring in the sample, to inhibit the peroxidation products of model lipids of the LDL-cholesterol fraction or linoleic acid. The course of the oxidation is monitored spectrophotometrically at 234 nm. During the absorption measurement, three phases can be observed (induction, propagation and termination of the reaction). During the induction phase, linoleic acid or polyunsaturated fatty acids of the LDL fraction are protected against oxidation by the sample's antioxidants. Once they have reacted, the peroxidation process moves into the propagation phase. In addition to the UV-VIS spectrophotometer, liquid or gas chromatographs are also applied [Cybul and Nowak 2008; Apak et al. 2016].

The advantages of this method are accuracy and precision [Zhang et al. 2006]. In its more advanced form, it requires specialized equipment [Zhang et al. 2006].

3.2.4. CBA Assay

Crocin, a carotenoid derivative naturally occurring in crocus, becomes discolored only by radical oxidation and this property is used in the crocin bleaching assay (CBA). The CBA is suitable for screening radical scavenging activity. Originally, an inhibition of crocin bleaching by a range of substances was monitored by competition kinetics in the presence of photolytically produced alkoxyl radicals. In CBA, abstraction of hydrogen atoms and/or addition of the radical to the polyene structure of crocin results in a disruption of the conjugated system accounting for crocin bleaching [Dontha 2016]. At the first stage, phosphate buffer is prepared, containing crocin and an appropriate amount of the analyzed antioxidants. Then, azo-initiator (AAPH or ABAP) is added to start the radical reaction. The course

of the oxidation process of samples, both with and without the addition of antioxidant, is usually monitored spectrophotometrically at 443 nm, for 10 minutes [Cybul and Nowak 2008; Zieniuk et al. 2021].

It is believed to be a suitable method for the analysis of complex samples containing many components and fast and slow acting antioxidants [Cybul and Nowak 2008].

This method measures the antioxidant activity of only hydrophilic antioxidants and is one of the most commonly used for the quantitative analysis of fruit and vegetable extracts, as well as individual compounds and body fluids. This method is characterized by low reproducibility, problematic quantification of results, differences in reagent preparation, doubtful need for a preheating phase and sensitivity to factors such as temperature, pH, solvents and metals [Caldwell et al. 2000; Ninfali et al. 2002; Cybul and Nowak 2008].

3.3. Methods using other mechanisms

3.3.1. TOSC Assay

The total oxidant scavenging capacity (TOSC) assay is a method allowing the determination of the ability of the examined solution to inhibit three strong oxidants, i.e. hydroxyl radicals, superoxide radicals and peroxynitrite radicals. In the total oxyradical scavenging capacity (TOSC) assay different reactive oxygen species can be generated at a constant rate. In this manner, reactive oxygen species can oxidize the substrate α-keto-γ-methiolbutyric acid (KMBA) to ethylene gas and the course of ethylene formation is measured. The efficiency of cellular antioxidants as scavengers of the generated reactive oxygen species is a function of their ability to inhibit the reaction between reactive oxygen species and KMBA. The degree of inhibition of ethylene formation relative to controls yields a parameter termed the TOSC value, which is an index of the antioxidant capacity of a sample for a defined reactive oxygen species [Regoli et al. 2000]. ethylene formation time is tracked using a gas chromatograph. The antioxidant properties of a sample are the greater, the greater the ability of its antioxidants to inhibit the reaction of ethylene formation. The analysis is carried out on the examined sample as well as on a control sample containing no antioxidants [Lichtenthäler et al. 2003; Cybul and Nowak 2008].

This method is used to determine both water- and lipid-soluble antioxidants and also is applied to testing a pure antioxidant solution as well as complex biological samples (liquids, tissues) [Cybul and Nowak 2008].

In this method large deviations of both hydrophilic and lipophilic substances can't be observed despite their sometimes lower concentration range. This method requires more advanced equipment [Regoli et al. 2000].

3.3.2. Chemiluminescent (CL) method

This method is based on the reaction of oxygen radicals with an appropriate tracer, resulting in the formation of excited chemiluminescence-emmiting forms. Among different chemiluminogenic species exploited for the evaluation of antioxidant activity, luminol seems to be the most commonly used CL reagent. The assays employing a luminol CL detection are based on the scavenging of free radicals (including reactive oxygen species) involved in the sequence leading to an electronically excited 3-aminophtalate dianion (3-APA*), which emit the light on return to its ground state. The determination of antioxidants is mainly based on the inhibiting of CL derived from few enzymatic reactions: luminol–H_2O_2–horseradish peroxidase, luminol–xanthine–xanthine oxidase, luminol–hypoxanthine–xanthine oxidase, but also luminol–H_2O_2–Co(II)/EDTA, luminol–H_2O_2–Fe(II), luminol–ClO^- and luminol-2,2'-azo-bis-(2-amidinopropane) CL system [Nalewajko-Sieliwoniuk et al. 2008]. The antioxidant activity of a sample is determined by comparing the reaction kinetics of a control sample (without chemiluminescence suppressants) to an analysis with antioxidants. The vast majority of chemiluminescent methods used to determine the total phenolic antioxidants are stationary methods; only a small part of them are the methods conducted in flow injection analysis (FIA) systems, flow sequential injection analysis (SIA) system, multi-pumping flow systems (*MPFS*), and multicommutation flow analysis (MCFA) system [Cybul and Nowak 2008; Koss-Mikołajczyk et al. 2017; Zadykowicz et al. 2018].

The advantages of the chemiluminescent method include a very low threshold of antioxidant detection, a wide range of linearity and a rate, faster than that of standard methods. The method is often used to determine the content of reactive oxygen species in various biological systems, and also as an indirect method for the analysis of antioxidant properties [Cybul and Nowak 2008]. Simplicity and low cost of the apparatus are its advantages. The SIA, MCFA and MPFS techniques are more advanced in terms of apparatus than the classic FIA techniques. So, they make it possible to increase the level of automation employed in measuring systems. In addition, their use is beneficial taking into account enviro-economic aspects, as they allow for the significant reduction of the amount of reagents used and produced waste, thus meeting the criteria for the so-called "Green analytical chemistry" [Atanassova et al. 2005; Cybul and Nowak 2008; Koss-Mikołajczyk et al. 2017].

The disadvantages of this method are the lack of analytical characteristics of the developed methods and their rarely-tested selectivity. In order to determine individual antioxidant compounds in raw materials and plant-derived products, as well as to find those most responsible for the antioxidant activity of the examined samples, it is necessary to apply the stage of their preliminary separation on the chromatographic column. Separation of plant phenols is mainly performed by means of high-performance liquid chromatography methods [Atanassova et al. 2005; Cybul and Nowak 2008; Koss-Mikołajczyk et al. 2017].

3.3.3. Electrochemical methods

These methods use the current generated during the electrochemical reaction of oxygen on the electrode. Antioxidants reduce the intensity of this current by reacting with oxygen and its derivatives. There are several variants of electrochemical measurement of antioxidant activity. The most important of them, cyclic voltammetry (CV) and differential pulse voltammetry (DPV), allow the measurement of the sample antioxidant potency using a special glass carbon electrode. In cyclic voltammetry, a glass carbon or platinum electrode is used as the working electrode, and a silver chloride or calomel electrode as the reference electrode [Zielinska et al. 2008; Chevion et al. 2000; Koss-Mikołajczyk et al. 2017].

This method is characterized by the high level of automation. The surface area may be taken as a parameter to compare the antioxidant capacity of a number of samples or relate its value to that of a given concentration of a reference substance. The most commonly used reference substances are Trolox and ascorbic acid [Chevion et al. 2000; Zielinska et al. 2008].

This method has limited efficiency in terms of the number of analyses performed per day (only 20 samples) due to the long electrode cleaning procedure. In addition, the signal observed for samples with a complex matrix is the result of the oxidation potentials for many compounds and there are problems in determining the value of the peak current or the total charge under the oxidation peak. This method will not provide information on the mechanism or kinetics of the free radicals neutralization reaction [Chevion et al. 2000; Zielinska et al. 2008].

3.3.4. Electron paramagnetic resonance (EPR) spectroscopy

This method allows the detection of compounds with unpaired electrons (paramagnetics), i.e. free radicals. Most EPR spectrometers use a constant frequency of radiation and an alternating magnetic field; resonance detection is performed by the continuous wave (CW) method [Epel et al. 2014]. CW EPR spectrometers

record the spectrum of a paramagnetic substance as an absorption curve, and this is usually displayed as the first derivative of the absorption curve due to this-way increased resolution and signal-to-noise ratio. Double integration allows the calculation of the signal area, which is directly proportional to the concentration of paramagnetic centers. The radical identification is conducted on the basis of the spectroscopic splitting factor (g), which determines the strength of the interaction with an external magnetic field. The difficulty in observing free radicals is their short lifetime. In order to avoid this problem, spin traps are used. These are diamagnetic compounds, which, due to the presence of –N=O bonds, form relatively stable spin adducts with free radicals [Zawada 2009; Epel et al. 2014; Jarco 2017].

EPR spectroscopy provides valuable information on a variety of paramagnetic systems, for example, with an unpaired electron, which attract the interest of pharmacy and medicine. Due to its specificity, it allows for the study of free radicals in various materials: drugs, tissues, body fluids [Zawada 2009].

The disadvantage of EPR imaging is the low spatial resolution of the method, resulting from a large spectral line width and the occurrence of hyperfine coupling [Ninfali et al. 2002; Zawada 2009].

3.3.5. Other, less frequently used methods

Mass spectrometer (MS), nuclear magnetic resonance (NMR) and Fourier transform infrared (FT-IR) spectroscopy are use occasionally to study antioxidant activity. In turn, there are methods using combined techniques, such as, for example, HPLC/MS or HPLC/MS/MS, which are applied for the detection of individual compounds with antioxidant activity as well as to determine antioxidant activity [Koss-Mikołajczyk et al. 2017].

These methods are characterized by high accuracy and innovative nature, depending to a large extent on the research skills of the person performing analyses [Szeleszczuk et al. 2018].

These techniques are time-consuming; require pre-treatment of the examined product, expensive equipment (detectors, chromatographic columns) and high-purity reagents [Szeleszczuk et al. 2018].

4. *In vivo* methods

For all *in vivo* methods the samples that are to be tested are usually administered to the testing animals (mice, rats, etc.) at a definite dosage regimen as described by the respective method. After a specified period of time, the animals are usually

sacrificed and blood or tissues are used for the assay [Alam et al. 2013]. In *in vivo* methods, liposomes and microsomes, due to their similarity to the composition of biological membranes, are used to assess antioxidant activity in oxidation reactions, in systems that mimic real conditions inside the body. The inhibition of low density lipoprotein (LDL) oxidation in the blood plasma of experimental animals and in humans after oral administration of a polyphenol mixture, is also used as a measure of antioxidant activity [Salleh et al. 2002]. The degree of inhibition of DNA damage occurring in biological systems (helix breakage, single-strand breakage or chromosomal abnormalities) is used to estimate the activity, too. *In vivo* methods applications include: free radical scavenging capacity of human blood; inhibition of apoptosis-inducing oxidation of living human cells; lipid peroxidation of liposome membranes exposed to UV radiation; oxidation of the rat liver cell-derived mitochondria; lipid oxidation in lecithin microsomes of chicken eggs; oxidation of human LDL induced by copper or radicals; NADPH/iron-induced peroxidation in liver microsomes; antioxidant capacity of rat blood plasma with induced formation of cholesterol ester hydroperoxides; and DNA oxidation and fragmentation assays [Moure et al. 2001; Cybul and Nowak 2008].

5. The problems with the objectivity of the methods used to determine antioxidant activity

5.1. The methods used to determine antioxidant activity *in vitro*

An extensive use of aforementioned assays for the evaluation of fruits, vegetables, leaves and stems, herbs and spices, caused that TEAC, DPPH, ABTS, ORAC, CUPRAC, and FRAP acronyms are today commonly used words in scientific publications and general audience popular science articles. However, none of the methods developed so far has been recognized as the standard method. These methods are characterized by great diversity, since they are based on different reaction mechanisms (e.g. single electron transfer, hydrogen atom transfer) and measurement conditions (different forms of analytes depending on the pH used). The selection of a suitable alcoholic/non-alcoholic/apolar extractant is also a serious problem as well as the measurement time used for methods where the sample becomes discolored. Usually, individual research groups rely on their previous experiences. As a result, no standards have been developed, as own modifications have been introduced to the commonly known methods. In addition, these methods use different standard substances and different ways of expressing re-

sults (e.g. the percentage of unreduced radical or as the EC_{5O} parameter, which indicates the antioxidant concentration causing a decrease of the initial radical concentration by 50% or expressed as Trolox). The differences described make it impossible to compare the values obtained in an unambiguous way. Unfortunately, the results obtained by means of spectrophotometric methods are subject to large errors. Doubts concerning the unambiguous classification of some simple reactions as following the SET mechanism have been reported in the literature. This includes suggestions of the co-occurrence of reactions based on SET and HAT mechanisms as well as the occurrence of more complex mechanisms – SPLET (sequential proton loss electron transfer) and PCET (proton coupled electron transfer). This also makes it impossible to clearly define the mechanism of the reactions. First of all, taking into account quantitative analyses, chemical aspects of methods are unclear. They were developed for rapid screening, so there are no detailed studies on basic initiators, objectives, antioxidant interactions, kinetics, and effects of solvents or the concentration used, etc. The routinely ignored problems include also such issues as: not fully understanding of ongoing reaction, some aspects of control, oxygen forms (dissolved and atmospheric), light, temperature, reagent concentrations, solvents, pH, and the blanks used. In the vast majority of methods, stoichiometry (capacity) rather than kinetics of antioxidant reactions is measured. Furthermore, in each laboratory, procedures develop to work with available instrumentation and under laboratory capabilities. It is observed that there is an almost complete lack of standardization of experimental procedures, especially in the expression of results. Here, there are various methods, often irrelevant in terms of *in situ* performance. Overall, the majority of "screening" methods and natural antioxidants are water-based, while lipid phases are ignored [Liang and Kitts 2014; Ilyasov et al. 2020].

5.2. The methods used to determine antioxidant activity *in vivo*

From many conceptual limitations, one of the most important relates to antioxidant assays designed to identify which antioxidants should ensure the strongest protective effects against free radicals *in vivo*. However, the radical quenching noted in test tubes probably does not take place *in vivo*. Majority of antioxidants are not easily absorbed or are rapidly conjugated and excreted in the urine. Therefore, the amount of circulating phenol reaches trace levels at best. There is low probability that such slight amounts can influence the physiological antioxidant's action by radical quenching only. In the vast majority of *in vitro* methods, chemical reactions and molecular targets are not reflecting *in vivo* conditions. These

methods apply antioxidants in the amounts, which are orders of magnitude higher than that occurring *in vivo*. As opposed to small, easily available but unstable radicals, which are active *in vivo*, in these assays, sterically-hindered stable radicals are used as targets. If an antioxidant needs minutes to hours for radical scavenging, its action *in vivo* in cells or even *in situ* in foods must be negligible [Schaich et al. 2015].

6. Conclusion

Chemical methods for the determination of antioxidant capacity are based on measurement of the effect of antioxidants on the rate of oxidation processes occurring in the sample (ORAC and TRAP), reduction of metal ions, e.g. iron (FRAP) or copper (CUPRAC), synthetic radical scavenging capacity (ABTS, DPPH) or measuring the amount of lipid oxidation products or LDL fractions. Independently of the analytical technique selected to evaluate the antioxidant activity against free radicals, the tests should fulfill to some main requirements. Firstly, all analytical methods used to quantify antioxidant activity must present repeatability, reproducibility and standardization to be validated. Secondly, all available methodologies should have their effectiveness tested by comparing the antioxidant compounds with an appropriate commercial standard to quantify their antioxidant capacity. Although a number of methods exist to assess antioxidant properties, there is no standardization of the obtained results. Unfortunately, this situation makes it impossible to compare the results achieved by different researchers. Therefore, it is a serious methodological challenge.

References

Alam M.N., Bristi N.J., Rafiquzzaman M. 2013. Review on in vivo and in vitro methods evaluation of antioxidant activity. Saudi Pharmaceutical Journal, 21(2), 143–152. https://doi.org/10.1016/j.jsps.2012.05.002

Ali S.S., Ahsan H., Zia M.K., Siddiqui T., Khan F.H. 2020. Understanding oxidants and antioxidants: Classical team with new players. Journal of Food Biochemistry, 44(3), e13145. https://doi.org/10.1111/jfbc.13145

Apak R., Güçlü K., Özyürek M., Karademir S.E. 2004. Novel total antioxidant capacity index for dietary polyphenols and vitamins C and E, using their cupric ion reducing capability

in the presence of neocuproine: CUPRAC method. Journal of Agricultural and Food Chemistry, 52(26), 7970–7981. https://doi.org/10.1021/jf048741x

Apak R., Güçlü K., Özyürek M., Karademir S.E., Altun M. 2005. Total antioxidant capacity assay of human serum using copper (II)-neocuproine as chromogenic oxidant: The CUPRAC method. Free Radical Research, 39(9), 949–961. https://doi.org/10.1080/10715760500210145

Apak R., Özyürek M., Güçlü K., Çapanoğlu E. 2016. Antioxidant activity/capacity measurement. 2. Hydrogen atom transfer (HAT)-based, mixed-mode (electron transfer (ET)/HAT), and lipid peroxidation assays. Journal of Agricultural and Food Chemistry, 64(5), 1028–1045. https://doi.org/10.1021/acs.jafc.5b04743

Arts M.J., Haenen G.R., Voss H.P., Bast A. 2004. Antioxidant capacity of reaction products limits the applicability of the Trolox Equivalent Antioxidant Capacity (TEAC) assay. Food and Chemical Toxicology, 42(1), 45–49. https://doi.org/10.1016/j.fct.2003.08.004

Atanassova D., Kefalas P., Psillakis E. 2005. Measuring the antioxidant activity of olive oil mill wastewater using chemiluminescence. Environment International, 31(2), 275–280. https://doi.org/10.1016/j.envint.2004.10.003

Bartoń H.J., Fołta M., Zachwieja Z. 2005. Zastosowanie metod FRAP, ABTS i DPPH w badaniu aktywności antyoksydacyjnej produktów spożywczych. Nowiny Lekarskie, 74(4), 510–513.

Bou-Fakhredin R., Dia B., Ghadieh H.E., Rivella S., Cappellini M.D., Eid A.A., Taher A.T. 2021. CYP450 mediates reactive oxygen species production in a mouse model of β-thalassemia through an increase in 20-HETE activity. International Journal of Molecular Sciences, 22(3), 1106. https://doi.org/10.3390/ijms22031106

Caldwell C.R. 2000. A device for the semiautomatic determination of oxygen-radical absorbance capacity. Analytical Biochemistry, 287(2), 226–233. https://doi.org/10.1006/abio.2000.4853

Capanoglu E., Kamiloglu S., Ozkan G., Apak R. 2018. Evaluation of antioxidant activity/capacity measurement methods for food products. [In:] Measurement of Antioxidant Activity and Capacity: Recent Trends and Applications. Eds. R. Apak, E. Capanoglu, F. Shahidi. John Wiley & Sons Ltd, Chicester, United Kingdom, 273–286. https://doi.org/10.1002/9781119135388.ch13

Chevion S., Roberts M.A., Chevion M. 2000. The use of cyclic voltammetry for the evaluation of antioxidant capacity. Free Radical Biology and Medicine, 28, 860–870. https://doi.org/10.1016/s0891-5849(00)00178-7

Cybul M., Nowak R. 2008. Przegląd metod stosowanych w analizie właściwości antyoksydacyjnych wyciągów roślinnych. Herba Polonica, 54(1), 68–78. http://www.herbapolonica.pl/magazinesfiles/4185443przeglad%20metod%20stosowanych.pdf [accessed: August 19, 2018].

Dontha S. 2016. A review on antioxidant methods. Asian Journal of Pharmaceutical and Clinical Research, 9(2), 14–32. https://doi.org/10.22159/ajpcr.2016.v9s2.13092

Dresch M.T.K., Rossato S.B., Kappel V.D., Biegelmeyer R., Hoff M.L.M., Mayorga P., Zuanazzi J.A.S., Henriques A.T., Moreira J.C.F. 2009. Optimization and validation of an alternative method to evaluate total reactive antioxidant potential. Analytical Biochemistry, 385, 107–114. https://doi.org/10.1016/j.ab.2008.10.036

Durazzo A. 2017. Study approach of antioxidant properties in foods: Update and considerations. Foods, 28, 6(3), 17. https://doi.org/10.3390/foods6030017

Epel B., Redler G., Halpern H.J. 2014. How in vivo EPR measures and images oxygen. Advances in Experimental Medicine and Biology, 812, 113–119. https://doi.org/10.1007/978-1-4939-0620-8_15

Firuzi O., Lacanna A., Petrucci R., Marrosu G., Saso L. 2005. Evaluation of the antioxidant activity of flavonoids by "ferric reducing antioxidant power" assay and cyclic voltammetry. Biochimica et Biophysica Acta, 1721(1–3), 174–184. https://doi.org/10.1016/j.bbagen.2004.11.001

Frezzini M.A., Castellani F., De Francesco N., Ristorini M., Canepari S. 2019. Application of DPPH assay for assessment of particulate matter reducing properties. Atmosphere, 10(12), 816. https://doi.org/10.3390/atmos10120816

Galadari S., Rahman A., Pallichankandy S., Thayyullathil F. 2017. Reactive oxygen species and cancer paradox: To promote or to suppress? Free Radical Biology and Medicine, 104, 144–164. https://doi.org/10.1016/j.freeradbiomed.2017.01.004

Grajek W. 2007. Przeciwutleniacze w żywności. Aspekty zdrowotne, technologiczne, molekularne i analityczne. Wydawnictwo Naukowo-Techniczne, Warszawa.

Ifeanyi O.E. 2018. A review on free radicals and antioxidants. International Journal of Current Research in Medical Sciences, 4(2), 123–133. https://doi.org/10.22192/ijcrms.2018.04.02.019

Ilyasov I.R., Beloborodov V.L., Selivanova I.A., Terekhov R.P. 2020. ABTS/PP decolorization assay of antioxidant capacity reaction pathways. Journal of Molecular Sciences, 21(3), 1131. https://doi.org/10.3390/ijms21031131

Jarco S. 2017. Effects of storage conditions on formation of free radicals in soybean extract – An EPR spectroscopy study. Annales Academiae Medicae Silesiensis, 71, 217–224. https://doi.org/10.18794/aams/67972

Kedare S.B., Singh R.P. 2011. Genesis and development of DPPH method of antioxidant assay. Journal of Food Science and Technology, 48(4), 412–22. https://10.1007/s13197-011-0251-1

Koss-Mikołajczyk I., Baranowska M., Namieśnik J., Bartoszek-Pączkowska A. 2017. Metody oznaczania właściwości przeciwutleniających fitozwiązków w systemach komórkowych z wykorzystaniem zjawiska fluorescencji/luminescencji. Postępy Higieny i Medycyny Doświadczalnej, 71, 602–616. https://doi.org/10.5604/01.3001.0010.3841

Liang N., Kitts D.D. 2014. Antioxidant property of coffee components: Assessment of methods that define mechanisms of action. Molecules, 19(11), 19180–19208. https://doi.org/10.3390/molecules191119180

Lichtenthäler R., Marx F., Kind O. 2003. Determination of antioxidative capacities using an enhanced total oxidant scavenging capacity (TOSC) assay. European Food Research and Technology, 216(2), 166–173. https://doi.org/10.1007/s00217-002-0635-6

Marchi R.C., Campos I.A.S., Santana V.T., Carlos R.M. 2022. Chemical implications and considerations on techniques used to assess the in vitro antioxidant activity of coordination compounds. Coordination Chemistry Reviews, 451, 21427. https://10.1016/j.ccr.2021.214275

Matschke V., Theiss C., Matschke J. 2019. Oxidative stress: The lowest common denominator of multiple diseases. Neural Regeneration Research, 14(2), 238. https://doi.org/10.4103/1673-5374.244780

Moharram A., Youssef M. 2014. Methods for determining the antioxidant activity: A review. Alexandria Journal of Food Science and Technology, 11(1), 31–42. https://journals.ekb.eg/article_20251_46bd1a0433e6dc694aa7953b19fd1868.pdf

Molyneux P. 2004. The use of the stable free radical diphenylpicrylhydrazyl (DPPH) for estimating antioxidant activity. Songklanakarin Journal of Science and Technology, 26(2), 211–219. http://rdo.psu.ac.th/sjstweb/journal/26-2/07-DPPH.pdf

Moure A., Cruz J.M., Franco D., Dominguez J.M., Sineiro J., Dominguez H., Nunez M.J., Parajo J.C. 2001. Natural antioxidants from residual sources. Food Chemistry, 72, 145–171. https://doi.org/10.1016/S0308-8146(00)00223-5

Nalewajko-Sieliwoniuk E., Nazaruk J., Antypiuk E., Kojło A. 2008. Determination of phenolic compounds and their antioxidant activity in Erigeron acris L. extracts and pharmaceutical formulation by flow injection analysis with inhibited chemiluminescent detection. Journal of Pharmaceutical and Biomedical Analysis, 48(3), 579-86. https://doi.org/10.1016/j.jpba.2008.05.026

Nenadis N., Tsimidou M. 2002. Observations on the estimation of scavenging activity of phenolic compounds using rapid 1,1-diphenyl-2-picrylhydrazyl (DPPH•) tests. Journal of the American Oil Chemists' Society, 79(12), 1191–1195. http://lib3.dss.go.th/fulltext/Journal/J.AOCS/J.AOCS/2002/no.12/v.79n12p1191-1195.pdf [accessed: August 21, 2018].

Ninfali P., Bacchiocca M., Biagiotti E., Servili M., Montedoro G. 2002. Validation of the oxygen radical absorbance capacity (ORAC) parameter as a new index of quality and stability of virgin olive oil. Journal of the American Oil Chemists' Society, 79(10), 977–982. https://doi.org/10.1007/s11746-002-0590-7

Osman A.M., Wong K.K.Y., Fernyhough A. 2006. ABTS radical-driven oxidation of polyphenols: Isolation and structural elucidation of covalent adducts. Biochemical and Biophysical Research Communications, 346(1), 321–329. https://doi.org/10.1016/j.bbrc.2006.05.118

Pastor F.T., Šegan D.M., Gorjanović S.Ž., Kalušević A.M., Sužnjević D.Ž. 2020. Development of voltammetric methods for antioxidant activity determination based on Fe(III) reduction. Microchemical Journal, 155, 104721. https://doi.org/10.1016/j.microc.2020.104721

Price J.A., Sanny C.G., Shevlin D. 2006. Application of manual assessment of oxygen radical absorbent capacity (ORAC) for use in high throughput assay of "total" antioxidant activity of drugs and natural products. Journal of Pharmacological and Toxicological Methods, 54(1), 56–61. https://doi.org/10.1016/j.vascn.2005.11.002

Prior R.L., Wu X., Schaich K. 2005. Standardized methods for the determination of antioxidant capacity and phenolics in foods and dietary supplements. Journal of Agriculture and Food Chemistry, 53(10), 4290–4302. https://doi.org/10.1021/jf0502698

Regoli F., Nigro M., Bompadre S., Winston G.W. 2000. Total oxidant scavenging capacity (TOSC) of microsomal and cytosolic fractions from Antarctic, Arctic and Mediterranean scallops: Differentiation between three potent oxidants. Aquatic Toxicology, 49(1–2), 13–25. https://doi.org/10.1016/s0166-445x(99)00070-3

Roginsky V., Lissi E.A. 2005. Review of methods to determine chainbreaking antioxidant activity in food. Food Chemistry, 92(2), 235–254. https://doi.org/ 10.1016/j.foodchem.2004.08.004

Salleh M.N., Runnie I., Roach P.D., Mohamed S., Abeywardena M.Y. 2002. Inhibition of low--density lipoprotein oxidation and up-regulation of low-density lipoprotein receptor in HepG2 cells by tropical plant extracts. Journal of Agriculture and Food Chemistry, 50(13), 3693–3697. https://doi.org/10.1021/jf011593f. PMID:12059144

Santos-Sánchez N.F., Salas-Coronado R., Villanueva-Cañongo C., Hernández-Carlos B. 2019. Antioxidant Compounds and their Antioxidant Mechanism. IntechOpen, London, UK. https://doi.org/10.5772/intechopen.85270

Schaich K.M., Tian X., Xie J. 2015. Hurdles and pitfalls in measuring antioxidant efficacy: A critical evaluation of ABTS, DPPH, and ORAC assays. Journal of Functional Foods, 14, 111–125. https://doi.org/10.1016/j.jff.2015.01.043

Siddeeg A., AlKehayez N.M., Abu-Hiamed H.A., Al-Sanea E.A., Al-Farga A.M. 2021. Mode of action and determination of antioxidant activity in the dietary sources: An overview. Saudi Journal of Biological Sciences, 28 (2021), 1633–1664. https://doi.org/10.1016/j.sjbs.2020.11.064

Sies H., Jones D.P. 2020. Reactive oxygen species (ROS) as pleiotropic physiological signalling agents. Nature Reviews Molecular Cell Biology, 21(7), 363–383. https://doi.org/10.1038/s41580-020-0230-3

Szeleszczuk Ł., Jurczak E., Zielińska-Pisklak M., Harwacki J., Pisklak D.M. 2018. Comparison of the analytical methods (solid state NMR, FT-IR, PXRD) in the analysis of the solid drug forms with low concentration of an active ingredient – 17-β-estradiol case. Journal of Pharmaceutical and Biomedical Analysis, 149, 160–165. https://doi.org/10.1016/j.jpba.2017.11.015

Yeo J., Shahidi F. 2019. Critical re-evaluation of DPPH assay: Presence of pigments affects the results. Journal of Agricultural and Food Chemistry, 67(26), 7526–7529. https://doi.org/10.1021/acs.jafc.9b02462

Zadykowicz B., Romanowska A., Pieńkos M. 2018. Fotofizyczne podstawy znakowania chemiluminescencyjnego – nowoczesnego narzędzia diagnostyki medycznej. Wiadomości Chemiczne, 72, 11–12. https://ptchem.pl/storage/pages/March2019/pdf/11_12.pdf [accessed: August 30, 2018].

Zawada K. 2009. Zastosowanie spektroskopii EPR w farmacji i medycynie. Farmacja Polska, 65(3), 224–228. https://ptfarm.pl/pub/File/FP/3_2009/13%20zastosowanie spektroskopii.pdf [accessed: August 31, 2018].

Zhang J., Stanley R.A., Melton L.D. 2006. Lipid peroxidation inhibition capacity assay for antioxidants based on liposomal membranes. Molecular Nutrition and Food Research, 50 (8), 714–24. https://doi.org/10.1002/mnfr.200600018

Zielinska D., Wiczkowski W., Piskula M.K. 2008. Determination of the relative contribution of quercetin and its glucosides to the antioxidant capacity of onion by cyclic voltammetry and spectrophotometric methods. Journal of Agricultural and Food Chemistry, 56, 3524–3531. https://doi.org/10.1021/jf073521f

Zieniuk B., Groborz K., Wołoszynowska M., Ratusz K., Białecka-Florjańczyk E., Fabiszewska A. 2021. Enzymatic synthesis of lipophilic esters of phenolic compounds, evaluation of their antioxidant activity and effect on the oxidative stability of selected oils. Biomolecules, 11(2), 314. https://doi.org/10.3390/biom11020314

ISBN 978-83-66602-61-8